

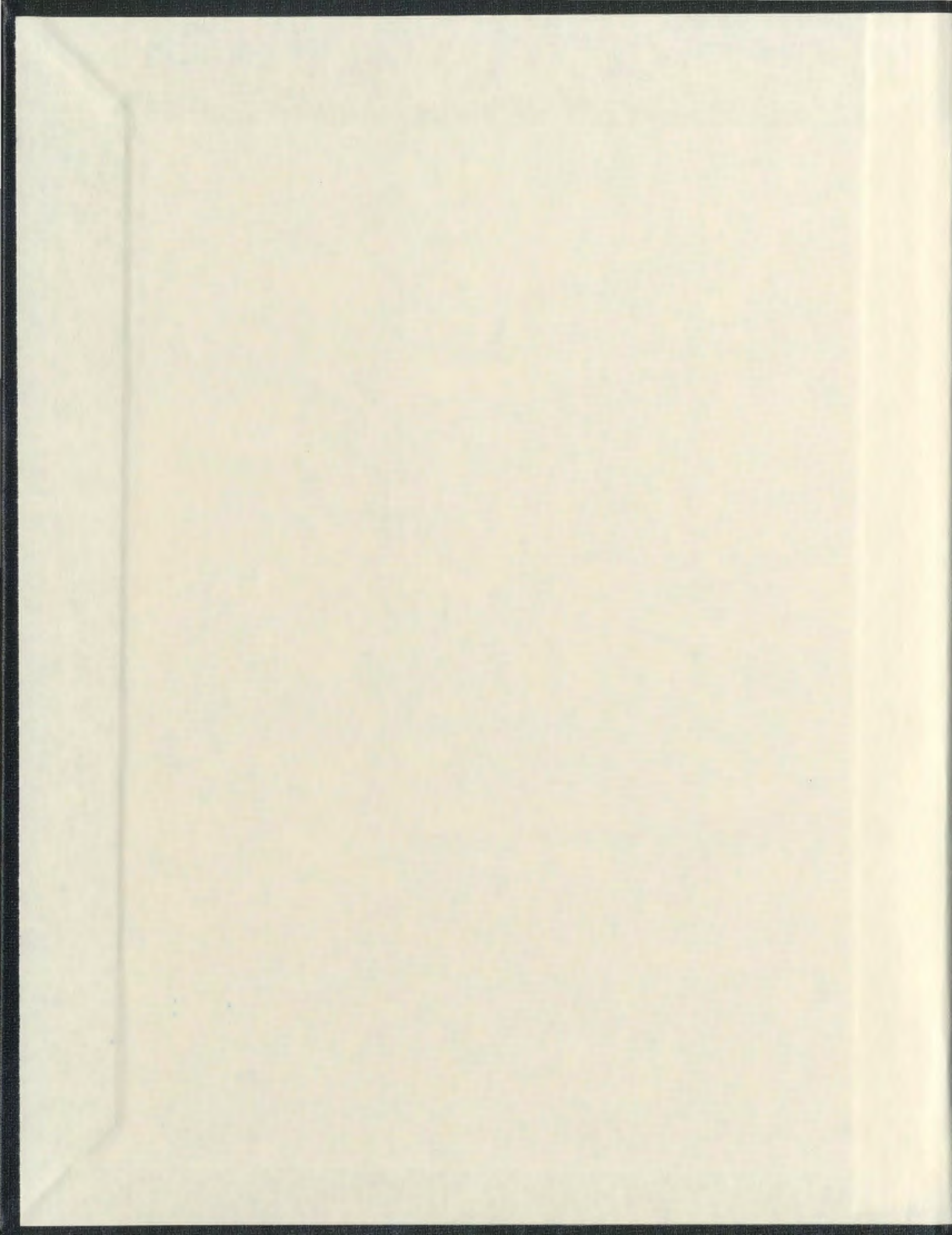
ALGEBRAIC COUPLED-STATE CALCULATION OF  
POSITRON-HYDROGEN COLLISIONS AT LOW ENERGY,  
USING LARGE COUPLING SCHEMES

CENTRE FOR NEWFOUNDLAND STUDIES

**TOTAL OF 10 PAGES ONLY  
MAY BE XEROXED**

(Without Author's Permission)

YU RANG KUANG







## **INFORMATION TO USERS**

This manuscript has been reproduced from the microfilm master. UMI films the text directly from the original or copy submitted. Thus, some thesis and dissertation copies are in typewriter face, while others may be from any type of computer printer.

The quality of this reproduction is dependent upon the quality of the copy submitted. Broken or indistinct print, colored or poor quality illustrations and photographs, print bleedthrough, substandard margins, and improper alignment can adversely affect reproduction.

In the unlikely event that the author did not send UMI a complete manuscript and there are missing pages, these will be noted. Also, if unauthorized copyright material had to be removed, a note will indicate the deletion.

Oversize materials (e.g., maps, drawings, charts) are reproduced by sectioning the original, beginning at the upper left-hand corner and continuing from left to right in equal sections with small overlaps. Each original is also photographed in one exposure and is included in reduced form at the back of the book.

Photographs included in the original manuscript have been reproduced xerographically in this copy. Higher quality 6" x 9" black and white photographic prints are available for any photographs or illustrations appearing in this copy for an additional charge. Contact UMI directly to order.

**UMI**

A Bell & Howell Information Company  
300 North Zeeb Road, Ann Arbor MI 48106-1346 USA  
313/761-4700 800/521-0600

**ALGEBRAIC COUPLED-STATE CALCULATION OF  
POSITRON-HYDROGEN COLLISIONS AT LOW ENERGY, USING  
LARGE COUPLING SCHEMES**

By

**Yu Rang Kuang**  
M. Sc., Sichuan Union University, PRC

**A THESIS SUBMITTED TO THE SCHOOL OF GRADUATE  
STUDIES IN PARTIAL FULFILLMENT OF THE  
REQUIREMENTS FOR THE DEGREE OF  
DOCTOR OF PHILOSOPHY**

**DEPARTMENT OF PHYSICS  
MEMORIAL UNIVERSITY OF NEWFOUNDLAND  
AUGUST, 1996**

**© Yu Rang Kuang, 1997**

## **Abstract**

The Harris-Nesbet algebraic approach is employed to carry out calculations of positron-hydrogen scattering at energy below the first excitation threshold of the hydrogen atom. The main work of this thesis is to extend the Harris-Nesbet method to large scale coupled-state calculations. With coupling schemes composed of lower physical states: 1s, 2s, 2p of both hydrogen and positronium, and a pseudo  $3\bar{p}$  of hydrogen associated with a number of short ranged correlation functions, calculations for positron-hydrogen scattering are accurately carried out for seven partial waves from  $L=0$  to 6. Comparison with available theoretical results shows that good agreement is obtained at energies considered. Our total elastic and total Ps formation cross sections are also in good agreement with existing accurate theoretical results. Our total Ps formation and integrated cross section (total elastic plus total Ps formation) agree with available experimental data. The scattering length obtained also agree well with the existing theoretical values. There are three, two and one resonances observed for the S-, P- and D-waves below the first excitation threshold of hydrogen, respectively, which confirms the existing observations.

On the other hand, we also carry out calculations for an 18-state and a 20-state coupling schemes. Both sets of results show reasonable agreement with each other and available findings.

## **Acknowledgements**

I wish to express my appreciation and gratitude to my thesis supervisor Dr. T. T. Gien for his guidance and encouragement throughout my studies, for suggesting this extended calculation and for correcting numerous errors and misprints of the formulas in Appendix B of the original version of this thesis.

Thanks are also extended to Dr. N. H. Rich, Dr. J. de Bruyn and Dr. S. P. Reddy for their great help during my studies in Memorial University of Newfoundland, to Dr. J. K. C. Lewis for his marvelous teaching. Special thanks to Dr. Rich and Dr. Lewis for their reading and correcting my thesis.

I am gratefully indebted to Dr. J. Mitroy, in Northern Territory University, Australia , for sharing his data in advance of publication and valuable suggestions.

I acknowledge Dr S. Zhou, Wayne State University, for sharing his experimental data in advance of publication.

I also wish to acknowledge the financial assistance from Memorial University of Newfoundland in the form of a University Fellowship and a teaching assistantship. A part of my financial support also came from Dr. T. T. Gien's NSERC Research Grant.

Finally, I thank my wife Huxiang for her understanding, encouragement and great support during my graduate studies, and my son Ningke who gives me a lot of happiness.

## Table of Contents

<b>Abstract</b>	<b>ii</b>
<b>Acknowledgements</b>	<b>iii</b>
<b>1 Introduction</b>	<b>1</b>
<b>2 Harris-Nesbet Algebraic Approximation</b>	<b>11</b>
2.1 Harris' Expansion Method . . . . .	12
2.2 Harris-Nesbet Algebraic Approach . . . . .	14
2.2.1 Single Channel . . . . .	14
2.2.2 Multichannel . . . . .	17
2.3 Optimized Harris-Nesbet Method in Transformed Space . . . . .	21
<b>3 Application for Positron-Hydrogen Scattering</b>	<b>25</b>
3.1 Hamiltonian and Channel wavefunctions . . . . .	25
3.2 Matrix Elements . . . . .	27
<b>4 Numerical Calculations and Results</b>	<b>32</b>
4.1 Calculations with Large Mixing bases . . . . .	32
4.1.1 The $e^+ + H(1s)$ entrance channel . . . . .	34
4.1.2 The $Ps + p$ entrance channel . . . . .	64
4.1.3 Resonance below the H First Excitation . . . . .	72
4.2 Calculations with 18- and 20-state bases . . . . .	87
4.2.1 Numerical Approaches . . . . .	87

4.2.2 Results . . . . .	88
<b>5 Conclusions</b>	<b>99</b>
<b>Bibliography</b>	<b>102</b>
<b>Appendix A: Variants of the Harris-Nesbet Method</b>	<b>110</b>
A.1 OMN Method . . . . .	110
A.2 OAF Method . . . . .	111
A.3 IAF and RIAF Methods . . . . .	113
<b>Appendix B: Analytical Reductions of Matrix Elements</b>	<b>114</b>
B.1 Bound-bound Matrix Elements . . . . .	114
B.2 Bound-free Matrix Elements . . . . .	119
B.3 Free-Free Matrix Elements . . . . .	127
B.4 Reduction of Angle Integral . . . . .	133
<b>Appendix C: Lists of Publications</b>	<b>138</b>
1 Positron-hydrogen collisions at low energies . . . . .	138
2 Large Scale Calculations of Positron-hydrogen System at Low Energies	139
<b>Appendix D: Fortran Programs</b>	<b>140</b>
1 18-state Coupling Scheme: 18-CC.f . . . . .	140
2 Mixing basis Coupling Scheme: 7-mixing.f . . . . .	140

## List of Figures

4.1	Partial S-wave phase shifts (Rad) as a function of positron momentum	37
4.2	Partial P-wave phase shifts (Rad) as a function of positron momentum (au). Phrases indicated in this picture have same meanings as in Figure 4.1 but Kleinman: variational by Kleinman et al. (1965); Chan: solving the coupled-equation associated with short range correlation functions by Chan and McEachran (1978). . . . .	43
4.3	Partial D-wave phase shifts (Rad) as a function of positron momentum (au). Phrases indicated in this picture have same meanings as in Figure 4.1. . . . .	44
4.4	Partial F-wave phase shifts (Rad) as a function of positron momentum (au). Phrases have same meanings as in Figure 4.1. . . . .	45
4.5	Partial S-wave elastic cross sections ( $\pi a_0^2$ ) from B7+ basis as a function of positron energy (Ryd). . . . .	48
4.6	Partial P-wave elastic cross sections ( $\pi a_0^2$ ) for $e^+ + H$ scattering are plotted as a function of positron energy (Ryd). Phrases in this picture have same meanings as in figure 4.5. . . . .	52
4.7	Partial D-wave elastic cross section ( $\pi a_0^2$ ) for $e^+ + H$ scattering is plotted as a function of positron energy (Ryd). Phrases in this picture have same meanings as in figure 4.5. . . . .	54
4.8	Partial F-wave elastic cross section ( $\pi a_0^2$ ) for $e^+ + H$ scattering is plotted as a function of positron energy (Ryd). Phrases in this picture have same meanings as in figure 4.5. . . . .	55

4.9	Partial S-wave Ps formation cross sections ( $\pi a_0^2$ ) for $e^+ + H$ scattering are plotted as a function of positron energy (Ryd). The phrases in this picture have the same meanings as in figure 4.5. . . . .	58
4.10	Partial P-wave Ps formation cross sections ( $\pi a_0^2$ ) for $e^+ + H$ scattering are plotted as a function of positron energy (Ryd). The phrases in this picture have the same meanings as in figure 4.5. . . . .	59
4.11	Partial D-wave Ps formation cross sections ( $\pi a_0^2$ ) for $e^+ + H$ scattering are plotted as a function of positron energy (Ryd). The phrases in this picture have the same meanings as in figure 4.5. . . . .	61
4.12	Partial F-wave Ps formation cross sections ( $\pi a_0^2$ ) for $e^+ + H$ scattering are plotted as a function of positron energy (Ryd). The phrases in this picture have the same meanings as in figure 4.5. . . . .	62
4.13	Total elastic, Ps formation and total $e^+ - H$ scattering cross sections ( $\pi a_0^2$ ) for $e^+ + H$ scattering are plotted as a function of positron energy. Experimental data are very recently reported by the Detroit group. . . . .	65
4.14	Partial wave Ps elastic cross sections ( $\pi a_0^2$ ) for $Ps + p$ scattering are plotted as a function of Ps energy. . . . .	68
4.15	Partial wave H formation cross sections ( $\pi a_0^2$ ) for $Ps + p$ scattering are plotted as a function of Ps energy. . . . .	69
4.16	Ps elastic, charge transfer and total $Ps + p$ scattering cross sections ( $\pi a_0^2$ ) for $Ps + p$ scattering are plotted as a function of Ps energy. . . . .	70
4.17	The eigenphase sum of positron-hydrogen scattering is plotted as a function of positron energy: the first resonance of the S-wave. . . . .	77
4.18	Elastic and Ps formation cross sections of positron-hydrogen scattering is plotted as a function of positron energy: the first resonance of the S-wave. . . . .	78

4.19 The eigenphase sum of positron-hydrogen scattering is plotted as a function of positron energy: the second resonance of the S-wave. . . . .	79
4.20 Elastic and Ps formation cross sections of positron-hydrogen scattering is plotted as a function of positron energy: the second resonance of the S-wave. . . . .	80
4.21 The eigenphase sum of positron-hydrogen scattering is plotted as a function of positron energy: the first resonance of the P-wave. . . . .	81
4.22 Elastic and Ps formation cross sections of positron-hydrogen scattering is plotted as a function of positron energy: the first resonance of the P-wave. . . . .	82
4.23 The eigenphase sum of positron-hydrogen scattering is plotted as a function of positron energy: the second resonance of the P-wave. . . . .	83
4.24 Elastic and Ps formation cross sections of positron-hydrogen scattering is plotted as a function of positron energy: the second resonance of the P-wave. . . . .	84
4.25 The eigenphase sum of positron-hydrogen scattering around the D-wave resonance is plotted as a function of positron energy. . . . .	85
4.26 Elastic and Ps formation cross sections of positron-hydrogen scattering around the D-wave resonance is plotted as a function of positron energy. . . . .	86

## List of Tables

4.1 The partial S-wave phase shifts (Rad.) for positron-hydrogen scattering as a function of incident momentum. The results B6+ and B7+ are from the bases B6+ and B7+ respectively. . . . .	36
4.2 The partial P-wave phase shifts (Rad.) for positron-hydrogen scattering as a function of incident momentum. The results B6+ and B7+ are from the bases B6+ and B7+ respectively. . . . .	41
4.3 The partial D- and F-wave phase shifts (Rad.) for positron-hydrogen scattering as a function of incident momentum. The results B6+ and B7+ are from the bases B6+ and B7+ respectively. The number in [ ] indicates powers of ten. . . . .	42
4.4 The L=4, 5 and 6 partial wave phase shifts (Rad.) and total elastic cross sections ( $\pi a_0^2$ ) for positron-hydrogen scattering as a function of positron momentum. The number in [ ] indicates powers of ten. . . .	46
4.5 The partial S- and P-wave elastic cross sections (in units of $\pi a_0^2$ ) as a function of incident momentum. . . . .	47
4.6 The partial D- and F-wave and total elastic cross sections (in units of $\pi a_0^2$ ) as a function of incident momentum. . . . .	53
4.7 L=0 and 1 partial wave positronium formation cross sections (in units of $\pi a_0^2$ ) as a function of incident momentum. . . . .	57
4.8 L=2, 3, 4, 5, and 6 partial wave and total positronium formation cross sections (in units of $\pi a_0^2$ ) as a function of incident momentum. The number in [ ] indicates powers of ten. . . . .	60

4.9	The S-wave reactance matrix elements. . . . .	64
4.10	Partial wave and total elastic cross sections ( $\pi a_0^2$ ) for Ps+p scattering. . . . .	67
4.11	Resonances of positron-hydrogen scattering below the first H excitation. . . . .	74
4.12	S, P and D partial wave phase shifts (in units of radiation) for positron-hydrogen scattering in 18- and 20-state approximations. The numbers in [ ] indicate the powers of 10. . . . .	89
4.13	F, G, H, and I partial wave phase shifts (in units of radiation) for positron-hydrogen scattering in 18- and 20-state approximations. The numbers in [ ] indicate the powers of 10. . . . .	91
4.14	S and P wave elastic cross sections ( $\pi a_0^2$ ) of positron-hydrogen scattering in 18- and 20-state approximations. The numbers in [ ] indicate the powers of 10. . . . .	92
4.15	D, F, G, H, and I partial wave elastic cross sections ( $\pi a_0^2$ ) of positron-hydrogen scattering in 18- and 20-state approximations. The numbers in [ ] indicate the powers of 1 . . . . .	95
4.16	S and P wave positronium formation cross sections ( $\pi a_0^2$ ) of positron-hydrogen scattering in 18- and 20-state approximations. The numbers in [ ] indicate the powers of 10. . . . .	96
4.17	D, F, G, H and I partial wave positronium formation cross sections ( $\pi a_0^2$ ) of positron-hydrogen scattering in 18- and 20-state approximations. The numbers in [ ] indicate the powers of 10. . . . .	97
4.18	The partial wave elastic cross sections ( $\pi a_0^2$ ) for Ps + p scattering in 18- and 20-state approximations. The numbers in [ ] indicate the powers of 10. . . . .	98

## Chapter 1

### Introduction

Since its prediction by Dirac (1928) [1, 2] and experimental confirmation by Anderson (1933) [3], the positron and positron physics have been an active subject in physics. Like its anti-particle the electron, a positron is a fermion with a spin quantum number  $\frac{1}{2}$  and possesses the same mass and magnitude of charge as that of an electron but a positive charge. A positron could form a new atom with its counterpart, electron, which was first named positronium by Ruark in 1945 [4], subsequently discovered by Deutsch in 1951 [5] and symbolized Ps by McGervey and DeBenedetti in 1959 [6]. The Ps atom is the lightest isotope of hydrogen. It has the same kind of energy levels and spectra series as the hydrogen atom. However, because the positron and the electron are distinguishable, a Ps atom has two ground states, called para-positronium  $^1S_0$  and ortho-positronium  $^3S_1$ . Moreover, in contrast to the hydrogen atom, the equal masses of the electron and positron make positronium an asymmetric system in charge. This drastic difference results in some special physical and chemical properties of positronium. A Ps atom has a relatively short lifetime,  $1.25 \times 10^{-10}$  seconds for a para-Ps and  $1.4 \times 10^{-7}$  seconds for a ortho-Ps. The annihilation of a positronium atom will produce two gamma photons with energy 0.511MeV for para-Ps and three gamma photons for ortho-Ps. Their lifetimes are also found to be very sensitive to the environment. These properties have been widely applied to probe the properties of matters which form some new branches of science such as positron solid state physics and positronium chemistry.

In the atomic collision field, the positron has been employed as a probe to test approximate theories developed for electron-atom and electron-molecule scatterings. It can be expected that the positron scattering with atoms and molecules is basically different from electron scattering, particularly at low energy. There are two major reasons for this. Firstly, the static interaction for positrons is positive, which tends to cancel the polarization potential; while for electrons, both are negative and tend to enhance the attractive potential. Secondly, the electron scattering is ruled by Pauli's exclusion principle, so we have to take into account the exchange effect between the incident electron and the target electrons; while in the case of the positron scattering, there is no exchange effect at all since the positron is distinguishable from the target electrons. Instead, a new rearrangement scattering, positronium formation, is energetically allowed. However, it is the rearrangement scattering of positron-atom system that brings a major challenge to theoretical studies. Of the positron scatterings, the positron-hydrogen system is the most fundamental one and the best test-ground of theoretical approaches because the exact eigenfunctions are well known for both hydrogen and positronium wavefunctions.

The experimental difficulties for positron-hydrogen scattering come from obtaining a good monoenergetic positron beam with enough intensity, and atomic hydrogen gas with high purity. So far, only two research groups have reported their measurements on positron-hydrogen scattering; experimental uncertainties are relatively large. The positronium formation cross section was reported by the Bielefeld-Brookhaven collaboration (Sperber et al. 1992 [7], Weber et al. 1994 [8]) and the total cross section was reported by the Detroit group (Zhou et al. 1994 [9]). It may need a special mention that great efforts have been made by the Detroit group to improve experimental measurements for this scattering system. They measured cross sections of the total scattering [10] and Ps formation [11]. The technical details

of experimental measurements positron-atom scatterings (not positron-hydrogen) can also be found in a number of review articles by Charlton and Laricchia (1990) [12], Charlton (1989 [13], 1985 [14]), Griffith and Heyland (1978) [15] and references therein.

Since the pioneering work by Massey and Mohr (1954) [16], study of positron-hydrogen scattering has been extensively carried out in recent years by using various theoretical approaches and the results are summarized by Bransden (1969) [17], Ghosh et al. (1982) [18], and Humberston (1991) [19], and references therein. The Kohn variational method proposed by Kohn in 1948 [20] has been widely applied to this scattering system. Spruch and Rosenberg (1960) [21] showed that the Kohn variational method does provide an upper bound for the scattering length at zero incident energy but not for the phase shifts at non-zero energies. For the phase shifts, Schwartz (1961) [22] first designed a definitive calculation for the S-wave positron-hydrogen scattering using the Kohn method with a Hylleraas-type basis. Stein and Sternicht (1972) [23] and Humberston and Wallace (1972) [24] also performed S-wave Kohn variational calculations. Armstead (1968) [25] extended the Kohn variational method to calculate P-wave phase shifts. The most significant applications of this method has been made by Humberston and his co-workers in the early 1980's [26, 27, 28, 29] for the incident energy in the Ore gap (a gap from Ps ground level to the H first excitation threshold). They also carried out the S-, P-, and D-wave partial elastic and Ps formation cross sections. Their results are generally considered as the most accurate [73].

The Kohn variational method has two undesirable features, the non-boundedness of phase shifts at non-zero energies and the singularities at some energies. Great efforts have been made to improve the Kohn variational method and many theoretical methods have been developed. These new approaches may be classified into

two categories: the general variational bound (GVB) of the New York group (Hahn and his co-workers 1962 [30], 1965 [31], 1967 [32]) and the Harris-Nesbet algebraic approach.

For the sake of simplifying the description in the following, we would like to introduce some common terms used in this field. We generally call each physical state of the scattering system a scattering channel or a channel. At a given scattering energy, some channels are open and the others are closed. The former are called open channels and the later closed channels. The whole scattering space could be considered to be spanned by all scattering channels, so we call it the scattering channel space or channel space. The channel space is divided into two parts: one is constituted of open channels, called the open channel space (also called the P-space), and the other called the closed channel space (also called the Q-space). Therefore, we can define two projection operators  $P$  and  $Q$ . The operator  $P$  projects the scattering wavefunction into the P-space and the operator  $Q$  projects it into the Q-space. So we have  $PQ = QP = 0$ ,  $PP = P$  and  $QQ = Q$ .

In order to improve the non-bounded feature, the GVB approach applied the above operators  $P$  and  $Q$  to "project" the scattering Schrödinger equation

$$(H - E)\Psi = 0 \quad (1.1)$$

into the open channel space, i.e. the P-space

$$P(H + V_{opt} - E)P\Psi = 0, \quad (1.2)$$

where the second term is called the optical potential

$$V_{opt} = -PHQ\frac{1}{Q(H - E)Q}QHP. \quad (1.3)$$

The above Eq. (1.1) is exactly equal to Eq. (1.2) but the former is solved in the whole scattering space and the later is solved just in the open channel space. The effect of the closed channel space is brought in the open channel Schrödinger equation

by the optical potential. Actually, the optical potential here represents the coupling between the open channel space and closed channel space. It has been proven that the lower bound of phase shifts can be obtained if the optical potential is negative definite (that means, when the system energy  $E$  is below the first eigenvalue of  $QHQ$ ). This method was applied to calculate the phase shifts of positron-hydrogen scattering [30, 31]. However, due to insufficient basis functions used, their theoretical results, although valuable, are not definite. The further applications for two open channels (elastic plus  $P_s$  formation) were carried out by Dirk and Hahn under the coupled-static (1970) [33] and effective distortion approximations(1971) [34]. For the coupled-static approximation, their results are quite accurate. Gailitis (1965) [35] improved this method numerically and showed how to compute a bound optical potential from an arbitrary bound function  $\Phi$ . Bhatia et al. (1971 [36], 1974 [37]) performed calculations for the S- and P-wave partial phase shifts following the Gailitis' method. These calculated phase shifts are considered to be the most accurate [73].

To avoid the singularities appearing in the Kohn variational method, Harris (1967) [38] proposed a new expansion method by taking the advantage of the singularities in the Kohn method. The details of this method will be given in Section 2.1. Houston and Drachman (1971) [39], using the Harris variational method with the Hylleraas bound function, calculated the S-wave phase shifts. Their results agree well with those from the Kohn variational by Schwartz. However, the Harris method can only give the scattering information at discrete eigenvalues of the Hamiltonian for a single channel scattering. A further improvement for a multichannel situation was made by Harris and Michels (1969) [40] by adopting the minimum norm method. But the minimum norm method does not straightforwardly give the scattering parameters.

Nesbet (1968) [41] (also see [42]) has analysed the Harris variational method and then proposed a new single channel variational method which is suitable for applications at continuous energies. Later, he (1969) [43] extended the single channel approach to multichannel scatterings, which is known as the Harris-Nesbet method. The details of this method will be given in Chapter 2. The key spirit of the Harris-Nesbet method is to express the internal part of the open channel wavefunction in terms of basis functions and to connect it with the external part by imposing a condition that the open channel wavefunction has no components in the space spanned by the basis functions. After determining the open channel wavefunctions, the standard Kohn and inverse Kohn methods have been applied to extract the reaction matrix.

The Harris-Nesbet method has been widely applied to the electron-atom scatterings, particularly to electron-hydrogen system, and the results appear in a review article by Callaway (1978) [44] and references therein. Further investigations of the electron-hydrogen scattering , using the Harris-Nesbet method, were carried out by Callaway (1985 [45], 1988 [46], 1991 [47]) and Callaway et al. (1987 [48], 1993 [49]). For positron-hydrogen scattering, the first successful application of the Harris-Nesbet method was made by Seiler et al. (1971) [50] in the 1s-2s-2p H close coupling approximation. Although the coupling scheme is quite simple, they observed three S-wave and two P-wave resonances below the first H excitation threshold. Wakid and LaBahn (1972) [51] carried out critical calculations using this method in a series of coupling schemes which directly included the positronium formation channels such as  $1sH+1sPs$ ,  $1s-2s-2pH+1sPs$ ,  $1s-2s-2pH+1s-2s-2pPs$ , and  $1s-2\bar{p}H+1s-2\bar{p}Ps$ . Some further calculations were also performed by Wakid (1973, 1975) [52, 53]. In addition to close coupling approximations, Register and Poe (1975) [54] performed the Harris-Nesbet calculation with a Hylleraas basis for the S-, P-, and D-wave partial

phase shifts. Their results are in close agreement with Bhatia et al.'s for the S- and P-waves.

In addition, there are a number of other theoretical approaches, such as the T-matrix approach in momentum space (Mitroy 1993 [55]), the R-matrix method (Higgins et al. 1991 [56]), the Schwinger variational method (Roy and Mandal 1993 [57]), the method of solving the Faddeev equation (1995) [58] and solving the coupled-equation in the configuration space with a short ranged correlation function basis (Chan and Fraser 1973 [59], Chan and McEachran 1976 [60]). Among these methods, the T-matrix and R-matrix approaches deserve a special mention. The T-matrix approach solves the Lippmann-Schwinger integral equation in momentum space and is employed mainly by the Calcutta group (Basu et al. 1976 [61], 1989 [62], Sarkar et al. 1993 [63, 64], 1994 [65]), Hewitt et al. (1990 [66], 1991 [67]), and the Mitroy group [55, 68, 69, 70, 71]. The key step of this method is how to handle the area around the momentum poles at the system thresholds. Mathematically, one can avoid these poles by splitting the integration into two parts: a  $\delta$ -function part and a principal-value part. The first part can be easily integrated out and the second part can only be done numerically. So how to accurately calculate the principal-value part determine whether the result obtained is reliable.

Of these three research groups, the scattering parameters obtained by the Mitroy's group are the more reliable. This method was also used to carry out large scale calculations of positron-hydrogen scattering recently at energy below the ionization threshold such as the 20-state (1994 [72]) and the 21-state (1995 [73, 74]) and the results converged to the accurate variational sets.

On the other hand, the R-matrix method is to divide the scattering space into two parts: internal and external parts. The Schrödinger equation is solved in each part of the scattering space and then two parts of the wavefunction are connected

at the boundary. Finally, the scattering information is extracted from the above connection. For positron-hydrogen scattering, the external part of the wavefunction is obtained by ignoring the coupling between hydrogen and positronium channels. The first application of the R-matrix approach for positron-hydrogen scattering was made by Higgins et al. for a six pseudo-state calculation (1990 [75], 1991 [56]). McAlinden et al. (1994) [76] and Kernoghan et al (1994 [77, 78], 1995 [79]) then performed 18-state close coupling calculations in the frame of the R-matrix approach. Their results showed reasonable agreement with those from the 21-state T-matrix calculation by Mitroy. Nevertheless, due to the omission of the couplings in the outer part of the scattering space between the hydrogen and positronium formation channels, the R-matrix in the 18-state approximation exhibited some numerical instabilities, especially at energies close to the threshold.

For a number of years, Gien has used the Harris-Nesbet algebraic method for coupled-state calculations of positron-hydrogen scattering at low energies [80, 81, 82, 83]. The method proved to work remarkably well at low energies. It could provide reliable numerical accuracy at low energies. By its high numerical accuracy, the method was also successfully used for the study of other interesting problems of positron-hydrogen scattering, such as resonances at intermediate energies [84, 85, 86] and Feshbach resonances [83, 87, 88, 89]. The feasibility of the Harris-Nesbet method for any large-scheme coupled-state calculation was established [83, 82]. The purpose of this work is, therefore, to carry out the calculation of "accurate" phase shift and cross section of  $e^+ - H$  scattering at low energy with the Harris-Nesbet method, using some large coupling schemes. The results are to be compared with the ones that have been obtained with other research groups who employed, however, different numerical methods.

We use some typical large coupling schemes, composed of either pseudo-states

and/or correlation functions, that other research groups had also considered for their coupled-state (close-coupling) calculations. In one calculation, we followed Chan et al. [59, 60] to add to the six-state  $[(1s, 2s, 2p)H - (1s, 2s, 2p)Ps]$  coupling scheme a sufficiently high number of short-range correlation functions and the  $3\bar{p}H$  pseudo-state [90]. We chose the six-state scheme for construction of the large couplings scheme, as initially we intend to extend our calculation to scattering energies above the Ore gap. With this coupling scheme, the cross section could have been obtained for H excitation and Ps formation in excited states. The  $3\bar{p}H$  pseudo-state was then added, simply to correct the well-known deficiency of the polarization effect of the six-state scheme. Indeed, together with the 2p H state, these two state can by themselves account for 100% of the dipole polarizability of H(1s) [90]. In this connection, it should be stressed that the long-range polarization effect has been known to predominate at low energy in high-partial wave scattering.

On the other hand, we use the 18- and 20-state coupling schemes that are composed of pseudo-states (instead of correlation functions). These schemes had been considered by Kernoghan et al. [76, 77, 78] and Mitroy et al. [71, 73, 74] for their coupled-state calculation of  $e^+H$  scattering. Indeed, the 20-state scheme is essentially the 21-state one of Mitroy with the  $4\bar{f}$  pseudo-pstate excluded. For some obvious reasons, the  $4\bar{f}$  pseudo-state was excluded from the scheme in the Harris-Nesbet calculation. We repeated these coupled-state calculations with the Harris-Nesbet method in order to reassert its numerical reliability. These results will also be used to check the accuracy that the large scheme we calculated with the correlation function mentioned above can provide for these cross sections at low energies.

This thesis is organized as follows: In Chapter 2, we will analyze the Harris-Nesbet method. More specifically, we will discuss the Harris expansion method and

Nesbet's extension of the Harris method. In the last section of chapter 2, we will propose a modified version of the Harris-Nesbet approach. Chapter 3 will give the details of applications of the Harris-Nesbet method for positron-hydrogen scattering. Chapter 4 presents the results of the calculation. By directly summing the partial wave cross sections, we plan to obtain the total elastic, total Ps formation, total  $e^+$ -H scattering, and Ps-p elastic cross sections and the theoretical results are compared with experimental data. In addition, we tentatively repeat the search for some low-lying resonances below the first hydrogen excitation threshold, although they have been determined by various authors. In Chapter 5, we will draw conclusion from these results.

The reduced formulas of the bound-bound, bound-free and free-free matrix elements that we rederived are given in Appendix B. A list of papers, reporting the results of the work done for this thesis, that have been published and/or presented at conferences and meetings will be shown in Appendix C. Listing of the FORTRAN programs that were used for this calculation is shown in Appendix D.

## Chapter 2

### Harris-Nesbet Algebraic Approximation

A quantum scattering system refers to a system containing at least two separate particles. One of the particles is a projectile, denoted by A, and the other a target, denoted by B. Both A and B can be either structureless or composite particles. If one or both of the particles are composite, the scattering is complicated. For a direct scattering process, the projectile may lose some energies to the target and pumps the target electron to some excitation state if it has enough energy. On the other hand, if the projectile is positive such as the positron, a rearrangement scattering process is possible if the positive projectile has enough energy to pick up an electron from the target. In quantum scattering theory, the partial wave analysis is often applied to study a scattering system. For multichannel scattering, the partial wave cross section for a transition from channel q to channel p is given by

$$Q_{pq} = \frac{4\pi}{k_p^2} | T_{pq} |^2, \quad (2.1)$$

where  $k_p$  is the momentum of an outgoing particle in channel p and T is a transition matrix. The element  $T_{pq}$  is a partial wave transition amplitude for a transition from channel q to channel p. The transition matrix T is related to the reactance matrix R through the following relation

$$T = \frac{R}{1 - iR}. \quad (2.2)$$

In some literature, the reactance matrix R is also called the K-matrix. The reactance matrix is a real and symmetric matrix; its trace equals the sum of tangent eigenphase

shifts for all possible scattering channels. The real and symmetric properties of the reactance matrix are very useful in performing numerical computations and checking the numerical accuracy. Its trace can be used to identify resonant structures of the scattering system. Moreover, one can automatically obtain scattering cross sections for different entrance channels at a given system energy E. In this thesis, we choose the Harris-Nesbet algebraic method to calculate the reactance matrix. Therefore, in the following sections we analyze the Harris-Nesbet method.

## 2.1 Harris' Expansion Method

In 1967, Harris [38, 91] proposed an expansion method for electron-atom scattering, which is considered as a pioneer work of the Harris-Nesbet approach. For a single channel scattering system with a Hamiltonian  $H$  at energy  $E$ , the Schrödinger equation is

$$(H - E)\Psi = 0, \quad (2.3)$$

where  $\Psi$  is a total scattering wavefunction. Following Harris [38], we can write

$$\Psi = \phi + \alpha_0 S + \alpha_1 C, \quad (2.4)$$

where  $S$  and  $C$  are asymptotic (also called free) wavefunctions of the system at large distance and a given system energy  $E$ .  $S$  corresponds to the spherical Bessel function and  $C$  corresponds to the spherical Neumann function. Both of them are quadratically integrable. However, the last two terms in the above are just asymptotic solution of the Schrödinger equation at large distance, so they do not represent any interaction within the scattering system. So we have

to introduce a short range function  $\phi$  to take care that. The major work in the Harris method is to find a short range wavefunction  $\phi_k$  with an eigenvalue  $\lambda_k = E$ .

For doing that, we choose a set of basis functions  $\xi_i$ ,  $i=1, \dots, n$ . In the space spanned by  $\xi_i$ , the above Schrödinger equation can be

written into its equivalent matrix form

$$(A - \lambda B)X = 0. \quad (2.5)$$

with

$$A_{ij} = \langle \xi_i | H | \xi_j \rangle, \quad (2.6)$$

$$B_{ij} = \langle \xi_i | \xi_j \rangle, \quad (2.7)$$

where A and B are the Hamiltonian and overlap matrices, respectively. If the selected basis functions are just the eigenfunctions of the Hamiltonian, the overlapping matrix B becomes the unit matrix. Where X is the system eigenfunction which also is an array in the space spanned by  $\xi_i$ . Solving Eq. (2.5), we obtain a set of eigenfunctions  $\phi_k = X_k$ , and a set of the corresponding eigenvalues  $\lambda_k$ ,  $k=1, \dots, n$ . Now Eq. (2.3) can, by imposing a condition that the total wavefunction has no components in the subspace spanned by the  $\phi_k$ , be reduced to the following form

$$\alpha_0 \langle \phi_k | H - \lambda_k | S \rangle + \alpha_1 \langle \phi_k | H - \lambda_k | C \rangle = 0, \quad (2.8)$$

at energy  $E = \lambda_k$ . Hence, we can obtain a ratio of  $\frac{\alpha_1}{\alpha_0}$  from the above equation which forms a  $1 \times 1$  reactance matrix R and equals the tangent of the scattering phase shift for single channel scattering.

Harris [38] summarized this method into four steps: (1) Choose a set of basis functions  $\xi_i$  and diagonalize Hamiltonian; (2) pick an eigenvalue  $\lambda_k$  appropriate to a scattering solution; (3) define the asymptotic wavefunctions S and C at this energy; and (4) solve for  $\frac{\alpha_1}{\alpha_0}$ . This method was first used by Michels and Harris (1967) [91] for single channel low-energy electron-hydrogen scattering.

A major characteristic of the Harris method is that it works for the eigenvalues of the system Hamiltonian. This nature makes the Harris approximation a very simple algebraic method. But the price paid is that it can only give the scattering information at separate system energies which are eigenvalues of the system under a set of selected basis functions. Of course, one can adjust parameters in the basis functions to produce different eigenvalues, but computing time is the price for doing that. Another feature of the Harris method is that it avoids the singularity of the Kohn variational method. However, there are some difficulties in direct extension of this method to multichannel scatterings. In order to overcome the above difficulties, Harris and Michels (1969,1971)[40, 92] proposed a method called minimum norm method which can be used for general energies and multichannel scatterings. This extension can not straightforwardly be applied to a general scattering case. Nesbet's development, usually referred to the Harris-Nesbet algebraic method, makes this method more suitable for general atomic scatterings.

## 2.2 Harris-Nesbet Algebraic Approach

### 2.2.1 Single Channel

Nesbet (1968)[41] first proposed an improvement of the Harris method by applying the Kohn variational method for a single channel scattering. Following Schwartz (1961)[22] who divided the short range function  $\phi$  into two parts: one is associated with S,  $\phi_S$  and the other with C,  $\phi_C$ , the total scattering wavefunction is separated into

$$\Psi = \alpha_0(\phi_S + S) + \alpha_1(\phi_C + C). \quad (2.9)$$

In order to find the short range functions  $\phi_S$  and  $\phi_C$ , suppose that we have a set of  $\phi_k$  eigenfunctions obtained by using the same steps as in the last section, we then

expand these two short range functions in terms of  $\phi_k$

$$\phi_S = \sum_k D_k \phi_k, \quad (2.10)$$

$$\phi_C = \sum_k G_k \phi_k, \quad (2.11)$$

Again the condition that  $\Psi$  has no components in the space spanned by  $\phi_k$  is imposed, i.e.

$$\langle \phi_k | H - E | \phi_S + S \rangle = 0, \quad (2.12)$$

$$\langle \phi_k | H - E | \phi_C + C \rangle = 0, \quad (2.13)$$

and we obtain the expansion coefficients

$$D_k = (E - E_k)^{-1} \langle \phi_k | H - E | S \rangle, \quad (2.14)$$

$$G_k = (E - E_k)^{-1} \langle \phi_k | H - E | C \rangle, \quad (2.15)$$

Up to now, two short range parts of the scattering wavefunction have been determined. Hence, we can define the variational functional as follows

$$\begin{aligned} I(\alpha_0, \alpha_1) &= \langle \Psi | H - E | \Psi \rangle \\ &= m_{00}\alpha_0^2 + (m_{01} + m_{10})\alpha_0\alpha_1 + m_{11}\alpha_1^2, \end{aligned} \quad (2.16)$$

where

$$m_{00} = \langle S | H - E | \phi_S + S \rangle, \quad (2.17)$$

$$m_{01} = \langle S | H - E | \phi_C + C \rangle, \quad (2.18)$$

$$m_{10} = \langle C | H - E | \phi_S + S \rangle, \quad (2.19)$$

$$m_{11} = \langle C | H - E | \phi_C + C \rangle, \quad (2.20)$$

Choosing proper normalizations of the asymptotic (free) functions,

$$S(r) \sim_{r \rightarrow \infty} k^{-1/2} \sin(kr - \frac{1}{2}l\pi), \quad (2.21)$$

$$C(r) \sim_{r \rightarrow \infty} k^{-1/2} \cos(kr - \frac{1}{2}l\pi), \quad (2.22)$$

we can prove that  $m_{01}$  and  $m_{10}$  matrices have the following relation

$$m_{01} = m_{10}^\dagger + \frac{1}{2}. \quad (2.23)$$

The variation of the functional is

$$dI(\alpha_0, \alpha_1) = (2m_{00}\alpha_0 + 2m_{01}\alpha_1 - \frac{1}{2}\alpha_1)d\alpha_0 + (2m_{11}\alpha_1 + 2m_{10}\alpha_0 + \frac{1}{2}\alpha_0)d\alpha_1 \quad (2.24)$$

For the Kohn method, the parameter  $\alpha_0=1$  and  $d\alpha_0=0$ , therefore, we can construct a quantity,  $I(\alpha_1)-\frac{1}{2}\alpha_1$ , which is stable at  $\alpha_1^0 = -m_{10}m_{11}^{-1}$  and obtain

$$\Delta(I - \frac{1}{2}\alpha_1) = 0. \quad (2.25)$$

Hence, a linear extrapolation

$$I(\alpha_1) - I(\alpha_1^0) = \frac{1}{2}(\alpha_1 - \alpha_1^0), \quad (2.26)$$

can be used to obtain the best value of  $\alpha_1 = R_K$

$$\begin{aligned} R_K &= \alpha_1^0 + 2(I(\alpha_1) - I(\alpha_1^0)), \\ &= -2(m_{00} - m_{10}m_{11}^{-1}m_{10}), \end{aligned} \quad (2.27)$$

where  $I(\alpha_1)$  has been chosen to be zero because the final  $\alpha_1$  is supposed to be exact. Similarly, if we apply the inverse Kohn method, i.e.  $\alpha_1=1$  and  $d\alpha_1=0$ , we can obtain the inverse reactance matrix

$$R_K^{-1} = 2(m_{11} - m_{01}m_{00}^{-1}m_{01}). \quad (2.28)$$

It is clear that the Nesbet's extension of the Harris method is suitable for any system energy. He also showed that the extension can recover the form of the Harris method if the system energy  $E$  tends to an eigenvalue  $E_k$  of the Hamiltonian. In addition, the above Kohn and inverse Kohn expressions are the linear parts of the Hulthen ones [41].

### 2.2.2 Multichannel

Soon after proposing the above extension of the Harris method, Nesbet (1969) [43] made a further great development of the Harris method suitable for multichannel scatterings. In this section, we will present the details of this method. For the sake of simplicity, we give its matrix derivation.

For a given system energy  $E$ , if the system has  $N$  open channels, we then have  $N$  degenerate system wavefunctions  $\Psi^\nu$ ,  $\nu = 1, 2, \dots, N$ , each corresponding to an possible entrance channel.  $\Psi^\mu$ , for an entrance channel  $\mu$ , can be written in terms of open channel wavefunctions  $\psi_{p\mu}$  which is related to a scattering from the entrance channel  $\mu$  to an outgoing (open) channel  $p$

$$\Psi^\mu = \sum_p \psi_{p\mu}, \quad (2.29)$$

where the channel wavefunctions  $\psi_{p\mu}$ , like what we did in the last section, is separated into two terms

$$\psi_{p\mu} = \alpha_{0p\mu}\psi_{0p} + \alpha_{1p\mu}\psi_{1p} = \sum_{i=0}^1 \alpha_{ip\mu}\psi_{ip}, \quad (2.30)$$

with

$$\psi_{0p} = \phi_S^p + S_p, \quad (2.31)$$

$$\psi_{1p} = \phi_C^p + C_p, \quad (2.32)$$

where  $\phi_S^p$  and  $\phi_C^p$  are short range functions of the channel wavefunction  $\psi_{ip}$ . Here the only difference from the single channel scattering is that we add a superscript  $p$  to indicate the outgoing channel because we may have several outgoing channels.  $S_p$  and  $C_p$  are the free functions in an outgoing channel  $p$ . Suppose that we already have a set of bound eigenfunctions  $\phi_k$  and eigenvalues  $E_k$  by diagonalizing the Hamiltonian matrix under a set of basis functions. Then the short range functions

$\phi_S^p$  and  $\phi_C^p$  are expanded in terms of the eigenfunctions  $\phi_k$

$$\phi_S^p = \sum_k b_k^p \phi_k, \quad (2.33)$$

$$\phi_C^p = \sum_k c_k^p \phi_k, \quad (2.34)$$

by imposing that  $\psi_{ip}$  has no components in the subspace spanned by  $\phi_k$ ,

$$\langle \phi_k | H - E | \psi_{ip} \rangle = 0, \quad (2.35)$$

we determine the expansion coefficients  $b_k^p$  and  $c_k^p$

$$b_k^p = (E - E_k)^{-1} \langle \phi_k | H - E | S_p \rangle = (E - E_k)^{-1} M_S^{pk}, \quad (2.36)$$

$$c_k^p = (E - E_k)^{-1} \langle \phi_k | H - E | C_p \rangle = (E - E_k)^{-1} M_C^{pk}, \quad (2.37)$$

where  $M_S^{pk}$  and  $M_C^{pk}$  are called the bound-free matrix elements. Now the channel wavefunctions  $\psi_{ip}$ ,  $i=0, 1$ , are completely determined. The total wavefunctions for an entrance channel  $\mu$  can then be simply expressed as

$$\Psi^\mu = \sum_p \sum_{i=0}^1 \alpha_{ip\mu} \psi_{ip}. \quad (2.38)$$

The variational functional  $\Phi^{\mu\nu}$  which is related to two degenerate wavefunctions  $\Psi^\mu$  and  $\Psi^\nu$  for entrance channels  $\mu$  and  $\nu$  at a system energy  $E$  is defined as

$$\begin{aligned} \Phi^{\mu\nu} &= \langle \Psi^\mu | H - E | \Psi^\nu \rangle \\ &= \sum_{i,j=0}^1 \sum_{pq} \alpha_{ip\mu}^* m_{ij}^{pq} \alpha_{jq\nu}, \end{aligned} \quad (2.39)$$

where the m-matrix elements  $m_{ij}^{pq}$  are

$$m_{ij}^{pq} = \langle \psi_{ip} | H - E | \psi_{jq} \rangle, \quad (2.40)$$

and their specific forms are as follows

$$m_{00}^{pq} = M_{SS}^{pq} + \sum_k M_S^{pk} (E - E_k)^{-1} M_S^{qk}, \quad (2.41)$$

$$m_{01}^{pq} = M_{SC}^{pq} + \sum_k M_S^{pk}(E - E_k)^{-1} M_C^{qk}, \quad (2.42)$$

$$m_{10}^{pq} = M_{CS}^{pq} + \sum_k M_C^{pk}(E - E_k)^{-1} M_S^{qk}, \quad (2.43)$$

$$m_{11}^{pq} = M_{CC}^{pq} + \sum_k M_C^{pk}(E - E_k)^{-1} M_C^{qk}, \quad (2.44)$$

where the free-free matrix elements are defined as

$$M_{SS}^{pq} = \langle S_p | H - E | S_q \rangle, \quad (2.45)$$

$$M_{SC}^{pq} = \langle S_p | H - E | C_q \rangle, \quad (2.46)$$

$$M_{CS}^{pq} = \langle C_p | H - E | S_q \rangle, \quad (2.47)$$

$$M_{CC}^{pq} = \langle C_p | H - E | C_q \rangle. \quad (2.48)$$

Then we make the following arrangements of the above matrices  $\alpha$  and  $m$

$$\alpha = \begin{pmatrix} \alpha_0 \\ \alpha_1 \end{pmatrix}, \quad (2.49)$$

$$m = \begin{pmatrix} m_{00} & m_{01} \\ m_{10} & m_{11} \end{pmatrix}, \quad (2.50)$$

where  $\alpha_i$  and  $m_{ij}$  are  $N \times N$  matrices for an  $N$  open channel scattering

$$\alpha_i = \begin{pmatrix} \alpha_i^{11} & \dots & \alpha_i^{1N} \\ \dots & \dots & \dots \\ \alpha_i^{N1} & \dots & \alpha_i^{NN} \end{pmatrix}, \quad (2.51)$$

and

$$m_{ij} = \begin{pmatrix} m_{ij}^{11} & \dots & m_{ij}^{1N} \\ \dots & \dots & \dots \\ m_{ij}^{N1} & \dots & m_{ij}^{NN} \end{pmatrix}, \quad (2.52)$$

with  $i, j = 0, 1$ . The above matrix elements are all real, and  $m_{00}$  and  $m_{11}$  are symmetric, but

$$m_{01} - m_{10}^\dagger = \frac{1}{2} I, \quad (2.53)$$

where  $I$  is an unit matrix. Using the above matrix notation, the variational functional  $\Phi^{\mu\nu}$ ,  $\mu, \nu=1, \dots, N$ , is an  $N \times N$  matrix of the form

$$\begin{aligned}\Phi &= \alpha^\dagger m \alpha \\ &= \alpha_0^\dagger (m_{00}\alpha_0 + m_{01}\alpha_1) + \alpha_1^\dagger (m_{10}\alpha_0 + m_{11}\alpha_1).\end{aligned}\quad (2.54)$$

Then a variation of the matrix functional  $\Phi$  due to a variation of  $\alpha$  is

$$\begin{aligned}\delta\Phi &= \delta\alpha^\dagger m \alpha + (m \alpha)^\dagger \delta\alpha + \alpha^\dagger (m - m^\dagger) \delta\alpha \\ &= \delta\alpha^\dagger m \alpha + (m \alpha)^\dagger \delta\alpha + \frac{1}{2}(\alpha_0^\dagger \delta\alpha_1 - \alpha_1^\dagger \delta\alpha_0).\end{aligned}\quad (2.55)$$

For the Kohn multichannel variational method, the matrices  $\alpha_0 = I$  and  $\alpha_1 = R$  which is the reactance matrix. So we have

$$\delta\alpha_0 = 0, \quad \delta\alpha_1 = \delta R, \quad (2.56)$$

the variation of the matrix variational functional  $\Phi$  is given by

$$\delta\Phi = \delta R^\dagger (m_{10} + m_{11}R) + (m_{10} + m_{11}R)^\dagger \delta R + \frac{1}{2}\delta R. \quad (2.57)$$

The trial reactance matrix  $R_{(0)}$  is chosen to make the matrix quantity  $\Phi - \frac{1}{2}R$  stable which is directly determined by

$$m_{10} + m_{11}R_{(0)} = 0, \quad R_{(0)} = -m_{11}^{-1}m_{10}. \quad (2.58)$$

Using the same procedure as in the single channel case, the  $N \times N$  reactance matrix  $R$  is obtained

$$\begin{aligned}R &= R_{(0)} + 2[\Phi(R) - \Phi(R_{(0)})] \\ &= -2(m_{00} - m_{10}^\dagger m_{11}^{-1}m_{10}),\end{aligned}\quad (2.59)$$

which has a form similar to Eq. (2.27) but now it is a general multichannel reactance matrix. Similarly, for the inverse Kohn method, we can obtain the same form of the

inverse reactance matrix as Eq. (2.28) in the multichannel case

$$R^{-1} = 2(m_{11} - m_{01}^\dagger m_{00}^{-1} m_{01}). \quad (2.60)$$

The Harris-Nesbet method is anomaly free (AF). In some cases, usually near zeroes of  $m_{00}$  or  $m_{11}$ , the Kohn and inverse Kohn reactance matrices disagree with each other. In order to avoid these situations, Nesbet and Oberoi (1972 [93], 1978 [94]) proposed several variants called optimized minimum norm (OMN), optimized anomaly free (OAF), interpolated anomaly free (IAF), and restricted interpolated anomaly free (RIAF). The detail of these variants are in Appendix A. In the following section, we propose a slightly different variant of the Harris-Nesbet method.

### 2.3 Optimized Harris-Nesbet Method in Transformed Space

The variants of the Harris-Nesbet approach, OMN, OAF, IAF, and RIAF, proposed by Nesbet and Oberoi (1972 [93], 1978 [94]) (also see Appendix A) still have some difficulties for a numerical calculation in certain situations. The OMN needs a condition  $\det(m'_{00}) < \det(m'_{11})$  and sometimes the transformed matrix  $m'_{11}$  still has zero points. The OAF and OAF2 need to reorder the eigenvalues of  $m$ . The IAF and RIAF seem better than others because they keep all of properties of the matrix  $m$ , but one must find a set of phase angles  $\phi_p$  to maximize  $|\det(m'_{11})|$ . Generally speaking, the disagreement between the Kohn and inverse Kohn results is from several aspects such as zeros of  $\det(m_{00})$  and  $\det(m_{11})$ , the system energy at the eigenvalues, as well as unproper free parameters in the factors before the free Neumann functions. Meanwhile, the AF criterion, i.e. using the Kohn method when  $\frac{\det(m_{00})}{\det(m_{11})} \ll 1$  and using the inverse Kohn when  $\frac{\det(m_{00})}{\det(m_{11})} \gg 1$ , may lose their validity in certain cases as we met in our numerical calculations, which is the main motivation to modify it. On the other hand, two independent versions, Kohn and

inverse Kohn, give us more options to easily check the reliability of our numerical computations. Therefore, we propose a more general and flexible modified version of the Harris-Nesbet variational method which meets all of the above requirements and can be easily applied to large scale calculations.

From the above discussion, the matrix form of the variational functional  $\Phi$  is

$$\Phi = \alpha^\dagger m \alpha. \quad (2.61)$$

We introduce an orthonormal unitary transformation matrix  $u$

$$u = \begin{pmatrix} \cos \theta & -\sin \theta \\ \sin \theta & \cos \theta \end{pmatrix}, \quad (2.62)$$

where  $\cos \theta$  and  $\sin \theta$  are symmetric block phase matrices which automatically satisfy the orthogonal and unitary conditions. Then the matrix functional becomes

$$\begin{aligned} \Phi &= \alpha^\dagger u u^\dagger m u u^\dagger \alpha \\ &= \alpha'^\dagger m' \alpha', \end{aligned} \quad (2.63)$$

where transformed m-matrix  $m'$  can be clearly written as follows

$$m'_{00} = m_{00} \cos^2 \theta + \frac{1}{2}(m_{10} + m_{01}) \sin 2\theta + m_{11} \sin^2 \theta, \quad (2.64)$$

$$m'_{01} = m_{01} \cos^2 \theta - \frac{1}{2}(m_{00} - m_{11}) \sin 2\theta - m_{10} \sin^2 \theta, \quad (2.65)$$

$$m'_{10} = m_{10} \cos^2 \theta - \frac{1}{2}(m_{00} - m_{11}) \sin 2\theta - m_{01} \sin^2 \theta, \quad (2.66)$$

$$m'_{11} = m_{11} \cos^2 \theta - \frac{1}{2}(m_{10} + m_{01}) \sin 2\theta + m_{00} \sin^2 \theta. \quad (2.67)$$

So the functional has the same form as in the original space. If we apply the Kohn and inverse Kohn methods in a given transformed space with phase angle matrix  $\theta$ , we will obtain stationary matrices  $[R_t]$  and  $[R_t^{-1}]$  formally similar to those in the original space

$$[R_t] = -2(m'_{00} - m'_{10} (m'_{11})^{-1} m'_{10}), \quad (2.68)$$

$$[R_t^{-1}] = 2(m'_{11} - m'_{01} (m'_{00})^{-1} m'_{01}). \quad (2.69)$$

It is clear from Eqs.(2.64)-(2.67) that one can easily avoid the anomalous feature of  $[R_t]$  and  $[R_t^{-1}]$  by properly selecting the transformed space in which both  $\det(m'_{00})$  and  $\det(m'_{11})$  are not close to zero. There exists a critical space in which the best agreement between the Kohn and inverse Kohn results can be obtained. Afterward we need a backward transformation to the original space by using  $\alpha = u\alpha'$ , more specifically,

$$\begin{aligned}\alpha &= \begin{pmatrix} \cos \theta & -\sin \theta \\ \sin \theta & \cos \theta \end{pmatrix} \begin{pmatrix} \alpha'_0 \\ \alpha'_1 \end{pmatrix} \\ &= \begin{pmatrix} \alpha'_0 \cos \theta - \alpha'_1 \sin \theta \\ \alpha'_0 \sin \theta + \alpha'_1 \cos \theta \end{pmatrix},\end{aligned}\quad (2.70)$$

Therefore, the  $\alpha_0$  and  $\alpha_1$  matrices in the original space are

$$\alpha_0 = \alpha'_0 \cos \theta - \alpha'_1 \sin \theta, \quad (2.71)$$

$$\alpha_1 = \alpha'_0 \sin \theta + \alpha'_1 \cos \theta. \quad (2.72)$$

The reactance matrix  $R$  is defined as

$$R = \frac{\alpha_1}{\alpha_0} = \frac{\alpha'_0 \sin \theta + \alpha'_1 \cos \theta}{\alpha'_0 \cos \theta - \alpha'_1 \sin \theta}. \quad (2.73)$$

So we can define two reactance matrices  $R_K$  and  $R_I$  which come respectively from the Kohn's and inverse Kohn's methods in the transformed space. For  $R_K$ , we have  $\alpha'_0 = I$  and  $\alpha'_1 = [R_t]$ , the reactance matrix is

$$R_K = \frac{\sin \theta + \cos \theta [R_t]}{\cos \theta - \sin \theta [R_t]}, \quad (2.74)$$

For  $R_I$ , we need to set  $\alpha'_1 = I$  and  $\alpha'_0 = [R_t^{-1}]$ , the reactance matrix  $R_I$  is

$$R_I = \frac{\sin \theta [R_t^{-1}] + \cos \theta}{\cos \theta [R_t^{-1}] - \sin \theta}. \quad (2.75)$$

There may exist several ways to choose the block phase matrices  $\cos \theta$  and  $\sin \theta$ . Of various possibilities, the simplest choice is that  $\sin \theta = \sin \theta_0 I$  and  $\cos \theta = \cos \theta_0 I$

where  $\theta_0$  is a common phase angle and  $I$  is a unit matrix. Under this choice, the Kohn and inverse Kohn reaction matrices are just special cases of Eqs. (2.74)-(2.75) at phase angle  $\phi_0 = 0$ .

The key difference between this modified version and the original Harris-Nesbet version is that the new version applies the Kohn and inversion Kohn variational principles in the critical transformed space but the original one does so in the untransformed (original) space. It can be noted that the system wavefunction in the untransformed space may not represent an actual scattering problem well, which causes disagreement between the Kohn and inverse Kohn results. Once this happens, one can adjust parameters both in the bound basis and in the factors which are exploited to avoid the undesirable feature of the Neuman function near the scattering center. The price paid is computing time. The unitary transformation applied here equals to searching a best scattering space to describe the scattering system without unnecessary repetitions of bound-bound, bound-free and free-free matrix elements. This point gives one more benefits for a large scale calculation. For accurate numerical computations, this version is automatically anomaly-free.

The implementation of this modified version of the Harris-Nesbet method is straightforward. After obtaining m-matrices, we transform them from the original space into a transformed space with a given phase angle  $\theta$ , then calculate  $[R_t]$  and  $[R_t^{-1}]$ , and finally calculate the reaction matrices  $R_K$  and  $R_I$  from Eqs. [2.74] and [2.75] respectively. By setting a loop, we repeat the above step automatically and select the best reaction matrix with minimum difference between the reaction matrices  $R_K$  and  $R_I$ .

## Chapter 3

### Application for Positron-Hydrogen Scattering

The Harris-Nesbet approach for positron-hydrogen scattering has been described elsewhere (Wakid and Labahm 1972 [51] and Gien 1995 [82]). In this Chapter, we will, for completeness, present it in some detail. The detailed reductions of the bound-bound, bound-free, and free-free matrix elements are given in Appendix B.

#### 3.1 Hamiltonian and Channel wavefunctions

For positron-hydrogen scattering, the system has two different kinds of outgoing channels: the hydrogen and positronium ones. Correspondingly, we have two equivalent forms of the Hamiltonian

$$H = -\frac{1}{2} \nabla_{r_1}^2 - \frac{1}{2} \nabla_{r_2}^2 - \frac{1}{r_1} + \frac{1}{r_2} - \frac{1}{|\mathbf{r}_1 - \mathbf{r}_2|}, \quad (3.1)$$

for the hydrogen channel space and

$$H = -\frac{1}{4} \nabla_R^2 - \nabla_\rho^2 + \frac{1}{|\mathbf{R} - \frac{1}{2}\rho|} - \frac{1}{|\mathbf{R} + \frac{1}{2}\rho|} - \frac{1}{\rho}, \quad (3.2)$$

for the positronium channel space.  $\mathbf{r}_1$  and  $\mathbf{r}_2$  are position vectors of the target electron and the positron to the target proton respectively.  $\rho = \mathbf{r}_1 - \mathbf{r}_2$  and  $\mathbf{R} = \frac{1}{2}(\mathbf{r}_1 + \mathbf{r}_2)$  are the internal position vector of the positronium and the position vector relative to the center-of-mass of the positronium to the proton, respectively. At a given system energy  $E$ , two kinds of possible open channel wavefunctions (see Eqs. (2.31, 2.32)) are

$$\psi_{0p}(\mathbf{r}_1, \mathbf{r}_2) = \phi_S^p + U_p(r_1) S_p^{l_2}(r_2) Y_{Ll_1l_2}^0(\hat{\mathbf{r}}_1 \cdot \hat{\mathbf{r}}_2), \quad (3.3)$$

$$\psi_{1p}(\mathbf{r}_1, \mathbf{r}_2) = \phi_C^p + U_p(r_1) C_p^{l_2}(r_2) Y_{Ll_1l_2}^0(\hat{\mathbf{r}}_1 \cdot \hat{\mathbf{r}}_2), \quad (3.4)$$

for the hydrogen channels and

$$\psi_{0q}(\rho, \mathbf{R}) = \phi_S^q + \phi_q(\rho) S_q^{l_4}(R) Y_{Ll_3l_4}^0(\hat{\rho} \cdot \hat{\mathbf{R}}), \quad (3.5)$$

$$\psi_{1q}(\rho, \mathbf{R}) = \phi_C^q + \phi_q(\rho) C_q^{l_4}(R) Y_{Ll_3l_4}^0(\hat{\rho} \cdot \hat{\mathbf{R}}), \quad (3.6)$$

for positronium channels. Where channel numbers p and q for hydrogen and positronium atoms denote sets of quantum numbers p={n<sub>p</sub>, l<sub>1</sub>} and q={n<sub>q</sub>, l<sub>3</sub>}, respectively. l<sub>2</sub> and l<sub>4</sub> are angular momentum quantum numbers of the positron and the center-of-mass of the positronium, respectively. Y<sub>Ll<sub>1</sub>l<sub>2</sub></sub><sup>0</sup>( ) and Y<sub>Ll<sub>3</sub>l<sub>4</sub></sub><sup>0</sup>( ) are the coupled spherical harmonic functions. L is the total angular momentum quantum number which is obtained by using the LS-coupling scheme from l<sub>1</sub> and l<sub>2</sub> or l<sub>3</sub> and l<sub>4</sub> (see Appendix B). It is not necessary for us to consider spins of the system particles since they are all distinguishable. The free functions are chosen to have the following forms

$$S_p^{l_2}(r_2) = k_p^{1/2} r_2 j_{l_2}(k_p r_2), \quad (3.7)$$

$$C_p^{l_2}(r_2) = -k_p^{1/2} r_2 (1 - e^{-\beta r_2})^{2l_2+1} n_{l_2}(k_p r_2), \quad (3.8)$$

for the positron and

$$S_q^{l_4}(R) = (2k_q)^{1/2} R j_{l_4}(k_q R), \quad (3.9)$$

$$C_q^{l_4}(R) = -(2k_q)^{1/2} R (1 - e^{-\gamma R})^{2l_4+1} n_{l_4}(k_q R), \quad (3.10)$$

for the center-of-mass of the positronium. Where k<sub>p</sub> and k<sub>q</sub> are momenta of the positron in channel p and the positronium in channel q respectively and are determined by

$$E = \frac{1}{2} k_p^2 - \frac{1}{2n_p^2} = \frac{1}{4} k_q^2 - \frac{1}{4n_q^2}. \quad (3.11)$$

The functions  $j_l(x)$  and  $n_l(x)$  in Eqs. (3.7-3.10) are the spherical Bessel and Neumann functions respectively. The factors before the Neumann functions are introduced to make the C functions have the same behaviour as the S functions. Strictly speaking, we only concern the asymptotic behaviour of the S and C functions because the internal part of the total scattering wavefunction  $\Psi$  is taken care by the short range functions  $\phi_S$  and  $\phi_C$ . Therefore, one can freely choose a way to make the C function decrease to zero as  $r_2$  or  $R$  tends to zero and quadratically integrable. Physically, the final scattering parameters should be independent of the parameters  $\beta$  and  $\gamma$  in some range of their variations. The short range functions  $\phi_S^p$ ,  $\phi_C^p$ ,  $\phi_S^q$  and  $\phi_C^q$  of the channel wavefunctions are expanded in terms of a set of eigenfunctions  $\phi_k$  and eigenvalues  $E_k$  of the system obtained by diagonalizing the bound-bound matrices.

### 3.2 Matrix Elements

#### Bound-bound

A trial eigenfunction of the system may be expanded into

$$\Psi = \sum_i c_i X_i^{12}(\mathbf{r}_1, \mathbf{r}_2) + \sum_j d_j X_j^{34}(\rho, \mathbf{R}), \quad (3.12)$$

where  $X_i^{12}$  and  $X_j^{34}$  are respectively hydrogen and positronium basis functions. Both kinds of functions are usually written in the following forms

$$X_i^{12}(\mathbf{r}_1, \mathbf{r}_2) = f_{1i}(r_1) f_{2i}(r_2) Y_{Ll_1l_2}^0(\hat{\mathbf{r}}_1 \cdot \hat{\mathbf{r}}_2), \quad (3.13)$$

$$X_j^{34}(\rho, \mathbf{R}) = f_{3j}(\rho) f_{4j}(R) Y_{Ll_3l_4}^0(\hat{\rho} \cdot \hat{\mathbf{R}}), \quad (3.14)$$

where  $f_{1i}$ ,  $f_{2i}$ ,  $f_{3j}$  and  $f_{4j}$  are the radial functions of the hydrogen electron, positron, positronium and center-of-mass of the positronium respectively. All of them may be chosen to be Slater-type functions (see, for example, Appendix B). In addition,  $f_{1i}$  and  $f_{3j}$  can be either physical or pseudo states of the hydrogen and positronium

atoms. Suitably arranging the order of the basis functions  $\xi_i$  ( $X_i^{12}$  or  $X_j^{34}$ ), we can obtain a matrix eigenvalue equation as follows

$$AX = \lambda BX, \quad (3.15)$$

with the Hamiltonian and overlapping matrix elements defined as

$$A_{ij} = \langle \xi_i(\mathbf{r}_1, \mathbf{r}_2; \rho, \mathbf{R}) | H | \xi_j(\mathbf{r}_1, \mathbf{r}_2; \rho, \mathbf{R}) \rangle,$$

$$B_{ij} = \langle \xi_i(\mathbf{r}_1, \mathbf{r}_2; \rho, \mathbf{R}) | \xi_j(\mathbf{r}_1, \mathbf{r}_2; \rho, \mathbf{R}) \rangle.$$

Where whether  $\xi_i$  takes the first two or the last two arguments depends on whether it is a  $X_i^{12}$  or  $X_j^{34}$  function. Then solving the eigenvalue equation (3.15), one obtains a set of eigenfunctions called  $\phi_k$  and a set of corresponding eigenvalues  $E_k$ ,  $k=1, \dots, n$ . This set of eigenfunctions is applied to expand the short range parts of the channel wavefunctions.

### Bound-Free and Free-Free

The major work using the Harris-Nesbet approach is to evaluate the so-called m-matrices. They are expressed in terms of the bound-free (see Eqs. (2.36, 2.37)) and free-free (see Eqs. (2.45-2.48)) matrices. For positron-hydrogen scattering, the bound-free matrices can be specifically expressed

$$\begin{aligned} M_S^{pk} &= \sum_i c_i^k \langle \xi_i(\mathbf{r}_1, \mathbf{r}_2; \rho, \mathbf{R}) | H - E | U_p(r_1) S_p^{l_2}(r_2) Y_{Ll_1l_2}^0(\hat{\mathbf{r}}_1 \cdot \hat{\mathbf{r}}_2) \rangle \\ &= \sum_i c_i^k M_{ip}^S, \end{aligned} \quad (3.16)$$

$$\begin{aligned} M_C^{pk} &= \sum_i c_i^k \langle \xi_i(\mathbf{r}_1, \mathbf{r}_2; \rho, \mathbf{R}) | H - E | U_p(r_1) C_p^{l_2}(r_2) Y_{Ll_1l_2}^0(\hat{\mathbf{r}}_1 \cdot \hat{\mathbf{r}}_2) \rangle \\ &= \sum_i c_i^k M_{ip}^C, \end{aligned} \quad (3.17)$$

$$\begin{aligned} M_S^{qk} &= \sum_i c_i^k \langle \xi_i(\mathbf{r}_1, \mathbf{r}_2; \rho, \mathbf{R}) | H - E | \phi_q(\rho) S_q^{l_4}(R) Y_{Ll_3l_4}^0(\hat{\rho} \cdot \hat{\mathbf{R}}) \rangle \\ &= \sum_i c_i^k M_{iq}^S, \end{aligned} \quad (3.18)$$

$$\begin{aligned} M_C^{qk} &= \sum_i c_i^k \langle \xi_i(\mathbf{r}_1, \mathbf{r}_2; \rho, \mathbf{R}) | H - E | \phi_q(\rho) C_q^{l_4}(R) Y_{Ll_3l_4}^0(\hat{\rho} \cdot \hat{\mathbf{R}}) \rangle \\ &= \sum_i c_i^k M_{iq}^C, \end{aligned} \quad (3.19)$$

where expansion coefficients  $c_i^k$  are just the  $k$ -th eigenvector of the system Hamiltonian obtained from solving the bound-bound eigenvalue equation. Suppose that there are  $N$  open channels at system energy  $E$  and  $M$  short range eigenfunctions, the above bound-free matrices then are all  $N \times M$ . In practical computation, we need to calculate all matrix elements between the free functions and basis functions  $\xi_i$ 's.

The free-free matrix elements classify into three groups, one-center hydrogen-hydrogen (H-H), one-center positronium-positronium (Ps-Ps) and two-center hydrogen-positronium (H-Ps) integrations. The one-center H-H elements have the following general forms

$$M_{SS}^{pp'} = \langle U_p(r_1) S_p^{l_2}(r_2) Y_{Ll_1l_2}^0(\hat{\mathbf{r}}_1 \cdot \hat{\mathbf{r}}_2) | H - E | U_{p'}(r_1) S_{p'}^{l_2}(r_2) Y_{Ll'_1l'_2}^0(\hat{\mathbf{r}}_1 \cdot \hat{\mathbf{r}}_2) \rangle, \quad (3.20)$$

$$M_{SC}^{pp'} = \langle U_p(r_1) S_p^{l_2}(r_2) Y_{Ll_1l_2}^0(\hat{\mathbf{r}}_1 \cdot \hat{\mathbf{r}}_2) | H - E | U_{p'}(r_1) C_{p'}^{l_2}(r_2) Y_{Ll'_1l'_2}^0(\hat{\mathbf{r}}_1 \cdot \hat{\mathbf{r}}_2) \rangle, \quad (3.21)$$

$$M_{CC}^{pp'} = \langle U_p(r_1) C_p^{l_2}(r_2) Y_{Ll_1l_2}^0(\hat{\mathbf{r}}_1 \cdot \hat{\mathbf{r}}_2) | H - E | U_{p'}(r_1) C_{p'}^{l_2}(r_2) Y_{Ll'_1l'_2}^0(\hat{\mathbf{r}}_1 \cdot \hat{\mathbf{r}}_2) \rangle, \quad (3.22)$$

with  $M_{CS}^{pp'} = M_{SC}^{pp'} - \frac{1}{2} \delta_{pp'}$ . The one-center Ps-Ps elements are defined as

$$M_{SS}^{qq'} = \langle \phi_q(\rho) S_q^{l_4}(R) Y_{Ll_3l_4}^0(\hat{\rho} \cdot \hat{\mathbf{R}}) | H - E | \phi_{q'}(\rho) S_{q'}^{l_4}(R) Y_{Ll'_3l'_4}^0(\hat{\rho} \cdot \hat{\mathbf{R}}) \rangle, \quad (3.23)$$

$$M_{SC}^{qq'} = \langle \phi_q(\rho) S_q^{l_4}(R) Y_{Ll_3l_4}^0(\hat{\rho} \cdot \hat{\mathbf{R}}) | H - E | \phi_{q'}(\rho) C_{q'}^{l_4}(R) Y_{Ll'_3l'_4}^0(\hat{\rho} \cdot \hat{\mathbf{R}}) \rangle, \quad (3.24)$$

$$M_{CC}^{qq'} = \langle \phi_q(\rho) C_q^{l_4}(R) Y_{Ll_3l_4}^0(\hat{\rho} \cdot \hat{\mathbf{R}}) | H - E | \phi_{q'}(\rho) C_{q'}^{l_4}(R) Y_{Ll'_3l'_4}^0(\hat{\rho} \cdot \hat{\mathbf{R}}) \rangle, \quad (3.25)$$

with  $M_{CS}^{qq'} = M_{SC}^{qq'} - \frac{1}{2} \delta_{qq'}$ . The two-center H-Ps elements are

$$M_{SS}^{pq} = \langle U_p(r_1) S_p^{l_2}(r_2) Y_{Ll_1l_2}^0(\hat{\mathbf{r}}_1 \cdot \hat{\mathbf{r}}_2) | H - E | \phi_q(\rho) S_q^{l_4}(R) Y_{Ll_3l_4}^0(\hat{\rho} \cdot \hat{\mathbf{R}}) \rangle, \quad (3.26)$$

$$M_{SC}^{pq} = \langle U_p(r_1) S_p^{l_2}(r_2) Y_{Ll_1l_2}^0(\hat{\mathbf{r}}_1 \cdot \hat{\mathbf{r}}_2) | H - E | \phi_q(\rho) C_q^{l_4}(R) Y_{Ll_3l_4}^0(\hat{\rho} \cdot \hat{\mathbf{R}}) \rangle, \quad (3.27)$$

$$M_{CC}^{pq} = \langle U_p(r_1) C_p^{l_2}(r_2) Y_{Ll_1l_2}^0(\hat{\mathbf{r}}_1 \cdot \hat{\mathbf{r}}_2) | H - E | \phi_q(\rho) C_q^{l_4}(R) Y_{Ll_3l_4}^0(\hat{\rho} \cdot \hat{\mathbf{R}}) \rangle, \quad (3.28)$$

with  $M_{CS}^{pq} = M_{SC}^{pq}$ . The above three kinds of matrix elements, bound-bound, bound-free, free-free, are analytically reduced to forms which are suitable for fast and accurate numerical evaluations.

To carry out these numerical calculations, these matrix elements must first be reduced to simpler forms. For the matrix elements where both "in" and "out" are either hydrogen channels or positronium channels (type I), a reduction to closed forms can be achieved (see for example, Gien 1995 [82]). For matrix elements where both hydrogen and positronium channels are involved (type II), it is necessary to use the spheroidal coordinates for the reduction. These matrix elements can at most be reduced to two-variable integrals (Gien 1995 [82]).

For the matrix element of type I, all the terms of the matrix elements can be straightforwardly reduced to closed forms. Only the terms that correspond to the interaction potential need some care. Fortunately, the reduction procedure of such a term has been available in the literature and it can be found in various text books of angular momentum theory such as [95] and references therein. For the matrix elements of type II, one needs to use the spheroidal coordinates ( $\xi$ ,  $\eta$ , and  $\phi$ , here  $\phi$  is not the wavefunction mentioned above but an angle ( see Ref. [51])) whose relationships to the spherical coordinates are

$$r_1 = \frac{1}{2}r_2(\xi + \eta), \quad (3.29)$$

$$\rho = \frac{1}{2}r_2(\xi - \eta), \quad (3.30)$$

$$R = \frac{1}{4}r_2\sqrt{\xi^2 + \eta^2 + 6\xi\eta + 8} \quad (3.31)$$

and

$$d^3\mathbf{r}_1 = \frac{1}{8}r_2^3(\xi^2 - \eta^2)d\xi d\eta d\phi. \quad (3.32)$$

where  $\phi$  is the angle between the plane containing the positron, electron and proton, and some arbitrary plane containing the positron and proton. The integrations over

the angular variables (the "angle part") can then be factorized and reduced to a closed form (see Appendix B.4). The relevant matrix elements could then be at most reduced to a two-variable integral (over  $\xi$  and  $\eta$ ), after the integration over  $r_2$  may be carried out. The detailed reductions of the relevant matrix elements are given in Appendix B.

## Chapter 4

### Numerical Calculations and Results

In this chapter, the details of numerical calculations and results are presented. Two kinds of calculations are carried out for obtaining accurate phase shifts and cross sections. One is to adopt a few lower close coupled-states: 1s, 2s, 2p or  $3\bar{p}$  states of hydrogen and 1s, 2s, 2p states of positronium, mixing with enough short ranged functions (called mixing basis) to simulate the interaction in the system, which will be in detail discussed in the first section. The other is to exploit large close-couplings. There have been two important large close-coupling calculations performed recently by McAlinden et al. [76] and Kerhnoghan et al. [79] (18-state R-matrix) and by Mitroy [73] (21-state T-matrix). The Harris-Nesbet method has also been applied to these large close-coupling calculations and presented in the last section.

#### 4.1 Calculations with Large Mixing bases

Due to its flexibility, the correlation function has been widely applied to express the short and long range interaction of a scattering system. In most situations, the Hylleraas-type correlation function is employed associated with a number of non-linear variational parameters such as Bhatia et al. 1971 [36], 1974 [37], Humberston 1972 [24], 1982 [26], 1984 [27, 28], Brown and Humberston 1985 [29]). These calculations produced the most accurate data sets of the positron-hydrogen scattering for S- and P-waves. However, these calculations are difficult to extend to higher partial waves. On the other hand, Chan and Fraser (1973) [59] and Chan and McEachran

(1976) [60] performed calculations for the S- and P-waves with channel spaces composed of  $1sH + 1sPs$  associated with a number of short range Slater-type correlation functions which can be considered as the linear variational method. In comparison with the coupled-static calculations, their results were greatly improved. But they just carried out the S- and P-waves and the evaluations did not reach a convergent limit. The main goal of this work is to perform full and physical convergent partial wave calculations by further extending both coupled-states and the size of the correlation functions.

Powers in the Slater basis functions are usually equal to the angular momentum quantum number of the particles. Such functions decrease rapidly with increase of the distance from the scattering center. In order to take care of the polarization well, some very small parameters  $Z_j$  in the radial function are needed, which brings some numerical difficulties for highly precise computations, and a relative large number of basis functions per bound channel is required to obtain satisfactory convergence of computations. In this work, we take the powers  $n_{ij} = l_i + n_j$ , where  $l_i$  is the angular momentum quantum number of the particle  $i$  (the positron or center-of-mass of positronium) and  $n_j$  is an integer. The test running for six state ( $1s, 2s, 2pH$  and  $1s, 2s, 2pPs$ ) scheme shows that the convergence is much faster than the traditional way and the number of basis functions per bound channel can be reduced to 12 or 15 if the basis functions contain  $n_j=0, 1, 2$ . We still use 18 basis functions for each bound channel in order to obtain a high numerical precision.

Two coupling schemes have been carried out. One is extended from six-state coupling,  $1s, 2s, 2pH$  and  $1s, 2s, 2pPs$ , associated with a number of short range correlation functions called B6+. The other is further extended from the basis B6+ by adding  $3\bar{p}$  pseudo-state of H (Burke et al. 1969 [90]) called B7+. The  $3\bar{p}H$  pseudo-state is included to speed up the convergence of the calculation at very low incident

momenta because the dipole polarization potential is quite important there. The short ranged correlation functions for the electron and positronium take the same forms as the functions of a positron considered above. The motivation of using correlation functions in the basis of lower physical states is to simulate the short range interaction of the scattering system, which somehow is equivalent to the application of pseudo-states. Moreover, general formulas of scattering matrix elements with correlation functions as a basis set can be applied to any close-coupling calculation. Numerically, the number of the correlation functions is gradually increased to search for the convergent limit. We first include the angular momentum  $l_1 = 0, 1$  subspaces of the electron and  $l_3 = 0, 1$  subspaces of the positronium, and then add  $l_1=2$  and  $l_3=2$  subspaces. Finally we add  $l_1=3, 4$  subspaces. We find that  $l_1=3, 4$  subspaces do not have significant contributions at energies considered. Therefore, results reported here are obtained without the inclusion of  $l_1=3, 4$  subspaces. The total number of short range correlation functions used are 126, 210 and 252 for  $L=0, 1$  and  $\geq 2$ , respectively, and the total number of basis functions used to span the scattering space are 234, 354, and 396 for B6+ basis and 252, 390 and 432 for B7+ basis at  $L=0, 1$  and  $\geq 2$ , respectively. We evaluated the phase shifts, elastic and positronium formation cross sections for the  $e^+ + H(1s)$  entrance channel and the elastic and hydrogen formation cross sections for the  $p + Ps$  entrance channel at energies below the first excitation threshold of hydrogen.

#### 4.1.1 The $e^+ + H(1s)$ entrance channel

The results of partial wave phase shifts, positron elastic and Ps formation cross sections are given in tables 4.1-4.4, 4.5-4.6, and 4.7-4.8 respectively, associated with existing theoretical data. In Table 4.9, we display the S-wave reaction matrix elements. The details of these results for the basis B7+ are plotted in figures 4.1 to

#### 4.12.

From Tables 4.1-4.4, it is obvious that two sets of data from basis sets B6+ and B7+ agree well with each other except at very low positron momentum where the phase shifts of the B6+ basis are smaller than those of the B7+ basis. But the S-wave phase shifts of both bases are in good agreement with each other. This can be explained in that the 2p state of hydrogen in the basis B6+ only represents 67% of the whole dipole polarization for the ground state hydrogen. The remaining part of the polarization may not completely be included by the short range correlation functions. Therefore, the incomplete inclusion of the long range polarization causes the phase shifts of the higher partial waves to be smaller than the actual ones. Taking into account this aspect, we think that our B7+ basis will give more accurate phase shifts at lower energies the 2p state in conjunction with  $3\bar{p}$  pseudo-state of hydrogen represents 100% of the dipole polarization. However, the overall agreement between two sets of cross sections shows that we reached physical convergence. In the following discussion, we just focus on our results from the basis B7+.

For the S-wave, Table 4.1 and Figure 4.1 show that our S wave phase shift demonstrates a peak at positron momentum around 0.2 and then decreases. At  $k$  larger than 0.6, the S-wave phase shift becomes negative. This indicates that the repulsive electrostatic potential begins to play the main role for this partial wave in such a momentum range. This feature also implies that both the long range dipole polarization and short range potentials are significant for the S-wave. In comparison with other theoretical results, we found that our S-wave phase shifts are in excellent agreement with the 21-state close coupling results [71] in the whole pure elastic region. The maximum absolute difference between two sets of data is less than 0.0009 Rad. The results of the convergent close coupling approach (Bray and Stelbovics 1994) [96] agree with ours within 2%. The Harris-Nesbet results of Register and

Table 4.1: The partial S-wave phase shifts (Rad.) for positron-hydrogen scattering as a function of incident momentum. The results B6+ and B7+ are from the bases B6+ and B7+ respectively.

$k(a_0^{-1})$	0.1	0.2	0.3	0.4	0.5	0.6	0.7
B6+	0.1481	0.1873	0.1668	0.1195	0.0618	0.00299	-0.0521
B7+	0.1483	0.1875	0.1670	0.1196	0.0621	0.00334	-0.0519
21-state <sup>a</sup>	0.1474	0.1868	0.1667	0.1191	0.0621	0.0031	-0.0518
Variational <sup>b</sup>	0.1479	0.1875	0.1672	0.1196	0.0619	0.00301	-0.0523
	0.1483	0.1877	0.1677	0.1201	0.0624	0.0039	-0.0512
CCC <sup>c</sup>	0.145	0.183	0.163	0.119	0.0624	0.0034	-0.0531
Schwinger <sup>d</sup>	0.1473	0.1869	0.1671	0.1202	0.0631	0.0041	-0.0514
IERM <sup>e</sup>	0.148	0.187	0.167	0.118	0.062	0.004	
Faddeev <sup>f</sup>	0.149	0.189	0.169	0.121	0.062	0.003	-0.050
Schwartz <sup>g</sup>	0.151	0.188	0.168	0.120	0.062	0.007	-0.054
Doolan <sup>h</sup>	0.1481	0.1876	0.1671	0.1199	0.0623	0.0034	-0.051
Register <sup>i</sup>	0.1460	0.1849	0.1649	0.1172	0.0593	-0.00003	-0.0569
Houston <sup>j</sup>	0.149	0.189	0.169	0.123	0.065	0.008	-0.049
Shimamura <sup>k</sup>	0.1506	0.1866	0.1667	0.1196	0.0623	0.002	-0.049
Stein <sup>l</sup>	0.148	0.187	0.167	0.120	0.062	0.0033	-0.0515
Humberston <sup>m</sup>	0.148	0.187	0.167	0.119	0.062	0.003	
Winick <sup>n</sup>	0.147	0.179	0.158	0.119	0.064	0.003	-0.051

<sup>a</sup>Close coupling, Mitroy (1995)[73]; <sup>b</sup>Variational, Bhatia et al. (1971)[36], the upper and lower entries with and without the extrapolation; <sup>c</sup>Convergent close coupling, Bray and Stelbovics (1994)[96]; <sup>d</sup>Schwinger principle, Roy and Mandal (1990,1993)[57]; <sup>e</sup>Intermediate Energy R-matrix with the extrapolation), Higgins et al. (1990)[75]; <sup>f</sup>Solving the modified Faddeev equations, Kvistinsky et al. (1995)[58]; <sup>g</sup>Variational, Schwartz (1961) [22]; <sup>h</sup>T-matrix, Doolan et al. (1971) [97]; <sup>i,j,k</sup>Harris-Nesbet variational, Register and Poe (1975)[54], Houston and Drachmen (1971) [39], Shimamura (1971) [98]; <sup>l,m</sup>Kohn variational, Stein and Sternlicht (1972) [23], Humberston and Wallace (1972) [24]; <sup>n</sup>moment T-matrix, Winick and Reinhardt (1978) [99].

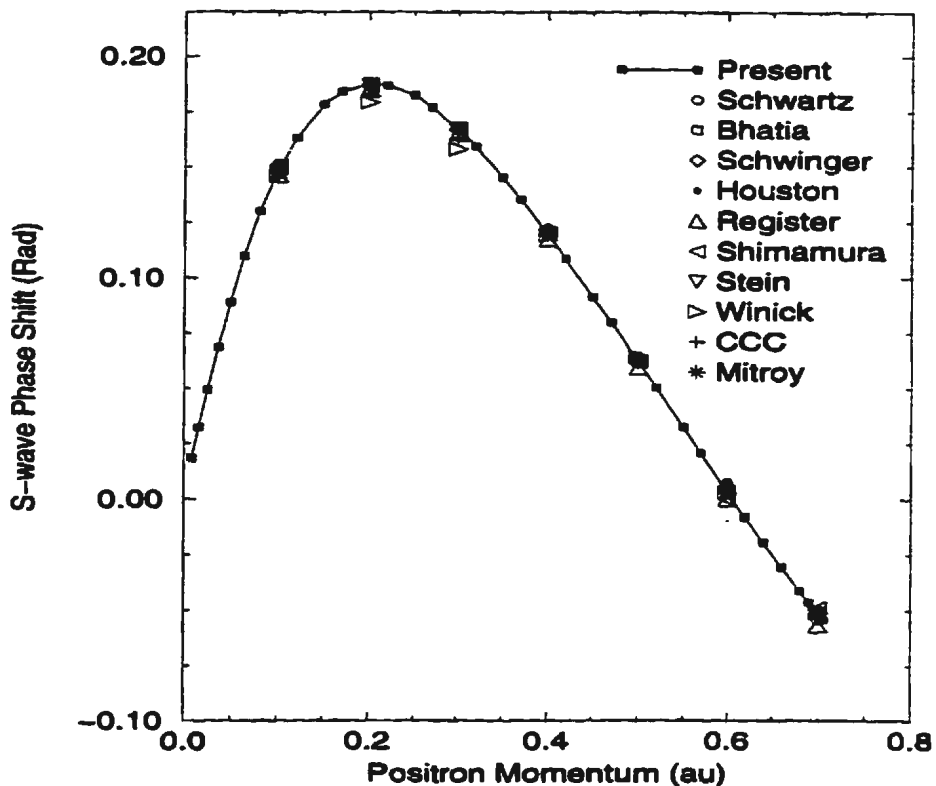


Figure 4.1: Partial S-wave phase shifts (Rad) as a function of positron momentum. Schwartz: variational by Schwartz (1961); Bhatia: variational by Bhatia et al. (1971); Schwinger: Schwinger principle by Roy and Mandal (1990,1993); Houston, Register, and Shimamura: Harris-Nesbet method by Houston and Drachman (1971)' Register and Poe (1978), and Shimamura (1971); Stein: Kohn variational by Stein and Sternlicht (1972); Winick: moment T-matrix by Winick and Reinhardt (1972); CCC: convergent close coupling by Bray and Stelbovics (1994); Mitroy: 21-state close coupling by Mitroy (1995).

Poe (1975) [54], Houston and Drachman (1971) [39] and Shimamura (1971) [98] generally agree with ours within 2%-10%. These differences may partly come from the relatively small bases applied in their calculations. Good agreement between ours and the variational data of Bhatia et al. (1971) [36] is also obtained. There is reasonable agreement between ours and the results from the methods of the Kohn variational principle by Schwartz (1961) [22], Stein and Sternlicht (1972) [23] and Humberston and Wallace (1972) [24], the T-matrix approach by Doolan (1971) [97] and Winick and Reinhardt (1978) [99], the Schwinger variational principle by Roy and Mandal (1990, 1993)[57], intermediate energy R-matrix by Higgins et al. [100] and an approach from solving the Faddeev equation by Kvistinsky et al. [58, 101].

The present scattering length is obtained by reducing the positron momentum to  $k = 0.01 a_0^{-1}$  and then using a number of polynomials to interpolate. The constant term of the polynomial, which gives the scattering length, is slightly different from one polynomial to another. Hence, we can determine the uncertainty of the scattering length. We obtain the scattering length  $a_S = -2.103 \pm 0.005 a_0$  which is in very good agreement with the variational values  $-2.1036 \pm 0.0004 a_0$  [39], and  $-2.103 \pm 0.001 a_0$ [24] and  $-2.104 \pm 0.001 a_0$  by solving the Faddeev equations [58, 101]. The 21-state close coupling calculation by Mitroy (1995) gives a scattering length  $-2.08 \pm 0.02 a_0$  which is also in reasonable agreement with the present value.

For the P-wave, Figure 4.2 shows that the P-wave phase shift monotonically increases with positron momentum in the whole pure elastic scattering region. Table 4.2 (also see Figure 4.2) indicates that the agreement between the present phase shifts and the 21-state ones is very good. The maximum relative difference between two phase shift sets is smaller than 0.3%. The convergent close coupling method by Bray and Stelbovics (1994) [96] also gives good agreement with our data. In comparison with the variational results of Bhatia et al. (1974) [37] , the present

data also indicate excellent agreement with their unextrapolated values. Looking at their data with the extrapolation and polarization corrections, the agreement even becomes a little worse. This may partly come from their extrapolation and polarization corrections. For their extrapolation, they carried out their calculations for different finite basis sizes and then extrapolate to an infinite basis size by using some formulas. That is, the extrapolated data correspond to a basis with infinite numbers of basis functions. This extrapolation has two problems. One is that the extrapolation from some small bases which are not good enough to span the scattering space to the infinite size basis would cause some undesirable compensations. The other problem is that different formulas give different compensations. For example, there is a difference  $0.0004\text{Rad}$  at  $k=0.4a_0^{-1}$  between their two different extrapolation formulas. On the other hand, their pure polarization correction from about 15 to  $100a_0$ , may slightly overestimate this effect because parts of the polarization potential may already be included in their calculations and extrapolations. In particular, this correction makes a change  $0.0013\text{Rad}$  at  $k=0.2a_0^{-1}$ . Considering the above facts, we may expect that the agreement will be further improved. In spite of those detailed small differences, the overall good agreement between the above three completely different methods may imply a high numerical precision achieved in these calculations. The phase shifts of Register and Poe (1975)[54], using Harris-Nesbet algebraic method, have the same situation as in the S-wave case, 2-10% smaller than ours and the 21-state data because of the reason mentioned above. The phase shifts from the Schwinger principle by Roy and Mandal (1993) [57] seem reasonably accurate. The results from the variational method by Kleinman (1965) [102] and from solving the coupled-equation in configuration space by Chan and McEachran (1976) [60], associated with short range correlation functions, show good agreement with ours at low momenta. At higher momenta, Kleinman's phase shifts are about

10% larger than ours but those of Chan and McEachran are about 10% lower than ours. The limited correlation functions (50) in Chan and McEachran's calculation may be a main reason for such disagreement. The results of the intermediate energy R-matrix method (IERM) (Higgins et al. 1990) [100] give good agreement with the present data and other accurate results. The moment T-matrix by Winick and Reinhardt (1978) [103] also show reasonable agreement, noting that this method mainly focused on high scattering energies.

For the D-wave case, Table 4.3 indicates a very good agreement with the accurate 21-state calculation. The maximum difference between two sets of data is lower than 0.0002 Rad. The phase shifts from the convergent close coupling calculation agree with ours within 5%. Again, the Harris-Nesbet results of Register and Poe (1975)[54] are about 2% smaller than ours. The phase shifts from the Schwinger principle by Roy and Mandal (1993)[57] are accurate at  $k \leq 0.4a_0^{-1}$  and about 2% smaller than ours and the 21-state values at higher momentum. The IERM values are in fair agreement with ours.

Our F-wave phase shifts in Table 4.3 and Figure 4.3 are slightly less than the 21-state results. The maximum deviation at momentum  $k=0.1a_0^{-1}$  is about 4%. The convergent close coupling data agree well with ours except for at momentum  $k=0.1$  and  $0.7a_0^{-1}$ , respectively, where the differences reach about 10%. The Schwinger phase shifts by Roy and Mandal (1993) are accurate at lower momentum, but show irregular deviation from the existing precise data at higher momentum. The IERM results are in good agreement with ours at the momentum considered.

It can be seen from Table 4.4 that the present phase shifts for the partial waves  $L=4$ , 5, and 6 are systematically a little less than the 21-state data. The difference between two sets is decreasing as the momentum increases and going up as the total angular momentum increases. The maximum discrepancies at  $k=0.1a_0^{-1}$  are

Table 4.2: The partial P-wave phase shifts (Rad.) for positron-hydrogen scattering as a function of incident momentum. The results B6+ and B7+ are from the bases B6+ and B7+ respectively.

$k(a_0^{-1})$	0.1	0.2	0.3	0.4	0.5	0.6	0.7
B6+	0.00875	0.0327	0.0657	0.1001	0.1303	0.1540	0.1781
B7+	0.00886	0.0327	0.0657	0.1002	0.1304	0.1542	0.1783
21-state <sup>a</sup>	0.00887	0.0327	0.0657	0.1002	0.1306	0.1542	0.1788
Variational <sup>b</sup>		0.0325	0.0656	0.1001	0.1303	0.1541	0.1777
		0.0338	0.0665	0.1016	0.1309	0.1547	0.1799
CCC <sup>c</sup>	0.0088	0.0325	0.0649	0.0986	0.128	0.151	0.171
Schwinger <sup>d</sup>	0.0088	0.0333	0.0658	0.1012	0.1318	0.1534	0.1739
Register <sup>e</sup>	0.005	0.030	0.063	0.097	0.128	0.146	0.169
Kleiman <sup>f</sup>	0.0086	0.032	0.066	0.11	0.14	0.17	0.19
Chan <sup>g</sup>	0.0080	0.0318	0.0637	0.0953	0.122	0.141	0.159
Winick <sup>h</sup>	0.0066	0.033	0.063	0.095	0.128	0.160	0.175
IERM <sup>i</sup>	0.009	0.033	0.066	0.102	0.132	0.156	0.185

<sup>a</sup>Close coupling, Mitroy (1995)[73].

<sup>b</sup>Variational calculations, Bhatia et al. (1974)[37], the upper entry without the extrapolation and the lower entry with both the extrapolation and polarization correction.

<sup>c</sup>Convergent close coupling, Bray and Stelbovics (1994)[96].

<sup>d</sup>Schwinger principle, Roy and Mandal (1990,1993)[57].

<sup>e</sup>Harris-Nesbet Variational calculation, Register and Poe (1975)[54].

<sup>f</sup>Variational, Kleiman et al. (1965) [102].

<sup>g</sup>Coupled static plus correlation functions, Chan and McEachran (1976) [60].

<sup>h</sup>Moment T-matrix, Winick and Reinhardt (1978)[99].

<sup>i</sup>Intermediate Energy R-matrix with the extrapolation), Higgins et al. (1990)[75].

Table 4.3: The partial D- and F-wave phase shifts (Rad.) for positron-hydrogen scattering as a function of incident momentum. The results B6+ and B7+ are from the bases B6+ and B7+ respectively. The number in [ ] indicates powers of ten.

$k(a_0^{-1})$	0.1	0.2	0.3	0.4	0.5	0.6	0.7
$L = 2$							
B6+	0.127[-2]	0.544[-2]	0.128[-1]	0.240[-1]	0.394[-1]	0.595[-1]	0.880[-1]
B7+	0.133[-2]	0.548[-2]	0.129[-1]	0.241[-1]	0.396[-1]	0.597[-1]	0.883[-1]
21-stat <sup>a</sup>	0.136[-2]	0.551[-2]	0.129[-1]	0.242[-1]	0.397[-1]	0.598[-1]	0.885[-1]
RP <sup>b</sup>	0.13[-2]	0.54 [-2]	0.125[-1]	0.235[-1]	0.389[-1]	0.598[-1]	0.863[-1]
CCC <sup>c</sup>	0.14[-2]	0.55 [-2]	0.127[-1]	0.239[-1]	0.389[-1]	0.582[-1]	0.839[-1]
Schwinger <sup>d</sup>	0.131[-2]	0.543[-2]	0.126[-1]	0.244[-1]	0.382[-1]	0.593[-1]	0.870[-1]
IERM <sup>e</sup>	0.5[-2]	0.13 [-1]	0.25 [-1]	0.41 [-1]	0.62[-1]		
$L = 3$							
B6+	0.376[-3]	0.174[-2]	0.403[-2]	0.746[-2]	0.124[-1]	0.195[-1]	0.304[-1]
B7+	0.436[-3]	0.177[-2]	0.406[-2]	0.750[-2]	0.125[-1]	0.197[-1]	0.305[-1]
21-state <sup>a</sup>	0.452[-3]	0.180[-2]	0.409[-2]	0.754[-2]	0.126[-1]	0.198[-1]	0.307[-1]
CCC <sup>c</sup>	0.4[-3]	0.18 [-2]	0.40 [-2]	0.75 [-2]	0.121[-1]	0.191[-1]	0.287[-1]
Schwinger <sup>d</sup>	0.454[-3]	0.178[-2]	0.404[-2]	0.710[-2]	0.133[-1]	0.161[-1]	0.218[-1]
IERM <sup>e</sup>	0.18 [-2]	0.40 [-2]	0.75 [-2]	0.126[-1]	0.207[-1]		

<sup>a</sup>Close coupling, Mitroy (1995)[73].

<sup>b</sup>Harris-Nesbet calculation, Register and Poe [54].

<sup>c</sup>Convergent close coupling, Bray and Stelbovics (1994)[96].

<sup>d</sup>Schwinger principle, Roy and Mandal (1990,1993)[57].

<sup>e</sup>Intermediate Energy R-matrix with the extrapolation), Higgins et al. (1990)[75].

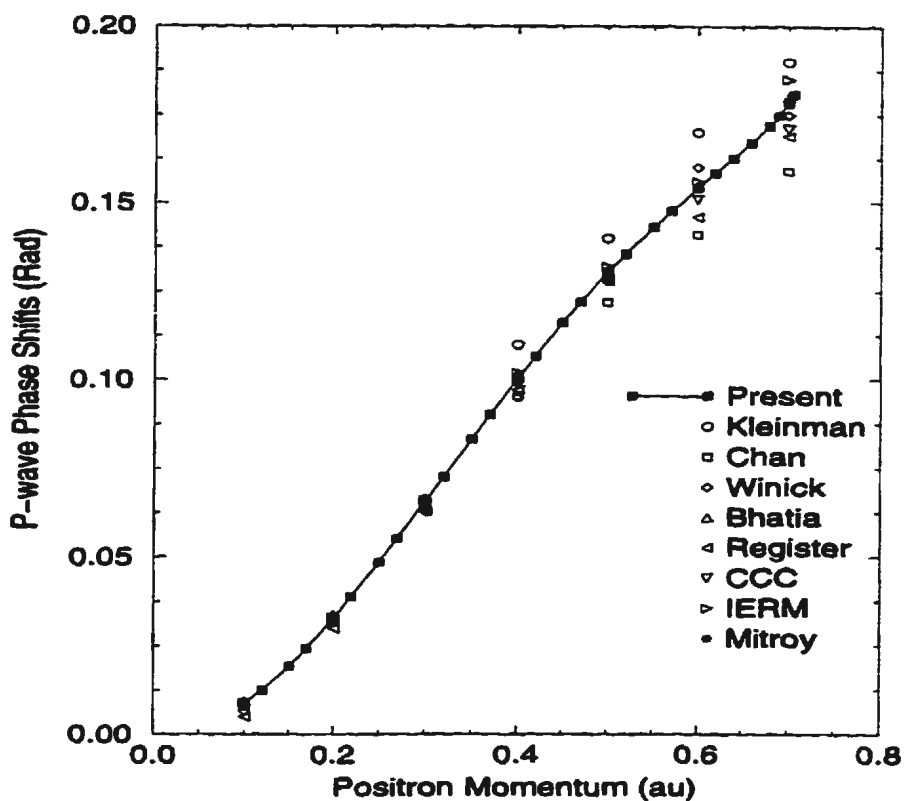


Figure 4.2: Partial P-wave phase shifts (Rad) as a function of positron momentum (au). Phrases indicated in this picture have same meanings as in Figure 4.1 but Kleinman: variational by Kleinman et al. (1965); Chan: solving the coupled-equation associated with short range correlation functions by Chan and McEachran (1978).

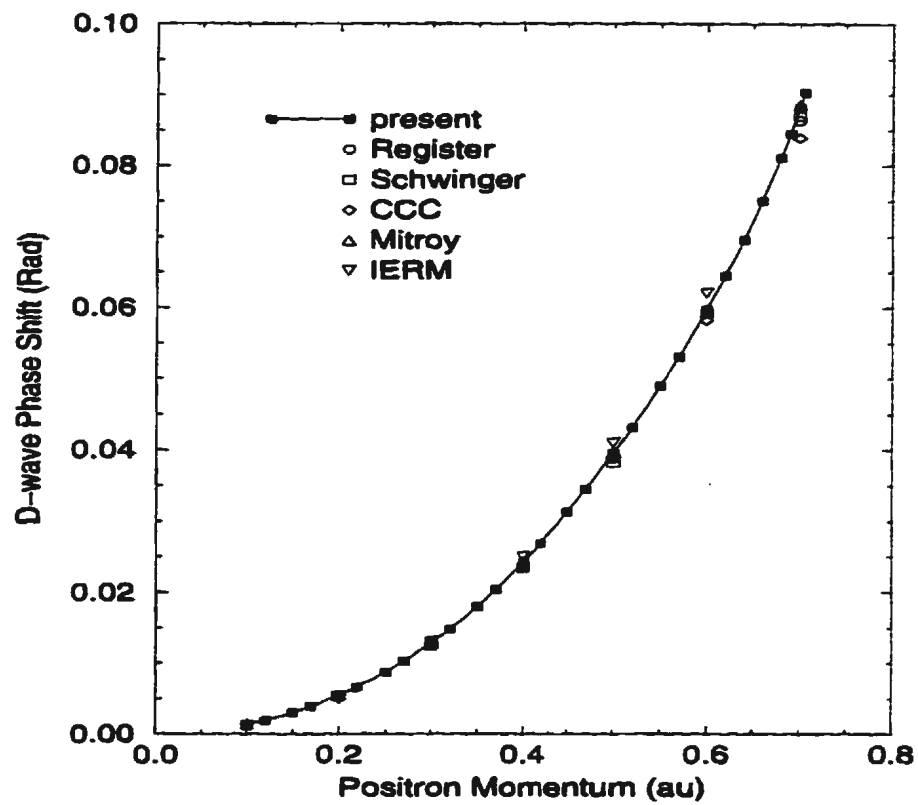


Figure 4.3: Partial D-wave phase shifts (Rad) as a function of positron momentum (au). Phrases indicated in this picture have same meanings as in Figure 4.1.

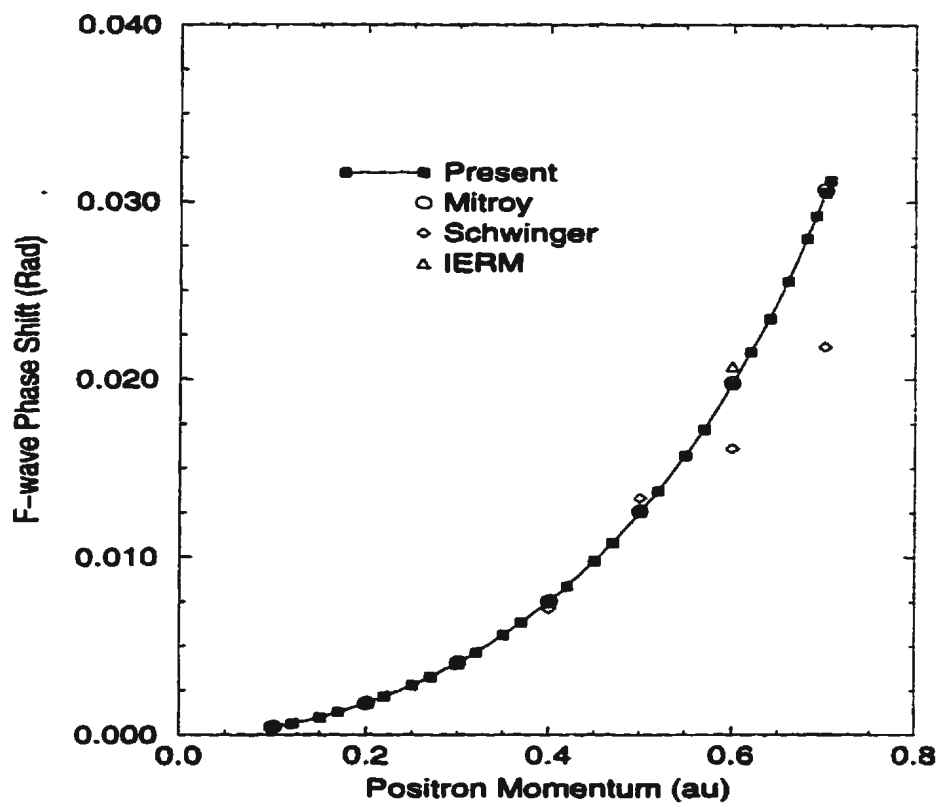


Figure 4.4: Partial F-wave phase shifts (Rad) as a function of positron momentum (au). Phrases have same meanings as in Figure 4.1.

6%, 9% and 10% for  $L=4$ , 5, and 6 partial waves, respectively. The reason for this systematic difference is presently unknown. In spite of this, the total cross sections for pure elastic scattering show very good agreement between the two sets, since the higher partial waves only have very small contributions to the total cross section.

Table 4.4: The  $L=4$ , 5 and 6 partial wave phase shifts (Rad.) and total elastic cross sections ( $\pi a_0^2$ ) for positron-hydrogen scattering as a function of positron momentum. The number in [ ] indicates powers of ten.

$k(a_0^{-1})$	0.1	0.2	0.3	0.4	0.5	0.6	0.7
$L = 4$							
This work(B7+)	0.193[-3]	0.793[-3]	0.180[-2]	0.325[-2]	0.525[-2]	0.799[-2]	0.119[-1]
21-state <sup>a</sup>	0.205[-3]	0.819[-3]	0.183[-2]	0.329[-2]	0.530[-2]	0.807[-2]	0.121[-1]
Schwinger <sup>b</sup>	0.204[-3]	0.813[-3]	0.188[-2]	0.323[-2]	0.507[-2]	0.746[-2]	0.994[-2]
$L = 5$							
This work(B7+)	0.100[-3]	0.420[-3]	0.958[-3]	0.172[-2]	0.272[-2]	0.403[-2]	0.576[-2]
21-state <sup>a</sup>	0.109[-3]	0.443[-3]	0.986[-3]	0.175[-2]	0.277[-2]	0.410[-2]	0.587[-2]
Schwinger <sup>b</sup>	0.109[-3]	0.436[-3]	0.987[-3]	0.177[-2]	0.273[-2]	0.396[-2]	0.535[-2]
$L = 6$							
This work(B7+)	0.570[-4]	0.248[-3]	0.566[-3]	0.101[-2]	0.160[-2]	0.234[-2]	0.326[-2]
21-state <sup>a</sup>	0.633[-4]	0.266[-3]	0.593[-3]	0.105[-2]	0.165[-2]	0.241[-2]	0.336[-2]
Schwinger <sup>b</sup>	0.650[-4]	0.259[-3]	0.589[-3]	0.105[-2]	0.167[-2]	0.241[-2]	0.326[-2]
$\sigma_{\text{elastic}}$							
This work(B7+)	8.826	3.815	1.847	1.193	1.022	1.024	1.177
21-state <sup>a</sup>	8.736	3.787	1.844	1.192	1.026	1.026	1.186

<sup>a</sup>Close coupling, Mitroy (1995)[73].

<sup>b</sup>Schwinger principle, Roy and Mandal (1990,1993)[57].

Tables 4.5 to 4.8 list the partial wave elastic and positronium formation cross sections at energies in the Ore gap. The details of the partial S, P, D, and F waves are plotted in Figures 4.5 to 4.8 for elastic cross sections and in Figures 4.9 to 4.12 for Ps formation cross sections. Table 4.5, as well as Figures 4.5 and 4.6, indicate a noticeable feature that very good agreement has been achieved among the present, 21-state and variational elastic cross sections for S and P partial waves.

Table 4.5: The partial S- and P-wave elastic cross sections (in units of  $\pi a_0^2$ ) as a function of incident momentum.

$k(a_0^{-1})$	0.71	0.75	0.80	0.85
$L = 0$				
This work(B6+)	0.0260	0.0434	0.0658	0.0866
This work(B7+)	0.0257	0.0431	0.0651	0.0858
21-state <sup>a</sup>	0.0258	0.0430	0.0657	0.0849
Variational <sup>b</sup>	0.026	0.043	0.065	0.085
18-state <sup>c</sup>			0.071	
Hyperspherical <sup>d</sup>	0.033	0.050	0.076	0.100
Hyperspherical <sup>e</sup>	0.0325	0.0548	0.0838	0.111
Hyperspherical <sup>f</sup>	0.0234	0.0415	0.0637	0.0863
Faddeev <sup>g</sup>	0.025	0.044	0.063	
$L = 1$				
This work(B6+)	0.799	0.722	0.622	0.546
This work(B7+)	0.800	0.724	0.624	0.549
21-state <sup>a</sup>	0.802	0.726	0.626	0.551
Variational <sup>b</sup>	0.789	0.724	0.622	0.547
18-state <sup>c</sup>			0.624	
Hyperspherical <sup>e</sup>	0.748	0.650	0.532	0.449
Hyperspherical <sup>f</sup>	0.810	0.720	0.608	0.528

<sup>a</sup>21-state close coupling, Mitroy (1995)[73].

<sup>b</sup>Variational calculation, Humberston (1984)[27], Brown et al. (1985) [29].

<sup>c</sup>18-state close coupling, McAlinden et al. (1994).

<sup>d<sub>f</sub></sup>Hyperspherical close coupling, Archer et al. (1990)[106] , Igarashi and Toshima (1994)[107], Zhou and Lin (1994)[104].

<sup>g</sup>Solving the modified Faddeev equations, Kvitsinsky et al. (1995)[58].

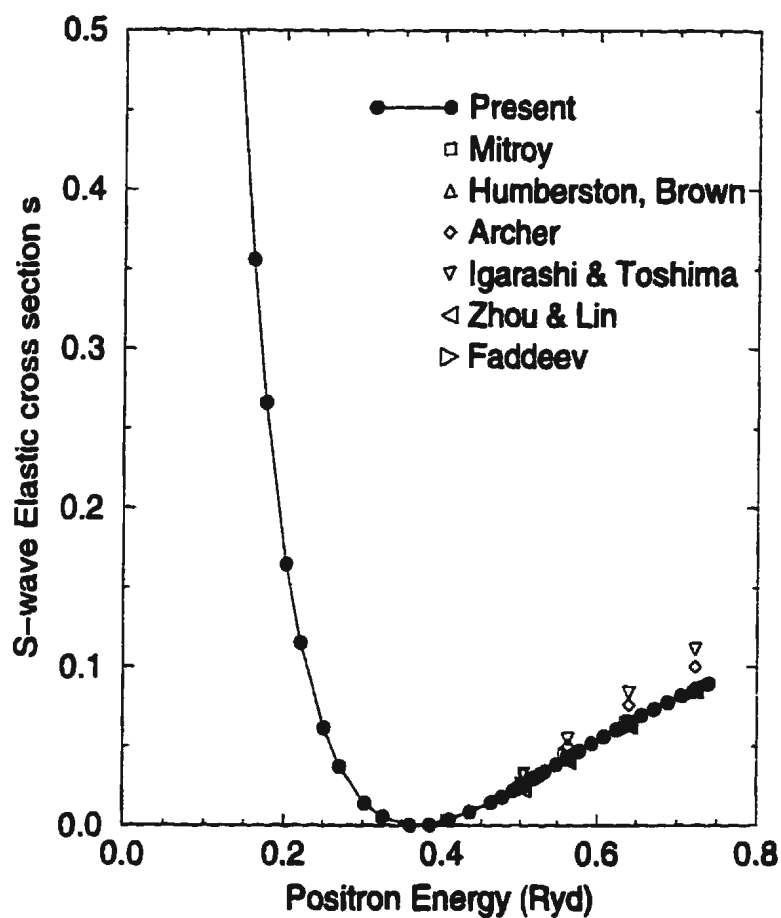


Figure 4.5: Partial S-wave elastic cross sections ( $\pi a_0^2$ ) from B7+ basis as a function of positron energy (Ryd).

Mitroy: 21-state close coupling by Mitroy (1995); Humberston, Brown: Kohn variational by Humberston (1984), Brown and Humberston (1985); Archer, Igarashi & Toshima, Zhou & Lin: hyperspherical close couplings by Archer et al. (1990), Igarashi and Toshima (1994) and Zhou and Lin (1994); Faddeev: solving the Faddeev equation by Kvistinsky et al. (1995).

The maximum difference is about 1% for the S wave at  $k=0.85a_0^{-1}$  and for the P wave at  $k=0.71a_0^{-1}$ . The 18-state result of McAlinden et al. (1994) at  $k=0.80a_0^{-1}$  indicates a reasonable agreement for the S wave and a very good agreement for the P wave with the above three accurate sets. For the hyperspherical calculations, data of Zhou and Lin (1994,1995)[104, 105] are in reasonable agreement with ours for both S and P waves. However, those of Archer et al. (1990) [106] and Igarashi and Toshima (1994) [107] are not very consistent with the existing accurate data.

In comparison with the variational D wave data, our elastic cross sections (Table 4.6 and Figure 4.7) confirm that the 21-state values are more precise. Both sets show almost the same data at energies in the whole Ore gap. There is a little surprise in that both sets come from completely different approaches and totally different basis sets. The 18-state value of McAlinden et al. (1994) at  $k=0.80a_0^{-1}$  is consistent with ours. Again, the hyperspherical values of Archer et al. (1990) [106] and Igarashi and Toshima (1994) [107] are not very accurate. The agreement between hyperspherical data of Igarashi and Toshima (1994) and variational results are probably coincidence. The same situation exists for the F wave elastic cross sections as for the D wave ones. The present total elastic cross sections obtained by just summing from  $L=0$  to 6 also reveal the excellent agreement with the 21-state data.

Figures 4.5-4.8 show that the S- and P-wave cross sections are major contributions to total elastic cross sections at positron energy below 0.2 Ryd. The contributions to total cross sections mainly come from the P and D waves at energies from 0.2 to 0.5 Ryd. At energies in the Ore gap, the P, D and F partial wave cross sections contribute about 90% to total elastic cross sections. One may notice a small shoulder in the P-wave cross section curve (see Figure 4.6) at energies around the Ps formation threshold. This small cusp-like structure was first observed by Chan

and McEachron (1976) in their calculation by solving the coupled equations in the configuration space[60]. They did not mention it although it appeared from their data. Such a structure has also been observed by Higgins et al. (1990) in IERM method[100], Higgins and Burke (1993) [108] almost at the same time and explicitly in their six pseudo-state close coupling, R-matrix calculation[108], Kernoghan et al. (1995) in an 18-state R-matrix calculation[77], Mitroy and Ratnavelu (1995)[71] and Mitroy (1995)[73] in their 12-state and 21-state close coupling calculations. Its existence seems to be independent from the coupling schemes used [82]. The physical origin of this structure is unknown. It is sure that this structure is not a resonance at energy around the Ps formation threshold. But we believe that it is special for positron-hydrogen scattering. In the following we try to give an informal explanation.

At energy just above the Ps formation threshold, the Ps formation channel is open and the incident positron may pick up the electron from the hydrogen atom, but the positron almost loses its all kinetic energy to form the positronium atom. That means, the outgoing positronium moves very slowly around the scattering center. So the strong attraction from the proton could pull back the electron to form a hydrogen atom and throw away the positron with its original energy. Therefore, this process is still elastic scattering. More specifically, the shoulder on the P-wave curve is due to the contribution of the Ps formation channel. If the above argument is a reasonable explanation of this P-wave structure, we then have to explain why there is no such structure in other partial waves. For doing that, let us look at the S-, D- and F-wave elastic cross sections in Figures 4.5, 4.7 and 4.8. All of these curves are going up at energy just above the Ps formation threshold. In contrast, the P-wave elastic cross section curve is going down. On the other hand, the S-, D- and F-wave Ps formation cross section curves (Figures 4.9, 4.11 and 4.12) show

that cross sections are all much smaller than the corresponding part of the P-wave (Figure 4.10) at energy just above the Ps formation threshold. Therefore, their contribution to their corresponding partial wave elastic cross sections, due to the pulling back effect from the Ps formation channel, should be much smaller than that for the P-wave. A very small contribution from the S-, D- and F-wave to the elastic cross section is immersed in the increasing cross section, which looks like nothing at all. However, for the P-wave, a relative large contribution added to the decreasing elastic cross section causes an obvious effects. This structure in the total cross section curve (see Figure 4.13) almost disappears due to a sharp increase of the D-wave cross section near the Ps formation threshold.

The S-wave positronium formation cross sections are sensitive to the basis set applied. A smaller basis set which is not enough to span the scattering space may cause some specific features such as a sharp dip in the six state  $(1s,2s,2p)H + (1s,2s,2p)Ps$  calculation [82]. However, the features will disappear if the selected basis can completely represent the scattering system in the energy range considered. The present calculations show that the S-wave Ps formation (see Figure 4.9) slowly and smoothly increases with the positron momentum in the Ore gap and then sharply goes up when the positron energy is close to the hydrogen first excitation threshold. This sharp increase indicates that a resonance will appear there. Again, two sets from B6+ and B7+ bases agree well with each other (see Table 4.7), which further shows that the channel electrostatic potential plays the main role in this situation. In comparison with other numerical data, our S wave positronium formation cross sections (see Table 4.7 and Figure 4.9) indicate good agreement with the variational and 21-state ones at energies in the whole Ore gap. The maximum difference among them is  $0.0003\pi a_0^2$ . The 18-state results of McAlinden et al. (1994) somehow disagree with the above three sets. In addition to possibly numerical instability, the

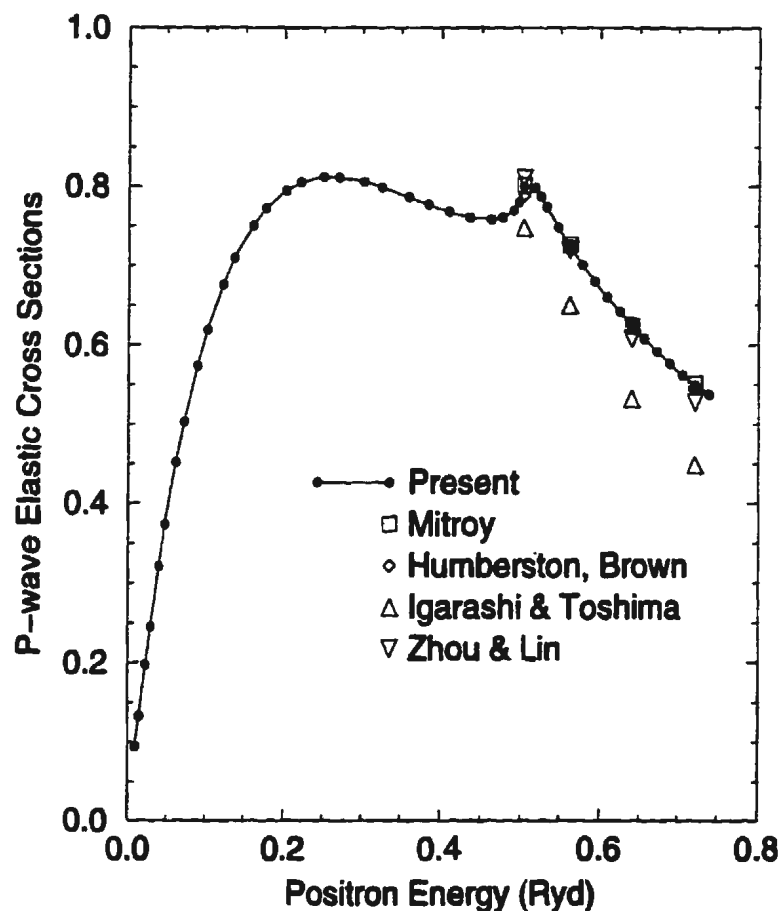


Figure 4.6: Partial P-wave elastic cross sections ( $\pi a_0^2$ ) for  $e^+ + H$  scattering are plotted as a function of positron energy (Ryd). Phrases in this picture have same meanings as in figure 4.5.

Table 4.6: The partial D- and F-wave and total elastic cross sections (in units of  $\pi a_0^2$ ) as a function of incident momentum.

$k(a_0^{-1})$	0.71	0.75	0.80	0.85
$L = 2$				
This work(B6+)	0.337	0.441	0.480	0.471
This work(B7+)	0.339	0.444	0.482	0.474
21-state <sup>a</sup>	0.341	0.446	0.484	0.477
Variational <sup>b</sup>	0.323	0.403	0.423	0.413
18-state <sup>c</sup>			0.482	
Hyperspherical <sup>d</sup>	0.304	0.376	0.389	0.366
Hyperspherical <sup>e</sup>	0.330	0.401	0.420	0.391
$L = 3$				
This work(B6+)	0.563[-1]	0.766[-1]	0.109	
This work(B7+)	0.568[-1]	0.773[-1]	0.110	0.134
21-state <sup>a</sup>	0.575[-1]	0.781[-1]	0.111	0.135
Hyperspherical <sup>d</sup>	0.471[-1]	0.541[-1]	0.675[-1]	0.761[-1]
Hyperspherical <sup>e</sup>	0.676[-1]	0.739[-1]	0.853[-1]	0.950[-1]
$L = 4$				
This work(B7+)	0.111[-1]	0.140[-1]	0.198[-1]	0.270[-1]
$L = 5$				
This work(B7+)	0.311[-2]	0.373[-2]	0.481[-2]	0.632[-2]
$L = 6$				
This work(B7+)	0.117[-2]	0.137[-2]	0.166[-2]	0.203[-2]
Total				
This work(B7+)	1.237	1.307	1.308	1.278
21-state <sup>a</sup>	1.242	1.313	1.316	1.285

<sup>a</sup>21-state close coupling, Mitroy (1995)[73].

<sup>b</sup>Variational calculation, Humberston (1984)[27], Brown et al. (1985) [29].

<sup>c</sup>18-state close coupling, McAlinden et al. (1994).

<sup>d</sup>eHyperspherical close coupling, Igarashi and Toshima (1994)[107] and Zhou and Lin.(1994) [104].

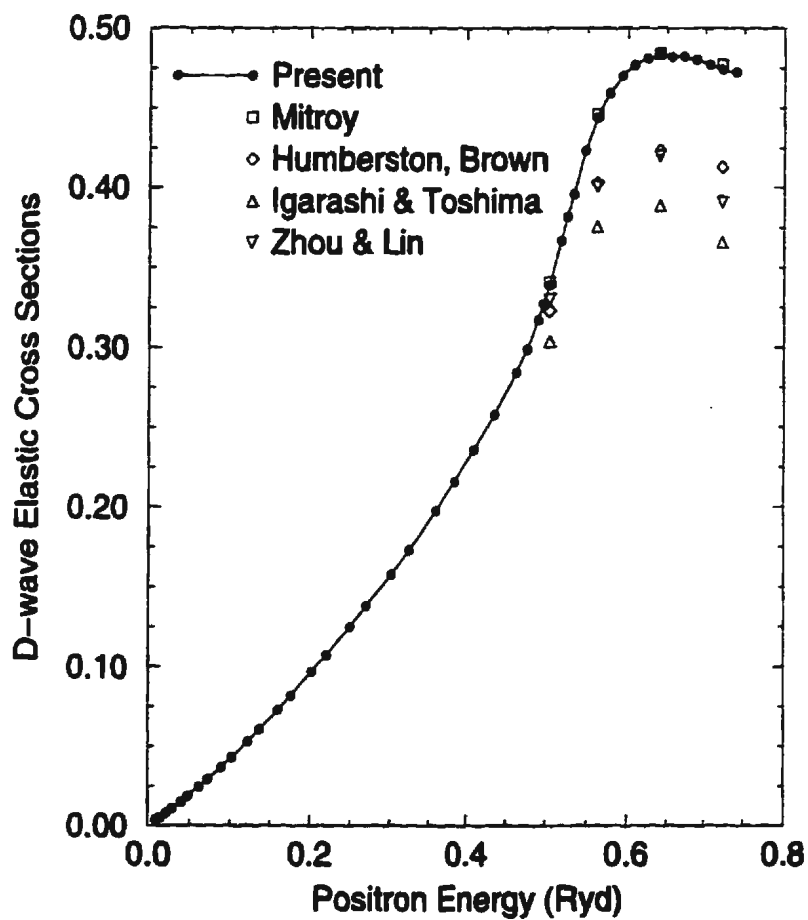


Figure 4.7: Partial D-wave elastic cross section ( $\pi a_0^2$ ) for  $e^+ + H$  scattering is plotted as a function of positron energy (Ryd). Phrases in this picture have same meanings as in figure 4.5.

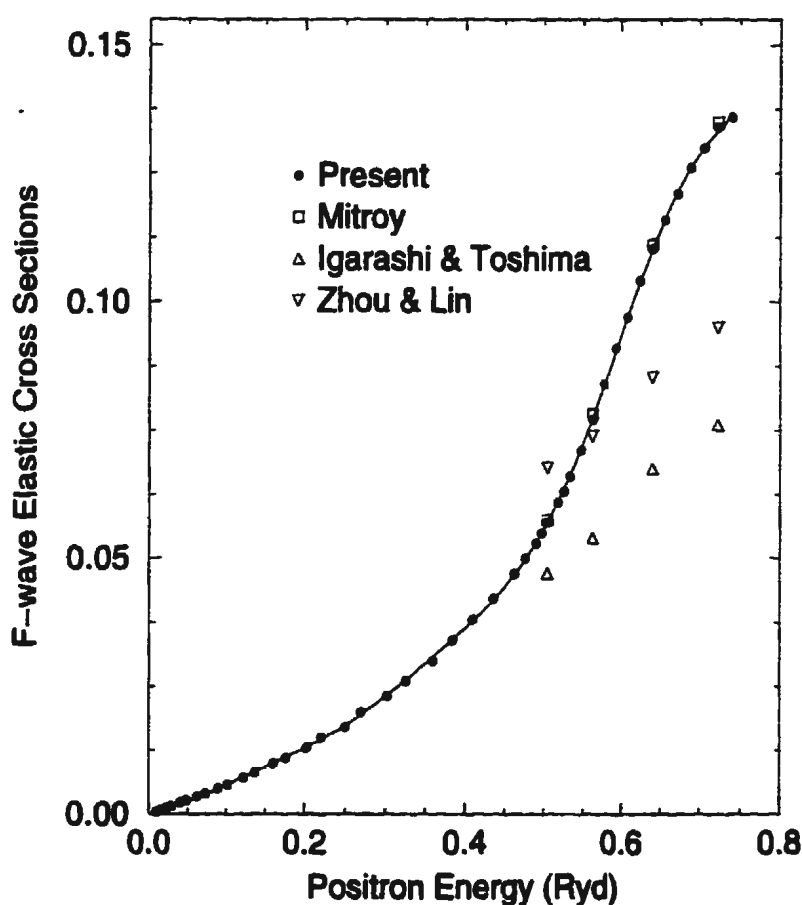


Figure 4.8: Partial F-wave elastic cross section ( $\pi a_0^2$ ) for  $e^+ + H$  scattering is plotted as a function of positron energy (Ryd). Phrases in this picture have same meanings as in figure 4.5.

coupling scheme itself may have some contributions for such a disagreement. For the hyperspherical data, reasonable agreement with the above three sets has been obtained except for those of Archer et al. (1990) [106]. Also, results from solving the Faddeev equations by Kvitsinsky et al. (1995) [58, 101] are consistent with ours.

Agreement with a maximum difference less than 1% (see Table 4.7 and Figure 4.10) has been achieved among the present, 21-state and variational P wave Ps formation cross sections. Moreover, the 18-state values for the P wave give good agreement with the above three sets except at  $k=0.71a_0^{-1}$  where the difference is about 70 calculation. We note that in their calculation they omit the coupling between the hydrogen and positronium channels in the external part of the scattering wavefunction, but we don't believe that the omission would cause this difference. The hyperspherical calculations of Archer et al. (1990) [106] and Igarashi and Toshima (1994) [107] also show reasonable agreement with ours.

Table 4.8 gives the partial wave Ps formation cross sections for  $L \geq 2$ . Good agreement between the present and 21-state data is obtained for both partial D- and F-waves except for the values at  $k=0.71a_0^{-1}$  where the difference reaches about 2%, although their absolute difference is very small. The variational data of Brown and Humberston (1985) [29] have a maximum deviation about 10% from ours for the D-wave, which is what they claimed in their publication. The hyperspherical results of Archer et al. (1990) [106] are in good agreement with ours. However, those of Igarashi and Toshima (1994) [107] have some deviations from the acceptable sets. The G-, H-, and I-wave cross sections demonstrate a quick decreasing trend as L increases at energies in the Ore gap. Our total Ps formation cross sections obtained by summing the partial wave's from  $L=0$  to 6 also agree very well with the 21-state ones.

Looking at the S-wave reactance matrix elements in Table 4.9, it can be easily

Table 4.7: L=0 and 1 partial wave positronium formation cross sections (in units of  $\pi a_0^2$ ) as a function of incident momentum.

$k(a_0^{-1})$	0.71	0.75	0.80	0.85
$L = 0$				
This work(B6+)	0.00407	0.00422	0.00486	0.00553
This work(B7+)	0.00407	0.00439	0.00492	0.00550
21-state <sup>a</sup>	0.00405	0.00427	0.00472	0.00560
Variational <sup>b</sup>	0.0041	0.0044	0.0049	0.0058
18-state <sup>c</sup>	0.0033	0.0030	0.0041	0.0047
Hyperspherical <sup>d</sup>	0.0034	0.0038	0.0043	0.0049
Hyperspherical <sup>e</sup>	0.00404	0.00398	0.00462	0.00535
Hyperspherical <sup>f</sup>	0.00407	0.00421	0.00473	0.00553
Faddeev <sup>g</sup>	0.0038	0.0043	0.0047	
$L = 1$				
This work(B6+)	0.0268	0.367	0.484	0.567
This work(B7+)	0.0267	0.367	0.483	0.564
21-state <sup>a</sup>	0.0266	0.366	0.483	0.563
Variational <sup>b</sup>	0.027	0.365	0.482	0.561
18-state <sup>c</sup>	0.046	0.376	0.485	0.573
Hyperspherical <sup>d</sup>	0.0366	0.376	0.490	0.570
Hyperspherical <sup>e</sup>	0.023	0.370	0.480	0.552

<sup>a</sup>21-state close coupling, Mitroy (1995)[73].

<sup>b</sup>Variational calculation, Humberston (1984)[27], Brown et al. (1985) [29].

<sup>c</sup>18-state close coupling, McAlinden et al. (1994) [76].

<sup>d,e,f</sup>Hyperspherical close coupling, Archer et al. (1990)[106]

, Igarashi and Toshima (1994)[107], Zhou and Lin (1994)[104].

<sup>g</sup>Solving the modified Faddeev equations, Kvitsinsky et al. (1995)[58].

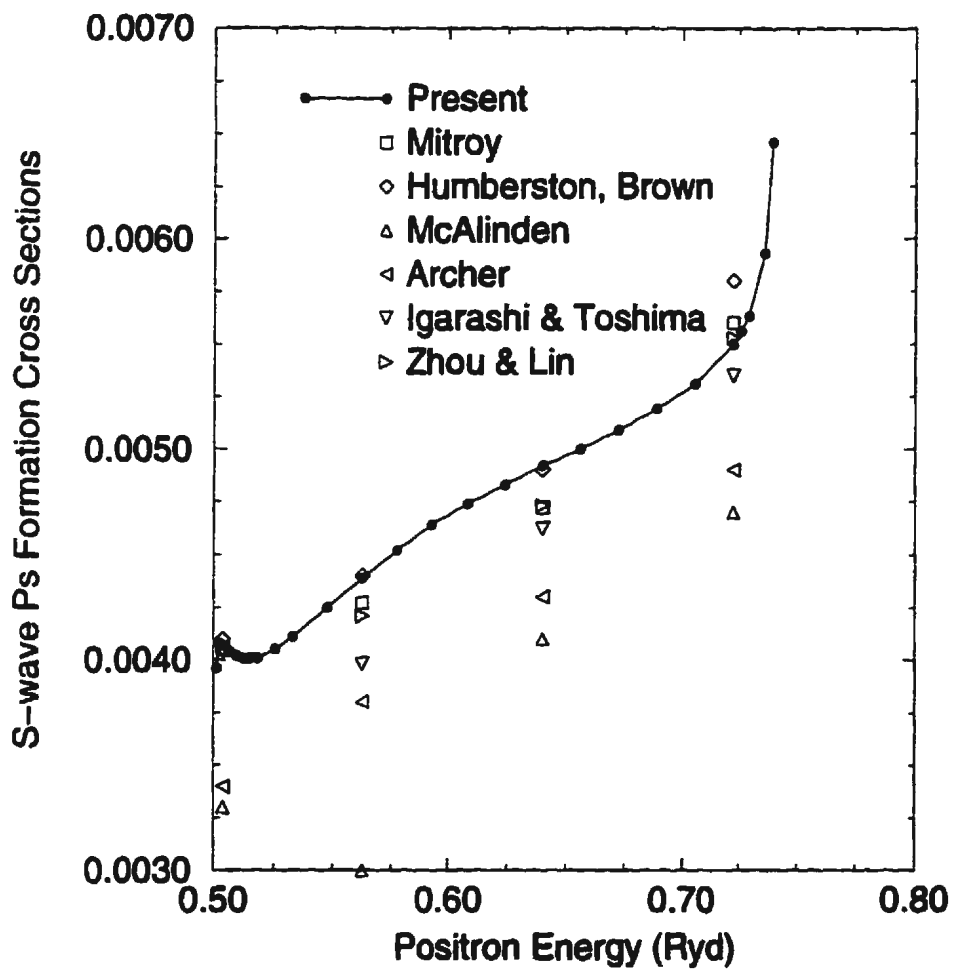


Figure 4.9: Partial S-wave Ps formation cross sections ( $\pi a_0^2$ ) for  $e^+ + H$  scattering are plotted as a function of positron energy (Ryd). The phrases in this picture have the same meanings as in figure 4.5.

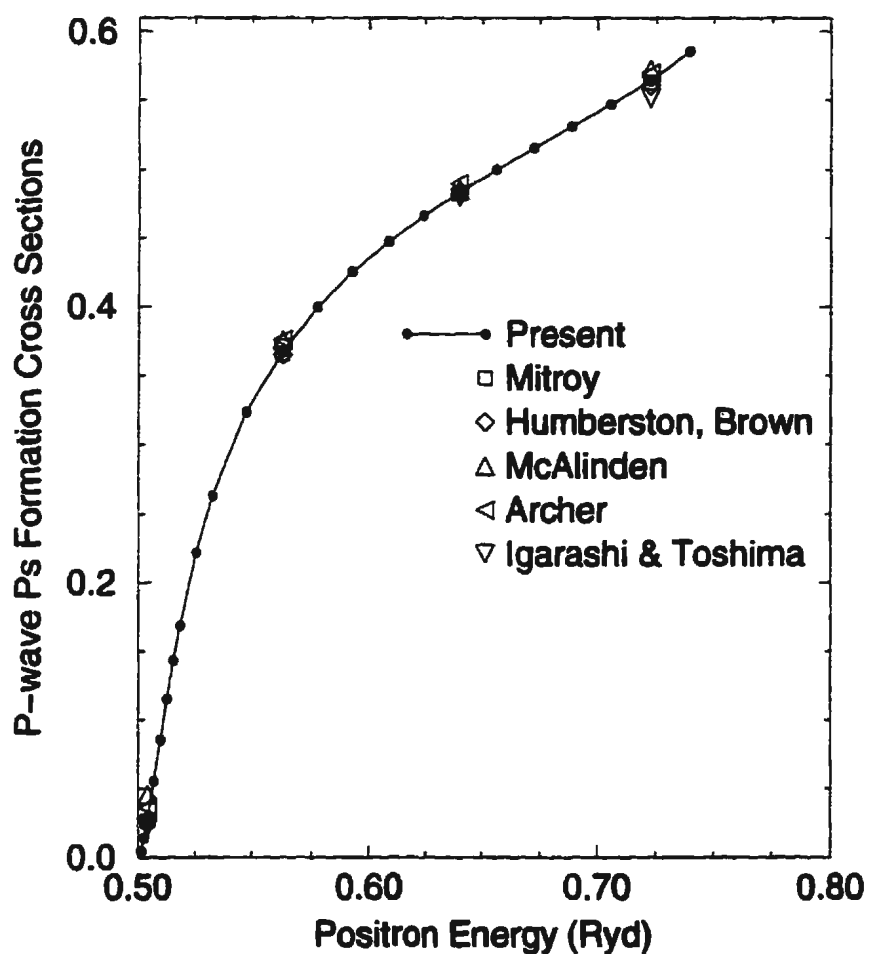


Figure 4.10: Partial P-wave Ps formation cross sections ( $\pi a_0^2$ ) for  $e^+ + H$  scattering are plotted as a function of positron energy (Ryd). The phrases in this picture have the same meanings as in figure 4.5.

Table 4.8: L=2, 3, 4, 5, and 6 partial wave and total positronium formation cross sections (in units of  $\pi a_0^2$ ) as a function of incident momentum. The number in [ ] indicates powers of ten.

$k(a_0^{-1})$	0.71	0.75	0.80	0.85
$L = 2$				
This work(B6+)	0.701[-3]	0.321	0.861	1.162
This work(B7+)	0.697[-3]	0.320	0.862	1.162
21-state <sup>a</sup>	0.682[-3]	0.320	0.859	1.158
Variational <sup>b</sup>	0.62[-3]	0.335	0.812	1.057
Hyperspherical <sup>c</sup>	0.934[-3]	0.334	0.866	1.16
Hyperspherical <sup>d</sup>	0.345[-3]	0.254	0.770	1.031
$L = 3$				
This work(B6+)	0.499[-5]	0.0354	0.271	
This work(B7+)	0.500[-5]	0.0354	0.271	0.596
21-state <sup>a</sup>	0.44[-5]	0.0356	0.270	0.596
Hyperspherical <sup>c</sup>	0.573[-5]	0.0382	0.276	0.592
Hyperspherical <sup>d</sup>	0.364[-4]	0.0133	0.188	0.484
$L = 4$				
This work(B7+)	0.32[-7]	0.219[-2]	0.388[-1]	0.143
$L = 5$				
This work(B7+)		0.113[-3]	0.426[-2]	0.240[-1]
$L = 6$				
This work(B7+)		0.521[-5]	0.414[-3]	0.347[-2]
Total				
This work(B7+)	0.0315	0.729	1.665	2.49
21-state <sup>a</sup>	0.0313	0.728	1.660	2.49

<sup>a</sup>Close coupling, Mitroy (1995)[73].

<sup>b</sup>Variational calculation, Humberston (1984)[27], Brown et al. (1985) [29].

<sup>c,d</sup>Hyperspherical close coupling, Igarashi and Toshima (1994)[107] and Zhou and Lin (1994) [104].

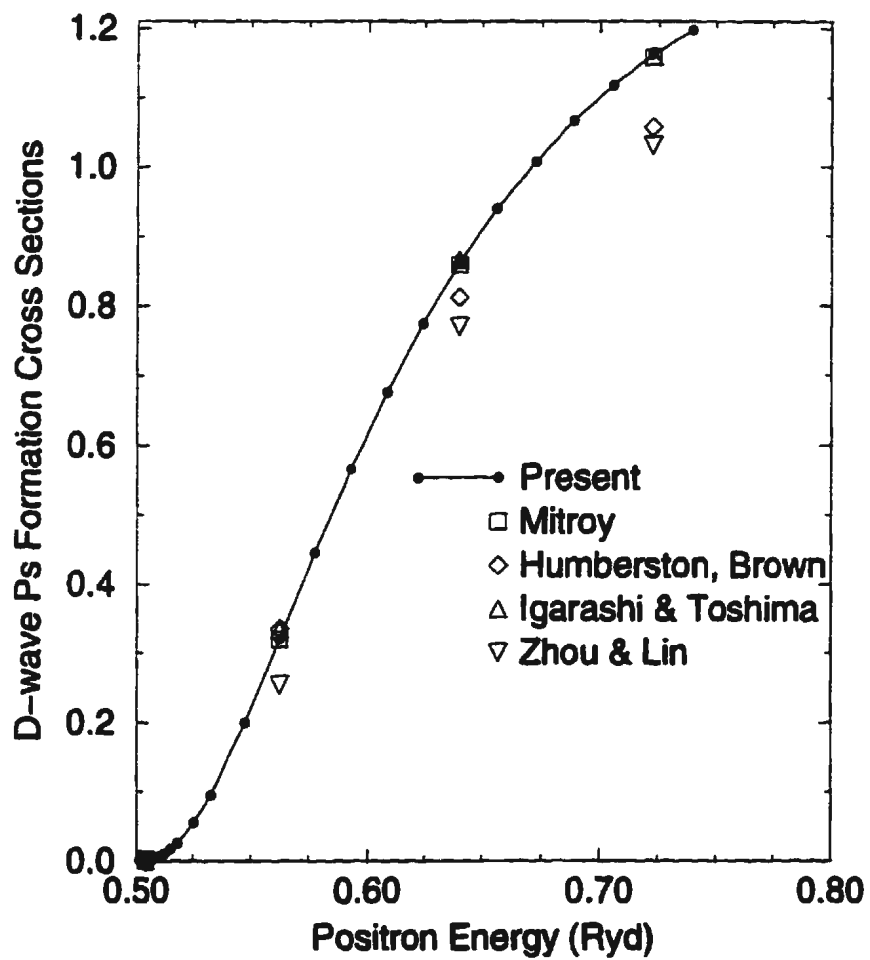


Figure 4.11: Partial D-wave Ps formation cross sections ( $\pi a_0^2$ ) for  $e^+ + H$  scattering are plotted as a function of positron energy (Ryd). The phrases in this picture have the same meanings as in figure 4.5.

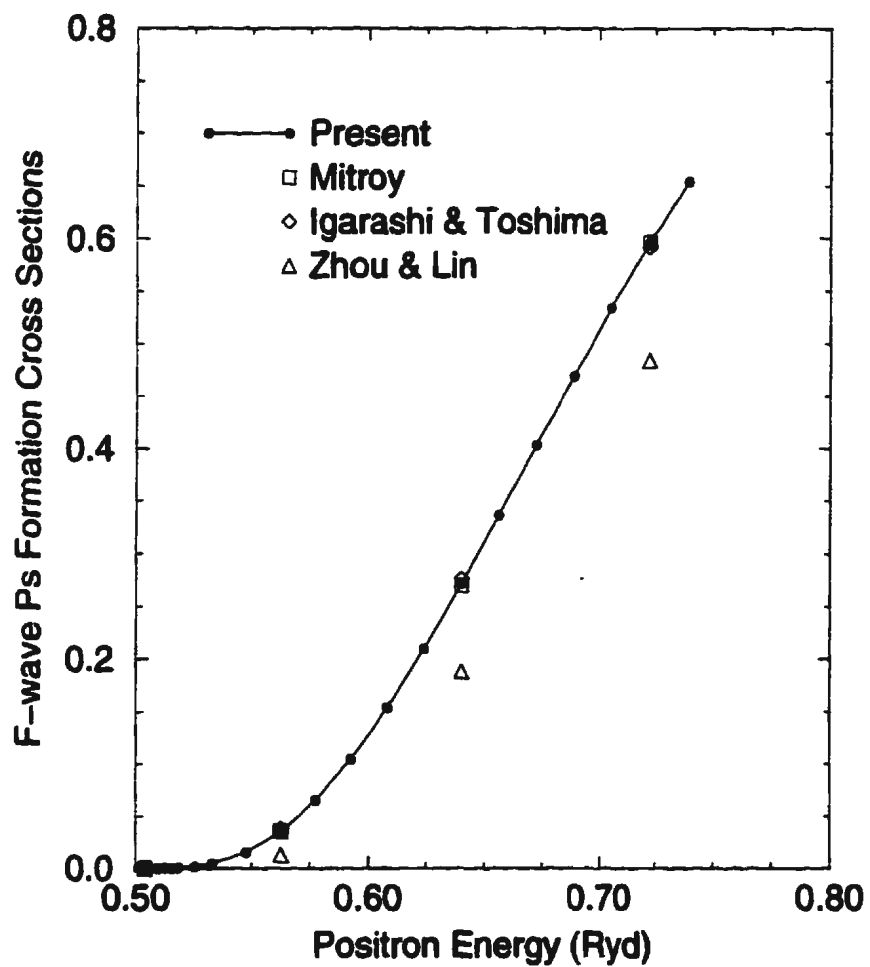


Figure 4.12: Partial F-wave Ps formation cross sections ( $\pi a_0^2$ ) for  $e^+ + H$  scattering are plotted as a function of positron energy (Ryd). The phrases in this picture have the same meanings as in figure 4.5.

seen that our reactance matrix elements at energies in the whole Ore gap agree very well with the most accurate variational values of Humberston (1982). The maximum difference is less than 1% for all elements K11, K12, and K22 except for K12 at  $k=0.85a_0^{-1}$  and K22 at  $k=0.71a_0^{-1}$  where they are about 2 to 3%. But compared with those from the Faddeev equations by Kvitsinsky et al. (1995), the agreement is not so perfect, especially at positron momentum  $k = 0.85a_0^{-1}$ .

Figure 4.13 plots the total elastic, positronium and total  $e^+$ -H scattering cross sections as a function of positron energy. It can be seen from this figure that the total elastic cross section monotonically decreases from positron energy 0.01 to 0.2 Ryd and then almost keeps the same value in the range from 0.2 to 0.75 Ryd except for a very slight bump at energies around the Ps threshold due to the cusp-like structure in the P partial wave. The total Ps formation cross section simply increases from the Ps formation threshold to the hydrogen first excitation. The figure also shows a broad bottom ("Ramsauser minimum") from about 0.2 to 0.5 Ryd in the total cross section curve. Compared with the electron-hydrogen system, this effect is special for positron-hydrogen scattering because of the rearrangement process. Our total elastic, Ps formation and total  $e^+$ -H scattering cross sections are all in excellent agreement with the 21-state results by Mitroy (1995) (not shown in the figure).

In comparison with most recent measurements by the Detroit group [10, 11], our total Ps formation cross section shows good agreement with experimental data except that the experimental data show a slightly flat trend of increase with positron energy. But their measurement also shows some data below the Ps formation threshold. Theoretically, these data are unphysical because the Ps formation channel is closed in that energy range. But it may have some experimental reasons, so we can not give any comment about this at the moment. For the total cross section, very good agreement between our values and experimental data is also obtained at

energy above 0.3 Ryd. Below that energy, the experiment shows a different trend from theoretical results. This is not surprising if we note the difficulties of this experiment (for example, it is very difficult to obtain a mono-energetic positron beam at such a low energy.). Although those differences, it can still be said that this is only experimental measurement which can be used to compare with theoretical results. We may expect that further measurements of this system at very low positron energies are required.

Table 4.9: The S-wave reactance matrix elements.

$k(a_0^{-1})$		K11	K12	K22
0.71	This work(B7+)	-0.05688	-0.02418	0.3691
	Variational <sup>a</sup>	-0.057	-0.024	0.363
	Faddeev <sup>b</sup>	-0.0565	-0.0232	0.348
	Faddeev <sup>c</sup>	-0.059	-0.024	0.33
0.75	This work(B7+)	-0.07844	-0.02826	-0.5322
	Variational <sup>a</sup>	-0.078	-0.028	-0.532
	Faddeev <sup>b</sup>	-0.0793	-0.0280	-0.536
	Faddeev <sup>c</sup>	-0.085	-0.029	-0.54
0.80	This work(B7+)	-0.1039	-0.05122	-1.5143
	Variational <sup>a</sup>	-0.104	-0.051	-1.513
	Faddeev <sup>b</sup>	-0.102	-0.050	-1.512
	Faddeev <sup>c</sup>	-0.109	-0.052	-1.52
0.85	This work(B7+)	-0.1294	-0.1225	-3.7216
	Variational <sup>a</sup>	-0.130	-0.126	-3.735
	Faddeev <sup>c</sup>	-0.169	-0.425	-6.40

<sup>a</sup>Variational calculation, Humberston (1982)[27].

<sup>b</sup>Faddeev equation, Kvitsinsky et al. (1995)[58].

<sup>c</sup>Faddeev equation, Kvitsinsky et al. (1995)[101].

#### 4.1.2 The Ps + p entrance channel

The Harris-Nesbet method directly calculates the reactance matrix. Hence, the transition cross sections for different entrance channels can be easily derived. The

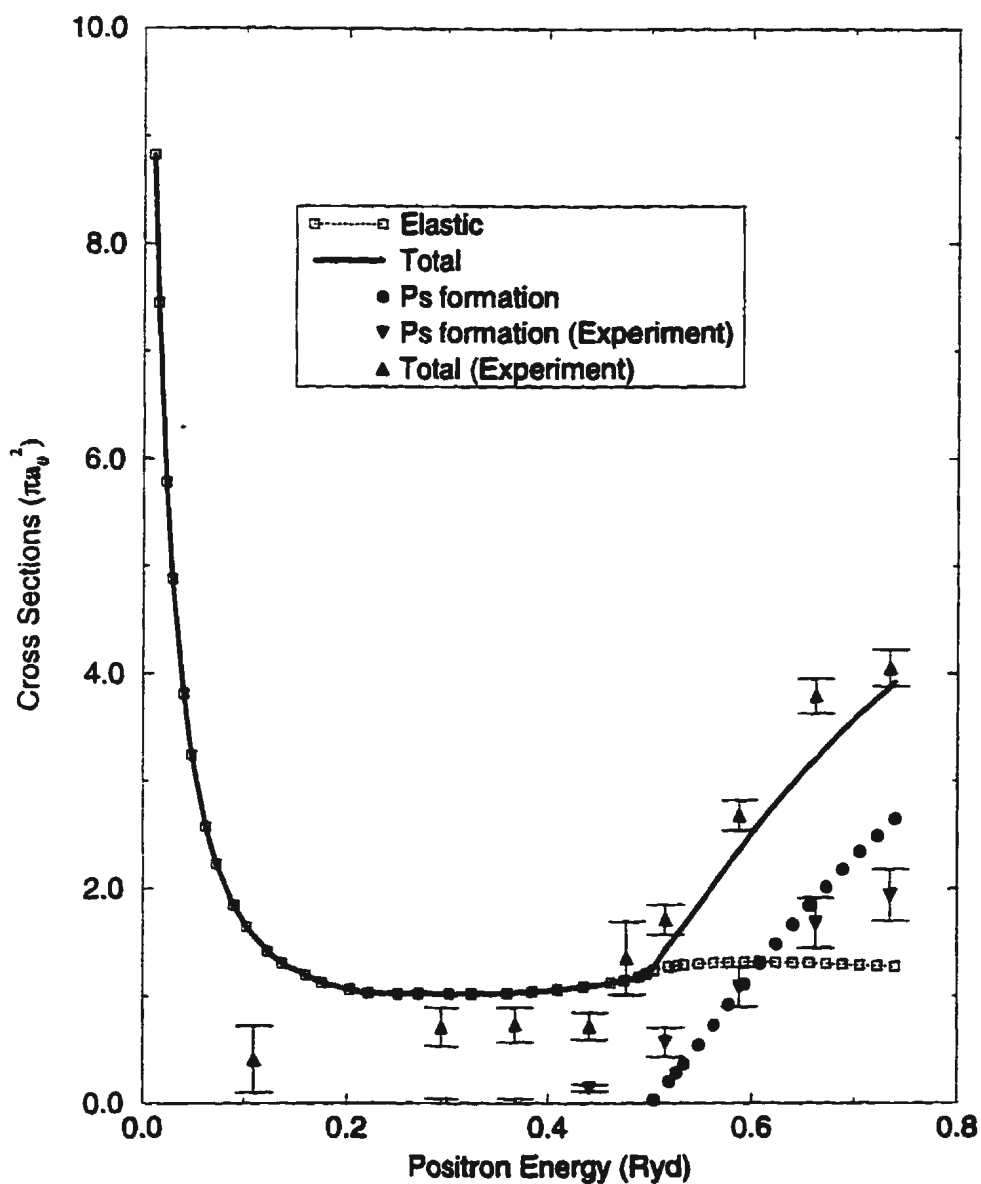


Figure 4.13: Total elastic, Ps formation and total  $e^+$ -H scattering cross sections ( $\pi a_0^2$ ) for  $e^+ + H$  scattering are plotted as a function of positron energy. Experimental data are very recently reported by the Detroit group.

excellent agreement with most accurate variational results and the 21-state close coupling calculation for  $e^+ + H$  entrance channel encourages us to present the transition cross sections for  $Ps + p$  entrance channel. The significance of this is to obtain the anti-hydrogen through a reaction  $Ps + \bar{p}$ . The charge transfer cross section for  $Ps + p$  entrance channel can be obtained by using the balance equation

$$Q_{12}k_1^2 = Q_{21}k_2^2 \quad (4.1)$$

from positronium formation cross sections. Where subscripts 1 and 2 denote the hydrogen and positronium channels respectively.  $k_1$  and  $k_2$  are momenta of the positron and the positronium respectively.

Table 4.10 lists the partial wave and total  $Ps$  elastic cross sections, and the details are illustrated in Figure 4.14. From Table 4.10, good agreement among the present, variational and 21-state results has been found for the S partial wave. However, the agreement between the present and 21-state calculations is just fair for other partial waves. We may expect that the polarization, not completely included in our basis set for the  $Ps$  channel, may be responsible.

The  $Ps$  elastic scattering length has been estimated by decreasing the  $Ps$  momentum to  $0.186 a_0^{-1}$  and using a number of polynomial interpolations as what did for  $e^+ + H$  entrance channel. The scattering length we obtain is  $-14.66 \pm 0.05 a_0$ , which is in good agreement with  $-15.5 \pm 0.4 a_0$  and  $-14.7 \pm 0.2 a_0$  from the 21-state and 12-state calculations by Mitroy (1995) [73]. This scattering length corresponds to a cross section of  $860 \pi a_0^2$ .

Figure 4.14 shows that the S-wave curve has a very sharp decrease as the  $Ps$  energy increases from 0 to 0.02Ryd. At about 0.02Ryd, the curve has a minimum and then slightly goes up and displays a long plateau to 0.25 Ryd at a value about  $10\pi a_0^2$ . However, the P wave curve has a peak as energy goes up to about 0.02 Ryd

Table 4.10: Partial wave and total elastic cross sections ( $\pi a_0^2$ ) for Ps+p scattering.

Energy(Ryd)	0.0041	0.0625	0.014	0.02225
L = 0				
This work(B7+)	58.4	7.05	9.93	8.37
Variational <sup>a</sup>	56.7	7.05	9.93	8.37
12-state <sup>c</sup>	56.4	7.07	9.92	8.34
21-state <sup>c</sup>	59.7	6.92	9.86	8.32
L = 1				
This work(B7+)	14.35	3.92	0.197	1.91
12-state <sup>b</sup>	15.0	3.97	0.181	1.82
21-state <sup>c</sup>	15.2	4.17	0.160	1.77
L = 2				
This work(B7+)	0.630	6.75	4.05	1.65
12-state <sup>b</sup>	0.785	6.86	4.07	1.71
21-state <sup>c</sup>	0.792	7.07	4.26	1.82
L = 3				
This work(B7+)	0.075	1.70	3.13	3.39
12-state <sup>b</sup>	0.113	1.82	3.18	3.46
21-state <sup>c</sup>	0.119	1.85	3.32	3.64
Total				
This work(B7+)	73.5	20.0	18.8	17.8
12-state <sup>b</sup>	72.7	20.5	19.2	18.3
21-state <sup>c</sup>	75.9	20.8	19.5	18.6

<sup>a</sup> Variational calculation, Humberston et al. (1984)[27].<sup>b</sup> Close coupling, Mitroy (1995c)[74].

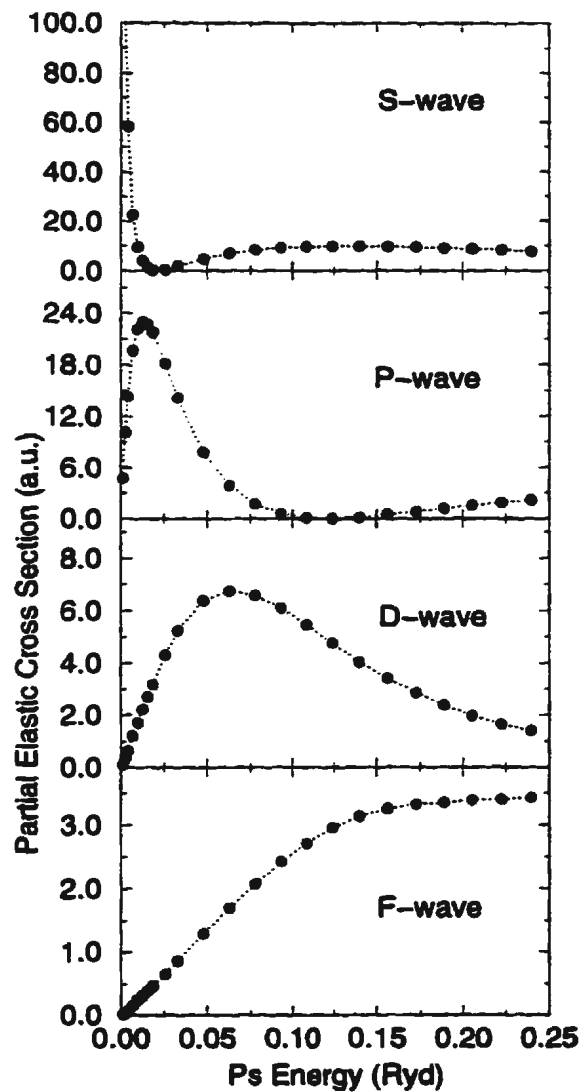


Figure 4.14: Partial wave Ps elastic cross sections ( $\pi a_0^2$ ) for Ps+p scattering are plotted as a function of Ps energy.

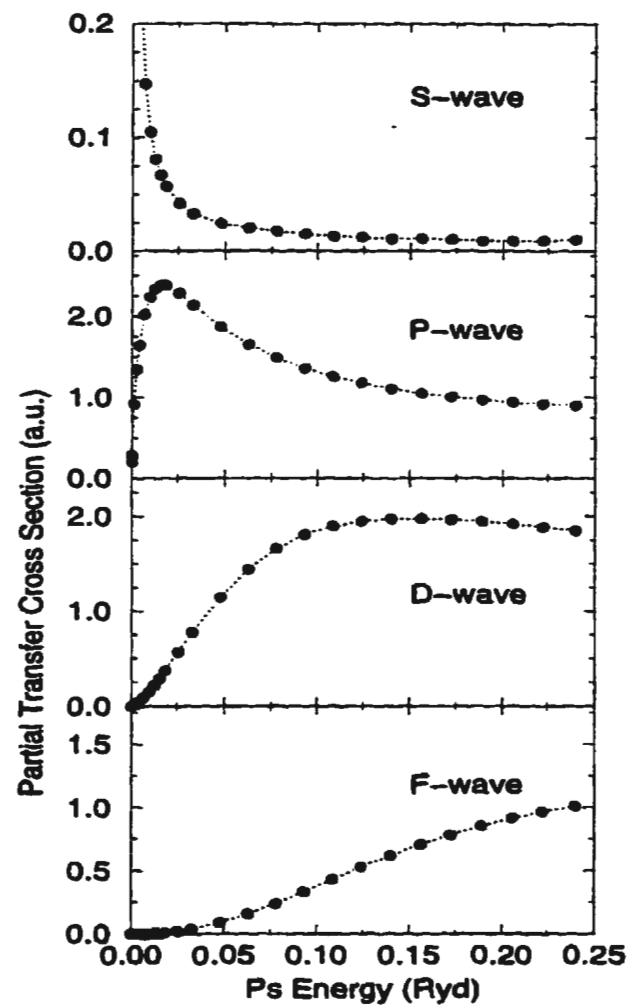


Figure 4.15: Partial wave H formation cross sections ( $\pi a_0^2$ ) for Ps+p scattering are plotted as a function of Ps energy.

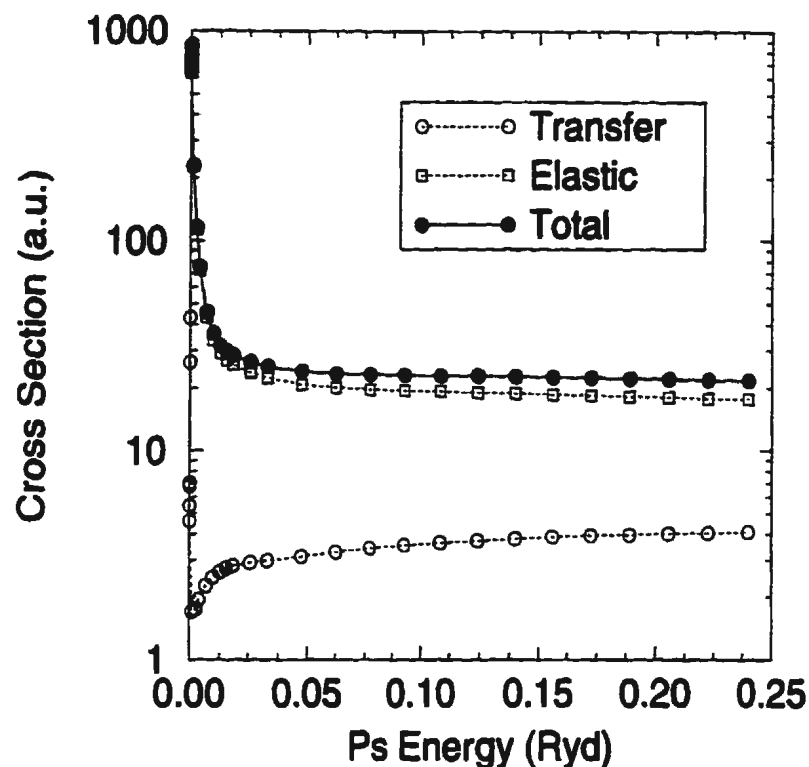


Figure 4.16: Ps elastic, charge transfer and total Ps+p scattering cross sections ( $\pi a_0^2$ ) for Ps+p scattering are plotted as a function of Ps energy.

and then decreases to a minimum at about 0.13Ryd. After the minimum, the P-wave Ps elastic cross section has very small values. The D wave curve just contains a simple wide peak at around 0.06Ryd and the F wave monotonically increases at energies considered here.

Figure 4.15 plots the detailed partial wave hydrogen formation cross sections. It shows that the S-wave cross section has a divergent behavior when Ps energy tends to zero, which can be explained by the characteristic of a superelastic collision (Mitroy 1995)[74]. The divergence is like  $E^{-1/2}$ , i.e.  $\sigma_S = \alpha/k_{Ps}$ , where  $\alpha$  is a constant. Our charge transfer cross sections at very low Ps momentum verifies this relation. For example, our cross section is  $43.31 \pi a_0^2$  at  $k_{Ps} = 0.0018567 a_0^{-1}$  and  $26.55 \pi a_0^2$  at  $k_{Ps} = 0.0030173 a_0^{-1}$ . The constant is about  $0.08 \pi$ . After  $E=0.05$  Ryd, the S-wave cross section slowly decreases. The P-wave curve has a very sharp increase with Ps energy from 0 to 0.01 Ryd and reaches a peak at about 0.2 Ryd. Finally it monotonically goes down. The D wave cross section goes up to  $2.0\pi a_0^2$  at about 0.1 Ryd and then keeps a plateau to 0.25 Ryd. The F wave monotonically increases from 0.0 to 0.25Ryd.

We plot the total charge transfer, total elastic and total Ps+p scattering (charge transfer plus elastic) cross sections as a function of Ps energy in Figure 4.16. One feature of this plot is that the total charge transfer cross section contains a minimum at about 0.0013 Ryd (about 0.02 eV)[74]. The minimum is caused by a sharp increase of the P-wave curve with large cross sections and a sharp decrease of the S-wave curve with relative small values in that energy range. The total elastic cross section has a sharp decrease at very low energies and then very slowly decreases. The total cross section has the same behavior as the elastic one.

#### 4.1.3 Resonance below the H First Excitation

Mittleman (1966) [109] predicted that there exist infinite resonances formed below the H first excitation threshold for positron-hydrogen scattering. The physical origin of these resonances arise from a long range force ( $\frac{1}{r^3}$ ) which stems from the degeneracy of the 2s and 2p hydrogen states (Mittleman 1966 [109], Gien 1996 [89]). Basu et al. (1989) [62] and Sarkar et al. (1993) [64] claimed they observed two resonances just above the Ps formation threshold. Mitroy and Stelbovics (1994) [70] and Gien and Liu (1994) [110] did not confirm the existence of the resonances at energy just above the Ps formation threshold. However, the three S-wave resonances observed by Seiler et al. (1971) [50] and Wakid (1975) [53] were reproduced by Mitroy and Stelbovics (1994) [70] for the first one in their six-state close coupling (CC) calculation and later for the first two in the 12-state (Mitroy and Ratnavelu 1995 [71]) and the 21-state (Mitroy 1995 [73]) CC calculations and by Gien (1994,1995) [83,87,88,89] for all of the three S-wave and two P-wave resonances in his six-state Harris-Nesbet calculation. Gien also observed a sequence of the resonances for the S-, P- and D-waves.

In this work, we also search for resonant structures for different partial waves. We do not find any resonance just above the Ps formation threshold. But we observed three S-wave, two P-wave and one D-wave resonances located below the first H excitation threshold (see Table 4.11). Besides, more resonances could be observed if a larger basis set is used. One may argue why the resonance depends on the selected basis. The reason is quite simple. Suppose that these resonances indeed exist for this scattering system, but theoretically how would we know they are really there? The only way we can theoretically do for this micro-system is to use our "theoretical detector"- a suitable basis and then do our calculations in the frame of quantum theory. If the "detector" is not good enough (that means, the basis is not

good or large enough) to detect some very narrow resonance, it won't appear in the theoretical results. However, the further resonances are very close to the threshold and with much narrower widths (less than  $10^{-8}$  Ryd, Gien 1996 [89]). Moreover, the numerical accuracy (thinking about we have to calculate thousands of hundreds of two dimensional integrals for each given scattering energy.) may not guarantee that we can give the correct positions and widths of these new and very narrow resonances. Meanwhile, further finer search for the resonances will be too CPU consumption for such a larger calculation. So we stop further searching for these resonances.

In order to identify a resonance for a multichannel scattering, we use the sum of eigenphase shifts for different open channels. The eigenphase shifts can be obtained by diagonalizing the reaction matrix  $R$ . By doing that, we obtain the eigenvalues of the matrix  $R$  which are equal to the tangents of the eigenphase shifts for different channels. So the sum of eigenphase shifts is a function of scattering energy. The eigenphase sum has a very slow change when it is away from a resonance energy (we call it the background) and a very sharp jump when it is reaching a resonance.

In Figures 4.17-4.25, we plot the sum of the eigenphase shifts, elastic and Ps formation cross sections of these resonances. We apply the following formula

$$\delta_L = \delta_L^0 + \tan^{-1}\left(\frac{\frac{1}{2}\Gamma}{E_{res} - E}\right) \quad (4.2)$$

to estimate the positions and widths of resonances. Where  $\delta_L$  and  $\delta_L^0$  are the sum of the eigenphase shift and its background respectively.  $\Gamma$  and  $E_{res}$  are the respective width and position of the resonance. Fitting this formula to an individual resonance, we obtained the positions and widths of these resonances and list them in the Table 4.11.

From Table 4.11, we can see that the present positions and widths of the resonances for S-, P- and D-waves are in good agreement with those from the 21-state

Table 4.11: Resonances of positron-hydrogen scattering below the first H excitation.

L	Position (Ryd)	Width (Ryd)	CC33 (Ryd)
0	0.74291	$1.62 \times 10^{-4}$	(0.744089, $4.92 \times 10^{-5}$ ) <sup>f</sup>
	0.74294 <sup>a</sup>	$1.56 \times 10^{-4}$	(0.74414, $5.1 \times 10^{-5}$ ) <sup>g</sup>
	0.742688 <sup>b</sup>	$1.328 \times 10^{-4}$	
	0.74294 <sup>c</sup>		
	0.742755 <sup>d</sup>	$1.332 \times 10^{-4}$	
	0.74298 <sup>e</sup>		
0	0.74964	$8.0 \times 10^{-6}$	(0.749670, $2.80 \times 10^{-6}$ ) <sup>f</sup>
	0.74964 <sup>a</sup>	$7.9 \times 10^{-6}$	(0.74967, $4.7 \times 10^{-6}$ ) <sup>g</sup>
	0.749698 <sup>b</sup>	$7.82 \times 10^{-6}$	
	0.74983 <sup>d</sup>	$< 2.0 \times 10^{-5}$	
0	0.749988	$\approx 10^{-7}$	(0.749981, $1.61 \times 10^{-7}$ ) <sup>f</sup>
1	0.74599	$1.53 \times 10^{-5}$	.
	0.74609 <sup>a</sup>	$1.58 \times 10^{-5}$	
	0.745868 <sup>b</sup>	$1.630 \times 10^{-5}$	
	0.745888 <sup>d</sup>	$1.62 \times 10^{-5}$	
1	0.74993	$7.6 \times 10^{-7}$	.
	0.74987 <sup>a</sup>	$4.5 \times 10^{-7}$	
	0.74989 <sup>b</sup>	$4.2 \times 10^{-7}$	
2	0.74994	$2.8 \times 10^{-6}$	.
	0.74990 <sup>a</sup>	$2.1 \times 10^{-6}$	

<sup>a</sup> 21-state close coupling calculation by Mitroy (1995) [71].<sup>b,c</sup>Hyperspherical close coupling by Zhou and Lin (1995) [105] and Archer et al. (1990) [106].<sup>d</sup> Complex coordinate rotation by Ho (1990) [111].<sup>e</sup> Peliken and Klar (1983) [112].<sup>f</sup> Gien (1994,1995) [83,87,88,89].<sup>g</sup> Mitroy and Ratnavelu (1995) [71].

close coupling calculation by Mitroy (1995) [71], the hyperspherical close coupling by Zhou and Lin (1995) [105], and some other calculations by Ho (1990) [111], using the complex coordinate rotation method, and by Peliken and Klar (1983) [112]. The slight differences among these positions are expected because of different coupling schemes used in different research groups, which represent slightly different optical potentials from the closed channels. In addition, we also observed the third S-wave resonance (not shown) which is located at positron energy 0.749988 Ryd. Its width is very narrow: about  $10^{-7}$  Ryd. This resonance was first found by Seiler et al. (1971) [50], by Wakid (1975) [53], and very recently by Gien (1994,1995) [83,87,88,89] in his six-state Harris-Nesbet calculation. The position and width of this resonance are in good agreement with what Gien obtained. The width of Seiler et al.'s resonance is much narrower than ours , which is predictable because the scheme just included three lowest hydrogen states. Wakid's width, however, is too broad. Looking at three resonances he observed, the widths of these resonances are several order in magnitude larger than those obtained by Gien and the present calculation.

In addition to the positions and widths of these resonances, we also compare their shapes with those from the 21-state (Mitroy 1995 [71]) and hyperspherical (Zhou and Lin 1995 [105]) close coupling calculations (not shown). We note that all of the present observed resonances, especially the first S-wave resonance (Gien[89]), display the detailed same shapes as those of Mitroy's and Zhou and Lin's. In comparison with those of the six-state calculation (Gien 1994,1995 [83,87,88,89]), we noted that the present S-wave resonances show the same shapes as the six-state's for the eigenphase sums and elastic cross sections, except for small shifts of the positions and completely different magnitudes. But the present Ps formation cross section curves (see Figure 4.17 and 4.19) demonstrate completely different shapes around the resonances. In the six-state calculation, the Ps formation cross section

curves first decrease, then pass a zero, after then sharply increase to the peak, and finally decrease to the background level. In contrast, the present results show that they first sharply increase to the peak, then decrease, after then pass a zero, and finally back to the background level. We may expect that the differences in shape are due to the incomplete inclusion of the optical potential from the Q-space in the six-state coupling scheme.

Further, we also observed that the S-wave resonances occur on a relatively large negative background of the eigenphase shift sum (see Figures 4.16 and 4.18). This large negative eigenphase shift implies that the repulsive short range potential plays a main role at these energies. This property causes the behaviour of the S-wave resonances different from the P- and D-waves. In the P- and D-wave cases (see Figures 4.20, 4.22 and 4.24) , the background eigenphase shift sums are very close to zero and the resonances display good symmetrical properties. These resonances could be considered to be close to the standard Breit-Wigner structures.

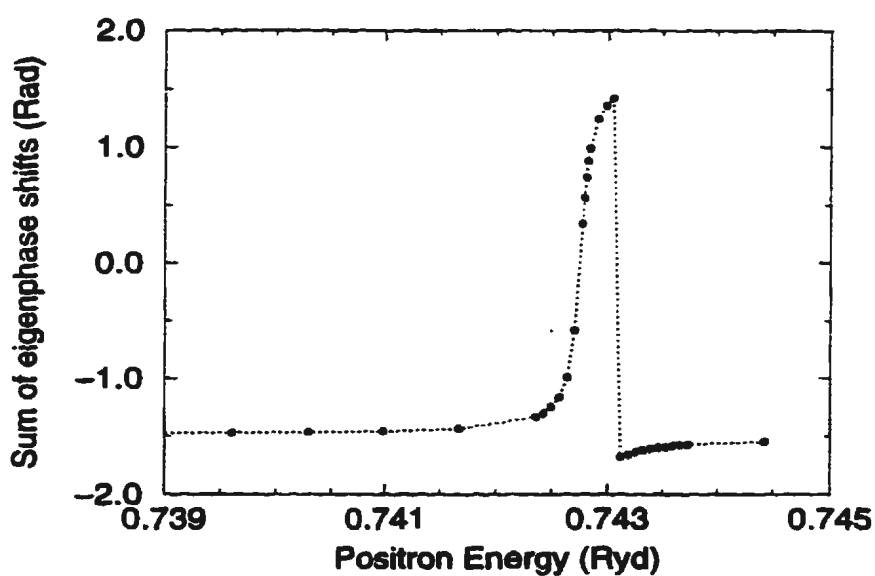


Figure 4.17: The eigenphase sum of positron-hydrogen scattering is plotted as a function of positron energy: the first resonance of the S-wave.

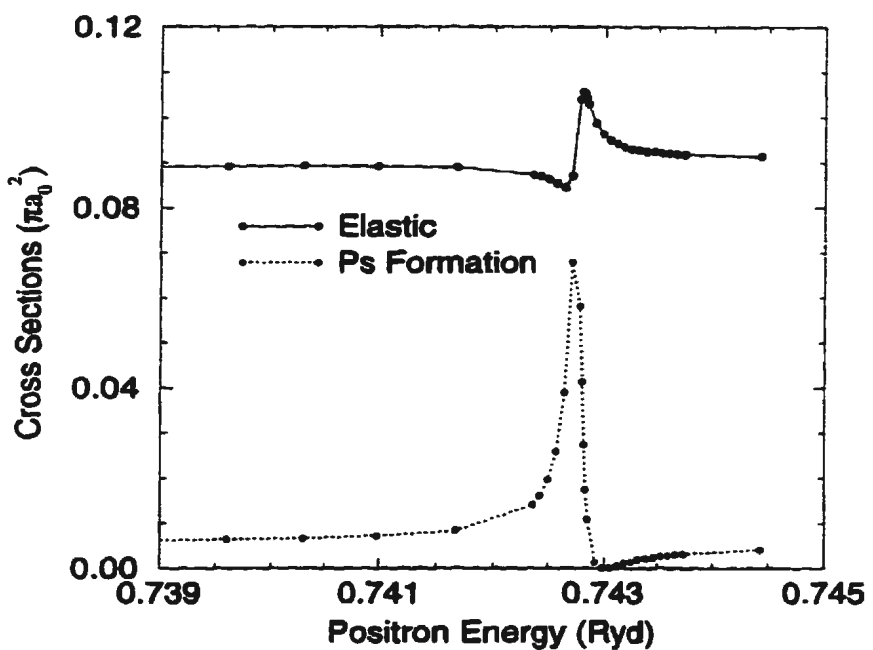


Figure 4.18: Elastic and Ps formation cross sections of positron-hydrogen scattering is plotted as a function of positron energy: the first resonance of the S-wave.

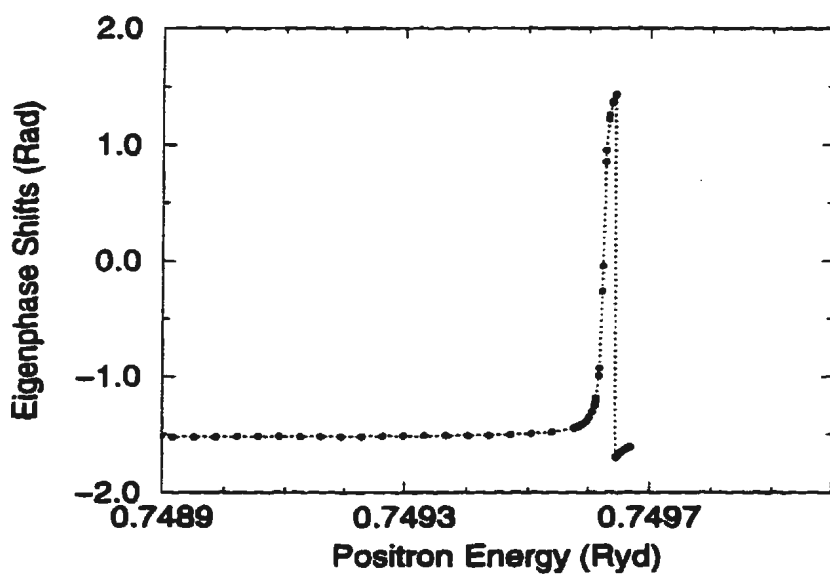


Figure 4.19: The eigenphase sum of positron-hydrogen scattering is plotted as a function of positron energy: the second resonance of the S-wave.

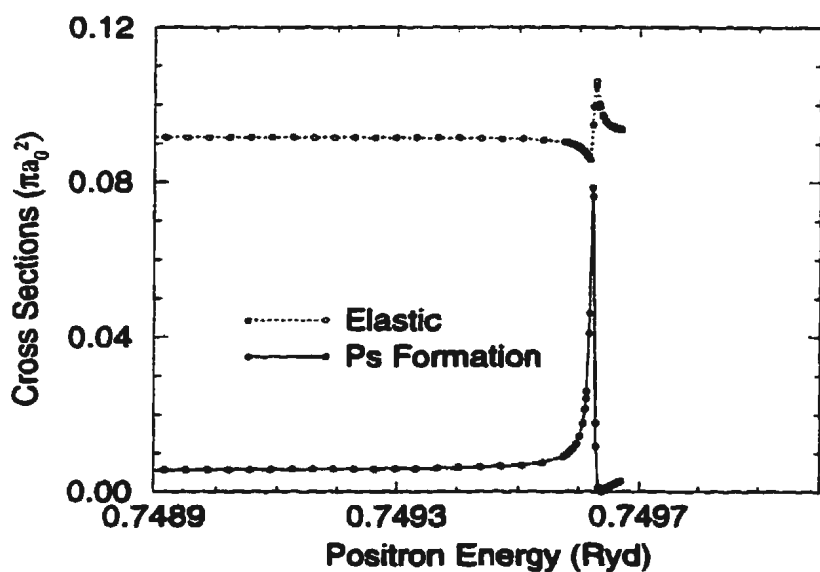


Figure 4.20: Elastic and Ps formation cross sections of positron-hydrogen scattering is plotted as a function of positron energy: the second resonance of the S-wave.

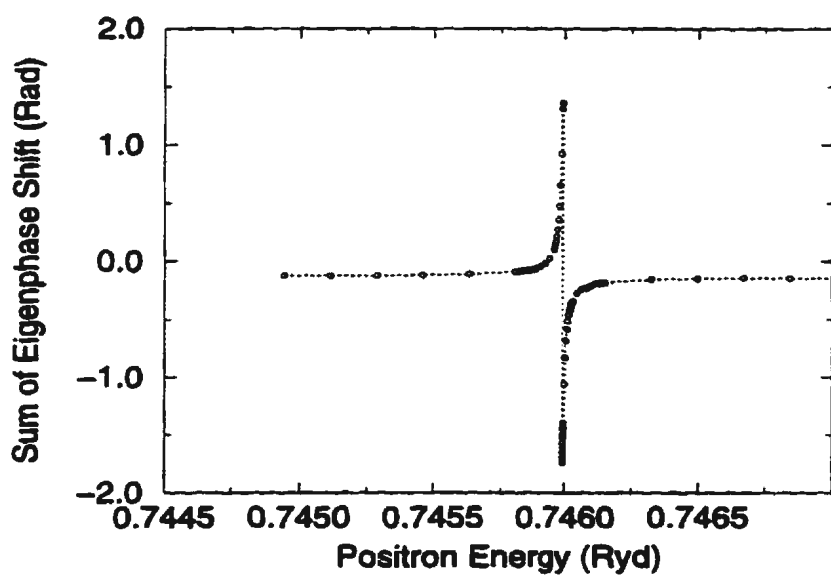


Figure 4.21: The eigenphase sum of positron-hydrogen scattering is plotted as a function of positron energy: the first resonance of the P-wave.

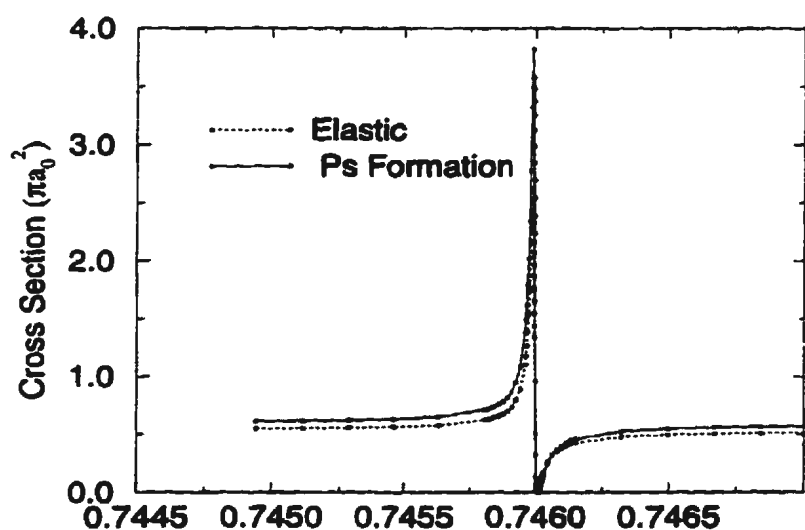


Figure 4.22: Elastic and Ps formation cross sections of positron-hydrogen scattering is plotted as a function of positron energy: the first resonance of the P-wave.

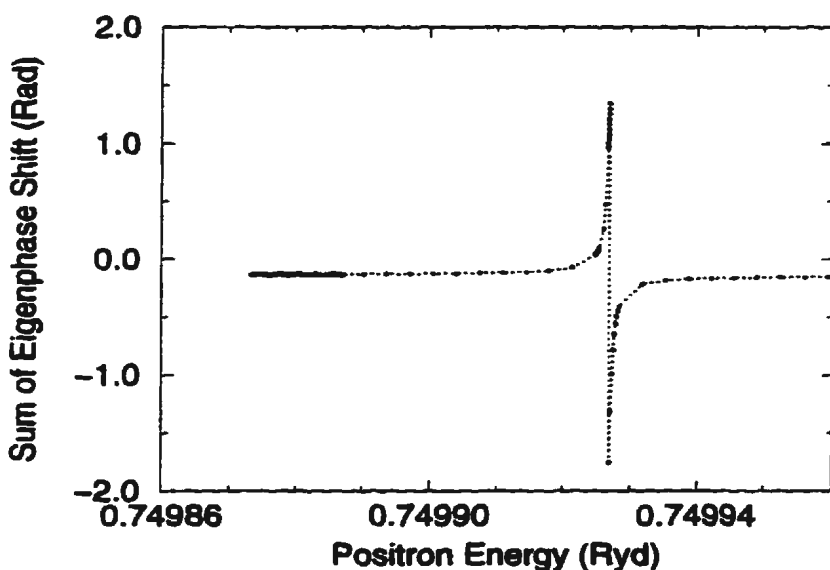


Figure 4.23: The eigenphase sum of positron-hydrogen scattering is plotted as a function of positron energy: the second resonance of the P-wave.

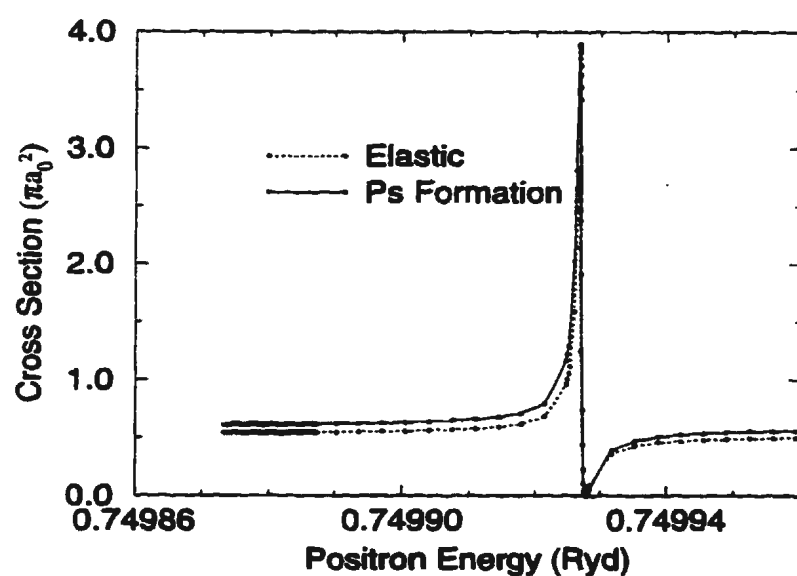


Figure 4.24: Elastic and Ps formation cross sections of positron-hydrogen scattering is plotted as a function of positron energy: the second resonance of the P-wave.

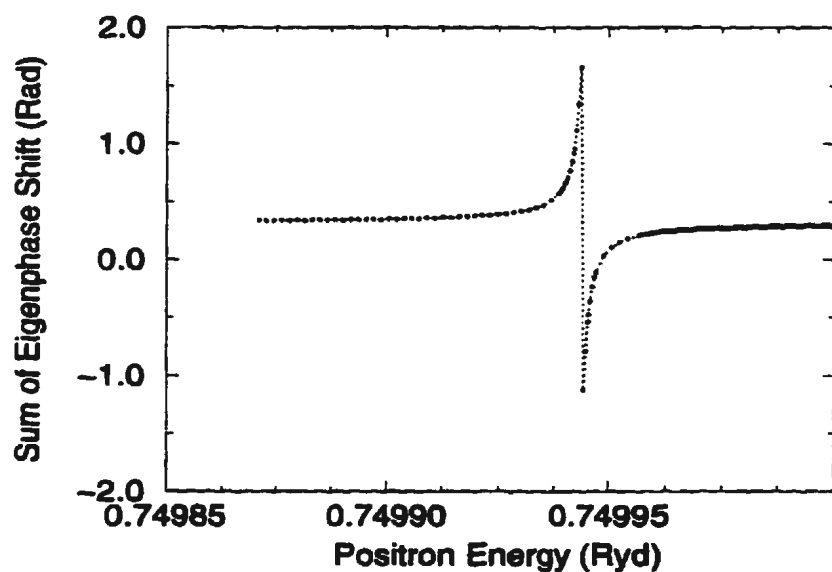


Figure 4.25: The eigenphase sum of positron-hydrogen scattering around the D-wave resonance is plotted as a function of positron energy.

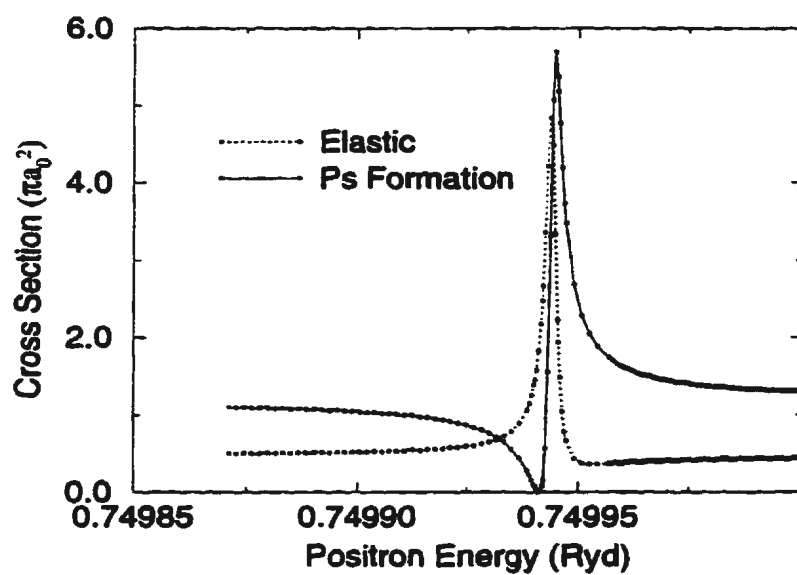


Figure 4.26: Elastic and Ps formation cross sections of positron-hydrogen scattering around the D-wave resonance is plotted as a function of positron energy.

## 4.2 Calculations with 18- and 20-state bases

### 4.2.1 Numerical Approaches

Our previous calculation using the B7+ basis in the last section achieved physical convergence and gave very accurate results of phase shifts, positron elastic and Ps formation cross sections for partial waves from  $L=0$  to 6. These results agreed well with the most accurate variational S- and P-wave scattering parameters of Bhatia et al. (1971, 1974) [36, 37] and Brown and Humberston (1985) [29] and with the 21-state T-matrix close coupling calculations by Mitroy (1995) [71]. Our Ps-p elastic cross sections, however, are not in perfect agreement with the 21-state results (Mitroy 1995 [73]), in particular for the higher partial waves. We expect that this disagreement may be due to the basis used, which did not include the whole dipole polarization potential of the ground Ps. Furthermore, some discrepancies visibly observed from the 18-state R-matrix calculation by Kernoghan et al. (1994,1995) [78, 79], especially for their S-wave cross sections, may not be simply said to be numerical inaccuracy. Trying to solve these problems formed our motivation of further investigation of this system by using the following scattering channel spaces (Kuang and Gien 1996 [115]):

- (1) 18-states. This basis is exactly the same as that used by McAlinden et al. (1994) [77] and Kernoghan et al. (1995) [79], which is composed of nine hydrogenic states and nine positronium states:  $(1s, 2s, 2p, 3\bar{s}, 3\bar{p}, 3\bar{d}, 4\bar{s}, 4\bar{p}, 4\bar{d})$  proposed by Fon et al. (1981) [113]. This basis gives good dipole but very poor quadrupole polarization.
- (2) 20-states. This basis contains 12 hydrogen states:  $1s, 2s, 2p, 3s, 3p, 3d, 4\bar{s}, 4\bar{p}, 4\bar{d}, 5\bar{s}, 5\bar{p}, 6\bar{p}$ , and 8 Ps states:  $1s, 2s, 2p, 3\bar{s}, 3\bar{p}, 3\bar{d}, 4\bar{s}$  and  $4\bar{p}$ , which are exactly the same as the 21-states used by Mitroy (1995) [71] without the pseudo-state  $4\bar{f}$  of

hydrogen. This basis gives the good dipole and quadruple polarization potentials.

#### 4.2.2 Results

The present partial wave phase shifts, positron elastic and Ps formation cross sections for the positron-hydrogen entrance channel are tabulated in Tables 4.12-4.13, Tables 4.14-4.15, and Tables 4.16-4.17, respectively. Ps elastic cross sections for the Ps-p entrance channel are listed in Table 4.18. Looking at Table 4.12 , the 20-state S- and P-wave phase shifts are in very good agreement with the 21-state data (Mitroy 1995) [71], our B7+ basis results (Kuang and Gien 1996) [114], and variational values of Bhatia et al. (1971) [36]. This good agreement implies that these values are what we physically expect. However, there obviously are discrepancies between the 18-state results and the other four data sets for the S-wave, as well as the P-wave at higher momenta. The above differences may imply that the 18-state basis does not describe the channel electrostatic potential well for the lower angular momentum partial waves; more specifically, they give slightly stronger electrostatic potential than the real one. This effect will partly cancel the long range polarization potential. At the low positron momenta, the cancellation has small effects on the phase shifts because the long range dipole potential is more important there. However, as the positron momentum increases, both the electrostatic and dipole polarization potentials are significant, especially around the zero point of the whole channel potential (electrostatic plus polarization) where the phase shifts are very sensitive to the cancellation. At  $k=0.6$ , the 18-state S-wave phase shifts even change their signs to negative which implies that the positive electrostatic potential begins to play an important role at  $k \geq 0.6$ . But the 20-state results and other calculations show this will happen at  $k$  larger than 0.6. Therefore, the sensitivity of the S-wave phase shift can be used to determine whether a basis is good enough for

this scattering system.

Using a similar way to the last section, we obtain the positron scattering lengths  $2.060 \pm 0.005 a_0$  and  $2.100 \pm 0.003 a_0$  for the 18-state and 20-state coupling schemes, respectively. In comparison with the result from B7+ basis, the 18-state scattering length seems small, which is expected from the reason discussed above. For the 20-state coupling scheme, the length is in quite good agreement with our mixing basis value and the 21-state T-matrix result:  $2.08 \pm 0.02 a_0$ .

For the D-wave case, four sets listed in Table 4.12 are in excellent agreement with each other since the dipole polarization becomes more important than the electrostatic potential for higher partial waves.

For partial waves  $L=3, 4, 5$ , and  $6$  (see Table 4.13), the present 18-state phase shifts, as well as the 20-state data for F partial wave, show good agreement with our mixing basis calculations and the 21-state results at higher momenta. At lower momenta, this work seems closer to the 21-state. The present total elastic cross sections summing the partial waves from  $L=0$  to  $6$  are about 1 to 2% smaller than our mixing basis and 21-state results.

Table 4.14 tabulates the present elastic cross sections for the S and P partial waves. The 18-state value of McAlinden et al. (1994) [76] at  $k=0.8$  agrees well with ours for the S partial wave. But their P-wave cross section is about 1.5% different from ours. The very good agreement is obtained between the 20-state, 21-state, mixing basis, and variational results. The very recent hyperspherical close coupling calculation by Zhou and Lin (1995) [105] also show reasonable agreement with ours at the hyper radii  $R_0 = 29.93 a_0$ . However, differences between the 18-state results and other four sets are about 10% and 1.5% for the S and P partial waves respectively. It may be interpreted that the stronger channel electrostatic potential of the 18-state basis may cause the S-wave elastic cross section to be larger and the

Table 4.12: S, P and D partial wave phase shifts (in units of radiation) for positron-hydrogen scattering in 18- and 20-state approximations. The numbers in [ ] indicate the powers of 10.

k(a.u.)	0.1	0.2	0.3	0.4	0.5	0.6	0.7
L = 0							
18-state <sup>a</sup>	0.1455	0.1834	0.1624	0.1148	0.573[-1]	-0.134[-2]	-0.564[-1]
20-state <sup>b</sup>	0.1474	0.1866	0.1662	0.1188	0.614[-1]	0.270[-2]	-0.523[-1]
21-state <sup>c</sup>	0.1474	0.1868	0.1667	0.1191	0.621[-1]	0.31 [-2]	-0.518[-1]
B7+ <sup>d</sup>	0.1483	0.1875	0.1670	0.1195	0.620[-1]	0.330[-2]	-0.519[-1]
Variational <sup>e</sup>	0.1483	0.1877	0.1677	0.1201	0.624[-1]	0.39 [-2]	-0.512[-1]
L = 1							
18-state <sup>a</sup>	0.885[-2]	0.326[-1]	0.653[-1]	0.0996	0.1295	0.1530	0.1770
20-state <sup>b</sup>	0.883[-2]	0.326[-1]	0.655[-1]	0.1000	0.1301	0.1538	0.1780
21-state <sup>c</sup>	0.887[-2]	0.327[-1]	0.657[-1]	0.1002	0.1306	0.1542	0.1788
B7+ <sup>d</sup>	0.886[-2]	0.327[-1]	0.657[-1]	0.1002	0.1305	0.1544	0.1782
Variational <sup>e</sup>	0.338[-1]	0.665[-1]	0.1016	0.1309	0.1547	0.1799	
L = 2							
18-state <sup>a</sup>	0.134[-2]	0.548[-2]	0.129[-1]	0.241[-1]	0.395[-1]	0.595[-1]	0.880[-1]
20-state <sup>b</sup>	0.133[-2]	0.546[-2]	0.129[-1]	0.241[-1]	0.395[-1]	0.595[-1]	0.881[-1]
21-state <sup>c</sup>	0.136[-2]	0.551[-2]	0.129[-1]	0.242[-1]	0.397[-1]	0.598[-1]	0.885[-1]
B7+ <sup>d</sup>	0.133[-2]	0.549[-2]	0.129[-1]	0.241[-1]	0.396[-1]	0.597[-1]	0.883[-1]

<sup>a,b</sup>the present 18-state and 20-state close couplings respectively.

<sup>c</sup>the 21-state close coupling, Mitroy (1995) [73].

<sup>d</sup>the mixing basis coupling, Kuang and Gien (1996) [114].

<sup>e</sup>the variational calculation, Brown and Humberston (1985) [29].

Table 4.13: F, G, H, and I partial wave phase shifts (in units of radiation) for positron-hydrogen scattering in 18- and 20-state approximations. The numbers in [ ] indicate the powers of 10.

k(a.u.)	0.1	0.2	0.3	0.4	0.5	0.6	0.7
L = 3							
18-state <sup>a</sup>	0.445[-3]	0.177[-2]	0.407[-2]	0.750[-2]	0.125[-1]	0.197[-1]	0.305[-1]
20-state <sup>b</sup>	0.444[-3]	0.177[-2]	0.404[-2]	0.747[-2]	0.124[-1]	0.196[-1]	0.304[-1]
21-state <sup>c</sup>	0.452[-3]	0.180[-2]	0.409[-2]	0.754[-2]	0.126[-1]	0.198[-1]	0.307[-1]
B7+ <sup>d</sup>	0.435[-3]	0.177[-2]	0.406[-2]	0.750[-2]	0.125[-1]	0.197[-1]	0.305[-1]
L = 4							
18-state <sup>a</sup>	0.200[-3]	0.804[-3]	0.180[-2]	0.326[-2]	0.523[-2]	0.793[-2]	0.119[-1]
21-state <sup>c</sup>	0.205[-3]	0.819[-3]	0.183[-2]	0.329[-2]	0.530[-2]	0.807[-2]	0.121[-1]
B7+ <sup>d</sup>	0.193[-3]	0.793[-3]	0.180[-2]	0.325[-2]	0.525[-2]	0.799[-2]	0.119[-1]
L = 5							
18-state <sup>a</sup>	0.106[-4]	0.429[-3]	0.967[-3]	0.172[-2]	0.271[-2]	0.398[-2]	0.574[-2]
21-state <sup>c</sup>	0.109[-3]	0.443[-3]	0.986[-3]	0.175[-2]	0.277[-2]	0.410[-2]	0.587[-2]
B7+ <sup>d</sup>	0.100[-3]	0.420[-3]	0.958[-3]	0.172[-2]	0.272[-2]	0.403[-2]	0.576[-2]
L = 6							
18-state <sup>a</sup>	0.628[-4]	0.255[-3]	0.575[-3]	0.102[-2]	0.160[-2]	0.231[-2]	0.325[-2]
21-state <sup>c</sup>	0.633[-4]	0.266[-3]	0.593[-3]	0.105[-2]	0.165[-2]	0.241[-2]	0.336[-2]
B7+ <sup>d</sup>	0.571[-4]	0.248[-3]	0.566[-3]	0.101[-2]	0.160[-2]	0.234[-2]	0.327[-2]
$\sigma_{\text{elastic}}$							
18-state <sup>a</sup>	8.567	3.676	1.776	1.153	0.998	1.008	1.141
21-state <sup>c</sup>	8.736	3.787	1.844	1.192	1.026	1.026	1.186
B7+ <sup>d</sup>	8.826	3.815	1.847	1.193	1.022	1.024	1.177

<sup>a,b</sup>the present 18-state and 20-state close couplings respectively.

<sup>c</sup>the 21-state close coupling, Mitroy (1995) [73].

<sup>d</sup>the mixing basis coupling, Kuang and Gien (1996) [114].

P-wave one to be smaller. The reason is that this potential plays the main role for the S-wave in the Ore gap but for the P-wave the polarization replaces it. For  $L=2, 3, 4$ , and  $5$  partial waves (see Table 4.15), the present close coupling elastic cross sections agree very well with the existing accurate data sets in the whole Ore gap. The present 18-state total cross sections also give good agreement with the 21-state ones and our B7+ basis results since small differences of the S and P partial waves do not affect the total cross sections.

Table 4.16 indicates the positronium formation cross sections. A main feature of this table for the S-wave is that all sets group into two classes: 18-state sets and other five sets. Within each class, the agreement is good. However, it is clear that the 18-state sets are up to 15% smaller than other four groups of data. It may be explained that the S-wave Ps formation cross section itself is very small, so any small effect from the channel electrostatic potential which conducts more probability into the elastic channel would cause a relatively large difference on the Ps formation cross section. For the P partial wave, all of the data sets display excellent agreement except for the 18-state result of McAlinden et al. (1994) at  $k=0.71$  where their value may contain some numerical inaccuracy. The present Ps formation cross sections for the partial waves  $L=2, 3, 4$ , and  $5$  (see Table 4.17) are also in very good agreement with the 21-state data (Mitroy 1995) and our B7+ basis values (Kuang and Gien 1996). The total Ps formation cross sections of the present 18-state calculation again agree well with the 21-state and our mixing basis results since the difference in the S partial wave only has small contribution to the total cross section.

An obvious feature of Table 4.18 for the Ps partial wave elastic cross sections is that very good agreement between different approaches has been achieved. Unlike

Table 4.14: S and P wave elastic cross sections ( $\pi a_0^2$ ) of positron-hydrogen scattering in 18- and 20-state approximations. The numbers in [ ] indicate the powers of 10.

k(a.u)	0.71	0.75	0.80	0.85
L = 0				
18-state <sup>a</sup>	0.300[-1]	0.481[-1]	0.706[-1]	0.915[-1]
18-state <sup>b</sup>			0.71[-1]	
20-state <sup>c</sup>	0.261[-1]	0.434[-1]	0.654[-1]	0.859[-1]
21-state <sup>d</sup>	0.258[-1]	0.430[-1]	0.657[-1]	0.849[-1]
B7+ <sup>e</sup>	0.258[-1]	0.431[-1]	0.651[-1]	0.858[-1]
HSCC <sup>f</sup>	0.238[-1]	0.415[-1]	0.624[-1]	0.862[-1]
Variational <sup>g</sup>	0.26[-1]	0.43 [-1]	0.65 [-1]	0.85 [-1]
L = 1				
18-state <sup>a</sup>	0.789	0.713	0.615	0.540
18-state <sup>b</sup>			0.624	
20-state <sup>c</sup>	0.798	0.721	0.622	0.547
21-state <sup>d</sup>	0.802	0.726	0.626	0.551
KG <sup>e</sup>	0.800	0.723	0.624	0.549
Variational <sup>g</sup>	0.789	0.724	0.622	0.547

<sup>a,c</sup>the present 18- and 20-state close couplings respectively.

<sup>b</sup>the 18-state close coupling, McAlinden et al. (1994) [76].

<sup>d</sup>the 21-state close coupling, Mitroy (1995) [73].

<sup>e</sup>the mixing basis coupling, Kuang and Gien (1996) [114].

<sup>f</sup>the hyperspherical close coupling with the hyper radii  $R_0=29.93 a_0$ , Zhou and Lin (1995) [105].

<sup>g</sup>the variational calculation, Humberston (1984) [27], Brown and Humberston (1984,1985) [28, 29].

the positron elastic cross sections for lower partial waves, the present 18- and 20-state and the 21-state results of Mitroy (1995) for all partial waves agree well with each other. This is because the dipole polarization potential is a much stronger and has much longer interaction range for the Ps ground state than that for the H ground state. Hence, the Ps channel electrostatic potential has an invisible effect on the Ps elastic scattering cross section at energies considered. However, our previous calculation, using a basis with an incomplete inclusion of the dipole polarization of Ps(1s), causes some inaccuracies in Ps elastic cross sections, especially at higher partial waves. Again summing from  $L=0$  to 6, we obtain the total Ps elastic cross section. The present 18-state total cross section agree very well with the 21-state one.

For the Ps scattering length, the 18-state value is, unlike in the positron case, in good agreement with the 20-state one. The former is  $-15.7 \pm 0.1$   $a_0$  and the later is  $-15.6 \pm 0.1$   $a_0$ , which also agree well with  $-15.5 \pm 0.4$   $a_0$  from the 21-state T-matrix calculation [74]. The reason for this agreement is that the dipole polarization of Ps(1s) is dominant at energies considered here and both coupling schemes can express the dipole polarization of Ps(1s) very well.

Table 4.15: D, F, G, H, and I partial wave elastic cross sections ( $\pi a_0^2$ ) of positron-hydrogen scattering in 18- and 20-state approximations. The numbers in [ ] indicate the powers of 1 .

k(a.u)	0.71	0.75	0.80	0.85
$L = 2$				
18-state <sup>a</sup>	0.337	0.441	0.480	0.472
18-state <sup>b</sup>			0.482	
20-state <sup>c</sup>	0.338	0.442	0.480	0.472
21-state <sup>d</sup>	0.341	0.446	0.484	0.477
B7+ <sup>e</sup>	0.339	0.444	0.482	0.474
Variational <sup>f</sup>	0.323	0.403	0.423	0.413
$L = 3$				
18-state <sup>a</sup>	0.567[-1]	0.772[-1]	0.110	0.133
20-state <sup>c</sup>	0.565[-1]	0.768[-1]	0.109	0.133
21-state <sup>d</sup>	0.575[-1]	0.781[-1]	0.111	0.135
B7+ <sup>e</sup>	0.568[-1]	0.773[-1]	0.110	0.134
$L = 4$				
18-state <sup>a</sup>	0.110[-1]	0.139[-1]	0.195[-1]	0.267[-1]
B7+ <sup>e</sup>	0.110[-1]	0.140[-1]	0.198[-1]	0.270[-1]
$L = 5$				
18-state <sup>a</sup>	0.308[-2]	0.367[-2]	0.468[-2]	0.621[-2]
B7+ <sup>e</sup>	0.311[-2]	0.373[-2]	0.481[-2]	0.632[-2]
$L = 6$				
18-state <sup>a</sup>	0.116[-2]	0.134[-2]	0.158[-2]	0.197[-2]
Total				
18-state <sup>a</sup>	1.227	1.297	1.300	1.272
21-state <sup>d</sup>	1.242	1.313	1.316	1.285
B7+ <sup>e</sup>	1.237	1.307	1.308	1.278

<sup>a,c</sup>the present 18- and 20-state close couplings respectively.

<sup>b</sup>the 18-state close coupling, McAlinden et al. (1994) [76].

<sup>d</sup>the 21-state close coupling, Mitroy (1995) [73].

<sup>e</sup>the mixing basis coupling, Kuang and Gien (1996) [114].

Table 4.16: S and P wave positronium formation cross sections ( $\pi a_0^2$ ) of positron-hydrogen scattering in 18- and 20-state approximations. The numbers in [ ] indicate the powers of 10.

$k(\text{a.u.)}$	0.71	0.75	0.80	0.85
$L = 0$				
18-state <sup>a</sup>	0.352[-2]	0.378[-2]	0.429[-2]	0.495[-2]
18-state <sup>b</sup>	0.33 [-2]	0.30 [-2]	0.41 [-2]	0.47 [-2]
20-state <sup>c</sup>	0.404[-2]	0.431[-2]	0.486[-2]	0.560[-2]
21-state <sup>d</sup>	0.405[-2]	0.427[-2]	0.472[-2]	0.560[-2]
B7+ <sup>e</sup>	0.404[-2]	0.441[-2]	0.493[-2]	0.549[-2]
HSCC <sup>f</sup>	0.394[-2]	0.427[-2]	0.483[-2]	0.557[-2]
Variational <sup>g</sup>	0.41[-2]	0.44 [-2]	0.49 [-2]	0.58[-2]
$L = 1$				
18-state <sup>a</sup>	0.269[-1]	0.369	0.485	0.566
18-state <sup>b</sup>	0.46 [-1]	0.376	0.485	0.573
20-state <sup>c</sup>	0.266[-1]	0.366	0.482	0.563
21-state <sup>d</sup>	0.266[-1]	0.366	0.483	0.563
B7+ <sup>e</sup>	0.267[-1]	0.367	0.483	0.565
Variational <sup>g</sup>	0.27 [-1]	0.365	0.482	0.561

<sup>a,c</sup>the present 18- and 20-state close couplings.

<sup>b</sup>the 18-state close coupling, McAlinden et al. (1994) [76].

<sup>d</sup>the 21-state close coupling, Mitroy (1995) [73].

<sup>e</sup>the mixing basis coupling, Kuang and Gien (1996) [114].

<sup>f</sup>the hyperspherical close coupling with the hyper radii  $R_0=29.93 a_0$ , Zhou and Lin (1995) [105].

<sup>g</sup>the variational calculation, Brown and Humberston (1985) [29].

Table 4.17: D, F, G, H and I partial wave positronium formation cross sections ( $\pi a_0^2$ ) of positron-hydrogen scattering in 18- and 20-state approximations. The numbers in [ ] indicate the powers of 10.

k(a.u)	0.71	0.75	0.80	0.85
L = 2				
18-state <sup>a</sup>	0.684[-3]	0.321	0.859	1.158
18-state <sup>b</sup>	0.85[-3]	0.373	0.871	1.170
20-state <sup>c</sup>	0.681[-3]	0.320	0.858	1.156
21-state <sup>d</sup>	0.682[-3]	0.320	0.859	1.158
B7+ <sup>e</sup>	0.683[-3]	0.320	0.862	1.162
Variational <sup>f</sup>	0.62[-3]	0.335	0.812	1.057
L = 3				
18-state <sup>a</sup>	0.445[-5]	0.356[-1]	0.270	0.594
20-state <sup>c</sup>	0.438[-5]	0.356[-1]	0.270	0.595
21-state <sup>d</sup>	0.44[-5]	0.356[-1]	0.270	0.596
B7+ <sup>e</sup>	0.500[-5]	0.354[-1]	0.271	0.596
L = 4				
18-state <sup>a</sup>		0.223[-2]	0.386[-1]	0.143
B7+ <sup>e</sup>		0.219[-2]	0.388[-1]	0.143
L = 5				
18-state <sup>a</sup>		0.117[-3]	0.415[-2]	0.238[-1]
B7+ <sup>e</sup>		0.113[-3]	0.425[-2]	0.241[-1]
L = 6				
18-state <sup>a</sup>			0.403[-3]	0.332[-2]
Total				
18-state <sup>a</sup>	0.310[-1]	0.731	1.663	2.492
21-state <sup>d</sup>	0.313[-1]	0.728	1.660	2.49
B7+ <sup>e</sup>	0.315[-1]	0.729	1.666	2.499

<sup>a,c</sup>the present 18- and 20-state close couplings.

<sup>b</sup>the 18-state close coupling, McAlinden et al.(1994) [76].

<sup>d</sup>the 21-state close coupling, Mitroy (1995) [73].

<sup>e</sup>the mixing basis coupling, Kuang and Gien (1996) [114].

Table 4.18: The partial wave elastic cross sections ( $\pi a_0^2$ ) for Ps + p scattering in 18- and 20-state approximations. The numbers in [ ] indicate the powers of 10.

Energy(Ryd)	0.0041	0.0625	0.014	0.02225
$L = 0$				
18-state <sup>a</sup>	59.7	6.95	9.88	8.34
20-state <sup>b</sup>	59.3	6.96	9.89	8.34
21-state <sup>c</sup>	59.7	6.92	9.86	8.32
B7+ <sup>d</sup>	58.4	7.05	9.93	8.37
Variational <sup>e</sup>	56.7	7.05	9.93	8.37
$L = 1$				
18-state <sup>a</sup>	15.1	4.10	0.172	1.80
20-state <sup>b</sup>	15.0	4.06	0.173	1.82
21-state <sup>c</sup>	15.2	4.17	0.160	1.77
B7+ <sup>d</sup>	14.4	3.93	0.197	1.92
$L = 2$				
18-state <sup>a</sup>	0.760	7.01	4.21	1.78
20-state <sup>b</sup>	0.760	6.95	4.17	1.76
21-state <sup>c</sup>	0.792	7.07	4.26	1.82
B7+ <sup>d</sup>	0.623	6.75	4.05	1.65
$L = 3$				
18-state <sup>a</sup>	0.112	1.81	3.27	3.59
20-state <sup>b</sup>	0.111	1.79	3.23	3.54
21-state <sup>c</sup>	0.119	1.85	3.32	3.64
B7+ <sup>d</sup>	0.075	1.70	3.13	3.39
$L = 4$				
18-state <sup>a</sup>	0.0251	0.464	1.094	1.762
B7+ <sup>d</sup>	0.016	0.423	1.019	1.653
$L = 5$				
18-state <sup>a</sup>	0.876[-2]	0.157	0.371	0.641
$L = 6$				
18-state <sup>a</sup>	0.315[-2]	0.674[-1]	0.149	0.246
Total				
18-state <sup>a</sup>	75.56	20.51	19.16	18.19
21-state <sup>c</sup>	75.9	20.8	19.5	18.6
B7+ <sup>d</sup>	73.49	20.04	18.79	17.80

<sup>a,b</sup>the present 18- and 20-state close couplings.

<sup>c</sup>the 21-state close coupling, Mitroy (1995) [74].

<sup>d</sup>the B7+ basis coupling, Kuang and Gien (1996) [114].

<sup>e</sup>the variational calculation, Brown and Humberston (1985) [29].

## Chapter 5

### Conclusions

In this thesis, the Harris-Nesbet algebraic approach has been applied to positron-hydrogen scattering. A modified version of this method was proposed to avoid singularity at some energies with the Kohn and inverse Kohn methods in a critical transformed space. The reaction matrix is obtained by applying a backward transformation to the original space. This modified version has been applied through all of the calculations presented in this thesis.

We have derived general formulas of the bound-bound and bound-free matrix elements for the Slater-type orbitals and free-free matrix elements for physical hydrogen and positronium states. These formulas can easily be constructed for applications of any pure physical or pseudo-state close coupling calculation and mixing basis (physical or pseudo-states plus correlation functions) calculation. In particular the general closed form of the angular integration between hydrogen and positronium formation channels enables us to perform our calculations with a more flexible choice of hydrogen and positronium channel wavefunctions. Correspondingly, we constructed our own computer codes to compute such general matrix elements. These codes have been applied to form three sets of programs used in this thesis research. It has been proven that these codes can generate numerical accurate results for positron-hydrogen scattering at energy below the hydrogen first threshold.

We extended the Harris-Nesbet method for calculations, in Section 4.1, to include the Slater short ranged functions in the basis of a six-state channel space. The motivation for such an extension is to simulate the short range and long range

interactions within the system by flexibly changing parameters of the Slater-type functions. It works well and gives quick convergence except at very low positron energies because the dipole polarization potential is quite important there. A pseudo-state  $3\bar{p}H$  was then included to improve this property of the basis which is called basis B7+. Using this basis, we carried out the full partial wave calculations and very accurate scattering parameters were obtained. Wide and good agreement for phase shifts, elastic and Ps formation cross sections has been achieved with the most accurate variational results of Bhatia et al. (1971, 1974) [36, 37] and the 21-state results from the T-matrix method by Mitroy (1995) [73]. Good agreement with new measurements of the Detroit group [10, 11] is obtained. However, this calculation also showed some disagreement with the 21-state calculations [73, 74] for the higher partial wave phase shifts and Ps+p elastic cross sections.

The 18- and 20-state calculations in Section 4.2 have achieved very good agreement with the 21-state phase shifts and Ps-p elastic cross sections. The improvements show that the complete inclusion of the dipole polarization of the Ps ground state is significant to obtain accurate Ps elastic cross sections and accurate phase shifts for higher partial waves need some special care with the Slater-type functions.

We also searched for resonances below the hydrogen first threshold, in our B7+ basis calculation. Three S-wave, two P-wave and one D-wave resonances have been observed. Their positions and widths agree well with those from other large close coupling calculations.

Finally, the Harris-Nesbet method could be applied for positron-hydrogen scattering at energy beyond the hydrogen first excitation threshold. The key problems met at such an extension are the degeneracy of H<sub>2s</sub> and H<sub>2p</sub> and the irregular behavior of the spherical Neuman function. We can not avoid the degeneracy of H<sub>2s</sub> and H<sub>2p</sub>. So the only way is to improve the Neuman function. In this thesis, we

applied a factor  $(1 - e^{-\beta r})^{2l+1}$  in front of  $n_l(kr)$  to improve the irregular behavior. But a big peak of the modified Neuman function, just as what Callaway (1985) [45] pointed out, occurred near the scattering center. The contributions of this big peak to the bound-free and free-free matrix elements cause both kinds of matrix elements to be very big, with almost same magnitudes but opposite signs. Therefore, the strong cancellations between the bound-free and free-free matrix elements will bring very inaccurate values back to the m-matrix, which is a key part of the Harris-Nesbet method. In electron-hydrogen scattering, Callaway et al. had chosen different forms of the Neuman functions and performed very accurate numerical computations by employing quadruple-precision. However, we can not exploit the quadruple-precision in positron-hydrogen scattering because hundreds of thousands of two-dimensional integrals could make CPU time extremely long. Therefore, the key step to make such an extension is to find a suitable modified Neuman function with correct asymptotic behaviour.

## Bibliography

- [1] P. A. M. Dirac. *Proc. Roy. Soc.*, **118**:351, 1928.
- [2] P. A. M. Dirac. *Proc. Roy. Soc.*, **117**:610, 1928.
- [3] C. D. Anderson. *Phys. Rev.*, **43**:491, 1933.
- [4] A. E. Ruark. *Phys. Rev.*, **68**:278, 1945.
- [5] M. Deutsch. *Prog. Nucl. Phys.*, **3**:131, 1951.
- [6] J. McGervey and S. DeBeneditti. *Phys. Rev.*, **114**:495, 1959.
- [7] W. Sperber, D. Becker, K. G. Lynn, W. Raith, A. Schwab, G. Sinapius, G. Spicher, and M. Weber. *Phys. Rev. Lett.*, **68**:690, 1992.
- [8] M. Weber, A. Hofmann, W. Raith, W. Sperber, F. Jacobsen, and K. G. Lynn. *Hypf. Int.*, **89**:221, 1994.
- [9] S. Zhou, S. P. Parikh, W. E. Kaupilla, C. K. Kwan, D. Lin, A. Surdutovich, and T. S. Stein. *Phys. Rev. Lett.*, **73**:236, 1994.
- [10] H. Li, S. Zhou, W. E. Kaupila, C. K. Kwan and T. S. stein. Bulletin of the American Physical Society, **Vol.41**:1141, 1996
- [11] S. Zhou private communication, 1996.
- [12] M. Charlton and G Laricchia. *J. Phys. B: At. Mol. Opt. Phys.*, **23**:1045, 1990.
- [13] M. Charlton. *Physica Scripta*, **42**:164–172, 1989.

- [14] M. Charlton. *Rep. Prog. Phys.*, **48**:737, 1985.
- [15] T. C. Griffith and G. R. Heyland. *Phys. Rep.*, **C39**:169–277, 1978.
- [16] H. S. W. Massey and C. B. O. Mohr. *Proc. Phys. Soc. Lond.*, **67**:695, 1954.
- [17] E. W. McDaniel and M. R. C. McDowell. *Case Studies in Atomic Collision Physics I* North-Holland, Amsterdam, (1969)p.169.
- [18] A. S. Ghosh, N. C. Sil, and P. Mandal. *Phys. Rep.*, **87**:314–406, 1982.
- [19] E. A. G. Armour and J. W. Humberston. *Phys. Rep.*, **204**:167, 1991.
- [20] W. Kohn. *Phys. Rev.*, **74**:1763, 1948.
- [21] L. Spruch and L. Rosenberg. *Phys. Rev.*, **117**:143, 1960.
- [22] C. Schwartz. *Ann. Phys. (N. Y.)*, **16**:36, 1961.
- [23] J. Stein and R. Sternlicht. *Phys. Rev.*, **A6**:2165, 1972.
- [24] J. W. Humberston and J. B. G. Wallace. *J. Phys. B: At. Mol. Phys.*, **5**:1138, 1972.
- [25] R. L. Armstead. *Phys. Rev.*, **171**:91, 1968.
- [26] J. W. Humberston. *Can. J. Phys.*, **60**:591, 1982.
- [27] J. W. Humberston. *J. Phys. B: At. Mol. Phys.*, **17**:2353, 1984.
- [28] C. J. Brown and J. W. Humberston. *J. Phys. B: At. Mol. Phys.*, **17**:L423, 1984.
- [29] C. J. Brown and J. W. Humberston. *J. Phys. B: At. Mol. Phys.*, **18**:L401, 1985.

- [30] Y. Hahn, T. F. O'Mally, and L. Spruch. *Phys. Rev.*, **128**:932, 1962.
- [31] Y. Hahn and L. Spruch. *Phys. Rev.*, **140**:A18, 1965.
- [32] Y. Hahn and L. Spruch. *Phys. Rev.*, **153**:1159, 1967.
- [33] J. F. Dirk and Y. Hahn. *Phys. Rev. A*, **2**:1861, 1970.
- [34] J. F. Dirk and Y. Hahn. *Phys. Rev. A*, **3**:310, 1971.
- [35] M. Gailitis. *Soviet Phys. JETP*, **20**:107, 1965.
- [36] A. K. Bhatia, A. Temkin, R. J. Drachman, and H Eiserike. *Phys. Rev.*, **A3**:1328, 1971.
- [37] A. K. Bhatia, A. Temkin, and H Eiserike. *Phys. Rev.*, **A9**:219, 1974.
- [38] F. E. Harris. *Phys. Rev. Lett.*, **19**:173, 1967.
- [39] S. K. Houston and R. J. Drachman. *Phys. Rev. A*, **3**:1335, 1971.
- [40] F. E. Harris and H. H. Michels. *Phys. Rev. Lett.*, **22**:1036, 1969.
- [41] R. K. Nesbet. *Phys. Rev.*, **175**:175, 1968.
- [42] R. K. Nesbet. *Variational Method in Electron-Atom Scattering Theory* Plenum Press(New York), 1980.
- [43] R. K. Nesbet. *Phys. Rev.*, **179**:60, 1969.
- [44] J. Callaway. *Phys. Rep.*, **45**:89, 1978.
- [45] J. Callaway. *Phys. Rev. A*, **32**:775, 1985.
- [46] J. Callaway. *Phys. Rev. A*, **37**:3692, 1988.

- [47] J. Callaway. *Phys. Rev. A*, **43**:5175, 1991.
- [48] J. Callaway, K. Unnikrishnan, and D. H. Oza. *Phys. Rev. A*, **36**:2576, 1991.
- [49] J. Callaway and K. Unnikrishnan. *J. Phys. B: At. Mol. Opt. Phys.*, **26**:L419, 1993.
- [50] G. J. Seiler, R. S. Oberoi, and J. Callaway. *Phys. Rev. A*, **3**:2006, 1971.
- [51] S. E. A. Wakid and R. W. Labahm. *Phys. Rev. A*, **6**:2039, 1972.
- [52] S. E. A. Wakid. *Phys. Rev. A*, **8**:2456, 1973.
- [53] S. E. A. Wakid and R. W. Labahm. *Phys. Rev. Lett.*, **54A**:103, 1975.
- [54] D. Register and R. T. Poe. *Phys. Lett.*, **51A**:431, 1975.
- [55] J. Mitroy. *Aust. J. Phys.*, **46**:751–71, 1993.
- [56] K. Higgins and P. G. Burke. *J. Phys. B: At. Mol. Opt. Phys.*, **24**:L343, 1991.
- [57] U. Roy and P. Mandal. *Phys. Rev.*, **A48**:2952, 1993.
- [58] A. A. Kvitsinsky, A. Wu, and C. Hu. *J. Phys. B: At. Mol. Opt. Phys.*, **28**:275, 1995.
- [59] Y. F. Chan and P. A. Fraser. *J. Phys. B: At. Mol. Phys.*, **6**:2504, 1973.
- [60] Y. F. Chan and R. P. McEachran. *J. Phys. B: At. Mol. Phys.*, **9**:2869, 1976.
- [61] D. Basu, G. Banerji, and A. S. Ghosh. *Phys. Rev. A*, **13**:1381, 1976.
- [62] M. Basu, M. Mukherjee, and A. S. Ghosh. *J. Phys. B: At. Mol. Opt. Phys.*, **22**:2195, 1989.

- [63] N. K. Sarkar, M Mukherjee, M. Basu, and A. S. Ghosh. *J. Phys. B: At. Mol. Opt. Phys.*, **26**:L427–L429, 1993.
- [64] N. K. Sarkar, M. Basu, and A. S. Ghosh. *J. Phys. B: At. Mol. Opt. Phys.*, **26**:L799, 1993.
- [65] N. K. Sarkar and A. S. Ghosh. *J. Phys. B: At. Mol. Opt. Phys.*, **27**:759, 1994.
- [66] R. N. Hewitt, C. J. Noble, and B. H. Bransden. *J. Phys. B: At. Mol. Opt. Phys.*, **23**:4185, 1990.
- [67] R. N. Hewitt. *J. Phys. B: At. Mol. Opt. Phys.*, **24**:L635, 1991.
- [68] J. Mitroy. *J. Phys. B: At. Mol. Opt. Phys.*, **26**:4861, 1993.
- [69] J. Mitroy. *J. Phys. B: At. Mol. Opt. Phys.*, **26**:L625, 1993.
- [70] J. Mitroy and A. T. Stelbovics. *J. Phys. B: At. Mol. Opt. Phys.*, **27**:3257–3275, 1994.
- [71] J. Mitroy and K. Ratnavelu. *J. Phys. B: At. Mol. Opt. Phys.*, **28**:287, 1995.
- [72] J. Mitroy, L. Berge, and A. Stelbovics. *Phys. Rev. Lett.*, **73**:2966, 1994.
- [73] J. Mitroy. *Aust. J. Phys.*, **48**:645, 1995.
- [74] J. Mitroy. *Ps-p. Aust. J. Phys.*, **48**:893, 1995.
- [75] K. Higgins, P. G. Burke, and H. R. J. Walters. *J. Phys. B: At. Mol. Phys.*, **23**:1345, 1990.
- [76] M. T. McAlinden, A. A. Kernaghan, and H. R. J. Walters. *Hypf. Int.*, **89**:161, 1994.

- [77] A. A. Kernoghan, M. T. McAlinden, and H. R. J. Walters. *J. Phys. B: At. Mol. Opt. Phys.*, **27**:L211, 1994.
- [78] A. A. Kernoghan, M. T. McAlinden, and H. R. J. Walters. *J. Phys. B: At. Mol. Opt. Phys.*, **27**:L543–L549, 1994.
- [79] A. A. Kernoghan, M. T. McAlinden, and H. R. J. Walters. *J. Phys. B: At. Mol. Opt. Phys.*, **28**:1079, 1995.
- [80] G. G. Liu and T. T. Gien. *Phys. Rev. A*, **46**:3918, 1992.
- [81] T. T. Gien and G. G. Liu. *Phys. Rev. A*, **48**:3386, 1993.
- [82] T. T. Gien. *Phys. Rev.*, **A50**:1186, 1995.
- [83] T. T. Gien. *Book of Abstracts, 14th ICAP*, pp 2P-1, July 31-August 5. 1994.
- [84] T. T. Gien. *J. Phys. B: At. Mol. Opt. Phys.*, **27**:L25–L31, 1994.
- [85] T. T. Gien. *Book of Abstracts, 14th ICAP*, pp 2P-2, July 31-August 5. 1994.
- [86] T. T. Gien. *J. Phys. B: At. Mol. Opt. Phys.*, **28**:103, 1995.
- [87] T. T. Gien. *J. Phys. B: At. Mol. Opt. Phys.*, **28**:L313, 1995.
- [88] T. T. Gien. *Can. J. Phys. (as Proc. of Positron Workshop 1995, Vancouver, BC)*, at press, 1995.
- [89] T. T. Gien. *J. Phys. B: At. Mol. Opt. Phys.*, **29**:2127, 1996.
- [90] P. G. Burke, D. F. Gallagher, and S. Getlman. *J. Phys. B: At. Mol.*, **2**, 1969.
- [91] H. H. Michels and F. E. Harris. *Phys. Rev. Lett.*, **19**:885, 1967.
- [92] F. E. Harris and H. H. Michels. *Meth. Comp. Phys.*, **10**:143, 1971.

- [93] R. K. Nesbet and R. S. Oberoi. *Phys. Rev.*, **A5**:1855, 1972.
- [94] R. K. Nesbet. *Phys. Rev.*, **A18**:955, 1978.
- [95] A. R. Edmonds. *Angular Momentum in Quantum Mechanics*. Princeton University Press, Princeton, New Jersey, (1957)p113-115.
- [96] I. Bray and T. Stelbovics. *Phys. Rev. A*, **48**:4787, 1993.
- [97] G. Doolan, G. McCarten, E. A. McDonald, and S. Nuttall. *Phys. Rev. A*, **4**:108, 1971.
- [98] I. Shimamura. *J. Phys. Soc. Japan*, **30**:1702, 1971.
- [99] J. R. Winick and W. P. Reinhardt. *Phys. Rev.*, **A18**:910, 1978.
- [100] K. Higgins, P. G. Burke, and H. R. Walters. *J. Phys. B: At. Mol. Opt. Phys.*, **23**:1345, 1990.
- [101] A. A. Kvitsinsky, J. Carbonell, and C. Gignoux. *Phys. Rev. A*, **51**:2997, 1995.
- [102] C. J. Kleiman, Y Hahn, and L. Spruch. *Phys. Rev.*, **140**:413, 1965.
- [103] J. R. Winick and W. P. Reinhardt. *Phys. Rev.*, **A18**:925, 1978.
- [104] Y. Zhou and C. D. Lin. *J. Phys. B: At. Mol. Opt. Phys.*, **27**:5065, 1994.
- [105] Y. Zhou and C. D. Lin. *J. Phys. B: At. Mol. Opt. Phys.*, **28**:4907, 1995.
- [106] B. J. Archer, G. A. Parker, and R. T. Pack. *Phys. Rev. A*, **41**:1303, 1990.
- [107] A. Igarashi and N. Toshima. *Phys. Rev. A*, **50**:232, 1994.
- [108] K. Higgins and P. G. Burke. *J. Phys. B: At. Mol. Opt. Phys.*, **26**:4269, 1993.
- [109] M. H. Mittleman. *Phys. Rev.*, **152**:76, 1966.

- [110] T. T. Gien and G. G. Liu. *J. Phys. B: At. Mol. Opt.*, **27**:L179–L185, 1994.
- [111] Y. K. Ho. *J. Phys. B: At. Mol. Opt. Phys.*, **23**:L419, 1990.
- [112] E. Peliken and H. Klar. *Z. Phys.*, **A 310**:153, 1983.
- [113] W. C. Fon, K. A. Berington, P. G. Burke, and A. E. Kingston. *J. Phys. B: At. Mol. Phys.*, **14**:1041, 1981.
- [114] Y. R. Kuang and T. T. Gien. *Phy. Rev.*, **A** : in press, 1996.
- [115] Y. R. Kuang and T. T. Gien. *Bulletin of the American Physical Society*, **41**:1140, 1996.
- [116] M. J. Weida, T. M. Schroeder, L. J. Wexer, and B. L. Whitten. *Ame. J. Phys.*, **60**:467, 1992.
- [117] I. S. Gradshteyn and I. M. Ryzhik. *Tables of Integrals, Series and Products*. Academic, New York, (1965).

## Appendix A: Variants of the Harris-Nesbet Method

In order to overcome some difficulties from the zeroes of the matrices  $m_{00}$  or  $m_{11}$  which cause some singularities of the Harris-Nesbet method, Nesbet and Oberoi developed the following modified versions of the Harris-Nesbet method.

### A.1 OMN Method

Harris and Michels (1969 [40], 1971 [92]) proposed a minimum norm method, that is, minimizing the trace of the quadratic form  $(m\alpha)^\dagger(m\alpha)$ . Nesbet and Oberoi (1972) [93] developed an optimized minimum norm (OMN) method by introducing a unitary transformation matrix  $u=(ab)$ ;  $a$  and  $b$  are both  $2N \times N$  matrices

$$a = \begin{pmatrix} a_0 \\ a_1 \end{pmatrix}, \quad (\text{A.1.1})$$

and

$$b = \begin{pmatrix} b_0 \\ b_1 \end{pmatrix}. \quad (\text{A.1.2})$$

So  $u$  is a  $2N \times 2N$  matrix.  $a$  and  $b$  satisfy the orthonormality conditions

$$a^\dagger a = b^\dagger b = I; a^\dagger b = b^\dagger a = 0. \quad (\text{A.1.3})$$

Then the variational functional  $\Phi$  can be expressed in the transformed space obtained by the unitary transformation  $u$

$$\Phi = \alpha'^\dagger m' \alpha', \quad (\text{A.1.4})$$

where

$$m' = u^\dagger m u, \quad \alpha' = u^\dagger \alpha. \quad (\text{A.1.5})$$

In this new transformed space, we exploit the Kohn method and obtain a stationary matrix  $[R']$  like that in the original space

$$[R'] = -2(m'_{00} - m'_{10}(m'_{11})^{-1}m'_{10}). \quad (\text{A.1.6})$$

Then, using  $\alpha = u\alpha'$  back to the original space, we can obtain a stationary matrix  $\alpha$ ,

$$[\alpha] = u\alpha' = (ab) \begin{pmatrix} I \\ R' \end{pmatrix} = a + b[R']. \quad (\text{A.1.7})$$

The reactance matrix  $R$  is

$$R = \frac{a_1 + b_1[R']}{a_0 + b_0[R']}. \quad (\text{A.1.8})$$

In the minimum norm method, the transformation  $u$  is constructed so that  $a^\dagger m^\dagger m a$  has minimum eigenvalues and  $b^\dagger m^\dagger m b$  has maximum eigenvalues. This implies that  $\det(m'_{00})$  is smaller in magnitude than  $\det(m'_{11})$ . The OMN method has some disadvantages such as the condition  $\det(m'_{00}) > \det(m'_{11})$  is not always fulfilled, sometimes  $m'_{11}$  can be still singular.

## A.2 OAF Method

In order to overcome the difficulties met in the OMN method, Nesbet and Oberoi proposed an optimized anomaly-free method by transforming  $m$  into a upper triangular matrix  $m'$ . That is,

$$m'_{10} = b^\dagger m a = 0. \quad (\text{A.2.1})$$

In the transformed space, using the Kohn method, we have a variation of the functional

$$\begin{aligned} \delta\Phi &= \delta R'^\dagger (m'_{10} + m'_{11} R') + (m'_{10} + m'_{11} R')^\dagger \delta R' + (m'_{01} - m'_{10}^\dagger) \delta R' \\ &= \delta R'^\dagger m'_{11} R' + (m'_{11} R')^\dagger \delta R' + m'_{01} \delta R', \end{aligned} \quad (\text{A.2.2})$$

where the last term is due to the break of the condition

$$m_{01} - m_{10}^\dagger = \frac{1}{2}I. \quad (\text{A.2.3})$$

So in the OAF method, the trial reactance matrix  $R'$  should be chosen to be zero. Hence

$$\delta(\Phi - m'_{01}R') = 0, \quad (\text{A.2.4})$$

and because  $\Phi(R'_{(0)}) = m'_{00}$

$$[R'] = -(m'_{01})^{-1}m'_{00}. \quad (\text{A.2.5})$$

We can use the same way to go back to the original space as Eq. (A.1.8) in OMN. Generally, the OAF gives an unsymmetric  $R$  matrix, so only the symmetric parts are used to compute cross sections. Especially, if  $m$  has complex eigenvalues, a transformation or reorder diagonal elements must be used to ensure that  $m'_{01}$  remain nonsingular in the limit of an exact scattering solution. To avoid this disadvantage of OAF, Nesbet and Oberoi developed a slightly different optimized anomaly-free (OAF2) method by choosing the transformation matrix  $u$

$$u = \begin{pmatrix} C & -S \\ S & C \end{pmatrix}, \quad (\text{A.2.6})$$

where submatrices  $C$  and  $S$  satisfy

$$C^2 + S^2 = I, \quad CS = SC, \quad (\text{A.2.7})$$

and

$$T = SC^{-1} = \tan \Delta, \quad (\text{A.2.8})$$

where  $\Delta$  is a real symmetric phase matrix such that  $C = \cos \Delta$  and  $S = \sin \Delta$ . So the trial  $R'$  matrix can again take the form

$$[R'] = -2(m'_{00} - m'_{10}(m'_{11})^{-1}m'_{10}), \quad (\text{A.2.9})$$

as what it is in the original space. In the OAF2 method,  $m'_{10}$  is no longer zero but keeps all properties of the original matrices  $m$ 's. The phase matrix  $\tan\Delta$  is chosen to be

$$\tan\Delta = \frac{1}{2}[\alpha_1\alpha_0^{-1} + (\alpha_1\alpha_0^{-1})^\dagger]. \quad (\text{A.2.10})$$

The model calculation by Nesbet and Oberoi (1972)[93] shows that it still needs to reorder the eigenvalues of  $m$ , which causes discontinuities when eigenvalues of opposite sign cross in magnitude.

### A.3 IAF and RIAF Methods

Trying to wipe out the discontinuities in the OAF2, Nesbet and Oberoi proposed to take a continuous transformation between the Kohn and inverse Kohn methods. They did not try to maximize  $m'_{11}$  this time but let it necessarily differ from zero. This method is called interpolated anomaly-free (IAF) method. If we further restrict the transformation matrix taking the following forms

$$C_{pq} = \delta_{pq}\cos\phi_p; \quad S_{pq} = \delta_{pq}\sin\phi_p, \quad (\text{A.3.1})$$

and choose the phase angle  $\phi_p$  to maximize  $| \det(m'_{11}) |$ , this restricted IAF method is called the RIAF method. If all  $\phi_p = 0$ , the RIAF becomes the Kohn method. Similarly, the inverse Kohn method corresponds to all  $\phi_p = \frac{\pi}{2}$ .

## Appendix B: Analytical Reductions of Matrix Elements

### B.1 Bound-bound Matrix Elements

As was indicated in Chapter 3, there are three types of matrix elements. One of them involves only H channels, another only Ps channels and the third one both H and Ps channels.

$$1) \quad A_{ij}(H) = \langle X_i(\mathbf{r}_1, \mathbf{r}_2) | H | X_j(\mathbf{r}_1, \mathbf{r}_2) \rangle$$

Consider the case of a single-term Slater-type wave function  $R_i(r)$  such that

$$U_i(r_1) = r_1 R_i(r_1) = B_{1i} r_1^{n_{1i}} e^{-\alpha_{1i} r_1}, \quad (B.1)$$

where  $B_{1i}$  is a normalization constant

$$B_{1i} = \left\{ \frac{(2\alpha_{1i})^{2n_{1i}+1}}{(2n_{1i})!} \right\}^{\frac{1}{2}}, \quad (B.2)$$

and hence  $X_i(\mathbf{r}_1, \mathbf{r}_2)$  is in the form

$$X_i(\mathbf{r}_1, \mathbf{r}_2) = B_{1i} r_1^{n_{1i}} e^{-\alpha_{1i} r_1} B_{2i} r_2^{n_{2i}} e^{-\alpha_{2i} r_2} Y_{Ll_{1i}l_{2i}}^0(\hat{\mathbf{r}}_1 \cdot \hat{\mathbf{r}}_2), \quad (B.3)$$

where

$$Y_{Ll_{1i}l_{2i}}^0(\hat{\mathbf{r}}_1 \cdot \hat{\mathbf{r}}_2) = \sum_{m=-l_<}^{l_<} (-1)^{l_{1i}-l_{2i}} \sqrt{2L+1} \begin{pmatrix} , l_{1i} & l_{2i} & L \\ m & -m & 0 \end{pmatrix} Y_{l_{1i}m}(\hat{\mathbf{r}}_1) Y_{l_{2i}-m}(\hat{\mathbf{r}}_2) \quad (B.4)$$

where  $l_< = \min(l_{1i}, l_{2i})$ . The Hamiltonian of the system can then be equivalently represented by

$$H = -\frac{d^2}{2dr_1^2} + \frac{\hat{l}_1^2}{2r_1} - \frac{1}{r_1} - \frac{d^2}{2dr_2^2} + \frac{\hat{l}_2^2}{2r_2} + \frac{1}{r_2} - \frac{1}{r_{12}} \quad (B.5)$$

where  $\hat{l}_j^2$  is the squared angular momentum operator of the  $j$ -th particle.

After operating  $H$  on the left, all the terms of the matrix elements can be reduced to closed forms by carrying out necessary integrations, except for the potential term  $-\frac{1}{r_{12}}$  which needs some care

$$\begin{aligned} A_{ij}(H) &= \frac{1}{2}(l_{1i}(l_{1i}+1) - n_{1i}(n_{1i}-1))\beta_{ij}(2,0) + (\alpha_{1i}n_{1i}-1)\beta_{ij}(1,0) - \\ &\quad \frac{1}{2}(\alpha_{1i}^2 + \alpha_{2i}^2)\beta_{ij}(0,0) + \frac{1}{2}(l_{2i}(l_{2i}+1) - n_{2i}(n_{2i}-1))\beta_{ij}(0,2) \\ &\quad (\alpha_{2i}n_{2i}+1)\beta_{ij}(0,1) + V_{ij}. \end{aligned} \quad (B.6)$$

To simplify the writing,  $\beta_{ij}(m,n)$  was used to indicate

$$\begin{aligned} \beta_{ij}(m,n) &= \langle X_i(\mathbf{r}_1, \mathbf{r}_2) | \frac{1}{r_1^m r_2^n} | X_j(\mathbf{r}_1, \mathbf{r}_2) \rangle \\ &= \delta_{l_{1i}, l_{2i}, l_{1j}, l_{2j}} B_{1i} B_{2i} B_{1j} B_{2j} \int_0^\infty dr_1 r_1^{n_{1i}+n_{1j}-m} e^{-(\alpha_{1i}+\alpha_{2i})r_1} \\ &\quad \int_0^\infty dr_2 r_2^{n_{2i}+n_{2j}-n} e^{-(\alpha_{2i}+\alpha_{2j})r_2} \\ &= \delta_{l_{1i}, l_{2i}, l_{1j}, l_{2j}} B_{1i} B_{2i} B_{1j} B_{2j} \frac{(n_{1i}+n_{1j}-m)!}{(\alpha_{1i}+\alpha_{1j})^{n_{1i}+n_{1j}-m+1}} \\ &\quad \frac{(n_{2i}+n_{2j}-n)!}{(\alpha_{2i}+\alpha_{2j})^{n_{2i}+n_{2j}-n+1}}, \end{aligned} \quad (B.7)$$

and

$$V_{ij} = \langle X_i(\mathbf{r}_1, \mathbf{r}_2) | -\frac{1}{r_{12}} | X_j(\mathbf{r}_1, \mathbf{r}_2) \rangle. \quad (B.8)$$

Fortunately, the method of reduction of this term  $V_{ij}$  has been well known. By applying this well-known reduction procedure described in various text books of angular momentum theory (see for example A. R. Edmonds (1957), Angular Momentum in Quantum Mechanics, pp113-115, [95] and references therein), this term can written as

$$\begin{aligned} V_{ij} &= -(-1)^{l_{1j}+l_{2i}+L} B_{1i} B_{2i} B_{1j} B_{2j} \sum_{k=k_{min}}^{k_{max}} \langle l_{1i} \| C^{(k)} \| l_{1j} \rangle \langle l_{2i} \| C^{(k)} \| l_{2j} \rangle \left\{ \begin{array}{ccc} l_{1i} & l_{2i} & L \\ l_{2j} & l_{1j} & k \end{array} \right\} \\ &\quad \int_0^\infty dr_1 \int_0^\infty dr_2 r_1^{n_{1i}+n_{1j}} r_2^{n_{2i}+n_{2j}} \frac{r_1^k}{r_2^{k+1}} e^{-(\alpha_{1i}+\alpha_{1j})r_1} e^{-(\alpha_{2i}+\alpha_{2j})r_2}, \end{aligned} \quad (B.9)$$

where  $r_{<,>}$  is the lesser or greater of  $r_1$  and  $r_2$ .  $\langle l_i || C^{(k)} || l_j \rangle$  is an irreducible matrix element of the renormalized spherical harmonics and is given by (Edmonds)

$$\langle l_i || C^{(k)} || l_j \rangle = (-1)^{l_i} \sqrt{(2l_i + 1)(2l_j + 1)} \begin{pmatrix} l_i & k & l_j \\ 0 & 0 & 0 \end{pmatrix}. \quad (\text{B.10})$$

In Eq.(B.10) and Eq.(B.9), a big ( ) and a big { } are 3-j and 6-j symbols of angular momentum couplings, respectively. The lower and upper limit of the sum in Eq.(B.9) take  $k_{min} = \max(|l_{1i} - l_{1j}|, |l_{2i} - l_{2j}|)$ ,  $k_{max} = \min(l_{1i} + l_{1j}, l_{2i} + l_{2j})$ . The sum over  $k$  jumps by 2 units. The radial integral was known to be "Slater integral"

$$S(n, m, \alpha, \beta, k) = \int_0^\infty dr_1 \int_0^\infty dr_2 r_1^{n+k+1} r_2^{m+k+1} e^{-\alpha r_1} e^{-\beta r_2} \frac{r_1^k}{r_2^{k+1}}. \quad (\text{B.11})$$

The closed form of this integral was given in the literature (Weida et al [116]). One then can write  $V_{ij}$  as

$$\begin{aligned} V_{ij} &= -B_{1i} B_{2i} B_{1j} B_{2j} \sum_k F_{l_{1i} l_{2i}; l_{1j} l_{2j}}^{L0}(k) \\ &\quad S(n_{1i} + n_{1j} - k - 1, n_{2i} + n_{2j} - k - 1, \alpha_{1i} + \alpha_{1j}, \alpha_{2i} + \alpha_{2j}, k), \end{aligned} \quad (\text{B.12})$$

where one defined

$$F_{l_{1i} l_{2i}; l_{1j} l_{2j}}^{L0}(k) = -(-1)^{l_{1i} + l_{2i} + L} \langle l_{1i} || C^{(k)} || l_{1j} \rangle \langle l_{2i} || C^{(k)} || l_{2j} \rangle \begin{Bmatrix} l_{1i} & l_{2i} & L \\ l_{2j} & l_{1j} & k \end{Bmatrix}. \quad (\text{B.13})$$

The so-called overlapping matrix element  $B_{ij}(H)$  is then given by

$$B_{ij}(H) = \langle X_i(\mathbf{r}_1, \mathbf{r}_2) | X_j(\mathbf{r}_1, \mathbf{r}_2) \rangle = \beta_{ij}(0, 0). \quad (\text{B.14})$$

2)  $A_{ij}(Ps) = \langle X_i(\rho, \mathbf{R}) | H | X_j(\rho, \mathbf{R}) \rangle$

With  $U_i(\rho) = \rho\phi_i(\rho) = B_{3i}\rho^{n_{3i}}e^{-\alpha_{3i}\rho}$ ,

$$X_i(\rho, \mathbf{R}) = B_{3i}\rho^{n_{3i}}e^{-\alpha_{3i}\rho}B_{4i}R^{n_{4i}}e^{\alpha_{4i}R}Y_{L_{3i}l_{4i}}^0(\hat{\rho} \cdot \hat{\mathbf{R}}). \quad (\text{B.15})$$

The Hamiltonian  $H$  for the Ps channel is then represented by

$$H = -\frac{d^2}{d\rho^2} + \frac{\hat{l}_3^2}{\rho^2} - \frac{1}{\rho} - \frac{d^2}{4dR^2} + \frac{\hat{l}_4^2}{4R^2} + \frac{1}{r_2} - \frac{1}{r_1}. \quad (\text{B.16})$$

In a similar fashion, by operating  $H$  on the left and carrying out the necessary integrations, one obtains

$$\begin{aligned} A_{ij}(Ps) &= [l_{3i}(l_{3i}+1) - n_{3i}(n_{3i}-1)]\beta_{ij}(2,0) + (2\alpha_{3i}n_{3i}-1)\beta_{ij}(1,0) - (\alpha_{3i}^2 + \frac{1}{4}\alpha_{4i}^2) \\ &\quad \beta_{ij}(0,0) + \frac{1}{4}[l_{4i}(l_{4i}+1) - n_{4i}(n_{4i}-1)]\beta_{ij}(0,2) + \frac{1}{2}\alpha_{4i}n_{4i}\beta_{ij}(0,1) + V'_{ij}, \end{aligned} \quad (\text{B.17})$$

where  $V'_{ij}$  is

$$V'_{ij} = \langle X_i(\rho, \mathbf{R}) | \frac{1}{r_2} - \frac{1}{r_1} | X_j(\rho, \mathbf{R}) \rangle. \quad (\text{B.18})$$

Using exactly the same procedure as that considered for  $V_{ij}$ , one obtains

$$\begin{aligned} V'_{ij} &= 2^{n_{3i}+n_{3j}+2}B_{3i}B_{4i}B_{3j}B_{4j} \sum_k F_{l_{3i}l_{4i};l_{3j}l_{4j}}^{LO}(k) \\ &\quad S(n_{3i}+n_{3j}-k-1, n_{4i}+n_{4j}-k-1, 2(\alpha_{3i}+\alpha_{3j}), \alpha_{4i}+\alpha_{4j}, k). \end{aligned} \quad (\text{B.19})$$

It may be worth noting that the two terms of  $V'_{ij}$  cancel each other when  $k$  is even. Thus,  $V'_{ij}$  will be different from zero only if the summation is over odd integers. Otherwise,  $V'_{ij} \equiv 0$ . Prior to carrying out the integration over  $\rho$ , one needs to change the variable  $\rho$  to  $\rho' = \frac{\rho}{2}$ . The overlapping matrix element is still equal to  $\beta_{ij}(0,0)$ ,

$$B_{ij}(Ps) = \langle X_i(\rho, \mathbf{R}) | X_j(\rho, \mathbf{R}) \rangle = \beta_{ij}(0,0). \quad (\text{B.20})$$

$$3) \underline{A_{ij}(H, Ps) = \langle X_i(\mathbf{r}_1, \mathbf{r}_2) | H | X_j(\rho, \mathbf{R}) \rangle}$$

After operating  $H$  on the left and performing the coordinate transformation from the spherical to the spheroidal ones (see Eqs. 3.29-3.31), the integration over the angular variables can be factorized out. This integral was called, for convenience, the "angle integral" of the matrix element and denoted by

$$H_{l_1 l_2; l_3 l_4}^L(\xi, \eta) = \int_0^{2\pi} d\phi \int d\hat{\mathbf{r}}_2 Y_{L l_1 l_2}^{(0)}(\mathbf{r}_1 \cdot \mathbf{r}_2) Y_{L l_3 l_4}^{(0)}(\rho \cdot \mathbf{R}). \quad (\text{B.21})$$

We shall describe in some details the reduction of this "angle integral" to closed form at the end of this Appendix. The integration over  $\mathbf{r}_2$  (that involves Euler's type) of the matrix element can be straightforwardly carried out and one obtained

$$\begin{aligned} A_{ij}(H, Ps) &= \langle X_i(\mathbf{r}_1, \mathbf{r}_2) | \frac{l_{1i}(l_{1i}+1) - n_{1i}(n_{1i}-1)}{2r_1^2} + \frac{\alpha_{1i}n_{1i}-1}{r_1} - \frac{1}{2}\alpha_{1i}^2 \\ &\quad + \frac{l_{2i}(l_{2i}+1) - n_{2i}(n_{2i}-1)}{2r_2^2} + \frac{\alpha_{2i}n_{2i}}{r_2} - \frac{1}{2}\alpha_{2i}^2 + \frac{1}{r_2} - \frac{1}{r_{12}} | X_j(\rho, \mathbf{R}) \rangle \\ &= \frac{1}{8} B_{1i} B_{2i} B_{3j} B_{4j} \int_1^\infty d\xi \int_{-1}^1 d\eta (\xi^2 - \eta^2) \left(\frac{\xi+\eta}{2}\right)^{n_{1i}-1} \left(\frac{\xi-\eta}{2}\right)^{n_{2i}-1} \\ &\quad \left(\frac{1}{4}\sqrt{\xi^2 + 6\xi\eta + \eta^2 + 8}\right)^{n_{4j}-1} H_{l_1 l_2; l_3 l_4}^L(\xi, \eta) [A' \frac{y^2}{m(m-1)} + B' \frac{y}{m} - \right. \\ &\quad \left. \frac{1}{2}(\alpha_{1i}^2 + \alpha_{2i}^2)] \frac{m!}{y^{m+1}}, \right. \end{aligned} \quad (\text{B.22})$$

where one defines

$$\begin{aligned} m &= 1 + n_{1i} + n_{2i} + n_{3j} + n_{4j}, \\ A' &= \frac{1}{2} \{ [l_{1i}(l_{1i}+1) - n_{1i}(n_{1i}-1)] \left(\frac{2}{\xi+\eta}\right)^2 + [l_{2i}(l_{2i}+1) - n_{2i}(n_{2i}-1)] \}, \\ B' &= (\alpha_{1i}n_{1i}-1) \frac{2}{\xi+\eta} + \alpha_{2i}n_{2i} + 1 - \frac{2}{\xi-\eta}, \\ y &= \frac{\xi+\eta}{2}\alpha_{1i} + \alpha_{2i} + \frac{\xi-\eta}{2}\alpha_{3j} + \frac{1}{4}\sqrt{\xi^2 + 6\xi\eta + \eta^2 + 8}\alpha_{4j}. \end{aligned} \quad (\text{B.23})$$

The overlapping matrix element for this case was, therefore, deduced to be

$$B_{ij}(H, Ps) = \langle X_i(\mathbf{r}_1, \mathbf{r}_2) | X_j(\rho, \mathbf{R}) \rangle$$

$$\begin{aligned}
&= \frac{1}{8} B_{1i} B_{2i} B_{3j} B_{4j} \int_1^\infty d\xi \int_{-1}^1 d\eta (\xi^2 - \eta^2) \left(\frac{\xi + \eta}{2}\right)^{n_{1i}-1} \left(\frac{\xi - \eta}{2}\right)^{n_{3j}-1} \\
&\quad \left(\frac{1}{4} \sqrt{\xi^2 + 6\xi\eta + \eta^2 + 8}\right)^{n_{4j}-1} H_{l_1, l_2, l_3, l_4}^L(\xi, \eta) \frac{m!}{y^{m+1}}. \quad (B.24)
\end{aligned}$$

## B.2 Bound-free Matrix Elements

Similar to the case of bound-bound matrix elements, these types of bound-free matrix elements exist. In addition, each of them will be subdivided into two which are corresponding to either S or C "free" wave functions.

$$1) M_{ip}^S(H) = \langle X_i(r_1, r_2) | H - E | U_{np} l_1(r_1) S_p^{l_2}(r_2) Y_{Ll_1 l_2}^0(\hat{r}_1 \cdot \hat{r}_2) \rangle$$

Here  $U_{np} l_1(r_1)$  is product of the radial wave function  $R_{np} l_1(r_1)$  of hydrogen atom by  $r_1$  and  $R_{np} l_1(r_1)$  is written as

$$R_{np} l_1(r_1) = \sum_{j_p=0}^{n_p-l_1-1} B_3(n_p, l_1, j_p) r_1^{l_1+j_p} e^{-\frac{1}{n_p} r_1}, \quad (B.25)$$

where

$$B_3(n_p, l_1, j_p) = \frac{(-1)^{j_p}}{n_p} \left(\frac{2}{n_p}\right)^{j_p+l_1+1} \frac{\sqrt{(n_p - l_1 - 1)!(n_p + l_1)!}}{j_p!(n_p - l_1 - 1 - j_p)!(2l_1 + 1 + j_p)!}. \quad (B.26)$$

After operating  $H$  on the right, using the same steps of reduction and carrying out the necessary integrations as done for the bound-bound matrix elements  $A_{ij}(H)$ , one obtains

$$\begin{aligned}
M_{ip}^S(H) &\equiv \langle X_i(r_1, r_2) | \frac{1}{r_2} - \frac{1}{r_{12}} | U_{np} l_1(r_1) S_p^{l_2}(r_2) Y_{Ll_1 l_2}^0(\hat{r}_1 \cdot \hat{r}_2) \rangle \\
&= B_{1i} B_{2i} \sqrt{k_p} \sum_{j_p=0}^{n_p-l_1-1} B_3(n_p, l_1, j_p) \{ \delta_{l_1, l_2, l_1 l_2} \int_0^\infty dr_2 r_2^{n_{2i}} e^{-\alpha_{2i} r_2} j_{l_2}(k_p r_2) \\
&\quad \int_0^\infty dr_1 r_1^{n_{1i}+l_1+j_p+1} e^{-\alpha_{1i} r_1} e^{-\frac{1}{n_p} r_1} - \sum_k F_{l_1, l_2, l_1 l_2}^{L0}(k) \\
&\quad \int_0^\infty dr_2 r_2^{n_{2i}+1} e^{-\alpha_{2i} r_2} j_{l_2}(k_p r_2) \int_0^\infty dr_1 r_1^{n_{1i}+l_1+j_p+1} e^{-(\alpha_{1i} + \frac{1}{n_p}) r_1} \frac{r_1^k}{r_1^{k+1}} \}
\end{aligned}$$

$$\begin{aligned}
& B_{1i} B_{2i} \sqrt{k_p} \sum_{j_p=0}^{n_p-l_1-1} B_3(n_p, l_1, j_p) \{ \delta_{l_{1i}, l_{2i}, l_1 l_2} V(n_{2i}, l_2, \alpha_{2i}, k_p) \\
& \frac{(n_{1i} + l_1 + j_p + 1)!}{(\frac{1}{n_p} + \alpha_{1i})^{n_{1i} + l_1 + j_p + 2}} - \sum_k F_{l_{1i} l_{2i}; l_1 l_2}^{L0}(k) \\
& G_j(n_{2i} + 1, \alpha_{2i}, k_p, l_2, n_{1i} + l_1 + j_p - k, \alpha_{1i} + \frac{1}{n_p}, k) \}. \quad (B.27)
\end{aligned}$$

where  $G_j$  is in a similar form of "generalized Slater integral" defined to be

$$\begin{aligned}
G_j(m, a, b, l, n, \alpha, k) &= \int_0^\infty dr_2 r_2^m e^{-ar_2} j_l(br_2) \int_0^\infty dr_1 r_1^{n+k+1} e^{-\alpha r_1} \frac{r_1^k}{r_1^{k+1}} \\
&= \frac{(n+2k+1)!}{\alpha^{n+2k+2}} [V(m-k-1, l, a, b) - \sum_{i=0}^{n+2k} \frac{1}{i!} \alpha^i V(m+i-k-1, l, a+\alpha, b)] \\
&+ \frac{n!}{\alpha^{n+1}} \sum_{j=0}^{n-1} \frac{1}{j!} \alpha^j V(m+k+j, l, a+\alpha, b). \quad (B.28)
\end{aligned}$$

The last line of Eq. (B.28) can be straightforwardly written down from the formulas of "incomplete gamma functions" (see for example, Gradshteyn and Ryzhik p.310. formulas 3.351 and 3.352 in Ref. [117])

The only slight difference from the bound-bound matrix case is that here one ended up with an integral over  $r_2$  involving the spherical Bessel function

$$V(n, l, a, b) = \int_0^\infty dx x^n e^{-ax} j_l(bx), \quad (B.29)$$

which can also be written in closed form, using an integral formula available in Tables of Integrals ( see for example Gradshteyn and Ryzhik, Formula 6.621 in Ref. [117])

$$V(n, l, a, b) = \frac{\sqrt{\pi} b^l (n+l)! 2^{-l-1}}{\Gamma(l + \frac{3}{2}) \sqrt{(a^2 + b^2)^{n+l+1}}} F\left(\frac{n+l+1}{2}, \frac{1-n+l}{2}; l + \frac{3}{2}; \frac{b^2}{a^2 + b^2}\right), \quad (B.30)$$

where  $\Gamma(x)$  and  $F(a,b,c,x)$  are the respective gamma function and Gaussian hypergeometrical function.

$$2) \underline{M_{ip}^C(H) = \langle X_i(\mathbf{r}_1, \mathbf{r}_2) | H - E | U_{n_p l_1}(r_1) C_p^{l_2}(r_2) Y_{L l_1 l_2}^0(\hat{\mathbf{r}}_1 \cdot \hat{\mathbf{r}}_2) \rangle}$$

Operating  $H$  on the left and using exactly the same procedure as that of  $M_{ip}^S$ , one obtains the following expression, with the integral over  $\mathbf{r}_2$  previously involving the spherical Bessel function replaced by an integral now involving the spherical Neumann function ( $V_1$ ),

$$\begin{aligned} M_{ip}^C(H) &= -B_{1i} B_{2i} \sqrt{k_p} \sum_{j_p=0}^{n_p - l_1 - 1} B_3(n_p, l_1, j_p) \{ \delta_{l_1 l_2 i, l_1 l_2} \left[ -\frac{1}{2} (k_p^2 + \alpha_{2i}^2) \right] \\ &= -B_{1i} B_{2i} \sqrt{k_p} \sum_{j_p=0}^{n_p - l_1 - 1} B_3(n_p, l_1, j_p) \{ \delta_{l_1 l_2 i, l_1 l_2} \left[ -\frac{1}{2} (k_p^2 + \alpha_{2i}^2) \right] \\ &\quad V_1(n_{2i} + 1, l_2, \alpha_{2i}, \beta, k_p) + \frac{1}{2} [l_{2i}(l_{2i} + 1) - n_{2i}(n_{2i} - 1)] \\ &\quad V_1(n_{2i} - 1, l_2, \alpha_{2i}, \beta, k_p) + (1 + \alpha_{2i} n_{2i}) V_1(n_{2i}, l_2, \alpha_{2i}, \beta, k_p) \} \\ &\quad \frac{(n_{1i} + l_1 + j_p + 1)!}{(\frac{1}{n_p} + \alpha_{1i})^{n_{1i} + l_1 + j_p + 2}} - \\ &\quad \sum_k F_{l_1 l_2 i, l_1 l_2}^{L0}(k) G_n(n_{2i} + 1, \alpha_{2i}, k_p, l_2, n_{1i} + l_1 + j_p - k, \alpha_{1i} + \frac{1}{n_p}, \beta, k) \}, \end{aligned} \tag{B.31}$$

where  $G_n$  is of the same form as  $G_j$  with the  $V$ -function replaced by the  $V_1$ -function

$$\begin{aligned} G_n(m, a, b, l, n, \alpha, \beta, k) &= \int_0^\infty dr_2 r_2^m e^{-ar_2} (1 - e^{-\beta r_2})^{2l+1} n_l(br_2) \int_0^\infty dr_1 r_1^{n+k+1} e^{-\alpha r_1} \frac{r_1^k}{r_1^{k+1}} \\ &= \frac{(n+2k+1)!}{\alpha^{n+2k+2}} [V_1(m-k-1, l, a, \beta, b) - \sum_{i=0}^{n+2k} \frac{\alpha^i}{i!} V_1(m+i-k-1, l, a+\alpha, \beta, b)] \\ &\quad + \frac{n!}{\alpha^{n+1}} \sum_{j=0}^{n-1} \frac{\alpha^j}{j!} V_1(m+k+j, l, a+\alpha, \beta, b), \end{aligned} \tag{B.32}$$

and

$$V_1(n, l, a, \beta, b) \equiv \int_0^\infty dx x^n e^{-ax} (1 - e^{-\beta x})^{2l+1} n_l(bx). \tag{B.33}$$

$V_1(n, l, a, \beta, b)$  can also be put in closed form, using various formulas already available in Tables of Integrals and Tables of Mathematical Function as described below.

By considering an expansion formula for the spherical Neumann function ( see for instance Gradshteyn and Ryzhik, Eq. (8.461.2) ), one can write,

$$\begin{aligned}
 & V_1(n, l, a, \beta, b) \\
 = & \frac{(-1)^{l+1}}{b} \left\{ \sum_{m=0}^{\lfloor \frac{l}{2} \rfloor} \frac{(-1)^m (l+2m)!}{(2m)!(l-2m)!(2b)^{2m}} V_{1C}(n-1-2m, 2l+1, l, a, \beta, b) \right. \\
 & + \sum_{k=0}^{\lfloor \frac{l-1}{2} \rfloor} \left. \frac{(-1)^k (l+2k+1)!}{(2k+1)!(l-2k-1)!(2b)^{2k+1}} V_{1C}(n-2k-2, 2l+1, l+1, a, \beta, b) \right\}, \\
 \end{aligned} \tag{B.34}$$

where  $V_{1C}$  function is defined as

$$\begin{aligned}
 V_{1C}(n, n_1, l, \alpha, \beta, a) &= \int_0^\infty dx x^n e^{-\alpha x} (1 - e^{-\beta x})^{n_1} \cos(ax + \frac{l\pi}{2}) \\
 &= Re\{V_{1E}(n, n_1, l, \alpha, \beta, a)\}
 \end{aligned} \tag{B.35}$$

with

$$V_{1E}(n, n_1, l, \alpha, \beta, a) = \int_0^\infty dx x^n e^{-\alpha x} (1 - e^{-\beta x})^{n_1} e^{i(ax + \frac{l\pi}{2})}. \tag{B.36}$$

For  $n \geq 0$ ,  $V_{1E}$  can be written in closed form, using an integral formula also available in Tables of Integrals (see for example, Gradshteyn and Ryzhik, p.333, formula 3.432) [117])

$$V_{1E}(n, n_1, l, \alpha, \beta, a) = e^{i\frac{l\pi}{2}} \Gamma(n+1) \sum_{j=0}^{n_1} (-1)^j C_j^{n_1} (\alpha + j\beta - ia)^{-n-1}, \tag{B.37}$$

where

$$C_j^{n_1} = \frac{n_1!}{(n_1 - j)! j!} \tag{B.38}$$

and For  $n < 0$ , but such that  $n' = -n < n_1$ , one notices that the integral  $V_{1E}$  (Eq. B.36) should be convergent. However the factor  $\Gamma(n+1)$  of Eq. (B.37) above is divergent in this case. Thus, the following identity is implied,

$$\sum_{j=0}^{n_1} (-1)^j C_j^{n_1} (\alpha + j\beta - ia)^{n'-1} \equiv 0. \tag{B.39}$$

Utilizing this identity and after carrying out expansion in power series of the integrand and splitting the range of the integration, one can easily obtain

$$V_{1E}(n, n_1, l, \alpha, \beta, a) = \frac{(-1)^{n'}}{(n' - 1)!} e^{i\frac{\pi}{2}} \sum_{j=0}^{n_1} (-1)^j C_j^{n_1} (\alpha + j\beta - ia)^{n'-1} \ln(\alpha + j\beta - ia). \quad (\text{B.40})$$

It should be noted that in practice this integral may be evaluated numerically by using appropriate Gaussian quadratures and that closed form expansion should be used only when  $\beta/\alpha$  is not too small.

$$3) \underline{M_{jq}^S(Ps)} = \langle X_j(\rho, \mathbf{R}) | H - E | \phi_{n_q l_3}(\rho) S_q^{l_4}(R) Y_{L l_3 l_4}^0(\hat{\rho} \cdot \hat{\mathbf{R}}) \rangle$$

Here  $\phi_{n_q l_3}(\rho)$  is the product of  $\rho$  by the radial wavefunction of the positronium. It was written as

$$\phi_{n_q l_3}(\rho) = \rho \sum_{j_q=0}^{n_q - l_q - 1} B'_3(n_q, l_q, j_q) \rho^{l_q + j_q} e^{-\frac{\rho}{2n_q}}, \quad (\text{B.41})$$

where

$$B'_3(n_q, l_q, j_q) = \frac{1}{\sqrt{8}} B_3(n_q, l_q, j_q). \quad (\text{B.42})$$

With the same steps of reduction previously used for  $M_{ip}^S$ , one obtains

$$\begin{aligned} M_{jq}^S(Ps) &= \langle X_j(\rho, \mathbf{R}) | \frac{1}{r_2} - \frac{1}{r_1} | \phi_{n_q l_3}(\rho) S_q^{l_4}(R) Y_{L l_3 l_4}^0(\hat{\rho} \cdot \hat{\mathbf{R}}) \rangle \\ &= B_{3j} B_{4j} \sqrt{2k_q} \sum_{(k)} F_{l_3 l_4; l_3 l_4}^{LO}(k) \sum_{j_q=0}^{n_q - l_3 - 1} B'_3(n_q, l_3, j_q) 2^{n_3, +l_3 + j_q + 3} \\ &\quad G_j(n_{4j} + 1, \alpha_{4j}, k_q, l_4, n_{3j} + l_3 + j_q - k, 2\alpha_{3j} + \frac{1}{n_q}, k). \end{aligned} \quad (\text{B.43})$$

Similar to the case of bound-bound matrix elements  $A_{ij}(Ps)$ , the summation  $k$  is over odd  $k$ .

$$4) \underline{M_{jq}^C(Ps) = \langle X_j(\rho, \mathbf{R}) | H - E | \phi_{n_q l_3}(\rho) C_q^{l_4}(R) Y_{L l_3 l_4}^0(\hat{\rho} \cdot \hat{\mathbf{R}}) \rangle}$$

Similar to  $M_{ip}^C(H)$ , applying  $H$  to operate on the left and using the defined  $V_1$ - and  $G_n$ -functions, one can analytically carry out this matrix element

$$\begin{aligned} M_{jq}^C(Ps) &= \langle X_j(\rho, \mathbf{R}) | -\frac{1}{4}(\alpha_{4j}^2 + k_q^2) + \frac{1}{4}(l_{4j}(l_{4j}+1) - n_{4j}(n_{4j}-1)) \frac{1}{R^2} + \frac{\alpha_{4j} n_{4j}}{2R} \\ &\quad + \frac{1}{r_2} - \frac{1}{r_1} | \phi_{n_q l_3}(\rho) C_q^{l_4}(R) Y_{L l_3 l_4}^0(\hat{\rho} \cdot \hat{\mathbf{R}}) \rangle \\ &= -B_{3j} B_{4j} \sqrt{2k_q} \sum_{j_q=0}^{n_q-l_3-1} B_3(n_q, l_3, j_q) \{ \delta_{l_3, l_4, l_3 l_4} \left[ -\frac{1}{4}(\alpha_{4j}^2 + k_q^2) \right. \\ &\quad V_1(n_{4j}+1, l_4, \alpha_{4j}, \gamma, k_q) + \frac{1}{4}(l_{4j}(l_{4j}+1) - n_{4j}(n_{4j}-1)) \\ &\quad V_1(n_{4j}-1, l_4, \alpha_{4j}, \gamma, k_q) + \frac{1}{2}\alpha_{4j} n_{4j} V_1(n_{4j}, l_4, \alpha_{4j}, \gamma, k_q) ] \\ &\quad \left. \frac{(n_{3j} + l_3 + j_q + 1)!}{(\alpha_{3j} + \frac{1}{2n_3})^{n_{3j} + l_3 + j_q + 2}} + \sum_k F_{l_3, l_4, l_3 l_4}^{L0}(k) 2^{n_{3j} + l_3 + j_q + 3} \right. \\ &\quad \left. G_n(n_{4j}+1, \alpha_{4j}, k_q, l_4, n_{3j} + l_3 + j_q - k, 2(\alpha_{3j} + \frac{1}{2n_3}), \gamma, k) \right\}. \quad (B.44) \end{aligned}$$

$$5) \underline{M_{jp}^S(Ps, H) = \langle X_j(\rho, \mathbf{R}) | H - E | U_{n_p l_1}(r_1) S_p^{l_2}(r_2) Y_{L l_1 l_2}^0(\hat{\mathbf{r}}_1 \cdot \hat{\mathbf{r}}_2) \rangle}$$

This matrix element can be easily reduced to a two-variable integral by operating  $H$  on the right, using the "angle integral" and  $V$ -function defined above

$$\begin{aligned} M_{jp}^S(Ps, H) &= \langle X_j(\rho, \mathbf{R}) | \frac{1}{r_2} - \frac{1}{r_{12}} | U_{n_p l_1}(r_1) S_p^{l_2}(r_2) Y_{L l_1 l_2}^0(\hat{\mathbf{r}}_1 \cdot \hat{\mathbf{r}}_2) \rangle \\ &= \sqrt{k_p} \frac{B_{3j} B_{4j}}{8} \sum_{j_p=0}^{n_p-l_1-1} B_3(n_p, l_1, j_p) \int_1^\infty d\xi \int_{-1}^1 d\eta (\xi^2 - \eta^2) \\ &\quad \left( \frac{\xi - \eta}{2} \right)^{n_{3j}-1} \left( \frac{1}{4} \sqrt{\xi^2 + 6\xi\eta + \eta^2 + 8} \right)^{n_{4j}-1} \left( \frac{\xi + \eta}{2} \right)^{l_1+j_p} \left( 1 - \frac{2}{\xi - \eta} \right) \\ &\quad H_{l_1 l_2; l_3, l_4}^L(\xi, \eta) V(2 + n_{3j} + n_{4j} + l_1 + j_p, l_2, y(\xi, \eta), k_p), \quad (B.45) \end{aligned}$$

where the function  $y(\xi, \eta)$  is

$$y(\xi, \eta) = \frac{\xi - \eta}{2} \alpha_{3j} + \frac{\xi + \eta}{2n_p} + \frac{1}{4} \sqrt{\xi^2 + 6\xi\eta + \eta^2 + 8} \alpha_{4j}. \quad (B.46)$$

$$6) \underline{M_{jp}^C(Ps, H) = \langle X_j(\rho, \mathbf{R}) | H - E | U_{n_p l_1}(r_1) C_p^{l_2}(r_2) Y_{L l_1 l_2}^0(\hat{\mathbf{r}}_1 \cdot \hat{\mathbf{r}}_2) \rangle}$$

With  $H$  operating on the left and using the "angle integral" and  $V_1$ -function, one obtains

$$\begin{aligned} M_{jp}^C(Ps, H) &= \langle X_j(\rho, \mathbf{R}) | [l_{3j}(l_{3j}+1) - n_{3j}(n_{3j}-1)] \frac{1}{\rho^2} + (2\alpha_{3j} - 1) \frac{1}{\rho} - (\alpha_{3j}^2 + \frac{1}{4}\alpha_{4j}^2) \\ &\quad + \frac{1}{4}[l_{4j}(l_{4j}+1) - n_{4j}(n_{4j}-1)] \frac{1}{R^2} + \frac{\alpha_{4j} n_{4j}}{2R} + \frac{1}{r_2} - \frac{1}{r_1} - E \\ &\quad | U_{n_p l_1}(r_1) C_p^{l_2}(r_2) Y_{L l_1 l_2}^0(\hat{\mathbf{r}}_1 \cdot \hat{\mathbf{r}}_2) \rangle \\ &= -\sqrt{k_p} \frac{B_{3j} B_{4j}}{8} \sum_{j_p=0}^{n_p-l_1-1} B_3(n_p, l_1, j_p) \int_1^\infty d\xi \int_{-1}^1 d\eta (\xi^2 - \eta^2) \left( \frac{\xi - \eta}{2} \right)^{n_{3j}-1} \\ &\quad \left( \frac{1}{4} \sqrt{\xi^2 + 6\xi\eta + \eta^2 + 8} \right)^{n_{4j}-1} \left( \frac{\xi + \eta}{2} \right)^{l_1+j_p} H_{l_1 l_2; l_{3j} l_{4j}}^L(\xi, \eta) \\ &\quad [A' V_1(1 + n_{3j} + n_{4j} + l_1 + j_p, l_2, y(\xi, \eta), \beta, k_p) \\ &\quad + B' V_1(2 + n_{3j} + n_{4j} + l_1 + j_p, l_2, y(\xi, \eta), \beta, k_p) \\ &\quad - \frac{1}{2}(2\alpha_{3j}^2 + \frac{1}{2}\alpha_{4j}^2 + 2E) V_1(3 + n_{3j} + n_{4j} + l_1 + j_p, y(\xi, \eta), \beta, k_p)], \quad (B.47) \end{aligned}$$

where

$$\begin{aligned} A' &= [l_{3j}(l_{3j}+1) - n_{3j}(n_{3j}-1)] \left( \frac{2}{\xi - \eta} \right)^2 + \frac{4[l_{4j}(l_{4j}+1) - n_{4j}(n_{4j}-1)]}{\xi^2 + 6\xi\eta + \eta^2 + 8}, \\ B' &= (2\alpha_{3j} n_{3j} - 1) \left( \frac{2}{\xi - \eta} \right) + \alpha_{4j} n_{4j} \frac{2}{\sqrt{\xi^2 + 6\xi\eta + \eta^2 + 8}} + 1 - \frac{2}{\xi + \eta}. \end{aligned}$$

$$7) \underline{M_{iq}^S(H, Ps) = \langle X_i(\mathbf{r}_1, \mathbf{r}_2) | H - E | \phi_{n_q l_3}(\rho) S_q^{l_4}(R) Y_{L l_3 l_4}^0(\hat{\rho} \cdot \hat{\mathbf{R}}) \rangle}$$

Using the same procedure as for  $M_{jp}^S(Ps, H)$ , this matrix element can be carried out

$$\begin{aligned} M_{iq}^S(H, Ps) &= \langle X_i(\mathbf{r}_1, \mathbf{r}_2) | \frac{1}{r_2} - \frac{1}{r_1} | \phi_{n_q l_3}(\rho) S_q^{l_4}(R) Y_{L l_3 l_4}^0(\hat{\rho} \cdot \hat{\mathbf{R}}) \rangle \\ &= B_{1i} B_{2i} \frac{\sqrt{2k_q}}{8} \sum_{j_q=0}^{n_q-l_3-1} B'_3(n_q, l_3, j_q) \int_1^\infty d\xi \int_{-1}^1 d\eta (\xi^2 - \eta^2) \\ &\quad \left( \frac{\xi + \eta}{2} \right)^{n_{1i}-1} \left( \frac{\xi - \eta}{2} \right)^{l_3+j_q} H_{l_1 l_2; l_{3i} l_{4i}}^L(\xi, \eta) \left( 1 - \frac{2}{\xi + \eta} \right) \\ &\quad V(2 + n_{1i} + n_{2i} + l_3 + j_q, l_4, y'(\xi, \eta), k'_q), \quad (B.48) \end{aligned}$$

where

$$y'(\xi, \eta) = \frac{\xi + \eta}{2} \alpha_{1i} + \alpha_{2i} + \frac{1}{2n_q} \frac{\xi - \eta}{2},$$

$$k'_q = \frac{1}{4} k_q \sqrt{\xi^2 + 6\xi\eta + \eta^2 + 8}.$$

8)  $M_{iq}^C(H, Ps) = \langle X_i(\mathbf{r}_1, \mathbf{r}_2) | H - E | \phi_{n_q l_3}(\rho) C_q^{l_4}(R) Y_{L l_3 l_4}^0(\hat{\rho} \cdot \hat{\mathbf{R}}) \rangle$

Again following the same procedure as for  $M_{jp}^C(Ps, H)$ , one can reduce this matrix element to

$$\begin{aligned} M_{iq}^C(H, Ps) &= \langle X_i(\mathbf{r}_1, \mathbf{r}_2) | \frac{1}{2}(l_{1i}(l_{1i}+1) - n_{1i}(n_{1i}-1)) \frac{1}{r_2} + (\alpha_{1i} n_{1i} - 1) \frac{1}{r_1} \\ &\quad - \frac{1}{2}(\alpha_{1i}^2 + \alpha_{2i}^2 + 2E) + \frac{1}{2}(l_{2i}(l_{2i}+1) - n_{2i}(n_{2i}-1)) \frac{1}{r_2^2} + (\alpha_{2i} n_{2i} + 1) \frac{1}{r_2} \\ &\quad - \frac{1}{\rho} | \phi_{n_q l_3}(\rho) C_q^{l_4}(R) Y_{L l_3 l_4}^0(\hat{\rho} \cdot \hat{\mathbf{R}}) \rangle \\ &= -B_{1i} B_{2i} \frac{\sqrt{2k_q}}{8} \sum_{j_q=0}^{n_q - l_3 - 1} B'_3(n_q, l_3, j_q) \int_1^\infty d\xi \int_{-1}^1 d\eta (\xi^2 - \eta^2) \left( \frac{\xi + \eta}{2} \right)^{n_{1i}-1} \\ &\quad \left( \frac{\xi - \eta}{2} \right)^{l_3 + j_q} H_{l_{1i} l_{2i}; l_3 l_4}^L(\xi, \eta) [A_1 V_1(1 + n_{1i} + n_{2i} + l_3 + j_q, l_4, y_1(\xi, \eta), \gamma', k'_q) \\ &\quad + B_1 V_1(2 + n_{1i} + n_{2i} + l_3 + j_q, l_4, y_1(\xi, \eta), \gamma', k'_q) \\ &\quad + C_1 V_1(3 + n_{1i} + n_{2i} + l_3 + j_q, l_4, y_1(\xi, \eta), \gamma', k'_q)], \end{aligned} \quad (B.49)$$

where parameters  $A_1$ ,  $B_1$  and  $C_1$  and the function  $y_1$  are defined as

$$A_1 = \frac{1}{2} [(l_{1i}(l_{1i}+1) - n_{1i}(n_{1i}-1)) \left( \frac{2}{\xi + \eta} \right)^2 + (l_{2i}(l_{2i}+1) - n_{2i}(n_{2i}-1))],$$

$$B_1 = (\alpha_{1i} n_{1i} - 1) \frac{2}{\xi + \eta} + \alpha_{2i} n_{2i} + 1 - \frac{2}{\xi - \eta},$$

$$C_1 = -\frac{1}{2}(\alpha_{1i}^2 + \alpha_{2i}^2 + 2E),$$

$$y_1(\xi, \eta) = \alpha_{1i} \frac{\xi + \eta}{2} + \alpha_{2i} + \frac{1}{2n_3} \frac{\xi - \eta}{2}.$$

The above formulas of the bound-bound and bound-free matrix elements can be straightforwardly generalized to apply for any physical or pseudo bound state of hydrogen and positronium by expressing it in terms of the Slater orbitals.

### B.3 Free-Free Matrix Elements

There still exist the same three types of the free-free matrix elements as in the case of the bound-free matrix elements, except that both wavefunctions involved are open channel ones.

#### 1) $M_{SS}^{pp'}(H)$ , $M_{CS}^{pp'}(H)$ and $M_{CC}^{pp'}(H)$

Operating  $H$  on the right, one can obtain  $M_{SS}^{pp'}(H)$

$$\begin{aligned} M_{SS}^{pp'}(H) &= \langle U_{n_p l_1}(r_1) S_p^{l_2}(r_2) Y_{L l_1 l_2}^0(\hat{\mathbf{r}}_1 \cdot \hat{\mathbf{r}}_2) | H - E | U_{n_{p'} l'_1}(r_1) S_{p'}^{l'_2}(r_2) Y_{L l'_1 l'_2}^0(\hat{\mathbf{r}}_1 \cdot \hat{\mathbf{r}}_2) \rangle \\ &= \langle U_{n_p l_1}(r_1) S_p^{l_2}(r_2) Y_{L l_1 l_2}^0(\hat{\mathbf{r}}_1 \cdot \hat{\mathbf{r}}_2) | \frac{1}{r_2} - \frac{1}{r_{12}} | U_{n_{p'} l'_1}(r_1) S_{p'}^{l'_2}(r_2) Y_{L l'_1 l'_2}^0(\hat{\mathbf{r}}_1 \cdot \hat{\mathbf{r}}_2) \rangle \\ &= \sqrt{k_p k_{p'}} \int_0^\infty dr_2 r_2^2 j_{l_2}(k_p r_2) j_{l'_2}(k_{p'} r_2) H_{pp'}(n_p, l_1, l_2, n_{p'}, l'_1, l'_2, L, r_2), \end{aligned} \quad (B.50)$$

where the  $H_{pp'}$ -function is defined

$$\begin{aligned} H_{pp'}(n_p, l_1, l_2, n_{p'}, l'_1, l'_2, L, r_2) &= \langle U_{n_p l_1}(r_1) Y_{L l_1 l_2}^0(\hat{\mathbf{r}}_1 \cdot \hat{\mathbf{r}}_2) | \frac{1}{r_2} - \frac{1}{r_{12}} | U_{n_{p'} l'_1}(r_1) Y_{L l'_1 l'_2}^0(\hat{\mathbf{r}}_1 \cdot \hat{\mathbf{r}}_2) \rangle \\ &= \delta_{n_p l_1 l_2 m_p l'_1 l'_2} \frac{1}{r_2} - \sum_k F_{l_1 l_2; l'_1 l'_2}^{LO} \sum_{j_p=0}^{n_p - l_1 - 1} B_3(n_p, l_1, j_p) \sum_{j_{p'}=0}^{n_{p'} - l'_1 - 1} B_3(n_{p'}, l'_1, j_{p'}) \\ &\quad \phi_{pp'}(l_1 + j_p + l'_1 + j_{p'} + 1 - k, \alpha_{pp'}, k, r_2), \end{aligned} \quad (B.51)$$

with

$$\alpha_{pp'} = \frac{1}{n_p} + \frac{1}{n_{p'}}, \quad (B.52)$$

and the function  $\phi_{pp'}$  is obtained by using the incomplete gamma functions (see for example, Gradshteyn and Ryzhik p.310, formulas 3.351 and 3.352)

$$\begin{aligned}\phi_{pp'}(n, \alpha, k, r_2) &= \int_0^\infty dr_1 r_1^{n+k+1} e^{-\alpha r_1} \frac{r_1^k}{r_1^{k+1}} \\ &= \frac{(n+2k+1)!}{\alpha^{n+2k+2}} \frac{1}{r_2^{k+1}} \left\{ 1 - e^{-\alpha r_2} \left[ \sum_{i=0}^{n+2k} \frac{1}{i!} (\alpha r_2)^i - \frac{n!}{(n+2k+1)!} \sum_{j=0}^{n-1} \frac{1}{j!} (\alpha r_2)^{j+2k+1} \right] \right\}. \end{aligned} \quad (\text{B.53})$$

Similarly, one obtains  $M_{CS}^{pp'}(H)$

$$\begin{aligned}M_{CS}^{pp'}(H) &= \langle U_{n_p l_1}(r_1) C_p^{l_2}(r_2) Y_{L l_1 l_2}^0(\hat{\mathbf{r}}_1 \cdot \hat{\mathbf{r}}_2) | H - E | U_{n_{p'} l'_1}(r_1) S_{p'}^{l'_2}(r_2) Y_{L l'_1 l'_2}^0(\hat{\mathbf{r}}_1 \cdot \hat{\mathbf{r}}_2) \rangle \\ &= \langle U_{n_p l_1}(r_1) C_p^{l_2}(r_2) Y_{L l_1 l_2}^0(\hat{\mathbf{r}}_1 \cdot \hat{\mathbf{r}}_2) | \frac{1}{r_2} - \frac{1}{r_{12}} | U_{n_{p'} l'_1}(r_1) S_{p'}^{l'_2}(r_2) Y_{L l'_1 l'_2}^0(\hat{\mathbf{r}}_1 \cdot \hat{\mathbf{r}}_2) \rangle \\ &= -\sqrt{k_p k_{p'}} \int_0^\infty dr_2 r_2^2 (1 - e^{-\beta r_2})^{2l_2+1} n_{l_2}(k_p r_2) j_{l'_2}(k_{p'} r_2) \\ &\quad H_{pp'}(n_p, l_1, l_2, n_{p'}, l'_1, l'_2, L, r_2). \end{aligned} \quad (\text{B.54})$$

For  $M_{CC}^{pp'}$ , by operating  $H$  on the left and introducing

$$\begin{aligned}f_l(\beta, k, r) &= [-\frac{1}{2r} \frac{d^2}{dr^2} + \frac{l(l+1)}{2r^2} - \frac{1}{2} k^2] (1 - e^{-\beta r})^{2l+1} n_l(kr) \\ &= \beta(l+\frac{1}{2}) e^{-\beta r} \left\{ -2\beta l (1 - e^{-\beta r})^{2l-1} n_l(kr) e^{-\beta r} + (\beta - 2\frac{l+1}{r}) \right. \\ &\quad \left. (1 - e^{-\beta r})^{2l} n_l(kr) + 2k (1 - e^{-\beta r})^{2l} n_{l+1}(kr) \right\}, \end{aligned} \quad (\text{B.55})$$

one obtains

$$\begin{aligned}M_{CC}^{pp'}(H) &= \langle U_{n_p l_1}(r_1) C_p^{l_2}(r_2) Y_{L l_1 l_2}^0(\hat{\mathbf{r}}_1 \cdot \hat{\mathbf{r}}_2) | H - E | U_{n_{p'} l'_1}(r_1) C_{p'}^{l'_2}(r_2) Y_{L l'_1 l'_2}^0(\hat{\mathbf{r}}_1 \cdot \hat{\mathbf{r}}_2) \rangle \\ &= \langle U_{n_p l_1}(r_1) Y_{L l_1 l_2}^0(\hat{\mathbf{r}}_1 \cdot \hat{\mathbf{r}}_2) | \sqrt{k_p} f_{l_2}(\beta, k_p, r_2) + C_p^{l_2}(r_2) \left( \frac{1}{r_2} - \frac{1}{r_{12}} \right) \\ &\quad | U_{n_{p'} l'_1}(r_1) C_{p'}^{l'_2}(r_2) Y_{L l'_1 l'_2}^0(\hat{\mathbf{r}}_1 \cdot \hat{\mathbf{r}}_2) \rangle \\ &= \sqrt{k_p k_{p'}} \int_0^\infty dr_2 r_2^2 [\delta_{n_p l_1 l_2; n_{p'} l'_1 l'_2} f_{l_2}(\beta, k_p, r_2) + (1 - e^{-\beta r_2})^{2l_2+1} n_{l_2}(k_p r_2) \\ &\quad H_{pp'}(n_p, l_1, l_2, n_{p'}, l'_1, l'_2, L, r_2)] (1 - e^{-\beta' r_2})^{2l'_2+1} n_{l'_2}(k_{p'} r_2). \end{aligned} \quad (\text{B.56})$$

## 2) $M_{SS}^{qq'}(Ps)$ , $M_{CS}^{pp'}(Ps)$ and $M_{CC}^{pp'}(Ps)$

Using the exactly same procedure as for the free-free matrix elements of hydrogen channels, One then obtains

$$\begin{aligned} M_{SS}^{qq'} &= \langle \phi_{n_q l_3}(\rho) S_q^{l_4}(R) Y_{Ll_3l_4}^0(\hat{\rho} \cdot \hat{\mathbf{R}}) | H - E | \phi_{n_{q'} l'_3}(\rho) S_{q'}^{l'_4}(R) Y_{Ll_3l_4}^0(\hat{\rho} \cdot \hat{\mathbf{R}}) \rangle \\ &= \langle \phi_{n_q l_3}(\rho) S_q^{l_4}(R) Y_{Ll_3l_4}^0(\hat{\rho} \cdot \hat{\mathbf{R}}) | \frac{1}{r_2} - \frac{1}{r_1} | \phi_{n_{q'} l'_3}(\rho) S_{q'}^{l'_4}(R) Y_{Ll_3l_4}^0(\hat{\rho} \cdot \hat{\mathbf{R}}) \rangle \\ &= 2\sqrt{k_q k_{q'}} \int_0^\infty dRR^2 j_{l_4}(k_q R) j_{l'_4}(k_{q'} R) H_{qq'}(n_q, l_3, l_4, n_{q'}, l'_3, l'_4, L, R), \end{aligned} \quad (\text{B.57})$$

with  $H_{qq'}$ -function defined

$$\begin{aligned} H_{qq'}(n_q, l_3, l_4, n_{q'}, l'_3, l'_4, L, R) &= \langle \phi_{n_q l_3}(\rho) Y_{Ll_3l_4}^0(\hat{\rho} \cdot \hat{\mathbf{R}}) | \frac{1}{r_2} - \frac{1}{r_1} | \phi_{n_{q'} l'_3}(\rho) Y_{Ll_3l_4}^0(\hat{\rho} \cdot \hat{\mathbf{R}}) \rangle \\ &= 2 \sum_k F_{l_3 l_4; l'_3 l'_4}^{L0}(k) \langle \phi_{n_q l_3}(\rho) | \frac{x_-^k}{x_+^{k+1}} | \phi_{n_{q'} l'_3}(\rho) \rangle \\ &= \sum_k F_{l_3 l_4; l'_3 l'_4}^{L0}(k) \sum_{j_q=0}^{n_q-l_3-1} B'_3(n_q, l_3, j_q) \sum_{j_{q'}=0}^{n_{q'}-l'_3-1} B'_3(n_{q'}, l'_3, j_{q'}) \\ &\quad 2^{l_3+j_3+l'_3+j'_3+4} \phi_{qq'}(l_3 + j_q + l'_3 + j_{q'} + 1 - k, \alpha_{qq'}, k, R), \end{aligned} \quad (\text{B.58})$$

where  $\phi_{qq'}$  function was defined in Eq. (B.53) and

$$\alpha_{qq'} = \frac{1}{n_q} + \frac{1}{n_{q'}}. \quad (\text{B.59})$$

The summation over  $k$  in Eq. B.58, as stated in Section C.1, just takes the possible odd integers. Similarly, one can obtain

$$\begin{aligned} M_{CS}^{qq'} &= \langle \phi_{n_q l_3}(\rho) C_q^{l_4}(R) Y_{Ll_3l_4}^0(\hat{\rho} \cdot \hat{\mathbf{R}}) | H - E | \phi_{n_{q'} l'_3}(\rho) S_{q'}^{l'_4}(R) Y_{Ll_3l_4}^0(\hat{\rho} \cdot \hat{\mathbf{R}}) \rangle \\ &= \langle \phi_{n_q l_3}(\rho) C_q^{l_4}(R) Y_{Ll_3l_4}^0(\hat{\rho} \cdot \hat{\mathbf{R}}) | \frac{1}{r_2} - \frac{1}{r_1} | \phi_{n_{q'} l'_3}(\rho) S_{q'}^{l'_4}(R) Y_{Ll_3l_4}^0(\hat{\rho} \cdot \hat{\mathbf{R}}) \rangle \\ &= -2\sqrt{k_q k_{q'}} \int_0^\infty dRR^2 (1 - e^{-\gamma R})^{2l_4+1} n_{l_4}(k_q R) j_{l'_4}(k_{q'} R) \\ &\quad H_{qq'}(n_q, l_3, l_4, n_{q'}, l'_3, l'_4, L, R), \end{aligned} \quad (\text{B.60})$$

and

$$\begin{aligned}
 M_{CC}^{qq'} &= \langle \phi_{n_q l_3}(\rho) C_q^{l_4}(R) Y_{Ll_3 l_4}^0(\hat{\rho} \cdot \hat{\mathbf{R}}) | H - E | \phi_{n_{q'} l'_3}(\rho) C_{q'}^{l'_4}(R) Y_{Ll'_3 l'_4}^0(\hat{\rho} \cdot \hat{\mathbf{R}}) \rangle \\
 &= \langle \phi_{n_q l_3}(\rho) C_q^{l_4}(R) Y_{Ll_3 l_4}^0(\hat{\rho} \cdot \hat{\mathbf{R}}) | -\frac{\sqrt{2k_q}}{2} f_{l_4}(\gamma, k_q, R) + C_q^{l_4}(R) \left( \frac{1}{r_2} - \frac{1}{r_1} \right) \\
 &\quad | \phi_{n_{q'} l'_3}(\rho) C_{q'}^{l'_4}(R) Y_{Ll'_3 l'_4}^0(\hat{\rho} \cdot \hat{\mathbf{R}}) \rangle \\
 &= 2\sqrt{k_q k_{q'}} \int_0^\infty dR R^2 [\delta_{n_q l_3 l_4; n_{q'} l'_3 l'_4} \frac{1}{2} f_{l_4}(\gamma, k_q, R) + (1 - e^{-\gamma R})^{2l_4+1} n_{l_4}(k_q R) \\
 &\quad H_{q q'}(n_q, l_3, l_4, n_{q'}, l'_3, l'_4, L, R)] (1 - e^{-\gamma R})^{2l'_4+1} n_{l'_4}(k_{q'} R). \tag{B.61}
 \end{aligned}$$

The above matrix elements could be further reduced to closed forms. But it is very feasible to carry out these one-dimensional integrals with these compact forms by using the Gaussian quadrature. Such a direct one-dimensional numerical integration is especially powerful for higher partial waves.

### 3) $M_{SS}^{pq}(H, Ps)$ , $M_{CS}^{pq}(H, Ps)$ , $M_{CS}^{qp}(Ps, H)$ and $M_{CC}^{pq}(H, Ps)$

With  $H$  operating on the right, one can obtain

$$\begin{aligned}
 M_{SS}^{pq} &= \langle U_{n_p l_1}(r_1) S_p^{l_2}(r_2) Y_{Ll_1 l_2}^0(\hat{\mathbf{r}}_1 \cdot \hat{\mathbf{r}}_2) | H - E | \phi_{n_q l_3}(\rho) S_q^{l_4}(R) Y_{Ll_3 l_4}^0(\hat{\rho} \cdot \hat{\mathbf{R}}) \rangle \\
 &= \langle U_{n_p l_1}(r_1) S_p^{l_2}(r_2) Y_{Ll_1 l_2}^0(\hat{\mathbf{r}}_1 \cdot \hat{\mathbf{r}}_2) | \frac{1}{r_2} - \frac{1}{r_1} | \phi_{n_{q'} l'_3}(\rho) S_{q'}^{l'_4}(R) Y_{Ll'_3 l'_4}^0(\hat{\rho} \cdot \hat{\mathbf{R}}) \rangle \\
 &= \frac{\sqrt{2k_p k_q}}{8} \sum_{j_p=0}^{n_p-l_1-1} B_3(n_p, l_1, j_p) \sum_{j_q=0}^{n_q-l_3-1} B'_3(n_q, l_3, j_q) \int_1^\infty d\xi \int_{-1}^1 d\eta (\xi^2 - \eta^2) \\
 &\quad \left( \frac{\xi + \eta}{2} \right)^{l_1+j_p} \left( \frac{\xi - \eta}{2} \right)^{l_3+j_q} \left( 1 - \frac{2}{\xi + \eta} \right) H_{l_1 l_2; l_3 l_4}^L(\xi, \eta) \\
 &\quad W_{j_j}(4 + l_1 + j_p + l_3 + j_q, y(\xi, \eta), k_p, k'_q, l_2, l_4), \tag{B.62}
 \end{aligned}$$

where

$$y(\xi, \eta) = \left( \frac{1}{2n_p} + \frac{1}{4n_q} \right) \xi + \left( \frac{1}{2n_p} - \frac{1}{4n_q} \right) \eta, \tag{B.63}$$

$$k'_q = \frac{k_q}{4} \sqrt{\xi^2 + 6\eta\xi + \eta^2 + 8}, \tag{B.64}$$

where the  $W_{jj}$ -function is defined as

$$W_{jj}(n, a, b, c, l_1, l_2) = \int_0^\infty dx x^n e^{-ax} j_{l_1}(bx) j_{l_2}(cx). \quad (\text{B.65})$$

For the integral Eq. (B.65), a formula is available for  $n=1$  and  $l_1=l_2=l$  (see Eq. (6.612.3) in Ref. [117]):

$$W_{jj}(1, l, l, a, b, c) = \frac{1}{2bc} Q_l\left(\frac{a^2 + b^2 + c^2}{2bc}\right), \quad (\text{B.66})$$

where  $Q_l(x)$  is the second kind of the Legendre function. For  $n>1$ , a closed form of the integration  $W_{jj}$  may be obtained by using parameter derivatives (Eq. (0.432(1)) in Ref. [117]) and the properties of the Legendre function  $Q_l^m(x)$  (see Eq. (8.752(4)) in Ref. [117])

$$\begin{aligned} W_{jj}(n, a, b, c, l, l) &= (-1)^{n-1} \frac{\partial^{n-1}}{\partial a^{n-1}} W_{jj}(1, a, b, c, l, l) \\ &= \frac{(-1)^{n-1}}{2bc} \frac{\partial^{n-1}}{\partial a^{n-1}} Q_l\left(\frac{a^2 + b^2 + c^2}{2bc}\right) \\ &= \frac{1}{2bc} \sum_{i=0}^{\lfloor \frac{n-1}{2} \rfloor} \frac{(-1)^i (n-1)!}{2^i (n-1-2i)! i!} \left(\frac{a}{bc}\right)^{n-1-2i} \left(\frac{1}{bc}\right)^i (x^2 - 1)^{-\frac{n-1-i}{2}} \bar{Q}_l^{n-1-i}(x), \end{aligned} \quad (\text{B.67})$$

where it was necessary to define

$$\bar{Q}_l^{n-l-i}(x) = (-1)^{n-l-i} Q_l^{n-l-i}(x), \quad (\text{B.68})$$

where the  $Q_l^m(x)$  is the second kind of the associated Legendre function and  $x = \frac{a^2+b^2+c^2}{2bc}$ . If  $l_1$  is different from  $l_2$ , a parameter derivative with respect to  $b$  or  $c$  will be carried out and the recursion relation of the Bessel function will be also used.

For matrix element  $M_{CS}^{pq}$ , still operating  $H$  on the right, one can obtain

$$\begin{aligned} M_{CS}^{pq} &= \langle U_{n_p l_1}(r_1) C_p^{l_2}(r_2) Y_{Ll_1 l_2}^0(\hat{r}_1 \cdot \hat{r}_2) | H - E | \phi_{n_q l_3}(\rho) S_q^{l_4}(R) Y_{Ll_3 l_4}^0(\hat{\rho} \cdot \hat{R}) \rangle \\ &= \langle U_{n_p l_1}(r_1) C_p^{l_2}(r_2) Y_{Ll_1 l_2}^0(\hat{r}_1 \cdot \hat{r}_2) | \frac{1}{r_2} - \frac{1}{r_1} | \phi_{n_q l_3}(\rho) S_q^{l_4}(R) Y_{Ll_3 l_4}^0(\hat{\rho} \cdot \hat{R}) \rangle \end{aligned}$$

$$\begin{aligned}
&= -\frac{\sqrt{2k_p k_q}}{8} \sum_{j_p=0}^{n_p-l_1-1} B_3(n_p, l_1, j_p) \sum_{j_q=0}^{n_q-l_3-1} B'_3(n_q, l_3, j_q) \int_1^\infty d\xi \int_{-1}^1 d\eta (\xi^2 - \eta^2) \\
&\quad (\frac{\xi + \eta}{2})^{l_1+j_p} (\frac{\xi - \eta}{2})^{l_3+j_q} (1 - \frac{2}{\xi + \eta}) H_{l_1 l_2; l_3 l_4}^L(\xi, \eta) \\
&\quad W_{jn}(4 + l_1 + j_p + l_3 + j_q, y(\xi, \eta), k'_q, \beta, k_p, l_4, l_2),
\end{aligned} \tag{B.69}$$

where  $W_{jn}$ -function is defined by

$$W_{jn}(n, a, b, \beta, c, l_1, l_2) = \int_0^\infty dx x^n e^{-ax} j_{l_1}(bx) (1 - e^{-\beta x})^{2l_2+1} n_{l_2}(cx). \tag{B.70}$$

Practically, we utilize direct numerical technique, the Gaussian quadrature, to carry out integrations Eq. (B.70). In all of our calculations for the bound-free and free-free matrix elements, the one-dimensional Gaussian integration is performed with 800 Gaussian node points, which can generally keep a high numerical precision.

Using exactly the same procedure as in  $M_{CS}^{pq}$ , one obtains

$$\begin{aligned}
M_{CS}^{qp} &= \langle \phi_{n_q l_3}(\rho) C_q^{l_4}(R) Y_{Ll_3 l_4}^0(\hat{\rho} \cdot \hat{\mathbf{R}}) | H - E | U_{n_p l_1}(r_1) S_p^{l_2}(r_2) Y_{Ll_1 l_2}^0(\hat{\mathbf{r}}_1 \cdot \hat{\mathbf{r}}_2) \rangle \\
&= \langle \phi_{n_q l_3}(\rho) S_q^{l_4}(R) Y_{Ll_3 l_4}^0(\hat{\rho} \cdot \hat{\mathbf{R}}) | \frac{1}{r_2} - \frac{1}{r_{12}} | U_{n_p l_1}(r_1) C_p^{l_2}(r_2) Y_{Ll_1 l_2}^0(\hat{\mathbf{r}}_1 \cdot \hat{\mathbf{r}}_2) \rangle \\
&= -\frac{\sqrt{2k_p k_q}}{8} \sum_{j_p=0}^{n_p-l_1-1} B_3(n_p, l_1, j_p) \sum_{j_q=0}^{n_q-l_3-1} B'_3(n_q, l_3, j_q) \int_1^\infty d\xi \int_{-1}^1 d\eta (\xi^2 - \eta^2) \\
&\quad (\frac{\xi + \eta}{2})^{l_1+j_p} (\frac{\xi - \eta}{2})^{l_3+j_q} (1 - \frac{2}{\xi - \eta}) H_{l_1 l_2; l_3 l_4}^L(\xi, \eta) \\
&\quad W_{jn}(4 + l_1 + j_p + l_3 + j_q, y(\xi, \eta), k_p, \gamma' k'_q, l_2, l_4),
\end{aligned} \tag{B.71}$$

where

$$\gamma' = \frac{\gamma}{4} \sqrt{\xi^2 + 6\eta\xi + \eta^2 + 8}. \tag{B.72}$$

Finally

$$\begin{aligned}
M_{CC}^{pq} &= \langle U_{n_p l_1}(r_1) C_p^{l_2}(r_2) Y_{Ll_1 l_2}^0(\hat{\mathbf{r}}_1 \cdot \hat{\mathbf{r}}_2) | H - E | \phi_{n_q l_3}(\rho) C_q^{l_4}(R) Y_{Ll_3 l_4}^0(\hat{\rho} \cdot \hat{\mathbf{R}}) \rangle \\
&= \langle U_{n_p l_1}(r_1) Y_{Ll_1 l_2}^0(\hat{\mathbf{r}}_1 \cdot \hat{\mathbf{r}}_2) | \sqrt{k_p} f_{l_2}(\beta, k_p, r_2) + C_p^{l_2}(r_2) (\frac{1}{r_2} - \frac{1}{r_{12}})
\end{aligned}$$

$$\begin{aligned}
& |\phi_{n_q l_3}(\rho) C_q^{l_4}(R) Y_{L l_3 l_4}^0(\hat{\rho} \cdot \hat{\mathbf{R}})\rangle \\
= & \frac{\sqrt{2k_p k_q}}{8} \sum_{j_p=0}^{n_p-l_1-1} B_3(n_p, l_1, j_p) \sum_{j_q=0}^{n_q-l_3-1} B'_3(n_q, l_3, j_q) \int_1^\infty d\xi \int_{-1}^1 d\eta (\xi^2 - \eta^2) \\
& \left( \frac{\xi + \eta}{2} \right)^{l_1+j_p} \left( \frac{\xi - \eta}{2} \right)^{l_3+j_q} H_{l_1 l_2; l_3 l_4}^L(\xi, \eta) \int_0^\infty dr_2 r_2^{5+l_1+j_p+l_3+j_q} e^{-y(\xi, \eta)r_2} \\
& [f_{l_2}(\beta, k_p, r_2) + (1 - \frac{2}{\xi - \eta}) \frac{1}{r_2} (1 - e^{-\beta r_2})^{2l_2+1} n_{l_2}(k_p r_2)] \\
& (1 - e^{-\gamma' r_2})^{2l_4+1} n_{l_4}(k'_q r_2). \tag{B.73}
\end{aligned}$$

#### B.4 Reduction of Angle Integral

Here we are going to reduce the "angle integral", Eq. (B.21), by transferring the spherical coordinates of the electron to spheroidal coordinates

$$\begin{aligned}
\xi &= \frac{r_1 + \rho}{r_2}, \\
\eta &= \frac{r_1 - \rho}{r_2},
\end{aligned}$$

and  $\phi$  which is an angle between a plane formed by particles  $e^+e^-p$  and an arbitrary plane through  $e^+p$ . The variables range from 1 to  $\infty$  for  $\xi$ , from -1 to 1 for  $\eta$  and from 0 to  $2\pi$  for  $\phi$ . To do this transformation, the following relations are basically necessary

$$\frac{z_1}{r_1} = a_1 \cos \theta_2 - a_2 \cos \phi \sin \theta_2, \tag{B.74}$$

$$\frac{x_1 + iy_1}{r_1} = (a_1 \sin \theta_2 + a_2 \cos \phi \cos \theta_2 + ia_2 \sin \phi) e^{i\phi_2}, \tag{B.75}$$

$$\frac{z_R}{R} = a_3 \cos \theta_2 - a_4 \cos \phi \sin \theta_2, \tag{B.76}$$

$$\frac{x_R + iy_R}{R} = (a_3 \sin \theta_2 + a_4 \cos \phi \cos \theta_2 + ia_4 \sin \phi) e^{i\phi_2}, \tag{B.77}$$

$$\frac{z_\rho}{\rho} = a_5 \cos \theta_2 - a_6 \cos \phi \sin \theta_2, \tag{B.78}$$

$$\frac{x_\rho + iy_\rho}{\rho} = (a_5 \sin \theta_2 + a_6 \cos \phi \cos \theta_2 + ia_6 \sin \phi) e^{i\phi_2}, \tag{B.79}$$

where subscripts 1,  $\rho$  and R respectively refer to the electron, positron and mass center of the positronium.  $\theta_2$  and  $\phi_2$  are the angle coordinates of the positron. The parameters  $a_i$ ,  $i=1, \dots, 6$ , are defined as

$$\begin{aligned} a_1 &= \frac{\xi\eta + 1}{\xi + \eta}, \\ a_2 &= \frac{\sqrt{(\xi^2 - 1)(1 - \eta^2)}}{\xi + \eta}, \\ a_3 &= \frac{\xi\eta + 3}{\sqrt{\xi^2 + 6\xi\eta + \eta^2 + 8}}, \\ a_4 &= \frac{\sqrt{(\xi^2 - 1)(1 - \eta^2)}}{\sqrt{\xi^2 + 6\xi\eta + \eta^2 + 8}}, \\ a_5 &= \frac{\xi\eta - 1}{\xi - \eta}, \\ a_6 &= \frac{\sqrt{(\xi^2 - 1)(1 - \eta^2)}}{\xi - \eta}. \end{aligned}$$

Using the angular momentum theory [95], we write the "angle integral", Eq. (B.21), into

$$\begin{aligned} H_{l_1 l_2; l_3 l_4}^L(\xi, \eta) &= \int_0^{2\pi} d\phi \int d\hat{\mathbf{r}}_2 Y_{L l_1 l_2}^0(\mathbf{r}_1 \cdot \mathbf{r}_2) Y_{L l_3 l_4}^0(\rho \cdot \mathbf{R}) \\ &= (-1)^{l_3 - l_4 + l_1 - l_2} (2L + 1) \sum_{m'=0}^{(l_3, l_4)_<} \lambda_{m'} \begin{pmatrix} l_3 & l_4 & L \\ m' & -m' & 0 \end{pmatrix} \\ &\quad \sum_{m=0}^{(l_1, l_2)_<} \lambda_m \begin{pmatrix} l_1 & l_2 & L \\ m & -m & 0 \end{pmatrix} H'_{l_1 l_2; l_3 l_4}(\xi, \eta, m, m'), \end{aligned} \quad (\text{B.80})$$

where  $\lambda_m = 0.5$  for  $m=0$ , 1 for  $m > 0$  and  $(n, m)_<$  the lesser of n and m.  $H'$  function is defined as

$$H'_{l_1 l_2; l_3 l_4}(\xi, \eta, m, m') = \int_0^{2\pi} d\phi \int d\hat{\mathbf{r}}_2 \Delta_{l_1 l_2 m} \Delta_{l_3 l_4 m'}, \quad (\text{B.81})$$

where

$$\Delta_{l_1 l_2 m} = Y_{l_1 m}(\hat{\mathbf{r}}_1) Y_{l_2 -m}(\hat{\mathbf{r}}_2) + Y_{l_1 -m}(\hat{\mathbf{r}}_1) Y_{l_2 m}(\hat{\mathbf{r}}_2), \quad (\text{B.82})$$

$$\Delta_{l_3 l_4 m'} = Y_{l_3 m'}(\hat{\rho}) Y_{l_4 -m'}(\hat{\mathbf{R}}) + Y_{l_3 -m'}(\hat{\rho}) Y_{l_4 m'}(\hat{\mathbf{R}}). \quad (\text{B.83})$$

Now we write down the specific forms of a spherical harmonics function [95] in the following form:

$$Y_{lm}(\theta, \phi) = \left(\frac{x + iy}{r}\right)^m \sum_{k=0}^{\lfloor \frac{l-m}{2} \rfloor} p_{lmk} \left(\frac{z}{r}\right)^{l-2k-m}, \quad (\text{B.84})$$

with a coefficient  $p_{lmk}$

$$p_{lmk} = (-1)^{m+k} \sqrt{\frac{2l+1}{4\pi} \frac{(l-m)!}{(l+m)!}} \frac{2^{-l}(2l-2k)!}{k!(l-k)!(l-2k-m)!}. \quad (\text{B.85})$$

Using the properties of the spherical harmonics [95] and the above expansion, we can rewrite  $\Delta_{l_1 l_2 m}$  into

$$\begin{aligned} \Delta_{l_1 l_2 m} &= (-1)^m [Y_{l_1 m}(\hat{r}_1) Y_{l_2 m}^*(\hat{r}_2) + Y_{l_1 m}^*(\hat{r}_1) Y_{l_2 m}(\hat{r}_2)] \\ &= 2(-1)^m \operatorname{Re}\left\{\left(\frac{x_1 + iy_1}{r_1}\right)^m e^{-im\phi_2}\right\} \bar{P}_{l_2}^m(\cos\theta_2) \sum_{k=0}^{\lfloor \frac{l_1-m}{2} \rfloor} p_{l_1 m k} \left(\frac{z_1}{r_1}\right)^{l_1-m-2k} \\ &= 2(-1)^m \bar{P}_{l_2}^m(\cos\theta_2) \sum_{k=0}^{\lfloor \frac{l_1-m}{2} \rfloor} p_{l_1 m k} a_1^{l_1-2k} \sum_{k_1=0}^{l_1-2k-m} (-1)^{k_1} C_{k_1}^{l_1-2k-m} \left(\frac{a_2}{a_1}\right)^{k_1} \\ &\quad \sum_{j=0}^{\lfloor \frac{m}{2} \rfloor} (-1)^j C_{2j}^m \sum_{j_0=0}^{m-2j} C_{j_0}^{m-2j} \left(\frac{a_2}{a_1}\right)^{2j+j_0} (\cos\theta_2)^{l_1-2k-m-k_1+j_0} \\ &\quad (\sin\theta_2)^{k_1+m-2j-j_0} (\cos\phi)^{k_1+j_0} (\sin\phi)^{2j}, \end{aligned} \quad (\text{B.86})$$

where  $\operatorname{Re}\{z\}$  is the real part of  $z$ .  $C_k^n$  is a binomial expansion coefficient.  $\bar{P}_l^m(x)$  is related to the associated Legendre function  $P_l^m(x)$

$$\bar{P}_l^m(x) = \sqrt{\frac{2l+1}{4\pi} \frac{(l-m)!}{(l+m)!}} P_l^m(x) = (1-x^2)^{\frac{m}{2}} \sum_{j=0}^{\lfloor \frac{l_1-m}{2} \rfloor} p_{l m j} x^{l-2j-m}. \quad (\text{B.87})$$

Then we define  $\Delta_{l_3 l_4 m'}$  as

$$\begin{aligned} \Delta_{l_3 l_4 m'} &= (-1)^{m'} [Y_{l_3 m'}(\hat{\rho}) Y_{l_4 m'}^*(\hat{R}) + Y_{l_3 m'}^*(\hat{\rho}) Y_{l_4 m'}(\hat{R})] \\ &= 2(-1)^{m'} \operatorname{Re}\left\{\left(\frac{x_\rho - iy_\rho}{\rho} \frac{x_R + iy_R}{R}\right)^{m'}\right\} \sum_{k_3}^{\lfloor \frac{l_3-m'}{2} \rfloor} p_{l_3 m' k_3} \left(\frac{z_\rho}{\rho}\right)^{l_3-m'-2k_3} \\ &\quad \sum_{k_4=0}^{\lfloor \frac{l_4-m'}{2} \rfloor} p_{l_4 m' k_4} \left(\frac{z_R}{R}\right)^{l_4-m'-2k_4} \end{aligned}$$

$$\begin{aligned}
&= 2(-1)^{m'}(a_3a_5)^{m'} \sum_{j_{13}=0}^{2m'} (-1)^{\frac{j_{13}}{2}} \sum_{j_1=[0,j_{13}-m']>}^{[j_{13},m']<} (-1)^{j_1} C_{j_1}^{m'} C_{j_{13}-j_1}^{m'} \\
&\quad \sum_{j_2=0}^{m'-j_1} C_{j_2}^{m'-j_1} \left(\frac{a_6}{a_5}\right)^{j_1+j_2} \sum_{j_4=0}^{m'+j_1-j_{13}} C_{j_4}^{m'+j_1-j_{13}} \left(\frac{a_4}{a_3}\right)^{j_{13}-j_1+j_4} \\
&\quad \sum_{k_3=0}^{\lfloor \frac{l_3-m'}{2} \rfloor} a_5^{l_s} p_{l_3 m' k_3} \sum_{k_s=0}^{l_s} \left(-\frac{a_6}{a_5}\right)^{k_s} C_{k_s}^{l_s} \sum_{k_t=0}^{\lfloor \frac{l_4-m'}{2} \rfloor} a_3^{l_t} p_{l_4 m' k_t} \sum_{k_t=0}^{l_t} C_{k_t}^{l_t} \left(-\frac{a_4}{a_3}\right)^{k_t} \\
&\quad (\cos\theta_2)^{l_s-k_s+l_t-k_t+j_2+j_4} (\sin\theta_2)^{k_s+k_t+2m'-j_{13}-j_2-j_4} (\cos\phi)^{k_s+k_t+j_2+j_4} (\sin\phi)^{j_{13}}, \\
\end{aligned} \tag{B.88}$$

where  $l_s = l_3 - m' - 2k_3$  and  $l_t = l_4 - m' - 2k_4$ . Using the following integral formula (see Eq. (3.621.5) in Ref. [117])

$$\int_0^{\frac{\pi}{2}} d\phi (\cos\phi)^n (\sin\phi)^m = \frac{1}{2} B\left(\frac{n+1}{2}, \frac{m+1}{2}\right), \tag{B.89}$$

where  $B(x,y)$  is the beta function (see Eq. (8.384.1) in Ref. [117]:  $B(x,y) = \frac{\Gamma(x)\Gamma(y)}{\Gamma(x+y)}$ , we can carry out the integration (see Eq. (3.621.5) in Ref. [117])

$$\begin{aligned}
\wp(n, k, l, m) &= \int_0^\pi d\theta (\cos\theta)^n (\sin\theta)^k \tilde{P}_l^m(\cos\theta) \\
&= \sum_{j=0}^{\lfloor \frac{l_1-m'}{2} \rfloor} p_{lmj} \int_0^\pi d\theta (\cos\theta)^{n+l-2j-m} (\sin\theta)^{k+m} \\
&= \frac{1}{2} \sum_{j=0}^{\lfloor \frac{l_1-m'}{2} \rfloor} ((-1)^{n+l-2j-m} + 1) p_{lmj} B\left(\frac{n+l-2j-m+1}{2}, \frac{k+m+1}{2}\right).
\end{aligned} \tag{B.90}$$

Now the  $H'$  function defined above can be analytically obtained as follows

$$\begin{aligned}
H'_{l_1 l_2 i_3 l_4}(\xi, \eta, m, m') &= \int_0^{2\pi} d\phi \int_0^{2\pi} d\phi_2 \int_0^\pi d\theta_2 \Delta_{l_1 l_2 m} \Delta_{l_3 l_4 m'} \\
&= 8\pi (-1)^{m+m'} \sum_{k=0}^{\lfloor \frac{l_1-m'}{2} \rfloor} p_{lmk} a_1^{l_1-2k} \sum_{k_1=0}^{l_1-2k-m} (-1)^{k_1} C_{k_1}^{l_1-2k-m} \left(\frac{a_2}{a_1}\right)^{k_1} \sum_{j=0}^{\lfloor \frac{m}{2} \rfloor} (-1)^j C_{2j}^m \\
&\quad \sum_{j_0=0}^{m-2j} C_{j_0}^{m-2j} \left(\frac{a_2}{a_1}\right)^{2j+j_0} \sum_{j_{13}=0}^{2m'} (-1)^{\frac{j_{13}}{2}} \sum_{j_1=[0,j_{13}-m']>}^{[j_{13},m']<} (-1)^{j_1} C_{j_1}^{m'} C_{j_{13}-j_1}^{m'}
\end{aligned}$$

$$\begin{aligned}
& \sum_{j_2=0}^{m'-j_1} C_{j_2}^{m'-j_1} \left(\frac{a_6}{a_5}\right)^{j_1+j_2} \sum_{j_4=0}^{m'+j_1-j_{13}} C_{j_4}^{m'+j_1-j_{13}} \left(\frac{a_4}{a_3}\right)^{j_{13}-j_1+j_4} \sum_{k_3=0}^{\lfloor \frac{j_3-m'}{2} \rfloor} a_5^{l_3-2k_3} p_{l_3 m' k_3} \\
& \sum_{k_s=0}^{l_s} \left(-\frac{a_6}{a_5}\right)^{k_s} C_{k_s}^{l_s} \sum_{k_4=0}^{\lfloor \frac{l_4-m'}{2} \rfloor} a_3^{l_4-2k_4} p_{l_4 m' k_4} \sum_{k_t=0}^{l_t} C_{k_t}^{l_t} \left(-\frac{a_4}{a_3}\right)^{k_t} \\
& \int_0^{2\pi} d\phi (\cos\phi)^M (\sin\phi)^{2j+j_{13}} \int_0^\pi d\theta_2 (\cos\theta_2)^N (\sin\theta_2)^K P_{l_2}^m(\cos\theta_2) \\
= & 8\pi (-1)^{m+m'} \sum_{k=0}^{\lfloor \frac{j_1-m}{2} \rfloor} p_{l_1 m k} a_1^{l_1-2k} \sum_{k_1=0}^{l_1-2k-m} (-1)^{k_1} C_{k_1}^{l_1-2k-m} \left(\frac{a_2}{a_1}\right)^{k_1} \sum_{j=0}^{\lfloor \frac{m}{2} \rfloor} (-1)^j C_{2j}^m \\
& \sum_{j_0=0}^{m-2j} C_{j_0}^{m-2j} \left(\frac{a_2}{a_1}\right)^{2j+j_0} \sum_{j_{13}=0}^{2m'} (-1)^{\frac{j_{13}}{2}} \sum_{j_1=[0,j_{13}-m']>}^{[j_{13},m']<} (-1)^{j_1} C_{j_1}^{m'} C_{j_{13}-j_1}^{m'} \\
& \sum_{j_2=0}^{m'-j_1} C_{j_2}^{m'-j_1} \left(\frac{a_6}{a_5}\right)^{j_1+j_2} \sum_{j_4=0}^{m'+j_1-j_{13}} C_{j_4}^{m'+j_1-j_{13}} \left(\frac{a_4}{a_3}\right)^{j_{13}-j_1+j_4} \sum_{k_3=0}^{\lfloor \frac{j_3-m'}{2} \rfloor} a_5^{l_3-2k_3} p_{l_3 m' k_3} \\
& \sum_{k_s=0}^{l_s} \left(-\frac{a_6}{a_5}\right)^{k_s} C_{k_s}^{l_s} \sum_{k_4=0}^{\lfloor \frac{l_4-m'}{2} \rfloor} a_3^{l_4-2k_4} p_{l_4 m' k_4} \sum_{k_t=0}^{l_t} C_{k_t}^{l_t} \left(-\frac{a_4}{a_3}\right)^{k_t} \\
& ((-1)^M + 1) B\left(\frac{M+1}{2}, \frac{2j+j_{13}+1}{2}\right) \varphi(N, K, l_2, m), \tag{B.91}
\end{aligned}$$

where M, N and K are

$$M = k_1 + j_0 + k_s + k_t + j_2 + j_4,$$

$$N = l_1 - 2k - m - k_1 + j_0 + l_s - k_s + l_t - k_t + j_2 + j_4,$$

$$K = k_1 + m - 2j - j_0 + k_s + k_t + 2m' - j_2 - j_4 - j_{13} + 1.$$

## **Appendix C: Lists of Publications**

### **1 Positron-hydrogen collisions at low energies**

**Y. R. Kuang and T. T. Gien**

#### **Abstract**

The Harris-Nesbet algebraic method was used to carry out a large coupled-state calculation of  $e^+$ -H scattering at energies below the first excitation of hydrogen. The six-state (1s, 2s, 2pH-1s, 2s, 2pPs) coupling scheme was extended to include an adequate number of short-ranged functions of both hydrogenic and positroniumic types and the H  $3\bar{p}$  pseudostate. Phase shifts and cross sections of partial waves from  $L=0$  to  $L=6$  were obtained for  $e^+$ -H(1s) scattering as well as for Ps(1s)-p scattering. Our results are to be compared with those obtained by other research groups with some large-scale calculations employing, however, different numerical methods of approach. Our results agree excellently with the values calculated with a variational method by Bhatia et al. and by Humberston et al. and with the 21-state close-coupling approximation by Mitroy.

Note: this paper has been underconsideration for publication in Phys. Rev. A.

## 2 Large Scale Calculations of Positron-hydrogen System at Low Energies

Y. R. Kuang and T. T. Gien

### Abstract

Two large scale, 18-state and 20-state, close coupling calculations of positron-hydrogen scattering have been carried out by using the Harris-Nesbet algebraic method at energies below the first hydrogen excitation threshold. Both sets of phase shifts, elastic and Ps formation cross sections for positron-H(1s) entrance channel and Ps elastic and H formation cross sections for Ps-p entrance channel are in good agreement with each other and with the existing accurate data, except for the S-wave phase shifts and S- and P-wave elastic cross sections in the Ore gap where the 20-state basis (Mitroy, Aust. J. Phys. v48 (1995) 645, without the 4f pseudostate in his 21-state) gives better results than the 18-state basis (A. A. Kernoghan et al, J. Phys. B28(1995) 1079). A possible reason for such a difference is that the 18-state scheme may not describe the short range interaction well. Our work confirms that the 20- or 21-state coupling scheme may be preferably chosen for low energy positron-hydrogen scattering.

Note: this work has been presented in DAMOP, Ann Arbor, Michigan, May 16-18, 1996; see **Bulletin of the American Physical Society**, Vol. 41, No. 3 (1996) p1140.

## **Appendix D: Fortran Programs**

### **1 18-state Coupling Scheme: 18-CC.f**

This set of programs is employed for obtaining the results of positron-hydrogen scattering presented in section 4.2. Similarly, the 20-state codes can be constructed by performing minor changes in parameters of coupled states.

### **2 Mixing basis Coupling Scheme: 7-mixing.f**

This set of programs is used to carry out positron-hydrogen calculations with a basis composed of  $(1s, 2s, 2p, \text{ or } 3\bar{p})H - (1s, 2s, 2p)Ps$  associated with sufficient number of short range correlation functions. The results presented in Section 4.1 are obtained by using this set of programs.

```

C##### MAIN PROGRAM #####
C
C THIS IS THE MAIN PROGRAM TO CARRY OUT CALCULATIONS OF POSITRON-
C HYDROGEN SCATTERING AT ENERGY BELOW THE FIRST HYDROGEN EXCITATION.
C
C INPUT-- L: THE TOTAL ANGULAR MOMENTUM QUANTUM NUMBER
C
C CALLING -- BB_18(L): CALCULATE THE BOUND-BOUND MATRICES A AND B
C EIGEN_NAG: USING THE NAG LIBRARY SUBROUTINE TO DIAGONALIZE
C           A X = E B X
C           CC_18(L): CALCULATE THE SCATTERING PHASE SHIFTS AND CROSS SECTIONS.
C
C##### IMPLICIT REAL*8(A-H,O-Z)
C      EXTERNAL BB_18, EIGEN_NAG, CC_18
C
L=3
CALL BB_18(L)
CALL EIGEN_NAG
CALL CC_18(L)

END

C##### Descriptions #####
C
C This is a SUB program to calculate the BOUND-BOUND matrix elements
C using the 18-state channel space of the Belfast group. The programs
C generate matrices A and B in a generalized eigenvalue equation:
C           A X = E B X
C where E is a diagonal eigenvalue matrix and X is the corresponding
C eigenvector matrix.
C
C Input-- L: the total angular momentum of the positron-hydrogen system
C
C Output--A: the Hamiltonian matrix
C             B: the overlapping matrix
C
C Parameters-- NH: number of basis functions per channel
C             N: number of the total basis functions
C             N=18*NH for the S-wave
C             N=28*NH for the P-wave
C             N=32*NH for the partial wave with L larger than 1.
C
C Arrays--
C           N24(I),A2(I): parameters of the Slater orbitals for a positron
C                         and a positronium
C           NHJ(9,4),LHJ(9),NPSJ(9,4),LPSJ(9): detailed descriptions of nine
C                         hydrogen and positronium states
C
C Callings--
C           PS_H_DATA: generate the detailed parameters of the 18-states
C           COMMON_DATA: produce some common data frequently used by some subs
C           ETA_PSI: produce Gaussian nodes and weights for 2-D integrations
C                         in the spheroidal system
C           MATRIX_MP(L): generate the angular integration between H and Ps channels
C           BB_PQ(..): Hamiltonian between hydrogen P and Q channels
C           SS_PQ(..): overlapping between hydrogen P and Q channels
C           BB_PU(..): Hamiltonian between hydrogen P and positronium U channels
C           SS_PU(..): overlapping between hydrogen P and positronium U channels
C           BB_UV(..): Hamiltonian between positronium U and V channels
C           SS_UV(..): overlapping between positronium U and V channels
C
C##### SUBROUTINE BB_18(L)
C
IMPLICIT REAL*8(A-H,O-Z)
PARAMETER(NH=18,N=576)
DIMENSION A(N,N),B(N,N),N24(NH),A2(NH)
EXTERNAL COMMON_DATA,ETA_PSI,MATRIX_MP
COMMON/N_H_PS/NHJ(9,4),LHJ(9),NPSJ(9,4),LPSJ(9)
DATA(N24(I),I=1,NH)/1.2,3.1,2.3,1,2,3,1,2,3,1,2,3,1,2,3/
DATA(A2(I),I=1,NH)/0.05d0,0.05d0,0.05d0,0.2d0,0.2d0,0.2d0
#,0.4d0,0.4d0,0.4d0,0.8d0,0.8d0,0.8d0,1.2d0,1.2d0,1.2d0
#,1.8d0,1.8d0,1.8d0/

```

```

OPEN(UNIT=8,FILE='BB_18_18F',STATUS='new')

L=3

CALL PS_H_DATA
CALL COMMON_DATA
CALL ETA_PSI
CALL MATRIX_HP(L)

NO_CHANNEL=9
          !H-H MATRIX ELEMENTS
NO_IP=-1
DO IP=1,NO_CHANNEL
DO L2I=INT(ABS(LHJ(IP)-L)),LHJ(IP)+L,2

NO_IP=NO_IP+1

NO_JQ=-1
DO JQ=1,NO_CHANNEL
DO L2J=INT(ABS(LHJ(JQ)-L)),LHJ(JQ)+L,2

NO_JQ=NO_JQ+1
DO I=1,NH
DO J=1,NH
NI=NO_IP*NH+I
NJ=NO_JQ*NH+J
N24I=N24(I)+L2I
N24J=N24(J)+L2J
A(NI,NJ)=BB_PQ(L,IP,JQ,N24I,A2(I),N24J,A2(J),L2I,L2J)
B(NI,NJ)=SS_PQ(L,IP,JQ,N24I,A2(I),N24J,A2(J),L2I,L2J)
ENDDO
ENDDO
ENDDO
ENDDO

ENDDO
ENDDO

          !Ps-H MATRIX ELEMENTS
NO_H=NO_IP
DO IU=1,NO_CHANNEL
DO L4I=INT(ABS(LPSJ(IU)-L)),LPSJ(IU)+L,2
NO_IP=NO_IP+1

NO_JQ=-1
DO JQ=1,NO_CHANNEL
DO L2J=INT(ABS(LHJ(JQ)-L)),LHJ(JQ)+L,2
NO_JQ=NO_JQ+1

DO I=1,NH
DO J=1,NH
NI=NO_IP*NH+I
NJ=NO_JQ*NH+J
N24I=N24(I)+L4I
N24J=N24(J)+L2J
A(NI,NJ)=BB_PU(L,JQ,IU,N24J,A2(J),N24I,A2(I),L2J,L4I)
B(NI,NJ)=SS_PU(L,JQ,IU,N24J,A2(J),N24I,A2(I),L2J,L4I)
ENDDO
ENDDO

ENDDO
ENDDO

          !Ps-Ps MATRIX ELEMENTS
NO_IP=NO_H
DO IU=1,NO_CHANNEL
DO L4I=INT(ABS(LPSJ(IU)-L)),LPSJ(IU)+L,2
NO_IP=NO_IP+1

NO_JQ=NO_H
DO JV=1,NO_CHANNEL
DO L4J=INT(ABS(LPSJ(JV)-L)),LPSJ(JV)+L,2
NO_JQ=NO_JQ+1

DO I=1,NH
DO J=1,NH
NI=NO_IP*NH+I

```

```

NJ=NO_JQ*NH+J
N24I=N24(I)+L4I
N24J=N24(j)+L4J
A(NI,NJ)=BB_UV(L,IU,JV,N24I,A2(I),N24J,A2(J),L4I,L4J)
B(NI,NJ)=SS_UV(L,IU,JV,N24I,A2(I),N24J,A2(J),L4I,L4J)
IF(ABS(A(NI,NJ)) .LT. 1D-13) A(NI,NJ)=0D0
IF(ABS(B(NI,NJ)) .LT. 1D-13) B(NI,NJ)=0D0
ENDDO
ENDDO
ENDDO
ENDDO

DO I=1,N
DO J=1,I
WRITE(6,29)A(I,J),B(I,J)
ENDDO
ENDDO

29 FORMAT(1X,2(D27.20,1X))

RETURN

END  *

C ****
C * < CHANNEL P; H | H | CHANNEL Q; H > *
C ****

C ##### Descriptions #####
C
C Input-- L: the total angular momentum number of the system
C          L2I,L2J: the angular momenta of the positron
C          IP, JQ: channel numbers of hydrogen which is from 1 to 9
C          N2I,A2I: parameters of the Slater orbital for the positron
C                      in channel IP
C          N2J,A2J: parameters of the Slater orbital for the positron
C                      in channel JQ
C Output--BB_PQ: the matrix element between hydrogen channels IP and JQ
C
C Calling-- BB_HH: general sub for the Slater orbitals of the electron
C
C #####
FUNCTION BB_PQ(L,IP,JQ,N2I,A2I,N2J,A2J,L2I,L2J)
IMPLICIT REAL*8(A-H,O-Z)
EXTERNAL BB_HH
COMMON/E_18/EH(9),EPS(9)/H_PS_DATA/AHJ(9,4),CHJ(9,4),APSJ(9,4),
#CPSJ(9,4)/N_H_PS/NHJ(9,4),LHJ(9),NPSJ(9,4),LFSJ(9)
SUM=0.
DO I=1,4
  IF(CHJ(IP,I) .NE. 0.)THEN
    DO J=1,4
      IF(CHJ(JQ,J) .NE. 0.)THEN
        SUM=SUM+CHJ(IP,I)*CHJ(JQ,J)*BB_HH(NHJ(IP,I),AHJ(IP,I),N2I,A2I,
#NHJ(JQ,J),AHJ(JQ,J),N2J,A2J,L,LHJ(IP),L2I,LHJ(JQ),L2J)
      ENDIF
    ENDDO
  ENDIF
ENDDO
BB_PQ=SUM
RETURN
END

C ****
C * < CHANNEL P; H | CHANNEL Q; H > *
C ****

C ##### Descriptions #####
C
C Input-- L: the total angular momentum number of the system
C          L2I,L2J: the angular momenta of the positron

```

```

C      IP, JQ: channel numbers of hydrogen which is from 1 to 9
C      N2I,A2I: parameters of the Slater orbital for the positron
C          in channel IP
C      N2J,A2J: parameters of the Slater orbital for the positron
C          in channel JQ
C Output--SS_PQ: the overlapping element between hydrogen channels IP and JQ
C Calling-- S_HH: general sub for the Slater orbitals of the electron
C
C#####
C
FUNCTION SS_PQ(L,IP,JQ,N2I,A2I,N2J,A2J,L2I,L2J)
IMPLICIT REAL*8(A-H,O-Z)
EXTERNAL S_HH
COMMON/E_18/EH(9),EPS(9)/H_PS_DATA/AHJ(9,4),CHJ(9,4),APSJ(9,4),
#CPSJ(9,4)/N_H_PS/NHJ(9,4),LHJ(9),NPSJ(9,4),LPSJ(9)

IF(IP .EQ. JQ .AND. L2I .EQ. L2J)THEN
  SS_PQ=B44(N2I,A2I)*B44(N2J,A2J)*FACT(N2I+N2J)/(A2I+A2J)
# **(N2I+N2J+1)
ELSE
  SUM=0.
  DO I=1,4
    IF(CHJ(IP,I) .NE. 0.)THEN
      DO J=1,4
        IF(CHJ(JQ,J) .NE. 0.)THEN
          SUM=SUM+CHJ(IP,I)*CHJ(JQ,J)*S_HH(NHJ(IP,I),AHJ(IP,I),N2I,A2I,
#NHJ(JQ,J),AHJ(JQ,J),N2J,A2J,L,LHJ(IP),L2I,LHJ(JQ),L2J)
        ENDIF
      ENDDO
    ENDIF
    ENDDO
    SS_PQ=SUM
  ENDIF
  RETURN
END

*****
* BB_HH(N1I,A1I,N2I,A2I,L,L1I,L1J,L2I)      *
*****

##### Descriptions #####
C
C Input-- L: the system total angular momentum number
C          L1I,L2I,L1J,L2J: angular momentum numbers of the electron and
C          positron in the I-th and J-th Slater orbitals respectively;
C          N1I,A1I,N2I,A2I: parameters of the electron and positron in the
C          I-th Slater orbital;
C          N1J,A1J,N2J,A2J: parameters of the electron and positron in the
C          J-th Slater orbital.
C Output-- BB_HH: matrix elements between two hydrogen Slater-type channel
C          functions
C Callings--
C          BET, F6J, CT, YRSF, B44 subs
C
C#####
C
FUNCTION BB_HH(N1I,A1I,N2I,A2I,N1J,A1J,N2J,A2J,L,L1I,L2I,L1J,L2J)
IMPLICIT REAL*8(A-H,O-Z)
EXTERNAL BET,F6J,CT,YRSF,B44
B4I=B44(N1I,A1I)*B44(N2I,A2I)
B4J=B44(N1J,A1J)*B44(N2J,A2J)

B1=BET(2,0,N1I,A1I,N2I,A2I,N1J,A1J,N2J,A2J,L,L1I,L2I,L1J,L2J)
B2=BET(1,0,N1I,A1I,N2I,A2I,N1J,A1J,N2J,A2J,L,L1I,L2I,L1J,L2J)
B3=BET(0,2,N1I,A1I,N2I,A2I,N1J,A1J,N2J,A2J,L,L1I,L2I,L1J,L2J)
B4=BET(0,1,N1I,A1I,N2I,A2I,N1J,A1J,N2J,A2J,L,L1I,L2I,L1J,L2J)
B5=BET(0,0,N1I,A1I,N2I,A2I,N1J,A1J,N2J,A2J,L,L1I,L2I,L1J,L2J)

BBO=0.5D0*AA(N1I,L1I)*B1+(A1I*N1I-1)*B2+0.5D0*AA(N2I,L2I)*B3
#+A2I*N2I*B4-0.5D0*(A1I**2+A2I**2)*B5

```

```

VIJ=B4
SIGN=-(LD0)**(L1J+L2I+L)*B4I
K1=MAX(ABS(L1I-L1J),ABS(L2I-L2J))
K2=MIN(L1I+L1J,L2I+L2J)

DO K=K1,K2,2
  VIJ=VIJ+SIGN*CT(L1I,K,L1J)*CT(L2I,K,L2J)*F6J(L1I,L2I,L,L2J,
#L1J,K)*YRSP(N1I+N1J-K-1,N2I+N2J-K-1,A1I+A1J,A2I+A2J,K)*B4J
ENDDO

BB_HH=BB0+VIJ
RETURN
END

*****
* OVERLAPPING ELEMENT BETWEEN TWO SLATER-TYPE BASIS FUNCTIONS *
*****

FUNCTION S_HH(N1I,A1I,N2I,A2I,N1J,A1J,N2J,A2J,L,L1I,L2I,L1J,L2J)
IMPLICIT REAL*8(A-H,O-Z)
EXTERNAL BET

S_HH=BET(0,0,N1I,A1I,N2I,A2I,N1J,A1J,N2J,A2J,L,L1I,L2I,L1J,L2J)
RETURN
END

*****
* BET = <I(r1,r2) | 1/(r1**m r2**n) | J(r1,r2) > *
*****
```

~~FUNCTION BET(M,N,N1I,A1I,N2I,A2I,N1J,A1J,N2J,A2J,L,L1I,~~
~~#L2I,L1J,L2J)~~
~~IMPLICIT REAL\*8(A-H,O-Z)~~
~~EXTERNAL FACT,B44~~
~~B4I=B44(N1I,A1I)\*B44(N2I,A2I)~~
~~B4J=B44(N1J,A1J)\*B44(N2J,A2J)~~
~~IF (L1I .EQ. L1J .AND. L2I .EQ. L2J)THEN~~
 ~~BET=B4I\*FACT(N1I+N1J-M)/(A1I+A1J)\*\*(N1I+N1J-M+1)\*~~
~~#FACT(N2I+N2J-N)/(A2I+A2J)\*\*(N2I+N2J-N+1)\*B4J~~
~~ELSE~~
 ~~BET=0~~
~~ENDIF~~

RETURN
END

\*\*\*\*\*
\* < CHANNEL U; Ps | H | CHANNEL V; Ps > \*
\*\*\*\*\*

```

##### Descriptions #####
C Input-- L: the total angular momentum number of the system
C           L4I,L4J: the angular momentum numbers of the mass center of Ps
C           IU, JV: channel numbers of positronium which is from 1 to 9
C           N4I,A4I: parameters of the Slater orbital for the mass center
C                     of Ps in channel IU
C           N4J,A4J:parameters of the Slater orbital for the mass center
C                     ofPs in channel JV
C Output--BB_UV: the matrix element between Ps channels IU and JV
C Calling-- BB_PSPS: general sub for the Slater orbitals of Ps
#####

FUNCTION BB_UV(L,IU,JV,N4I,A4I,N4J,A4J,L4I,L4J)
IMPLICIT REAL*8(A-H,O-Z)
EXTERNAL BB_PSPS
COMMON/E_18/EH(9),EPS(9)/H_PS_DATA/AHJ(9,4),CHJ(9,4),APSJ(9,4),
#CPSJ(9,4)/N_H_PS/NHJ(9,4),LHJ(9),NPSJ(9,4),LPSJ(9)

SUM=0.
DO I=1,4
  IF(CPSJ(IU,I) .NE. 0.)THEN
    DO J=1,4
      IF(CPSJ(JV,J) .NE. 0.)THEN
        SUM=SUM+CPSJ(IU,I)*CPSJ(JV,J)*BB_PSPS(NPSJ(IU,I),APSJ(IU,I),N4I,
```

```

#A4I,NPSJ(JV,J),APSJ(JV,J),N4J,A4J,L,LPSJ(IU),L4I,LPSJ(JV),L4J

      ENDIF

      ENDDO
      ENDIF

      ENDDO
      BB_UV=SUM
      RETURN
      END

C *****
C * < CHANNEL U; Ps | CHANNEL V; Ps > *
C *****

C ##### Descriptions #####
C
C Input-- L: the total angular momentum number of the system
C          L4I,L4J: the angular momentum numbers of the mass center of Ps
C          IU, JV: channel numbers of positronium which is from 1 to 9
C          N4I,A4I: parameters of the Slater orbital for the mass center
C                      of Ps in channel IU
C          N4J,A4J:parameters of the Slater orbital for the mass center
C                      ofPs in channel JV
C Output--SS_UV: the overlapping element between Ps channels IU and JV
C
C Calling-- S_HH: general sub for the Slater orbitals of the hydrogen
C
C ##### Descriptions #####
C
FUNCTION SS_UV(L,IU,JV,N4I,A4I,N4J,A4J,L4I,L4J)
IMPLICIT REAL*8(A-H,O-Z)
EXTERNAL S_HH
COMMON/E_18/EH(9),EPS(9)/H_PS_DATA/AHJ(9,4),CHJ(9,4),APSJ(9,4),
#CPSJ(9,4)/N_H_PS/NHJ(9,4),LHK(9),NPSJ(9,4),LPSJ(9)

      IF (IU .EQ. JV .AND. L4I .EQ. L4J)THEN
      SS_UV=B44(N4I,A4I)*B44(N4J,A4J)*FACT(N4I+N4J)/(A4I+A4J)
      # **(N4I+N4J+1)
      ELSE
      SUM=0.
      DO I=1,4
      IF(CPSJ(IU,I) .NE. 0.)THEN
      DO J=1,4
      IF(CPSJ(JV,J) .NE. 0.)THEN
      SUM=SUM+CPSJ(IU,I)*CPSJ(JV,J)*S_HH(NPSJ(IU,I),APSJ(IU,I),N4I,
#A4I,NPSJ(JV,J),APSJ(JV,J),N4J,A4J,L,LPSJ(IU),L4I,LPSJ(JV),L4J)
      ENDIF
      ENDDO
      ENDIF
      ENDDO
      SS_UV=SUM
      ENDIF
      RETURN
      END

C *****
C * matrix elements between Ps states *
C *****

C ##### Descriptions #####
C
C Input-- L: the system total angular momentum number
C          L3I,L4I,L3J,L4J: angular momentum numbers of Ps and the mass
C          center of Ps in the I-th and J-th Slater orbitals respectively;
C          N3I,A3I,N4I,A4I: parameters of Ps and the mass center of Ps in the
C          I-th Slater orbital;
C          N3J,A3J,N4J,A4J: parameters of Ps and the mass center of Ps in the
C          J-th Slater orbital;
C
C Output-- BB_PSPS: matrix elements between two Ps Slater-type channel

```

```

C           functions
C Callings-- 
C     BET, F6J, CT, YRSF, B44 subs
C
C#####
C FUNCTION BB_PSPS(N3I,A3I,N4I,A4I,N3J,A3J,N4J,A4J,
#L,L3I,L4I,L3J,L4J)
IMPLICIT REAL*8(A-H,O-Z)
EXTERNAL BET,F6J,CT,YRSF,B44

B1=BET(2,0,N3I,A3I,N4I,A4I,N3J,A3J,N4J,A4J,L,L3I,L4I,L3J,L4J)
B2=BET(1,0,N3I,A3I,N4I,A4I,N3J,A3J,N4J,A4J,L,L3I,L4I,L3J,L4J)

B3=BET(0,2,N3I,A3I,N4I,A4I,N3J,A3J,N4J,A4J,L,L3I,L4I,L3J,L4J)
B4=BET(0,1,N3I,A3I,N4I,A4I,N3J,A3J,N4J,A4J,L,L3I,L4I,L3J,L4J)
B5=BET(0,0,N3I,A3I,N4I,A4I,N3J,A3J,N4J,A4J,L,L3I,L4I,L3J,L4J)

BB0=AA(N3I,L3I)*B1+(2*A3I*N3I-1)*B2+0.25D0*AA(N4I,L4I)*B3
#+0.5d0*A4I*N4I*B4-(A3I**2+0.25D0*A4I**2)*B5

K1=MAX(ABS(L3I-L3J),ABS(L4I-L4J))
K2=MIN(L3I+L3J,L4I+L4J)

IF (K1/2**2 .EQ. K1)THEN
  BB1=0.
ELSE
  BB1=0.
  DO K=K1,K2,2
    BB1=BB1+(-1D0)**(L3J+L4I+L)*CT(L3I,K,L3J)*CT(L4I,K,L4J)
#*F6J(L3I,L4I,L,L4J,L3J,K)*2D0***(N3I+N3J+2)*YRSF(N3I+N3J-1-K,
#N4I+N4J-1-K,2*(A3I+A3J),A4I+A4J,K)
  ENDDO
ENDIF
BB_PSPS=BB0+B44(N3I,A3I)*B44(N4I,A4I)*
#BB1*B44(N3J,A3J)*B44(N4J,A4J)

RETURN
END

C#####
C * <CHANNEL P; H | H | CHANNEL U; Ps > *
C#####

C#####
C Descriptions #####
C
C Input-- L: the total angular momentum number of the system
C          L2I,L4J: the angular momenta of the positron and mass center of Ps
C          IP, JU: channel numbers of H and Ps which are from 1 to 9
C          N2I,A2I: parameters of the Slater orbital for the mass center
C                      of H in channel IP
C          N4J,A4J:parameters of the Slater orbital for the mass center
C                      of Ps in channel JU
C Output--BB_PU: the matrix element between H-IP and Ps-JU channels
C
C Calling-- BB_HPS: general sub for the Slater orbitals of H and Ps
C
C#####
C
FUNCTION BB_PU(L,IP,JU,N2I,A2I,N4J,A4J,L2I,L4J)
IMPLICIT REAL*8(A-H,O-Z)
EXTERNAL BB_HPS
COMMON/E_18/EH(9),EPS(9)/H_PS_DATA/AHJ(9,4),CHJ(9,4),APSJ(9,4),
#CPSJ(9,4)/N_H_PS/NHJ(9,4),LHJ(9),NPSJ(9,4),LPSJ(9)

SUM=0.
DO I=1,4
  IF(CHJ(IP,I) .NE. 0.)THEN
    DO J=1,4
      IF(CPSJ(JU,J) .NE. 0)THEN
        SUM=SUM+CHJ(IP,I)*CPSJ(JU,J)*BB_HPS(NHJ(IP,I),AHJ(IP,I),N2I,A2I,
#NPSJ(JU,J),APSJ(JU,J),N4J,A4J,L,LHJ(IP),L2I,LPSJ(JU),L4J)
      ENDIF
    ENDDO
  ENDIF
ENDDO
BB_PU=SUM

```

```

      RETURN
      END

C ****
C * <CHANNEL P; H | CHANNEL U; Ps > *
C ****

C ##### Descriptions #####
C
C Input-- L: the total angular momentum number of the system
C          L2I,L4J: the angular momenta of the positron and mass center of Ps
C          IP, JU: channel numbers of H and Ps which are from 1 to 9
C          N2I,A2I: parameters of the Slater orbital for the mass center
C                      of H in channel IP
C          N4J,A4J:parameters of the Slater orbital for the mass center
C                      of Ps in channel JU
C Output--SS_PU: the overlapping element between H-IP and Ps-JU channels
C
C Calling-- S_HPS: general sub for the Slater orbitals of H and Ps
C
C #####
FUNCTION SS_PU(L,IP,JU,N2I,A2I,N4J,A4J,L2I,L4J)
IMPLICIT REAL*8(A-H,O-Z)
EXTERNAL S_HPS
COMMON/E_18/EH(9),EPS(9)/H_PS_DATA/AHJ(9,4),CHJ(9,4),APSJ(9,4),
#CPSJ(9,4)/N_H_PS/NHJ(9,4),LHJ(9),NPSJ(9,4),LPSJ(9)

SUM=0.
DO I=1,4
  IF(CHJ(IP,I) .NE. 0.)THEN
    DO J=1,4
      IF(CPSJ(JU,J) .NE. 0)THEN
        SUM=SUM+CHJ(IP,I)*CPSJ(JU,J)*S_HPS(NHJ(IP,I),AHJ(IP,I),N2I,A2I,
#NPSJ(JU,J),APSJ(JU,J),N4J,A4J,L,LHJ(IP),L2I,LPSJ(JU),L4J)
      ENDIF
    ENDDO
    ENDDO
    SS_PU=SUM
    RETURN
  END

C ****
C * INTEGRATION OF 2-D: <I(1,2) | H | J(3,4) > *
C ****

C ##### Descriptions #####
C
C Input-- L: the system total angular momentum number
C          L1I,L2I,L1J,L2J: angular momentum numbers of the electron and
C          positron in the I-th and J-th Slater orbitals respectively;
C          N1I,A1I,N2I,A2I: parameters of the electron and positron in the
C          I-th Slater orbital;
C          N3J,A3J,N4J,A4J: parameters of the positronium and mass center of
C          of Ps in the J-th Slater orbital.
C Output-- BB_HPS: matrix elements between a hydrogen I-th and a Ps J-th
C          Slater-type channel functions
C Callings-- B44: normalization factor
C
C #####
FUNCTION BB_HPS(N1I,A1I,N2I,A2I,N3J,A3J,N4J,A4J,L,L1I,L2I,L3J,L4J)
IMPLICIT REAL*8(A-H,O-Z)
EXTERNAL B44
COMMON/D_HP/DHP(5,5,3,3,100,150)/PSI_ETA/DPSI(100),
# DETA(150)/W_W/W_PSI(100),W_ETA(150)

L2I0=INT(ABS(L-L1I))
L4J0=INT(ABS(L-L3J))
M=1+N1I+N2I+N3J+N4J

SUM1=0.
DO I=1,100
  PSI=1/DPSI(I)

```

```

SUM2=0.
DO J=1,150
ETA=DETA(J)
X0=(PSI**2+6*ETA*PSI+ETA**2+8)**0.5D0
Y=0.5D0*(PSI+ETA)*A1I+A2I+0.5D0*(PSI-ETA)*A3J+0.25D0*X0*A4J
A1=0.5D0*(AA(N1I,L1I)*(2/(PSI+ETA))**2+AA(N2I,L2I))
B1=(A1I*N1I-1)*2/(PSI+ETA)+A2I*N2I-1-2/(PSI-ETA)

BB_HPS1=(PSI**2-ETA**2)*((PSI+ETA)/2)**(N1I-1)*((PSI-ETA)
#/2)**(N3J-1)*(0.25D0*X0)**(N4J-1)*DHP(L1I+1,(L2I-L2I0)/2+1,L3J+1,
#(L4J-L4J0)/2+1,I,J)*((A1*Y/(M-1)+B1)*Y/M-0.5D0*(A1I**2+A2I**2))
#*(1/Y)**(M+1)
SUM2=SUM2+BB_HPS1*W_ETA(J)
ENDDO

SUM1=SUM1+W_PSI(I)*SUM2*PSI**2
ENDDO

BB_HPS=0.125d0*B44(N1I,A1I)*B44(N2I,A2I)*B44(N3J,A3J)*
#B44(N4J,A4J)*SUM1*FACT(M)
RETURN
END

*****
* <I: (1,2) | J: (3,4)>
*****

C ##### Descriptions #####
C
C Input-- L: the system total angular momentum number
C          L1I,L2I,L1J,L2J: angular momentum numbers of the electron and
C          positron in the I-th and J-th Slater orbitals respectively;
C          N1I,A1I,N2I,A2I: parameters of the electron and positron in the
C          I-th Slater orbital;
C          N3J,A3J,N4J,A4J: parameters of the positronium and mass center of
C          of Ps in the J-th Slater orbital.
C Output-- S_HPS: overlapping elements between a hydrogen I-th and a Ps J-th
C          Slater-type channel functions
C Callings-- B44: normalization factor
C
C #####
FUNCTION S_HPS(N1I,A1I,N2I,A2I,N3J,A3J,N4J,A4J,L,L1I,L2I,L3J,L4J)
IMPLICIT REAL*8(A-H,O-Z)
EXTERNAL B44
COMMON/D_HP/DHP(5,5,3,3,100,150)/PSI_ETA/DPSI(100),
# DETA(150)/W_W/W_PSI(100),W_ETA(150)

L2I0=INT(ABS(L-L1I))
L4J0=INT(ABS(L-L3J))
M=1+N1I+N2I+N3J+N4J

SUM1=0.
DO I=1,100
PSI=1/DPSI(I)

SUM2=0.
DO J=1,150
ETA=DETA(J)

X0=(PSI**2+6*ETA*PSI+ETA**2+8)**0.5D0
Y=0.5D0*(PSI+ETA)*A1I+A2I+0.5D0*(PSI-ETA)*A3J+0.25D0*X0*A4J

SS1=(PSI**2-ETA**2)*((PSI+ETA)/2)**(N1I-1)*((PSI-ETA)
#/2)**(N3J-1)*(0.25D0*X0)**(N4J-1)*DHP(L1I+1,(L2I-L2I0)/2+1,L3J+1,
#(L4J-L4J0)/2+1,I,J)*(1/Y)**(M+1)

SUM2=SUM2+SS1*W_ETA(J)
ENDDO

SUM1=SUM1+W_PSI(I)*SUM2*PSI**2
ENDDO

S_HPS=0.125d0*B44(N1I,A1I)*B44(N2I,A2I)*B44(N3J,A3J)*
#B44(N4J,A4J)*SUM1*FACT(M)
RETURN
END

*****
* NORMALIZATION FACTOR B44
*****

```

```

FUNCTION B44(N,A)
IMPLICIT REAL*8(A-H,O-Z)
EXTERNAL FACT

B44=((2*A)**(2*N+1)/FACT(2*N))**0.5D0

RETURN
END

C *****
C *AA(NI,LI)=-NI*(NI-1)+LI*(LI+1) *
C *****
FUNCTION AA(NI,LI)
IMPLICIT REAL*8(A-H,O-Z)
AA=-NI*(NI-1)+LI*(LI+1)
RETURN
END

C*****
C S-FUNC IS AN INTEGRAL:
C <R_(1)^(N+K-1)EXP(-A R_(1)|OP(K)|R_(2)^(M+K-1)EXP(-B R_(2))>
C OP(K)- OPERATOR :R_(<)^K/R_(>)^{K+1}
C****

REAL*8 FUNCTION YRSF(N,M,A,B,K)
IMPLICIT REAL*8(A-H,O-Z)
EXTERNAL FACT
S=0.D0
DO I=0,N
  S1=1D0/FACT(N-I)/A**(I+1)
  DO J=0,M
    LN=2*K+N+M-I-J
    sn=dlog(fact(ln))-(j+1)*dlog(b)-(ln+1)*dlog(a+b)-
      dlog(fact(m-j))+dlog(s1)
    s=s+dexp(sn)
  ENDDO
ENDDO
YRSF=S*(2D0*K+1D0)*FACT(M)*FACT(N)
RETURN
END

SUBROUTINE EIGEN_NAG
IMPLICIT REAL*8(A-H,O-Z)
PARAMETER(NHN=576,LDA=NHN,LDB=NHN,LDEVEC=NHN)
EXTERNAL F02AEF
DIMENSION A(LDA,NHN),B(LDB,NHN),DL(NHN),E(NHN)
#,VV(NHN,NHN),Y(NHN,NHN),VB(NHN),INDX(NHN),C(NHN,NHN)
#,EVAL(NHN),EVEC(NHN,NHN)
OPEN(UNIT=5,FILE='BB_18_18F',STATUS='OLD')
OPEN(UNIT=12,FILE='EIGEN_18_18F',STATUS='new')

DO I=1,NHN
  DO J=1,I
    READ(5,29)A(i,j),B(i,j)
    A(j,i)=A(i,j)
    B(j,i)=B(i,j)
  ENDDO
ENDDO

CALL F02AEF(A,LDA,B,LDB,NHN,EVAL,EVEC,LDEVEC,DL,E,IFAIL)

DO I=0,NHN
  DO J=1,NHN,3
    IF (I .EQ. 0) THEN
      WRITE(12,30)EVAL(J),EVAL(J+1),EVAL(J+2)
    ELSE
      WRITE(12,30)EVEC(I,J),EVEC(I,J+1),EVEC(I,J+2)
    ENDIF
  ENDDO
ENDDO

29 FORMAT(1X,2(D27.20,1X))
30 FORMAT(1X,3(d23.17,1X))

close(5)

RETURN

```

```

      END

C#####
C      This is a SUB program calculating phase shifts and cross sections
C      at energies below the 2sH, using a modified version of the Harris-Nesbet
C      approach. The channel space is spanned by 18 coupled-states used by
C      Belfast group.
C

C INPUT---L: the partial wave angular momentum
C           beta: parameter in the factor before the spherical Neumann functions
C                   for hydrogen channel
C           gamma: parameter in the factor before the spherical Neumann functions
C                   for Ps channel
C

C Callings--- PS_H_DATA: generate the parameters of H and Ps physical and pseudo
C           states
C           GAUSS:   read in the Gaussian node points and weights for 1-D
C                   integration
C           ETA_PSI: generate the Gaussian node points and weights for two
C                   dimensional integrations in spheroidal coordinate system.
C           MATRIX_HP(L): produce a matrix of the angular integration between
C                   H and Ps channels at a given L
C

C           COMMON_DATA: generate common block data for some subroutines
C           Q1_MATRIX: single channel phase shifts and elastic cross
C                   sections
C           Q2_MATRIX: two open channel reaction matrix and cross sections
C#####

SUBROUTINE CC_18(L)

IMPLICIT REAL*8(A-H,O-Z)
EXTERNAL Q1_MATRIX,Q2_MATRIX,COMMON_DATA,ETA_PSI,MATRIX_HP
COMMON/B_G/BETA,GAMMA

OPEN(UNIT=8,FILE='Q_18_18F',STATUS='new')

CALL PS_H_DATA
CALL GAUSS
CALL COMMON_DATA
CALL ETA_PSI
CALL MATRIX_HP(L)
  beta=0.3d0
  gamma=0.3d0

write(8,*)"18-state H-N calculation, 18 functions/channel"
write(8,*)"phase shifts (Rad.) and cross sections (pi a0**2)"
write(8,*)"Beta=",beta,"Gamma=",gamma

CALL Q1_MATRIX(L)
CALL Q2_MATRIX(L)

END

C ****
C * OPEN CHANNEL: H1s *
C ****

C#####
C      Descriptions #####
C Callings--- R_MATRIX: calculate the reaction matrix
C           T_MATRIX: calculate the transition matrix
C           FFM:   the free-free matrices
C           BFMATRIX: the bound-free matrices
C Input----- PPK(I): array stored moments of positron
C Output----- R1, R2: the Kohn and inverse Kohn reaction matrices
C           T11, T22: store the transition cross sections
C                   from the Kohn and inverse Kohn respectively
C           T12, T21: temporary storages
C#####

SUBROUTINE Q1_MATRIX(L)
IMPLICIT REAL*8(A-H,O-Z)
PARAMETER(N=1)
external R_MATRIX,T_MATRIX,FFM,BFMATRIX
DIMENSION X00(N,N),X01(N,N),X10(N,N),X11(N,N),Y(N,N),INDX(N)
# ,R1(N,N),R2(N,N),T11(N,N),T12(N,N),T21(N,N),T22(N,N),PPK(13)
# ,PKK(N)

DATA(PPK(I),I=1,13)=0.1D0,0.2D0,0.3D0,0.4D0,0.5D0,0.6D0,

```

```

# 0.62d0,0.64d0,0.66d0,0.68d0,0.69d0,0.7d0,0.705d0/
WRITE(8,123)'PK','PHASE_K','PHASE-IK','Q1-K','Q2-IK'
WRITE(8,*)

DO KK=1,13

PKK(1)=PPK(KK)

NO=N

C
C   Output-- X00, X01, X10, and X11: temporary storages of free-free matrices
C   FFSS,FFSC,FFCS, and FFCC, respectively.

CALL FFM(NO,PKK(1),L,X00,X10,X01,X11)      !FREE-FREE

C
C   Input-- the free-free matrices: X00, X01, X10, and X11
C   Output-- the m-matrix: X00=m00, X01=m01, X10=m10, and X11=m11
C

CALL BFMATRIX(NO,PKK(1),L,X00,X10,X01,X11) ! (FREE-FREE)+(FREE-BOUND)
                                                !--->M_matrices

C change the normalization of the free functions

DO I=1,NO
  DO J=1,NO
    PKIJ=DSQRT(PKK(I)*PKK(J))
    X00(I,J)=X00(I,J)/PKIJ
    X01(I,J)=X01(I,J)/PKIJ
    X10(I,J)=X10(I,J)/PKIJ
    X11(I,J)=X11(I,J)/PKIJ
  ENDDO
ENDDO

C   Input-- the m-matrix
C   Output-- the optimized reaction matrices
C   R1, R2: from the Kohn and inverse Kohn methods

CALL R_MATRIX(X00,X01,X10,X11,Y,INDX,R1,R2,N)

CALL T_MATRIX(R1,T11,T12,INDX,N)
CALL T_MATRIX(R2,T21,T22,INDX,N)

DO I=1,N
  DO J=1,N
    T11(I,J)=T11(I,J)**2+T12(I,J)**2           !T11(I,J)=|Tk(I,J)|^2
    T22(I,J)=T21(I,J)**2+T22(I,J)**2           !T22(I,J)=|Ti(I,J)|^2
  ENDDO
ENDDO

PI=1D0/PKK(1)**2*(2*L+1)
Q1=T11(1,1)*PI
Q2=T22(1,1)*PI

A1=R1(1,1)
A2=R2(1,1)
if(A1 .gt. 0.)then
  phi1= atan(A1)
  phi2= atan(A2)
else
  phi1= -atan(abs(A1))
  phi2= -atan(abs(A2))
endif
WRITE(8,124)PKK(1), phi1 , phi2,Q1,Q2
ENDDO

123  FORMAT(A5,2x,A13,3(5X,A13))
124  FORMAT(f7.5,4(2x,E15.10))

RETURN
end

C ****
C * OPEN CHANNELS: H1s,Ps(1s) *
C ****

C##### subs and arrays have the same meanings as in Q1_MATRIX(L)

SUBROUTINE Q2_MATRIX(L)

```

```

IMPLICIT REAL*8(A-H,O-Z)
PARAMETER(N=2)
external R_MATRIX,T_MATRIX,FFM,BFMATRIX
DIMENSION X00(N,N),X01(N,N),X10(N,N),X11(N,N),Y(N,N),INDX(N)
#,R1(N,N),R2(N,N),T11(N,N),T12(N,N),T21(N,N),T22(N,N),PPK(25)
#,PKK(N)

DATA(PPK(I),I=1,17)/0.71D0,0.72D0,0.725D0,0.73D0,0.74D0,0.75D0,
#0.76D0,0.77D0,0.78D0,0.79D0,0.80D0,0.81D0,0.82D0,0.83D0,0.84D0,
#0.85D0,0.86D0/
!Open channel:Ps(1s);N=2

NO=N
WRITE(8,124)'PK','Q11(1,1)', 'Q22(1,1)', 'Q11(1,2)', 'Q22(1,2)'
WRITE(8,124)'QK','Q22(2,2)', 'Q11(2,2)', 'Q11(2,1)', 'Q22(2,1)'
WRITE(8,"")'-----'

DO KK=1,3

PKK(1)=PPK(KK)
IF(NO .EQ. 2)THEN
PKK(2)=(2*PKK(1)**2-1)**0.5D0

C## the following options for future uses at high energies

ELSEIF(NO .GT. 2 .AND. NO .LE. 5)THEN
PKK(2)=(2*PKK(1)**2-1)**0.5D0
PKK(3)=DSQRT(-0.75D0+PKK(1)**2)
PKK(4)=PKK(3)
PKK(5)=PKK(3)
ENDIF

CALL FFM(NO,PKK(1),L,X00,X10,X01,X11)      !FREE-FREE
CALL BFMATRIX(NO,PKK(1),L,X00,X10,X01,X11)  !(FREE-FREE)+(FREE-BOUND)
!----> M_matrices

DO I=1,N
  DO J=1,N
    PKIJ=DSQRT(PKK(I)*PKK(J))
    X00(I,J)=X00(I,J)/PKIJ
    X01(I,J)=X01(I,J)/PKIJ
    X10(I,J)=X10(I,J)/PKIJ
    X11(I,J)=X11(I,J)/PKIJ
  ENDDO
ENDDO

CALL R_MATRIX(X00,X01,X10,X11,Y,INDX,R1,R2,N)
CALL T_MATRIX(R1,T11,T12,INDX,N)
CALL T_MATRIX(R2,T21,T22,INDX,N)

DO I=1,N
  DO J=1,N
    T11(I,J)=T11(I,J)**2+T12(I,J)**2          !T11(I,J)=|Tk(I,J)|^2
    T22(I,J)=T21(I,J)**2+T22(I,J)**2          !T22(I,J)=|Ti(I,J)|^2
  ENDDO
ENDDO

DO I=1,N                                         !Transition cross sections
  PI=1D0/PKK(I)**2*(2*L+1)

  DO J=1,N
    T11(I,J)=PI*T11(I,J)
    T22(I,J)=PI*T22(I,J)
  ENDDO

  IF(NO .GT. 4 )THEN
    T11(I,4)=T11(I,4)+T11(I,5)
    T22(I,4)=T22(I,4)+T22(I,5)
  ENDIF
ENDDO

IF(NO .EQ. 2)THEN
C H entrance channel kp   ls->ls_k ls->ls_i ls->Ps_k ls->Ps_i
WRITE(8,126)'PKK(1),T11(1,1),T22(1,1),T11(1,2),T22(1,2),
write(2,126)'PKK(1),T11(1,1),T22(1,1),T11(1,2),T22(1,2)

C Ps entrance channel kq   Ps->Ps_k Ps->Ps_i Ps->ls_K Ps->ls_i
WRITE(8,126)'PKK(2),T11(2,2),T22(2,2),T11(2,1),T22(2,1)

```

```

      WRITE(8,*)
      write(2,126)PKK(1),T11(1,1),T22(1,1),T11(1,2),T22(1,2)
      close(2)

      ELSEIF(NO .GT. 2 .AND. NO .LT. 6)THEN
C H entrance channel kp,   ls->ls   ls->Ps  ls->2s   ls->2p_,  2p+
      WRITE(8,126)PKK(1),T11(1,1),T11(1,2),T11(1,3),T11(1,4)
      WRITE(8,126)PKK(1),T22(1,1),T22(1,2),T22(1,3),T22(1,4)

C Ps entrance channel kq   Ps->ls   Ps->Ps   Ps->2s   Ps->2p_,  2p+
      WRITE(8,126)PKK(2),T11(2,1),T11(2,2),T11(2,3),T11(2,4)
      WRITE(8,126)PKK(2),T22(2,1),T22(2,2),T22(2,3),T22(2,4)

      ENDIF

      ENDDO
124  FORMAT(A5,4(5X,A13))
126  FORMAT(F10.8,1X,4(1X,E14.9))
      RETURN
      END

C ****
C * CALCULATE FREE-FREE MATRICE:FFSS,FFCS,FFSC,FFCC *
C * NO --> NO. OF OPEN CHANNEL *
C ****

C ##### Descriptions #####
C Input-- NO: number of the open channels
C          PK: the positron momentum
C          L: the total angular momentum of the system
C Output-- the free-free matrices: FFSS,FFCS,FFSC,FFCC
C
C Callings---
C          FFSS_PQ,FFCS_PQ,FFCC_PQ: free-free subs between H-P and H-Q channels
C          FFSS_PU,FFCS_PU,FFCS_UP,FFCC_UP: free-free subs between H and Ps
C          FFCC_UV: free-free sub between Ps and Ps
C          Note: FFSS_UV=0 and FFCS_UV=0 for just two open channels
C
C #####
SUBROUTINE FFM(NO,PK,L,FFSS,FFCS,FFSC,FFCC)
IMPLICIT REAL*8(A-H,O-Z)
EXTERNAL FFSS_PQ,FFCS_PQ,FFCC_PQ,FFSS_PU,FFCS_PU,FFCS_UP,
#FFCC_UP
DIMENSION FFSS(NO,NO),FFCS(NO,NO),FFSC(NO,NO),FFCC(NO,NO)
COMMON/B_G/BETA,GAMMA

FFSS(1,1)=FFSS_PQ(PK,PK,L,1,0,L,1,0,L)
FFCS(1,1)=FFCS_PQ(PK,PK,L,1,0,L,1,0,L,beta)
FFSC(1,1)=FFCS(1,1)+0.5D0*PK
FFCC(1,1)=FFCC_PQ(PK,PK,L,1,0,L,1,0,L,BETA,BETA)

IF (NO .GT. 1) THEN                                !Ps channel open
PK2=DSQRT(2*PK*PK-1)
FFSS(1,2)=FFSS_PU(PK,PK2,L,1,0,L,1,0,L)
FFSS(2,1)=FFSS(1,2)
FFSS(2,2)=0.

FFCS(1,2)=FFCS_PU(PK,PK2,L,1,0,L,1,0,L,BETA)
FFCS(2,1)=FFCS_UP(PK2,PK,L,1,0,L,1,0,L,GAMMA)
FFCS(2,2)=0.

FFSC(1,2)=FFCS(2,1)
FFSC(2,1)=FFCS(1,2)
FFSC(2,2)=0.5D0*PK2

FFCC(1,2)=FFCC_PU(PK,PK2,L,1,0,L,1,0,L,BETA,GAMMA)
FFCC(2,1)=FFCC(1,2)
FFCC(2,2)=FFCC_UV(PK2,PK2,L,1,0,L,1,0,L,BETA,GAMMA)
ENDIF

RETURN
END

C ##### Descriptions #####
C Input-- NO: number of open channels
C          L: the total angular momentum of the system
C          PK: the positron momentum
C          FB00, FB01, FB10, and FB11: the free-free matrices

```



```

      DO I=1,NH
      NI=NO_IP*NH+I
      N24I=N24(I)+L2I
      FBS(2,NI)=FBS_PIU(UK,IP,N24I,ZII(I),L2I,1,0,L,L)
      FBC(2,NI)=FBC_QJU(UK,IP,N24I,ZII(I),L2I,1,0,L,L,GAMMA)
      ENDDO
      ENDDO
      ENDDO

      !Ps(bound,V)-Ps(1s)

      NO_H=NO_IP
      DO IU=1,9
      DO L4I=INT(ABS(LPSJ(IU)-L)),LPSJ(IU)+L,2
      NO_IP=NO_IP+1
      DO I=1,NH
      NI=NO_IP*NH+I
      N24I=N24(I)+L4I
      FBS(2,NI)=FBS_VU(UK,IU,N24I,ZII(I),L4I,1,0,L,L)
      FBC(2,NI)=FBC_VU(UK,IU,N24I,ZII(I),L4I,1,0,L,L,GAMMA)
      ENDDO
      ENDDO
      ENDDO

      ENDDIF

C##### READ IN THE EIGENVALUES AND EIGENFUNCTIONS #####
      IF(NO_READ .NE. 1)THEN
      DO I=0,NHN
      DO J=1,NHN,3
      IF (I .EQ. 0)THEN
      READ(5,30) EVAL(J),EVAL(J+1),EVAL(J+2)
      ELSE
      READ(5,30) EVEC(I,J),EVEC(I,J+1),EVEC(I,J+2)
      ENDIF

      ENDDO
      ENDDO
      NO_READ=1
      close(5)
      ENDDIF

C##### CALCULATE FB00,FB01,FB10,FB11 #####
      E=-0.5D0+0.5D0*PK**2
      DO I=1,NO
      DO J=1,NH
      BFMS(I,J)=0.
      BFMC(I,J)=0.
      DO K=1,NHN
      BFMS(I,J)=BFMS(I,J)+FBS(I,K)*EVEC(K,J)
      BFMC(I,J)=BFMC(I,J)+FBC(I,K)*EVEC(K,J)
      ENDDO
      ENDDO
      ENDDO

      DO I=1,NO
      DO J=1,NO
      s00=0.
      s01=0.
      s10=0.
      s11=0.

      DO K=1,NHN
      S00=S00+BFMS(I,K)/(E-EVAL(K))*BFMS(J,K)
      S01=S01+BFMS(I,K)/(E-EVAL(K))*BFMC(J,K)
      S10=S10+BFMC(I,K)/(E-EVAL(K))*BFMS(J,K)
      S11=S11+BFMC(I,K)/(E-EVAL(K))*BFMC(J,K)
      ENDDO
      FB00(I,J)=FB00(I,J)+S00
      FB01(I,J)=FB01(I,J)+S01
      FB10(I,J)=FB10(I,J)+S10
      FB11(I,J)=FB11(I,J)+S11

      ENDDO
      ENDDO

30   FORMAT(1X,3(d23.17,1X))
118  format(1x,a5.2a23)
119  format(1x,i5.2d23.16)
      RETURN
      END

```

```

C ****
C * REACTANCE MATRIX R: Using a modified version of the Harris-Nesbet *
C ****
C ##### Descriptions #####
C Input-- X00, X01, X10, X11: the m-matrices in the Harris Nesbet method
C N: number of open channels. So Xij(N,N)--square matrices
C
C Output-- R1, R2: the Kohn and inverse Kohn reaction matrices obtained
C by optimized in the transformed space
C
C Temperary storages: Y, INDEX, X00_1,X01_1,X10_1, X11_1,T1, and T2 arrays
C
C Callings-- AA_INVERSE: the inverse of matrix AA
C
C#####
SUBROUTINE R_MATRIX(X00,X01,X10,X11,Y,indx,R1,R2,N)
IMPLICIT REAL*8(A-H,O-Z)
EXTERNAL AA_INVERSE
DIMENSION X00(N,N),X01(N,N),X10(N,N),X11(N,N),Y(N,N),INDX(N)
# .R1(N,N),R2(N,N),X00_1(15,15),X01_1(15,15),X10_1(15,15),
# X11_1(15,15),T1(15,15),T2(15,15)

DO I=1,N                         !deposit x00,x01,x10,x11 into
  DO J=1,N                         !x00_1,x01_1,x10_1,x11_1
    X00_1(I,J)=X00(I,J)
    X01_1(I,J)=X01(I,J)
    X10_1(I,J)=X10(I,J)
    X11_1(I,J)=X11(I,J)
  ENDDO
ENDDO

DELTA0=1D6
DO 3039 X=0D0,180D0,1D0
Z=X/180D0*3.1415926535897932d0

C transform the original space to a transformed space

DO I=1,N
  DO J=1,N
    X00(I,J)=(COS(Z))**2*X00_1(I,J)+0.5D0*SIN(2*Z)*(X01_1(I,J) +
#   X10_1(I,J))+(SIN(Z))**2*X11_1(I,J)
    X11(I,J)=(SIN(Z))**2*X00_1(I,J)-0.5D0*SIN(2*Z)*(X01_1(I,J) +
#   X10_1(I,J))+(COS(Z))**2*X11_1(I,J)
    X01(I,J)=-(SIN(Z))**2*X10_1(I,J)-0.5D0*SIN(2*Z)*(X00_1(I,J) -
#   X11_1(I,J))+(COS(Z))**2*X01_1(I,J)
    X10(I,J)=(COS(Z))**2*X10_1(I,J)-0.5D0*SIN(2*Z)*(X00_1(I,J) -
#   X11_1(I,J))-(SIN(Z))**2*X01_1(I,J)
  ENDDO
ENDDO

C calculate the reactance matrix using the Kohn method in new space

DO I=1,N
  DO J=1,N
    R1(I,J)=-2*X00+2*X10/X11*X10           !R1=-2*X00+2*X10/X11*X10
    R2(I,J)=2*X11(I,J)                      !R2=2*(X11-X01/X00*X01)
  ENDDO
ENDDO

CALL AA_INVERSE(X11,Y,indx,N)

DO I=1,N
  DO J=1,N
    DO K1=1,N
      SUM=0.
      DO K2=1,N
        SUM=SUM+Y(K1,K2)*X10(K2,J)
      ENDDO
      R1(I,J)=R1(I,J)+2*X10(K1,I)*SUM
    ENDDO
  ENDDO
ENDDO

C calculate the reactance matrix using the inverse Kohn method in new space

CALL AA_INVERSE(X00,Y,indx,N)

```

```

DO I=1,N
  DO J=1,N
    DO K1=1,N
      SUM=0.
      DO K2=1,N
        SUM=SUM+Y(K1,K2)*X01(K2,J)
      ENDDO
      R2(I,J)=R2(I,J)-2*X01(K1,I)*SUM
    ENDDO
  ENDDO

CALL AA_INVERSE(R2,Y,INDX,N) !inverse of R2

C change memories: inverse of R2=>Y deposite into R2

DO I=1,N
  DO J=1,N
    R2(I,J)=Y(I,J)
  ENDDO
ENDDO

C change back to original space
DO I=1,N
  DO J=1,N
    X00(I,J)=-SIN(Z)*R1(I,J)
    R1(I,J)=COS(Z)*R1(I,J)
    !R_o-----sin(z)+cos(z) R_n
    !R_o-----cos(z)-sin(z) R_n
    !R_o: R-matrix in original
    !R_n: R-matrix in new space
    X11(I,J)=-SIN(Z)*R2(I,J)
    R2(I,J)=COS(Z)*R2(I,J)
  ENDDO
  X00(I,I)=COS(Z)+X00(I,I)
  R1(I,I)=SIN(Z)+R1(I,I)

  X11(I,I)=COS(Z)+X11(I,I)
  R2(I,I)=SIN(Z)+R2(I,I)
ENDDO

CALL AA_INVERSE(X00,X01,INDX,N) !inverse of X00 = X01
CALL AA_INVERSE(X11,X10,INDX,N) !inverse of X11 = X10

DO I=1,N
  DO J=1,N
    X00(I,J)=0.
    X11(I,J)=0.
    DO K=1,N
      X00(I,J)=X00(I,J)+R1(I,K)*X01(K,J)
      X11(I,J)=X11(I,J)+R2(I,K)*X10(K,J)
    ENDDO
  ENDDO
ENDDO

DELTA=abs(X00(1,1)-X11(1,1))
IF( DELTA .LT. DELTA0)THEN
  DELTA0=DELTA
  DO I=1,N
    DO J=1,N
      T1(I,J)=X00(I,J) ! from the Kohn method
      T2(I,J)=X11(I,J) ! from the inverse Kohn method
    ENDDO
  ENDIF
ENDIF

3039 CONTINUE

write(8,*)'I,J,R1(i,j),R2(i,j)'

DO I=1,N
  DO J=1,N
    R1(I,J)=T1(I,J)
    R2(I,J)=T2(I,J)
    write(8,*)i,j,R1(i,j),R2(i,j)
  ENDDO
ENDDO

RETURN
END

C ****
C * MATRIX: T=-2*R/(1-iR)=T1+iT2 *
C ****

```

```

C##### Descriptions #####
C
C Input--- R-matrix: reactiona matrix
C      N:          number of open channels
C
C Output-- T1 and T2: the real and imaginary parts of transition matrix T
C
C Temperary storage: INDX(N)
C
C#####
C
SUBROUTINE T_matrix(R,T1,T2,INDX,N)
IMPLICIT REAL*8(A-H,O-Z)
EXTERNAL AA_INVERSE
DIMENSION R(N,N),T1(N,N),T2(N,N),INDX(N)
DO I=1,N
  DO J=1,N
    T1(I,J)=0.
    DO K=1,N
      T1(I,J)=T1(I,J)+R(I,K)*R(K,J)
    ENDDO
  ENDDO
  T1(I,I)=1+T1(I,I)           !deposite 1+R^2 into T1
ENDDO

CALL AA_INVERSE(T1,T2,INDX,N)      !inverse of 1+R^2 into T2

DO I=1,N
  DO J=1,N
    T1(I,J)=0.
    DO K=1,N
      T1(I,J)=T1(I,J)+R(I,K)*T2(K,J)           !real part of T: T1=-2R/(1+R^2)
    ENDDO
    T1(I,J)=-2*T1(I,J)
  ENDDO
ENDDO

DO I=1,N
  DO J=1,N
    T2(I,J)=0.
    DO K=1,N
      T2(I,J)=T2(I,J)+R(I,K)*T1(K,J)           !image part of T: T2=RT1
    ENDDO
  ENDDO
RETURN
END

C *****
C * MATRIX INVERSE: AA-->Y *
C *****

C##### Descriptions #####
C
C Input -- AA: N X N square matrix
C
C Output-- Y: inverse of AA. INDX(N) is a temperary storage matrix
C
C#####
C
SUBROUTINE AA_INVERSE(AA,Y,INDX,N)
IMPLICIT REAL*8(A-H,O-Z)
DIMENSION AA(N,N),Y(N,N),INDX(N)
EXTERNAL LUDCMP,LUBKSB
NP=N
DO I=1,N
  DO J=1,N
    Y(I,J)=0.
  ENDDO
  Y(I,I)=1D0
ENDDO

CALL LUDCMP(AA,N,np,INDX,D)

DO J=1,N
  CALL LUBKSB(AA,N,np,INDX,Y(1,J))
ENDDO

do i=1,n
do j=i,n
  aa(j,i)=aa(i,j)
enddo
enddo

```

```

      RETURN
      END

C *****decomposition of A into LU matrix *****
C This sub is down-loaded from linpack
C *****

SUBROUTINE ludcmp(a,n,np,indx,d)
implicit real*8(a-h,o-z)
PARAMETER (NMAX=500,TINY=1.0e-20)
dimension a(np,np),vv(nmax),indx(n)
d=1d0
do 12 i=1,n
   aamax=0.
   do 11 j=1,n
      if (abs(a(i,j)).gt.aamax) aamax=abs(a(i,j))
11  continue
      if (aamax.eq.0.) pause 'singular matrix in ludcmp'
      vv(i)=1d0/aamax
12  continue
   do 19 j=1,n
      do 14 i=1,j-1
         sum=a(i,j)
         do 13 k=1,i-1
            sum=sum-a(i,k)*a(k,j)
13  continue
         a(i,j)=sum
14  continue
      aamax=0.
      do 16 i=j,n
         sum=a(i,j)
         do 15 k=1,j-1
            sum=sum-a(i,k)*a(k,j)
15  continue
         a(i,j)=sum
         dum=vv(i)*abs(sum)
         if (dum.ge.aamax) then
            imax=i
            aamax=dum
         endif
16  continue
      if (j.ne.imax)then
         do 17 k=1,n
            dum=a(imax,k)
            a(imax,k)=a(j,k)
            a(j,k)=dum
17  continue
         d=-d
         vv(imax)=vv(j)
      endif
      indx(j)=imax
      if(a(j,j).eq.0.)a(j,j)=TINY
      if(j.ne.n)then
         dum=1d0/a(j,j)
         do 18 i=j+1,n
            a(i,j)=a(i,j)*dum
18  continue
      endif
19  continue
      return
      END

C ***** Solving A1 X =B *****
C This sub is down-loaded from linpack
C *****

SUBROUTINE lubksb(a,n,np,indx,b)
IMPLICIT REAL*8(A-H,O-Z)
DIMENSION a(np,np),b(n),INDX(N)
ii=0

```

```

do 12 i=1,n
  ll=indx(i)
  sum=b(ll)
  b(ll)=b(i)
  if (ii.ne.0)then
    do 11 j=ii,i-1
      sum=sum-a(i,j)*b(j)
  11   continue
  else if (sum.ne.0.) then
    ii=i
  endif
  b(i)=sum
12  continue
do 14 i=n,1,-1
  sum=b(i)
  do 13 j=i+1,n
    sum=sum-a(i,j)*b(j)
  13   continue
  b(i)=sum/a(i,i)
14  continue
return
END

C ****
C * GAUSSIAN NODE POINTS FOR ETA AND PSI *
C ****

C ##### Descriptions #####
C Argument:
C   NPSI-- number of segments chopped in an interval [0,1]
C   NETA-- number of segments chopped in an interval [-1,1]
C           in each segment, we use 10 Gaussian Node points
C Arrays:
C   DPSI, W_PSI-- Nodes and Weights for spheroidal argument (psi)
C   DETA, W_ETA-- Nodes and Weights for spheroidal argument (eta)
C

SUBROUTINE ETA_PSI
IMPLICIT REAL*8(A-H,O-Z)
PARAMETER(NPSI=8,NETA=15)
COMMON/QXQWW/XX(5),WW(5)/PSI_ETA/DPSI(NPSI*10),DETA(NETA*10)
# /W_W/W_PSI(80),W_ETA(150)

# DATA XX/0.1488743389816312D0,0.4333953941292473D0,
# 0.6794095682990244D0,0.865063366889846D0,0.9739065285171717D0/
# DATA WW/0.2955242247147529D0,0.2692567193099963D0,
# 0.2190863625159821D0,0.1494513491505806D0,0.6667134430868818D-1/

WIDTH=1D0/NPSI
DO J=1,NPSI
  A=(J-1)*WIDTH
  B=A-WIDTH
  XM=0.5D0*(B+A)
  XR=0.5D0*(B-A)

  DO I=6,10
    DX=XR*XX(I-5)
    DPSI(I+(J-1)*10)=(XM+DX)
    DPSI(J*10-I+1)=(XM-DX)
    W_PSI(I+(J-1)*10)=WW(I-5)*0.5d0*WIDTH
    W_PSI(J*10-I+1)=WW(I-5)*0.5d0*WIDTH
  ENDDO
ENDDO

WIDTH=2D0/NETA
DO J=1,NETA
  A=-1D0+(J-1)*WIDTH
  B=A+WIDTH

  XM=0.5D0*(B+A)
  XR=0.5D0*(B-A)

  DO I=6,10
    DX=XR*XX(I-5)
    DETA(I+(J-1)*10)=XM+DX
    DETA(J*10-I+1)=XM-DX
    W_ETA(I+(J-1)*10)=WW(I-5)*0.5d0*WIDTH
    W_ETA(J*10-I+1)=WW(I-5)*0.5d0*WIDTH
  ENDDO
ENDDO

```

```

      RETURN
      END

C*****+
C   The angular integration matrix between a hydrogen and a Ps channels
C   This is a general program for any angular momentum numbers (L1,L2) and
C   (LU,LV) under a given system total angular momentum number L. But If L1
C   or LU is larger than 2, one should change the upper limits in DO-loops.
C*****+

C##### Descriptions #####
C
C Input-- L: the total angular momentum
C
C Calling-- HP(...): angular integration matrix
C
C DHP(...)-- Common angular integration Matrix which will be frequently used in
C             Ps-H bound-free and free-free, as well as the bound-bound,
C             integrations
C
C L1: the angular momentum number of the hydrogen electron
C L2: the angular momentum number of the positron
C LU: the angular momentum number of the positronium
C LV: the angular momentum number of the mass center of Ps
C
C One can change the maxima of L1 and LU to include higher angular momentum
C orbitals
C
C##### Descriptions #####
C
SUBROUTINE MATRIX_HP(L)
IMPLICIT REAL*8(A-H,O-Z)
EXTERNAL HP
COMMON/D_HP/DHP(5,5,3,3,80,150)
# /PSI_ETA/DPSI(80),DETA(150)
DO 1321 L1=0,2
L20=INT(ABS(L-L1))
DO 1321 L2=L20,L+L1,2
DO 1321 LU=0,2
LV0=INT(ABS(L-LU))
DO 1321 LV=LV0,L+LU,2
DO 1321 I=1,150
DO 1321 J=1,150
DHP(L1+1,(L2-L20)/2+1,LU+1,(LV-LV0)/2+1,I,J)=HP(L,L1,L2,LU,LV,
# 1/DPSI(I),DETA(J))
1321 CONTINUE
RETURN
END

C *****+
C *2pi *
C * |d(phi) <L(11)(12);(1,2) | L(lu)(lv);(3,4) > *
C * 0   *
C *****+

C##### Description #####
C
C Input-- L1/ L2: angular momentum of the electron/positron
C          LU/LV : angular momentum of the positronium/mass center of Ps
C          PSI,ETA: spheroidal coordinates
C
C Output-- HP(L,L1,L2,LU,LV,PSI,ETA)
C
C Calling-- HPMM(..): angular integration matrix element for given magnetic
C                  quantum numbers m1 and m
C                  F3J(..): 3-j symbol from angular momentum coupling
C
C##### Descriptions #####
C
FUNCTION HP(L,L1,L2,LU,LV,PSI,ETA)
IMPLICIT REAL*8(A-H,O-Z)
EXTERNAL HPMM ,F3J
DIMENSION DLAMDA(3)
DLAMDA(1)=0.5D0
DLAMDA(2)=1D0
DLAMDA(3)=1D0

SUM=0.
DO M1=0,MIN(LU,LV)
SUM1=0.

```

```

DO M=0,MIN(L1,L2)
  SUM1=SUM1+DLAMDA(M+1)*F3J(L1,L2,L,M,-M,0)*
#    HPMM(L1,L2,M,LU,LV,M1,PSI,ETA)
  ENDDO
  SUM=SUM+DLAMDA(M1+1)*F3J(LU,LV,L,M1,-M1,0)*SUM1
ENDDO
HP=(-1D0)**(LU-LV+L1-L2)*(2*L+1)*SUM
RETURN
END

C **** -----
C * <L1ML2(-M) | LUM'LV(-M') > *
C **** -----

C ##### Descriptions #####
C Input--L1, L2: the angular momentum quantum number of the electron and
C                  positron
C LU, LV: the angular momentum quantum number of the Ps and mass
C                  center of Ps
C M, M1 : the magnetic quantum number of the electron and Ps
C PSI,ETA:the spheroidal coordinates
C
C Output-- the angular integration HPMM
C #####
FUNCTION HPMM(L1,L2,M,LU,LV,M1,PSI,ETA)
IMPLICIT REAL*8 (A-H,O-Z)
COMMON/D_BINC/dbinc(21,21) /D_BB/DBB(30,10)

AA=((PSI**2-1)*(1-ETA**2))**0.5D0
BB=(PSI**2+6*PSI*ETA+ETA**2+8)**0.5D0

A1=(PSI*ETA+1)/(PSI+ETA)
A2=AA/(PSI+ETA)

A3=(PSI*ETA+3)/BB
A4=AA/BB
A5=(PSI*ETA-1)/(PSI-ETA)
A6=AA/(PSI-ETA)

A65=A6/A5
A43=A4/A3

SUM=0.
DO 5013 K=0,(L1-M)/2
H1=PM1(L1,M,K)*A1**((L1-2*K)
DO 5013 K1=0,L1-2*K-M
H2=H1*DBINC(L1-2*K-M+1,K1+1)*(-A2/A1)**K1

DO 5013 J=0,M/2
H3=H2*(-1D0)**J*DBINC(M+1,2*J+1)

DO 5013 J0=0,M-2*J
H4=H3*DBINC(M-2*J+1,J0+1)*(A2/A1)**(2*J+J0)

DO 5013 J13=0,2*M1,2
H5=H4*(-1D0)**(J13/2)

DO 5013 J1=MAX(0,J13-M1),MIN(J13,M1)
H6=H5*(-1D0)**J1*DBINC(M1+1,J1+1)*DBINC(M1+1,J13-J1+1)

DO 5013 J2=0,M1-J1
H7=H6*DBINC(M1-J1+1,J2+1)*A65**((J1+J2)

DO 5013 J4=0,M1+J1-J13
H8=H7*DBINC(M1+J1-J13+1,J4+1)*A43**((J13-J1+J4)

DO 5013 KU=0,(LU-M1)/2
H9=H8*A5**((LU-2*KU)*PM1(LU,M1,KU)

LS=LU-M1-2*KU
DO 5013 KS=0,LS
H10=H9*DBINC(LS+1,KS+1)*(-A65)**KS

DO 5013 KV=0,(LV-M1)/2
H11=H10*A3**((LV-2*KV)*PM1(LV,M1,KV)

LT=LV-M1-2*KV
DO 5013 KT=0,LT

```

```

H12=H11*DBINC(LT+1,KT+1)*(-A43)**KT
IX=K1+J0+KS+KT+J2+J4+1
IY=2*J+J13+1
II=L1-2*K-M-K1+J0+LS-KS+LT-KT+J2+J4
JJ=K1+M-2*J-J0+KS+KT+2*M1-J2-J4-J13+1
H13=H12*((-1D0)**(IX-1)+1D0)*DBB(IX,IY)*
# PM(II,JJ,L2,M)
sum=sum+h13
5013 CONTINUE
HPPM=(-1D0)**(M+M1)*8D0*3.1415926535897932D0*APM(L1,M)
# *APM(L2,M)*APM(LU,M1)*APM(LV,M1)*SUM
RETURN
END

*****
C * PROVIDING COMMON DATA: FACT(N),CT(N1,N2,N3),B3(N,L,NU)*
C * B3PS(N,L,NU),BINC(N,J) *
*****
SUBROUTINE COMMON_DATA
IMPLICIT REAL*8(A-H,O-Z)
EXTERNAL FACT,CT,B3,B3PS,BINC,WK,WK,APM,PML,PM,F3J
COMMON/D_FACT/DFACT(150)
# /D_BINC/dbinc(21,21)/D_WMK/DWM(15,8),DWK(15,8)
# /D_BB/DBB(30,10)

DFACT(1)=1D0
DO I=1,149
    DFACT(I+1)=DFACT(I)*I
ENDDO

DO N=0,20
    DO I=0,N
        DBINC(N+1,I+1)=BINC(N,I)
    ENDDO
ENDDO

DO L=0,14
    DO M=0,L/2
        DWM(L+1,M+1)=WM(L,M)
    ENDDO
ENDDO

IF(L .GE. 1)THEN
    DO K=0,(L-1)/2
        DWK(L+1,K+1)=WK(L,K)
    ENDDO
ENDIF
ENDDO

DO I=1,30
    DO J=1,10
        DBB(I,J)=GAMA(0.5D0*I)*GAMA(0.5D0*J)/GAMA(0.5D0*(I+J))
    ENDDO
ENDDO

RETURN
END

*****
C * FFSS_PQ(...)=<NP LP;L LP LP1;S|H-E|NQ LQ;L LQ LQ1;S> *
*****
C ##### Descriptions #####
C Input--NP,LP,LPI: quantum numbers of H channel P with the angular momentum LPI
C          of the positron
C      NQ,LQ,LQ1: quantum numbers of H channel Q with the angular momentum LQ1
C          of the positron
C      L, PK, QK: total angular momentum number, psoitron momenta in channels
C          P and Q
C
C Callings--
C      BJ: the spherical Bessel function

```

```

C      H_PQ: the interaction matrix element between H channels P and Q
C
C Common block--GAUS/QX(354),QW(354): one-dimensional Gaussian quadrature using
C      800 node points but only the first 354 points used because the remainings
C      have zero weights.
C#####
C
FUNCTION FFSS_PQ(PK,QK,L,NP,LP,LP1,NQ,LQ,LQ1)
IMPLICIT REAL*8(A-H,O-Z)
EXTERNAL BJ,H_PQ
COMMON/GAUS/QX(354),QW(354)

SUM=0.
DO I=1,354
  X=QX(I)
  SUM=SUM+X**2*BJ(LP1,PK*X)*BJ(LQ1,QK*X)*H_PQ(NP,LP,LP1,
#NQ,LQ,LQ1,L,X)*QW(I)
ENDDO
FFSS_PQ=PK*QK*SUM
RETURN
END

C *****
C *FFSS_UV(...)=<NU LU;L LU LUL1;S|H-E|NV LV;L LV LV1;S> *
C *****
C#####
C      Descriptions #####
C
C Input--NU,LU,LUL1: quantum numbers of Ps channel U with the angular momentum LP1
C      of the positron with the free Bessel function for mass center
C      of Ps
C      NV,LV,LV1: quantum numbers of Ps channel V with the angular momentum LQ1
C      of the positron
C      L, UK, VK: total angular momentum number, positronium momenta in
C      channels U and V
C
C Callings--
C      BJ: the spherical Bessel function
C      PS_UV: the interaction matrix element between Ps channels U and V
C
C#####
C
FUNCTION FFSS_UV(UK,VK,L,NU,LU,LUL1,NV,LV,LV1)
IMPLICIT REAL*8(A-H,O-Z)
EXTERNAL PS_UV,BJ
COMMON/GAUS/QX(354),QW(354)

SUM=0.
DO I=1,354
  X=QX(I)
  SUM=SUM+X*X*BJ(LUL1,UK*X)*BJ(LV1,VK*X)*
#PS_UV(NU,LU,LUL1,NV,LV,LV1,L,X)*QW(I)
ENDDO

FFSS_UV=UK*VK*SUM
RETURN
END

C *****
C * FFCS_PQ(...)=<NP LP;L LP LP1;C|H-E|NQ LQ;L LQ LQ1;S> *
C *****
C#####
C      Description #####
C
C The same as in sub FUNCTION FFSS_PQ, but
C Calling-- BESSELN: the modified Neumann function
C      BETA: parameter in the factor before the Neuman function
C
C#####
C
FUNCTION FFCS_PQ(PK,QK,L,NP,LP,LP1,NQ,LQ,LQ1,BETA)
IMPLICIT REAL*8(A-H,O-Z)
EXTERNAL H_PQ,BJ,BESSELN
COMMON/GAUS/QX(354),QW(354)

SUM=0.
DO I=1,354
  X=QX(I)
  SUM=SUM+X*X*BESSELN(2*LP1+1,LP1,BETA,PK,X)*BJ(LQ1,QK*X)*
#H_PQ(NP,LP,LP1,NQ,LQ,LQ1,L,X)*QW(I)
ENDDO

```

```

FFCS_PQ=-PK*QK*SUM
RETURN
END

C ****
C *FFCS_UV(..)=<NU LU;L LU LUL;C|H-E|NV LV;L LV LVL;S> *
C ****

C##### Description #####
C
C The same as in sub FUNCTION FFSS_UV, but
C Calling-- BESSELN: the modified Neumann function
C           GAMMA: parameter in the factor before the Neuman function
C
C#####

FUNCTION FFCS_UV(UK,VK,L,NU,LU,LUL,NV,LV,LVL,GAMMA)
IMPLICIT REAL*8(A-H,O-Z)
EXTERNAL BESSELN,BJ,PS_UV
COMMON/GAUS/QX(354),QW(354)

SUM=0.
DO I=1,354
  X=QX(I)
  SUM=SUM+X*X*BESSELN(2*LU1+1,LUL,GAMMA,UK,X)*BJ(LVL1,VK*X)-
#PS_UV(NU,LU,LUL,NV,LV,LVL,X)*QW(I)
ENDDO

FFCS_UV=-2*UK*VK*SUM
RETURN
END

C ****
C *FFCC_PQ(..)=<NP LP;L LP LP1;C|H-E|NQ LQ;L LQ LQ1;C> *
C ****

FUNCTION FFCC_PQ(PK,QK,L,NP,LP,LPL,NQ,LQ,LQ1,beta1,beta2)
IMPLICIT REAL*8(A-H,O-Z)
EXTERNAL H_PQ,FF_N,BESSELN
COMMON/GAUS/QX(354),QW(354)

SUM1=0.
DO K=1,354
  X=QX(K)
  IF(NP.EQ.NQ .AND. LP.EQ.LQ .AND. LPL.EQ.LQ1)THEN
    FFCC1=FF_N(LPL,beta1,PK,X)
  ELSE
    FFCC1=0.
  ENDIF

  SUM1=SUM1+X**2*(FFCC1+BESSELN(2*LPL+1,LPL,beta1,PK,X)-
#*H_PQ(NP,LP,LPL,NQ,LQ,LQ1,L,X))-
#*BESSELN(2*LQ1+1,LQ1,beta2,qk,X)*QW(K)
ENDDO

FFCC_PQ=PK*QK*SUM1
RETURN
END

C ****
C * Hamiltonian operates on the modified neuman function*
C ****

FUNCTION FF_N(L,B,P,X)
IMPLICIT REAL*8(A-H,O-Z)
EXTERNAL BESSELN
BNJN=BESSELN(2*L,1,B,P,X)
XY=DEXP(-B*X)
FF_N=(L+0.5D0)*B*XY*(-2*B*L*BNJN/(1-XY)*XY+(B-2*(L+1)/X)*BNJN
#+2*P*BESSELN(2*L,L+1,B,P,X))

RETURN
END

C ****
C *FFCC_UV(..)=<NU LU;L LU LUL;C|H-E|NV LV;L LV LVL;C> *
C ****

FUNCTION FFCC_UV(UK,VK,L,NU,LU,LUL,NV,LV,LVL,GAMMA1,GAMMA2)
IMPLICIT REAL*8(A-H,O-Z)
EXTERNAL FF_N,PS_UV,BESSELN
COMMON/GAUS/QX(354),QW(354)

SUM=0.

```

```

DO I=1,354
  X=QX(I)
  IF(NU.EQ.NV .AND. LU.EQ.LV .AND. LU1.EQ.LV1)THEN
    FFCC2=0.5D0*FF_N(LU1,GAMMA1,UK,X)
  ELSE
    FFCC2=0.
  ENDIF
  SUM=SUM+X*X*(FFCC2+BESSELN(2*LU1+1,LU1,GAMMA1,UK,X)*PS_UV(
#NU,LU,LU1,NV,LV,LV1,L,X))*BESSELN(2*LV1+1,LV1,GAMMA2,VK,X)
*QW(I)
  ENDDO

  FFCC_UV=2*UK*VK*SUM
  RETURN
END

C *****
C *PFSS_PU(..)=<NP LP;L LP LP1;S|K-E|NU LU;L LU LU1;S> *
C *****

C ##### Descriptions #####
C
C Input---L: total angular momentum of the system
C           NP,LP,LP1: quantum numbers of H channel p
C           NU,LU,LU1: quantum numbers of Ps channel U
C           PK,UK:      momenta of the positron and positronium
C
C Callings--
C           WWJJ: sub of an integration related to two spherical Bessel functions
C           B3 and B3PS: coeffs of H and Ps physical states
C
C Common Blocks--
C           DHP: the angular integration between Ps and H channels
C           DPSI,W_PSI: Gaussian nodes and weights of the spheroidal coordinate (psi)
C           DETA,W_ETA: Gaussian nodes and weights of the spheroidal coordinate (eta)
C
C #####
FUNCTION FFSS_PU(PK,UK,L,NP,LP,LP1,NU,LU,LU1)
IMPLICIT REAL*8(A-H,O-Z)
EXTERNAL WWJJ,B3PS,B3
COMMON/D_MP/DHP(5,5,3,3,80,150)/PSI_ETA/DPSI(80),
# DETA(150)/W_W/W_PSI(80),W_ETA(150)

LP2=(LP1-INT(ABS(L-LP))/2
LU2=(LU1-INT(ABS(L-LU))/2

SUM=0.
DO I=1,80
  PSI=1/DPSI(I)

  SUM1=0.
  DO J=1,150
    ETA=DETA(J)
    UK1=0.25D0*UK*DSQRT(PSI**2+6D0*ETA*PSI+ETA**2+8D0)
    Y=0.25D0*((2D0/NP+1D0/NU)*PSI+(2D0/NP-1D0/NU)*ETA)
    SUM2=0.
    DO JP=0,NP-LP-1

      SUM3=0.
      DO JU=0,NU-LU-1
        SUM3=SUM3+B3PS(NU,LU,JU)*(0.5D0*(PSI-ETA))**((LU+JU)*
#WWJJ(4+LP+JP+LU+JU,Y,PK,UK1,LP1,LU1)
      ENDDO

      SUM2=SUM2+B3(NP,LP,JP)*(0.5D0*(PSI-ETA))**((LP+JP)*SUM3
    ENDDO

    SUM1=SUM1+(PSI**2-ETA**2-2*(PSI-ETA))*SUM2*W_ETA(J)*
#DHP(LP+1,LP2+1,LU+1,LU2+1,I,J)
    ENDDO

    SUM=SUM+SUM1/DPSI(I)**2*W_PSI(I)
  ENDDO

  FFSS_PU=0.5D0**2.5D0*PK*UK*SUM
  RETURN
END

C *****
C *PFCS_PU(..)=<NP LP;L LP LP1;C|K-E|NU LU;L LU LU1;S> *
C *****

```

```

C##### Descriptions #####
C Input---L: total angular momentum of the system
C           NP,LP,LPI: quantum numbers of H channel p, with the spherical Bessel
C           NU,LU,LUI: quantum numbers of Ps channel U,with the spherical Neumann
C           PK,UK:    momenta of the positron and positronium
C
C Callings--
C     WJN: sub of an integration related to a spherical Bessel and a modified
C           Neumann functions
C     B3 and B3PS: coeffs of H and Ps physical states
C
C Common Blocks--
C     DHP: the angular integration between Ps and H channels
C     DPSI,W_PSI: Gaussian nodes and weights of the spheroidal coordinate (psi)
C     DETA,W_ETA: Gaussian nodes and weights of the spheroidal coordinate (eta)
C
C#####
FUNCTION FFCS_PU(PK,UK,L,NP,LP,LPI,NU,LU,LUI,BETA)
IMPLICIT REAL*8(A-H,O-Z)
EXTERNAL WJN,B3,B3PS
COMMON/D_HP/DHP(5,5,3,3,80,150)/PSI_ETA/DPSI(80),
# DETA(150)/W_W/W_PSI(80),W_ETA(150)/D_BINC/DBINC(21,21)

LP2=(LPI-INT(ABS(L-LP)))/2
LU2=(LUI-INT(ABS(L-LU)))/2

SUM=0.
DO I=1,80
PSI=1/DPSI(I)

SUM1=0.
DO J=1,150
ETA=DETA(J)
UK1=0.25D0*UK*DSQRT(PSI**2+6D0*ETA*PSI+ETA**2+8D0)
Y=0.25D0*((2D0/NP+1D0/NU)*PSI+(2D0/NP-1D0/NU)*ETA)
SUM2=0.
DO JP=0,NP-LP-1

SUM3=0.
DO JU=0,NU-LU-1

SUM3=SUM3+B3PS(NU,LJ,JU)*(0.5D0*(PSI-ETA))**2*(LU+JU)*
#WJN(4+LP+JP+LU+JU,Y,UK1,BETA,PK,LUI,LPI)
ENDDO

SUM2=SUM2+B3(NP,LP,JP)*(0.5D0*(PSI+ETA))**2*(LP+JP)*SUM3
ENDDO

SUM1=SUM1+(PSI**2-ETA**2-2*(PSI-ETA))*SUM2*W_ETA(J)*
#DHP(LP+1,LP2+1,LU+1,LU2+1,I,J)
ENDDO

SUM=SUM+SUM1/DPSI(I)**2*W_PSI(I)
ENDDO

FFCS_PU=-0.5D0**2.5D0*PK*UK*SUM
RETURN
END

C ***** FFCS_UP(..)=<NU LU;L LU LUI;C|H-E|NP LP;L LP LPI;S> *
C
C##### Descriptions #####
C Input---L: total angular momentum of the system
C           NP,LP,LPI: quantum numbers of H channel p, with the spherical Neumann
C           NU,LU,LUI: quantum numbers of Ps channel U,with the spherical Bessel
C           PK,UK:    momenta of the positron and positronium
C
C Callings--
C     WJN: sub of an integration related to a spherical Bessel and a modified
C           Neumann functions
C     B3 and B3PS: coeffs of H and Ps physical states
C
C Common Blocks--
C     DHP: the angular integration between Ps and H channels
C     DPSI,W_PSI: Gaussian nodes and weights of the spheroidal coordinate (psi)
C     DETA,W_ETA: Gaussian nodes and weights of the spheroidal coordinate (eta)

```

```

C
C#####
FUNCTION FFCS_UP(UK,PK,L,NU,LU,LUI,NP,LP,LP1,GAMMA)
IMPLICIT REAL*8(A-H,O-Z)
EXTERNAL WJN,B3,B3PS
COMMON/D_HP/DHP(5,5,3,3,80,150)/PSI_ETA/DPSI(80),
# DETA(150)/W_W/W_PSI(80),W_ETA(150)/D_BINC/DBINC(21,21)

LP2=(LP1-INT(ABS(L-LP)))/2
LU2=(LUI-INT(ABS(L-LU)))/2

SUM=0.
DO I=1,80
PSI=1/DPSI(I)

SUM1=0.
DO J=1,150
ETA=DETA(J)
X=DSQRT(PSI**2+6D0*ETA*PSI+ETA**2+8D0)
UK1=0.25D0*UK*X
GAM=0.25D0*GAMMA*X
Y=0.25D0*((2D0/NP+1D0/NU)*PSI+(2D0/NP-1D0/NU)*ETA)
SUM2=0.
DO JP=0,NP-LP-1

SUM3=0.
DO JU=0,NU-LU-1

SUM3=SUM3+B3PS(NU,LU,JU)*(0.5D0*(PSI-ETA))**(LU+JU)*
#WJN(4+LP+JP+LU+JU,Y,PK,GAM,UK1,LP1,LUI)
ENDDO

SUM2=SUM2+B3(NP,LP,JP)*(0.5D0*(PSI+ETA))**(LP+JP)*SUM3
ENDDO

SUM1=SUM1+(PSI**2-ETA**2-2*(PSI+ETA))*SUM2*W_ETA(J)*
#DHP(LP+1,LP2+1,LU+1,LU2+1,I,J)
ENDDO

SUM=SUM+SUM1/DPSI(I)**2*W_PSI(I)
ENDDO

FFCS_UP=-0.5D0**2.5D0*PK*UK*SUM
RETURN
END

*****+
C *FFCC_PU(..)=<NP LP;L LP LP1;C|H-E|NU LU;L LU LUI;C> *
C ****+
C##### Descriptions #####
C
C Input---L: total angular momentum of the system
C          NP,LP,LP1: quantum numbers of H channel p, with the spherical Neumann
C          NU,LU,LUI: quantum numbers of Ps channel U,with the spherical Neumann
C          PK,UK:      momenta of the positron and positronium
C
C Callings--
C     B3 and B3PS: coeffs of H and Ps physical states
C
C Common Blocks--
C     DHP: the angular integration between Ps and H channels
C     DPSI,W_PSI: Gaussian nodes and weights of the spheroidal coordinate (psi)
C     DETA,W_ETA: Gaussian nodes and weights of the spheroidal coordinate (eta)
C
C#####
FUNCTION FFCC_PU(PK,UK,L,NP,LP,LP1,NU,LU,LUI,BETA,GAMMA)
IMPLICIT REAL*8(A-H,O-Z)
EXTERNAL FF_N,BESSELN,B3,B3PS
COMMON/D_HP/DHP(5,5,3,3,80,150)/PSI_ETA/DPSI(80),
# DETA(150)/W_W/W_PSI(80),W_ETA(150)/GAUS/QX(354),QW(354)

LP2=(LP1-INT(ABS(L-LP)))/2
LU2=(LUI-INT(ABS(L-LU)))/2

SUM=0.
DO I=1,80
PSI=1/DPSI(I)

SUM1=0.

```

```

DO J=1,150
ETA=DETA(J)
XXX=DSQRT(PSI**2+6D0*ETA*PSI+ETA**2+8D0)
UK1=0.25D0*UK*XXX
GAM=0.25D0*GAMMA*XXX
Y=0.25D0*((2D0/NP+1D0/NU)*PSI+(2D0/NP-1D0/NU)*ETA)
SUM2=0.
DO JP=0,NP-LP-1

SUM3=0.
DO JU=0,NU-LU-1

NN=5+LP+JP+LU+JU
SUM4=0.
DO K=1,354
    SSS=SUM4
    X=QX(K)
    SUM4=SUM4+X**NN*DEXP(-Y*X)*(FF_N(LP1,BETA,PK,X)+  

#(1-2/(PSI-ETA))/X*BESSELN(2*LP1+1,LP1,BETA,PK,X))  

#BESSELN(2*LU1+1,LU1,GAM,UK1,X)*QW(K)
    IF(SUM4 .NE. 0.)THEN
        IF(ABS(1-SUM4/SSS) .LE. 1D-15 .AND. K .GE. 30)GO TO 4031
    ENDIF
ENDDO

4031 SUM3=SUM3+B3PS(NU,LU,JU)*(0.5D0*(PSI-ETA))**((LU+JU)*SUM4
ENDDO

SUM2=SUM2+B3(NP,LP,JP)*(0.5D0*(PSI-ETA))**((LP+JP)*SUM3
ENDDO

SUM1=SUM1+(PSI**2-ETA**2)*DNP(LP+1,LP2+1,LU+1,LU2+1,I,J)*SUM2
#*W_ETA(J)
ENDDO

SUM=SUM+SUM1/DPSI(I)**2*W_PSI(I)
ENDDO

FFCC_PU=2D0**(-2.5D0)*PK*UK*SUM
RETURN
END

*****
C * MODIFIED NEUMAN: (1-EXP(-BX))**N n_L(x) *
*****
FUNCTION BESSELN(N,L,B,A,Y)
IMPLICIT REAL*8(A-H,O-Z)
DIMENSION DNJ(15)

X=A**Y
BX=N*DLOG(1-DEXP(-B*Y))
DNJ(1)=DSIN(X)/X
DNJ(2)=-DCOS(X)

DO I=0,L-1
    DNJ(I+3)=(2*I+1)*DNJ(I+2)-X**2*DNJ(I+1)
ENDDO
BESSELN=DEXP(BX-(L+1)*DLOG(X))*DNJ(L+2)

return
end

*****
C *          000
C *WWJJ(N,A,B1,C1,L1,L2)= | dx x^n exp(-ax) j_(L1)(bx) j_(L2)(cx) *
C *          0
*****
C ##### Descriptions #####
C
C Callings-- WJJ: integration with "L1=L12"
C           DWJJ: first derivative with respect to parameter 'a'
C
C##### Descriptions #####
FUNCTION WWJJ(N,A,B1,C1,L1,L2)
IMPLICIT REAL*8(A-H,O-Z)
EXTERNAL WJJ,DWJJ
COMMON/GAUS/QX(354),QW(354)

IF(L11 .LE. L12)THEN
    B=B1
    C=C1

```

```

L1=L11
L2=L12
ELSE
  B=C1
  C=B1
  L1=L12
  L2=L11
ENDIF

IF(L1 .EQ. L2)THEN
  WWJJ=WJJ(N,A,B,C,L1)
ELSEIF(L2 .EQ. L1+1)THEN
  WWJJ=(L2+1)/B*WJJ(N-1,A,B,C,L2)+DWJJ(N-1,A,B,C,L2)
ELSEIF(L2 .EQ. L1+2)THEN
  L=(L1+L2)/2
  WWJJ=-WJJ(N,A,B,C,L-1)+(2*L+1)/C*((L+1)/B*WJJ(N-2,A,B,C,L)+*
#DWJJ(N-2,A,B,C,L))
ENDIF
RETURN
END

*****
*          000
*Wjj(N,A,B,C,L)= | dx x^n exp(-ax) j_(L)(bx) j_(L)(cx) *
*          0
*****


REAL*8 FUNCTION Wjj(N,A,B,C,L)
IMPLICIT REAL*8(A-H,O-Z)
EXTERNAL FLEG2Q
COMMON/D_FACT/DFACT(150)
BC=B*C
X=0.5D0*(A*A+B*B+C*C)/BC

SUM=0
DO I=0,(N-1)/2
  SUM=SUM+(A/BC)**(N-2*I)/DFACT(N-2*I)/DFACT(I+1)*
#(-0.5d0/BC)**I*(X*X-1)**(-0.5D0*(N-I-I))*FLEG2Q(L,N-1-I,X)
ENDDO
WJJ=0.5D0/B/C*SUM*dfact(n)
RETURN
END

*****
*DWjj(N,A,B,C,L)= derivative of Wjj with respect to b *
*****


FUNCTION DWjj(N,A,B,C,L)
IMPLICIT REAL*8(A-H,O-Z)
EXTERNAL FLEG2Q
COMMON/D_FACT/DFACT(150)
X=0.5d0*(A*A+B*B+C*C)/B/C
SUM=0.
DO I=0,(N-1)/2
  SUM=SUM+(-1D0)**I*(B*C/A**2)**I/2**I/DFACT(N-2*I)/DFACT(I+1)
#*(X*X-1)**(-0.5D0*(N-I-I))*((N-I)*DSQRT(X*X-1)*FLEG2Q(L,N-1-I,X)
#+FLEG2Q(L,N-I,X)*(B*B-A*A-C*C)/B/C/2)
ENDDO
DWJJ=-0.5D0/A/B*(A/B/C)**N*DFACT(N)*SUM
RETURN
END

*****
* LEGENDQ(L,M,X) --> THE LEGENDRE FOUNCTION OF THE 2-ND KIND *
*****


REAL*8 FUNCTION FLEG2Q(L,M,X)
IMPLICIT REAL*8(A-H,O-Z)
EXTERNAL GEOF,GAMA,FACT
COMMON/D_FACT/DFACT(150)
FLEG2Q=0.5D0**((L+1)*DFACT(L+M+1)*GAMA(0.5D0)/
&      GAMA(L+1.5D0)/(X*X-1D0)**(0.5D0*M)/X**((L-M+1)*
#      GEOF(0.5D0*(L-M+1),0.5D0*(L-M+2),L+1.5D0,1D0/X**2)
RETURN
END

*****
* bessel function j_(l)(x)   *
*****


FUNCTION BJ(L,X)
IMPLICIT REAL*8(A-H,O-Z)
EXTERNAL GAMA
DIMENSION DBJ(15)

```

```

IF(X .LE. 2D0)THEN
  AK=(0.5D0*X)**L/GAMA(L+1.5D0)
  SUM=AK
  DO K=1,10000
    AK=-AK/K/(L+K+0.5D0)*0.25D0*X*X
    SUM=SUM+AK
    IF(ABS(AK/SUM) .LE. 1D-8)GO TO 1891
  ENDDO
1891  BJ=DSQRT(3.1415926535897932D0)/2*SUM

  ELSE

    DBJ(1)=DCOS(X)/X           !--> j_{-1}(x)
    DBJ(2)=DSIN(X)/X
    DO I=0,L-1
      DBJ(I+3)=(2D0*I+1)/X*DBJ(I+2)-DBJ(I+1)
    ENDDO
    BJ=DBJ(L+2)
    ENDIF

    RETURN
  END

C*****
C*          000
C* Wjn(..)=| dx x**n exp(-ax) j_{[L1]}(ax) (1-exp(-bx)) **(2L2+1)n_{(12(bx)} *
C*          0
C*****


FUNCTION WJN(N,A0,A,B0,B,L1,L2)
IMPLICIT REAL*8(A-H,O-Z)
EXTERNAL BJ,BESSELN
COMMON/GAUS/QX(354),QW(354)

sum=0.
DO I=1,354
  SUM0=SUM
  X=QX(I)
  SUM=SUM+X**N*DEXP(-A0*X)*BJ(L1,A*X)*BESSELN(2*L2+1,L2,
#B0,B,X)*QW(I)
  IF(SUM .NE. 0.)THEN
    IF(ABS(1-SUM0/SUM) .LE. 1D-15)GO TO 4103
    ENDIF
  ENDDO
4103  WJN=SUM
  RETURN
END

REAL*8 FUNCTION WWjn(N,A0,A,B,L1,L2)
IMPLICIT REAL*8(A-H,O-Z)
EXTERNAL WM,WK,UR
1230  SUM=0.
DO M=0,L2/2
  SUM=SUM+WM(L2,M)/B**((2*M)*UR(N-2*M-1,A0,B,A,-L2,L1))
ENDDO
1231  IF (L2) 1234,1234,1232
1232  DO K=0,(L2-1)/2
  SUM=SUM+WK(L2,K)/B**((2*K+1)*UR(N-2*K-2,A0,B,A,-L2-1,L1))
ENDDO
1234  WWjn=(-1)**(L2+1)*SUM/B
  RETURN
END

C*****
C*          000
C* UR(M,A,B,C,L1,L)=| dx x**m exp(-ax) cos(bx-L1*3.1415/2) j_{(1)}(cx) *
C*          0
C*****


REAL*8 FUNCTION UR(M,A,B,C,L1,L)
IMPLICIT REAL*8(A-H,O-Z)
EXTERNAL GAMA,FACT
PI=3.1415926535897932D0
X0=A*A-B*B+C*C
IF (X0 .GE. 0) THEN
  X=DATAN(2D0*A*B/X0)
ELSE
  X=PI-DATAN(2D0*A*B/ABS(X0))
ENDIF
Y=1D0/((A*A-B*B+C*C)**2+(2D0*A*B)**2)
UR1=DSQRT(PI)*(C/2D0)**L*FACT(M+L)/2D0
&   /GAMA(L+1.5D0)*Y**((0.25D0*(M+L+1D0))
A0=0.5D0*(M+L+1D0)
B0=0.5D0*(1D0-M+L)

```

```

C0=L+1.5D0
SUM=DCOS(A0*X-0.5D0*LI*PI)
PIK=1D0
K=1
1211    SUM0=SUM
        K1=K-1

        PIK=PIK*(A0+K1)/K*(B0+K1)/(C0+K1)*C*C*DSQRT(Y)
        SUM=SUM+PIK*DCOS((K+A0)*X-0.5D0*LI*PI)
        K=K+1
        IF (ABS(1D0-SUM0/SUM)-1D-15)1212,1212,1211
1212    UR=URL*SUM
        RETURN
        END

C ****
C *WM(L,M,A)--->COEFF. OF the neuman function   *
C ****
REAL*8 FUNCTION WM(L,M)
IMPLICIT REAL*8(A-H,O-Z)
COMMON/D_FACT/DFACT(150)

WM=(-1d0)**M*DFACT(L+2*M+1)/DFACT(2*M+1)/DFACT(L-2*M+1)
*   /(2d0)**(2*M)
RETURN
END

C ****
C *WK(L,K,A)--->2nd coef. of the neuman function   *
C ****
REAL*8 FUNCTION WK(L,K)
IMPLICIT REAL*8(A-H,O-Z)
COMMON/D_FACT/DFACT(150)

WK=(-1d0)**K*DFACT(L+2*K+2)/DFACT(2*K+2)/DFACT(L-2*K)/
*   (2d0)**(2*K+1)
RETURN
END

C ****
C *H_PQ=<NP LP;L LP LP1 | 1/r2-1/r12 |NQ LQ;L LQ LQ1> *
C ****
FUNCTION H_PQ(NP,LP,LP1,NQ,LQ,LQ1,L,X)
IMPLICIT REAL*8(A-H,O-Z)
EXTERNAL PHI,F6J,CT,B3

H11=0.
APQ=1D0/NP+1D0/NQ
K1=MAX(ABS(LP-LQ),ABS(LP1-LQ1))
K2=MIN(LP+LQ,LP1+LQ1)
DO K=K1,K2,2

SUM1=0.
DO JP=0,NP-LP-1

SUM2=0.
DO JQ=0,NQ-LQ-1
SUM2=SUM2+B3(NQ,LQ,JQ)*PHI(LP+JP+LQ+JQ+1-K,APQ,K,X)
ENDDO

SUM1=SUM1+B3(NP,LP,JP)*SUM2
ENDDO

H11=H11-(-1D0)**(LQ+LP1+L)*CT(LP,K,LQ)*CT(LP1,K
*,LQ1)*F6J(LP,LP1,L,LQ1,LQ,K)*SUM1
ENDDO
H_PQ=H11
RETURN
END

C ****
C *PS_UV(..)=<NU LU;L LU LU1|1/r2-1/r1|NV LV;L LV LV1> *
C ****
FUNCTION PS_UV(NU,LU,LU1,NV,LV,LV1,L,X)
IMPLICIT REAL*8(A-H,O-Z)
EXTERNAL PHI,F6J

AUV=1D0/NU+1D0/NV
K1=MAX(ABS(LU-LV),ABS(LU1-LV1))
K2=MIN(LU+LV,LU1+LV1)
IF((-1)**K1+1 .NE. 0)THEN
  PS_UV=0.
  RETURN
END

```

```

ELSE
  SUM=0.
  DO K=K1,K2,2

    SUM1=0.
    DO JU=0,NU-LU-1

      SUM2=0.
      DO JV=0,NV-LV-1
        SUM2=SUM2+2D0**((LU+JU+LV+JV+4)*PHI(LU+JU+LV+JV+1-K,AUV,K,X))
      *B3PS(NV,LV,JV)
      ENDDO

      SUM1=SUM1+B3PS(NU,LU,JU)*SUM2
    ENDDO

    SUM=SUM+CT(LU,K,LV)*CT(LU1,K,LV1)*F6J(LU,LU1,L,
#LV1,LV,K)*SUM1
    ENDDO

  PS_UV=(-1D0)*(LV+LU1+L)*SUM
ENDIF
RETURN
END

C *****
C      000
C      *PHI(N,A,K,X) = |dr r**(n+k+1) exp(-ar) r<**k/r>**(k+1) *
C      0
C *****
FUNCTION PHI(N,A,K,X)
IMPLICIT REAL*8(A-H,O-Z)
COMMON/D_FACT/DFACT(150)/D_BINC/dbinc(21,21)
S11=DFACT(N+2*K+2)/A**(N+2*K+2)

IF(K .EQ. 0)THEN
SUM=0d0
ELSE
SUM=1d0
ENDIF

DO I=0,N+2*K
SUM=SUM-(A*X)**I/DFACT(I+1)*DEXP(-A*X)
ENDDO

SUM=S11*SUM/X**(K+1)
DO J=0,N-1
SUM=SUM+DBINC(N+1,J+1)*DFACT(N-J+1)/A** (N+1-J)*X** (K+J) *
#DEXP(-A*X)
ENDDO

PHI=SUM
RETURN
END

C ##### The following is to calculate free-bound matrix elements #####
C      * < PSEUDO_Q,J; Bound of H | H-E | H;NP,LP,LP1,L; free of H> *
C *****

C ##### Descriptions #####
C
C Input-- NP,LP,LP1,L: quantum numbers of a H channel P with the Bessel free
C           function of the positron
C           PK: positron momentum in channel P
C           IP: channel number of hydrogen from 0 to 9, which specifies a bound
C           wavefunction of hydrogen
C           N2I,A2I,L2I: parameters of the positron wavefunction in the H bound
C           channel IP
C
C Calling--
C           FBS_HJP(...): bound-free matrix element with a Slater orbital as a bound
C           function of hydrogen
C
C Common Block--
C           H_PS_DATA, N_H_PS: details of the 18-state channel wavefunctions
C
C #####

```

```

FUNCTION FBS_QP(PK,IP,N2I,A2I,L2I,NP,LP,LP1,L)
IMPLICIT REAL*8(A-H,O-Z)
EXTERNAL FBS_HJP
COMMON/E_18/EH(9),EPS(9)/H_PS_DATA/AHJ(9,4),CHJ(9,4),APSJ(9,4),
#CPSJ(9,4)/N_H_PS/NHJ(9,4),LHJ(9),NPSJ(9,4),LPSJ(9)

IF(IP .EQ. 1 .AND. L2I .EQ. LP1)THEN
  FBS1=VV(N2I,LP1,A2I,PK)           !only for physical and pseudostate
ELSE                               !calculation and HIs open
  FBS1=0.
ENDIF
  FBS1=PK*FBS1*B44(N2I,A2I)

SUM=0.
DO I=1,4

  IF(CHJ(IP,I) .NE. 0.)THEN
    SUM=SUM+CHJ(IP,I)*FBS_HJP(PK,NHJ(IP,I),AHJ(IP,I),N2I,A2I,
#LHJ(IP),L2I,NP,LP,LP1,L)
  ENDIF

ENDDO
FBS_QP=SUM +FBS1
RETURN
END

*****
* < H; J | H-E | H; NP LP LP1,L >
*****

C##### Descriptions #####
C
C Input--N1J,A1J,N2J,A2J,L1J,L2J: parameters in bound slater orbitals of the
C                                electron and positron
C      NP,LP,LP1,L: quantum numbers of the free channel P of hydrogen
C      PK:          positron momentum
C Calling--
C      VV: integration related to one spherical Bessel function
C      GJ: integration related to one spherical Bessel function and interaction
C      F6J: six J symbol
C      B4: normalization factor of a Slater orbital
C      B3: coeffs of hydrogen physical wavefunction
C#####

FUNCTION FBS_HJP(PK,N1J,A1J,N2J,A2J,L1J,L2J,NP,LP,LP1,L)
IMPLICIT REAL*8(A-H,O-Z)
EXTERNAL VV,GJ,F6J,B4,B3

K1=MAX(ABS(L1J-LP),ABS(L2J-LP1))
K2=MIN(L1J+LP,L2J+LP1)
SUM=0.
DO K=K1,K2,2

  SUM1=0.
  DO JP=0,NP-LP-1
    SUM1=SUM1+B3(NP,LP,JP)*GJ(N2J+1,A2J,PK,LP1,N1J+LP+JP-K,
#A1J+1D0/NP,K)
  ENDDO

  SUM=SUM+CT(L1J,K,LP)*CT(L2J,K,LP1)*
#F6J(L1J,L2J,L,LP1,LP,K)*SUM1
  ENDDO

  FBS_HJP=PK*(-(-1D0)**(LP+L2J+L)*SUM)*B44(N1J,A1J)*B44(N2J,A2J)

  RETURN
END

*****
* <PS; V,J| H-E| Ps; NU LU LU1,L>
*****



C##### Descriptions #####
C
C Input-- NU,LU,LU1,L: quantum numbers of a Ps channel U with the Bessel free
C                                function of the positronium
C      UK: positronium momentum in channel U
C      JV: channel number of Ps from 0 to 9, which specifies a bound
C            wavefunction of Ps

```

```

C      N4J,A4J,L4J: parameters of the positronium wavefunction in the Ps
C      bound channel JV
C
C Calling--
C      FBS_PSJU(..): bound-free matrix element with a Slater orbital as a bound
C      function of Ps
C
C Common Block--
C      H_PS_DATA, N_H_PS: details of the 18-state channel wavefunctions
C
C#####
C
FUNCTION FBS_VU(UK,JV,N4J,A4J,L4J,NU,LU,LU1,L)
IMPLICIT REAL*8(A-H,O-Z)
EXTERNAL FBS_PSJU
COMMON/E_18/EH(9),EPS(9)/H_PS_DATA/AHJ(9,4),CHJ(9,4),APSJ(9,4),
#CPSJ(9,4)/N_H_PS/NHJ(9,4),LHJ(9),NPSJ(9,4),LPSJ(9)

SUM=0.
DO J=1,4
  IF(CPSJ(JV,J) .NE. 0.)THEN
    SUM=SUM+CPSJ(JV,J)*FBS_PSJU(UK,NPSJ(JV,J),APSJ(JV,J),
#N4J,A4J,LPSJ(JV),L4J,NU,LU,LU1,L)
  ENDIF
ENDDO
FBS_VU=SUM
RETURN
END

C#####
C      * <Ps; J | H-E | Ps; NU LU LU1, L>
C#####

C#####
C Descriptions #####
C
C Input--N3J,A3J,N4J,A4J,L3J,L4J: parameters in bound slater orbitals of the
C      Ps and mass center of Ps
C      NU,LU,LU1,L: quantum numbers of the free channel U of Ps
C      UK: positronium momentum
C Calling--
C      GJ: integration related to one spherical Bessel function and
C      interaction
C      F6J: six J symbol
C      B4: normalization factor of a Slater orbital
C      B3PS: coeffs of Ps physical wavefunction
C
C#####
C
FUNCTION FBS_PSJU(UK,N3J,A3J,N4J,A4J,L3J,L4J,NU,LU,LU1,L)
IMPLICIT REAL*8(A-H,O-Z)
EXTERNAL F6J,GJ,B4,B3PS

K1=MAX(ABS(LU-L3J),ABS(LU1-L4J))
K2=MIN(LU+L3J,LU1+L4J)
IF(K1/2**2 .EQ. K1)THEN
  FBS_PSJU=0
  RETURN
ELSE
  SUM=0.
  DO K=K1,K2,2
    SUM1=0.
    DO JU=0,NU-LU-1
      SUM1=SUM1+B3PS(NU,LU,JU)*2D0** (N3J+LU+JU+2)*GJ(N4J+1,A4J,UK,LU1,
#N3J+LU+JU-K,2*A3J+1D0/NU,K)
    ENDDO
    SUM=SUM+CT(L3J,K,LU)*CT(L4J,K,LU1)*F6J(L3J,L4J,
#L,LU1,LU,K)*SUM1
  ENDDO
  FBS_PSJU=2**1.5D0*UK*(-1D0)** (LU+L4J+L)*SUM*B44(N3J,A3J)*B44(N4J,A4J)
  ENDIF
  RETURN
END

C#####
C      * < Ps; i, | H - E | H; NP LP LPI, L >
C#####

```

```

C##### Descriptions #####
C Input-- NP,LP,LPI,L: quantum numbers of a H channel P with the Bessel free
C function of the positron
C PK: positron momentum in channel P
C IU: channel number of Ps from 0 to 9, which specifies a bound
C wavefunction of Ps
C N4I,A4I,L4I: parameters of the positronium wavefunction in the Ps
C bound channel IU
C
C Calling--
C     PBS_PSJP(..): bound-free matrix element with a Slater orbital as a
C     bound function of Ps
C
C Common Block--
C     H_PS_DATA, N_H_PS: details of the 18-state channel wavefunctions
C
C#####
FUNCTION PBS_UIP(PK,IU,N4I,A4I,L4I,NP,LP,LPI,L)
IMPLICIT REAL*8(A-H,O-Z)
EXTERNAL PBS_PSJP
COMMON/E_18/EH(9),EPS(9)/H_PS_DATA/AHJ(9,4),CHJ(9,4),APSJ(9,4),
#CPSJ(9,4)/N_H_PS/NHJ(9,4),LHJ(9),NPSJ(9,4),LPSJ(9)

SUM=0.
DO I=1,4

IF (CPSJ(IU,I) .NE. 0.)THEN
SUM=SUM+CPSJ(IU,I)*PBS_PSJP(PK,NPSJ(IU,I),APSJ(IU,I),N4I,A4I,
#LPSJ(IU),L4I,NP,LP,LPI,L)
ENDIF

ENDDO
FBS_UIP=SUM
RETURN
END

*****
C     <Ps ; J | H-E | H; NP LP LPI, L >
*****
C#####
C Descriptions #####
C Input--N3J,A3J,N4J,A4J,L3J,L4J: parameters in bound slater orbitals of the
C positron and positronium
C     NP,LP,LPI,L: quantum numbers of the free channel P of hydrogen
C     PK: positron momentum
C Calling--
C     VV: integration related to one spherical Bessel function
C     B4: normalization factor of a Slater orbital
C     B3: coeffs of hydrogen physical wavefunction
C
C Common Block--
C     DHP(..): angular integration between Ps and H channels
C     DPSI,W_PSI: Gaussian nodes and weights of the spheroidal coordinate (psi)
C     DETA,W_ETA: Gaussian nodes and weights of the spheroidal coordinate (eta)
C
C#####
FUNCTION PBS_PSJP(PK,N3J,A3J,N4J,A4J,L3J,L4J,NP,LP,LPI,L)
IMPLICIT REAL*8(A-H,O-Z)
EXTERNAL VV,B4,B3
COMMON/D_HP/DHP(5,5,3,3,80,150)
#/PSI_ETA/DPSI(80),DETA(150)/W_W/W_PSI(80),W_ETA(150)
#/D_FACT/DFACT(150)

LP2=(LPI-INT(ABS(L-LP)))/2
L4J2=(L4J-INT(ABS(L-L3J)))/2

SUM=0.
DO I=1,80
PSI=1/DPSI(I)

SUM1=0.
DO J=1,150
ETA=DETA(J)

X=DSQRT(PSI**2+6D0*ETA*PSI+ETA**2+8D0)
Y=0.5D0*(PSI-ETA)*A3J+0.5D0*(PSI+ETA)/NP+0.25D0*A4J*X

```

```

SUM2=0.
DO JP=0,NP-LP-1
SUM2=SUM2+B3(NP,LP,JP)*(0.5D0*(PSI+ETA))**2*(LP+JP)*
#VV(2+N3J+N4J+LP+JP,LPI,Y,PK)
ENDDO

SUM1=SUM1+SUM2*((PSI-ETA)/2)**2*(N3J-1)*(X/4)**2*(N4J-1)*
#(1-2/(PSI-ETA))*DHP(LP+1,LP2+1,L3J+1,L4J2+1,I,J)*(PSI**2-ETA**2)
#*W_ETA(J)
ENDDO

SUM=SUM+SUM1/DPSI(I)**2*W_PSI(I)
ENDDO

FBS_PSJP=0.125D0*PK*B44(N3J,A3J)*B44(N4J,A4J)*SUM
RETURN
END

***** < H; P(pseudo) | H-E | PS; NU LU LUI,L > ****
***** Descriptions *****
C Input-- NU,LU,LUI,L: quantum numbers of a Ps channel U with the Bessel free
C function of the positron
C UK: positronium momentum in channel U
C IP: channel number of H from 0 to 9, which specifies a bound
C wavefunction of H
C N2I,A2I,L2I: parameters of the positron wavefunction in the H bound
C channel IP
C Calling--
C     FBS_HJU(..): bound-free matrix element with a Slater orbital as a bound
C function of H
C Common Block--
C     H_PS_DATA, N_H_PS: details of the 18-state channel wavefunctions
C **** Descriptions *****
FUNCTION FBS_PIU(UK,IP,N2I,A2I,L2I,NU,LU,LUI,L)
IMPLICIT REAL*8(A-H,O-Z)
EXTERNAL FBS_HJU
COMMON/E_18/EH(9),EPS(9)/H_PS_DATA/AHJ(9,4),CHJ(9,4),APSJ(9,4),
#CPSJ(9,4)/N_H_PS/NHJ(9,4),LHJ(9),NPSJ(9,4),LPSJ(9)

SUM=0.
DO I=1,4
IF(CHJ(IP,I).NE.0.)THEN
SUM=SUM+CHJ(IP,I)*FBS_HJU(UK,NHJ(IP,I),AHJ(IP,I),N2I,A2I,
#LHJ(IP),L2I,NU,LU,LUI,L)
ENDIF

ENDDO
PBS_PIU=SUM
RETURN
END

***** < H ;J | H-E | PS; NU LU LUI,L > ****
***** Descriptions *****
C Input--N1J,A1J,N2J,A2J,L1J,L2J: parameters in bound slater orbitals of the
C electron and Ps
C NU,LU,LUI,L: quantum numbers of the free channel U of Ps
C UK: positronium momentum
C Calling--
C VV: integration related to one spherical Bessel function
C B4: normalization factor of a Slater orbital
C B3PS: coeffs of Ps physical wavefunction
C **** Descriptions *****
FUNCTION PBS_HJU(UK,N1J,A1J,N2J,A2J,L1J,L2J,NU,LU,LUI,L)
IMPLICIT REAL*8(A-H,O-Z)
EXTERNAL VV,B4,B3PS

```

```

COMMON/D_HP/DHP(5,5,3,3,80,150)
# /PSI_ETA/DPSI(80),DETA(150)/W_W/W_PSI(80),W_ETA(150)
# /D_FACT/DFACT(150)

L2J2=(L2J-INT(ABS(L-L1J)))/2
LU2=(LU1-INT(ABS(L-LU)))/2

SUM=0.
DO I=1,80
PSI=1/DPSI(I)

SUM1=0.
DO J=1,150
ETA=DETA(J)

X=DSQRT(PSI**2+6D0*ETA*PSI+ETA**2+8D0)
Y=0.5D0*(PSI+ETA)*A1J+A2J+0.25D0/NU*(PSI-ETA)
UK1=0.25D0*UK*X

SUM2=0.
DO JU=0,NU-LU-1

SUM2=SUM2+B3PS(NU,LU,JU)*(0.5D0*(PSI-ETA))**2*(LU+JU)
#*VV(2+N1J+N2J+LU+JU,LU1,Y,UK1)
ENDDO

SUM1=SUM1+SUM2*(PSI**2-ETA**2-2*(PSI-ETA))*((PSI+ETA)/2)**2
#(N1J-1)*DHP(L1J+1,L2J2+1,LU+1,LU2+1,I,J)*W_ETA(J)
ENDDO

SUM=SUM+SUM1/DPSI(I)**2*W_PSI(I)
ENDDO

FBS_HJU=0.125D0*2**0.5D0*UK*B44(N1J,A1J)*B44(N2J,A2J)*SUM
RETURN
END

*****
* <H; Q,J| H-E | H;NP LP LP1,L;>*
*****

C##### Descriptions #####
C
C Input-- NP,LP,LP1,L: quantum numbers of a H channel P with the Neumann free
C function of the positron
C PK: positron momentum in channel P
C IP: channel number of hydrogen from 0 to 9, which specifies a bound
C wavefunction of hydrogen
C N2I,A2I,L2I: parameters of the positron wavefunction in the H bound
C channel IP
C
C Callings--
C     FBC_HJP(...): bound-free matrix element with a Slater orbital as a
C     bound function of hydrogen
C
C Common Block--
C     H_PS_DATA, N_H_PS: details of the 18-state channel wavefunctions
C
FUNCTION FBC_QP(PK,JQ,N2J,A2J,L2J,NP,LP,LP1,L,BETA)
IMPLICIT REAL*8(A-H,O-Z)
EXTERNAL FBC_HJP
COMMON/E_18/ER(9),EPS(9)/H_PS_DATA/AHJ(9,4),CHJ(9,4),APSJ(9,4),
#CPSJ(9,4)/N_H_PS/NHJ(9,4),LHJ(9),NPSJ(9,4),LPSJ(9)

IF(JQ .EQ. 1 .AND. L2J .EQ. LP1)THEN
    FBC1=-0.5D0*(PK*PK+A2J*A2J)*VV1(N2J+1,LP1,A2J,BETA,PK) +
#0.5D0*(L2J*(L2J+1)-N2J*(N2J-1))*VV1(N2J-1,LP1,A2J,BETA,PK) +
#(A2J*N2J+1)*VV1(N2J,LP1,A2J,BETA,PK)
ELSE
    FBC1=0.
ENDIF
FBC2=-PK*B44(N2J,A2J)*FBC1

SUM=0.
DO J=1,4

IF(CHJ(JQ,J) .NE. 0.)THEN
    SUM=SUM+CHJ(JQ,J)*FBC_HJP(PK,NHJ(JQ,J),AHJ(JQ,J),N2J,A2J
#,LHJ(JQ),L2J,NP,LP,LP1,L,BETA)

```

```

ENDIF

ENDDO
FBC_QP=SUM+FBC2
RETURN
END

C **** < H; J | H-E | H;NP LP LP1,L > ****
C **** *****

C##### Descriptions #####
C Input--N1J,A1J,N2J,A2J,L1J,L2J: parameters in bound slater orbitals of the
C electron and positron
C NP,LP,LP1,L: quantum numbers of the free channel P of hydrogen
C PK: positron momentum
C BETA: Parameter in the factor before Neumann function
C
C Calling--
C   VV1: integration related to one spherical Neumann function
C   GN: integration related to one spherical Neumann function and interaction
C   F6J: six J symbol
C   B4: normalization factor of a Slater orbital
C   B3: coeffs of hydrogen physical wavefunction
C
C#####
FUNCTION FBC_HJP(PK,N1J,A1J,N2J,A2J,L1J,L2J,NP,LP,LP1,L,BETA)
IMPLICIT REAL*8(A-H,O-Z)
EXTERNAL F6J,GN,B4,VV1,B3

K1=MAX(ABS(L1J-LP),ABS(L2J-LP1))
K2=MIN(ABS(L1J+LP),ABS(L2J+LP1))

SUM=0.
DO K=K1,K2,2

SUM1=0.
DO JP=0,NP-LP-1
SUM1=SUM1+B3(NP,LP,JP)*GN(N2J+1,A2J,PK,LP1,N1J+LP+JP-K,
#A1J+1D0/NP,K,BETA)
ENDDO

SUM=SUM+(-1D0)**(LP+L2J+L)*CT(L1J,K,LP)*CT(L2J,K,
#LP1)*F6J(L1J,L2J,L,LP1,LP,K)*SUM1
ENDDO

FBC_HJP=-PK*B44(N1J,A1J)*B44(N2J,A2J)*(-SUM)
RETURN
END

C **** < PS; JV(pseudo) | H-E | PS; NU LU LU1,L,C > ****
C **** *****

C##### Descriptions #####
C Input-- NU,LU,LU1,L: quantum numbers of a Ps channel U with the Neumann free
C function of the positronium
C UK: positronium momentum in channel U
C JV: channel number of Ps from 0 to 9, which specifies a bound
C wavefunction of Ps
C N4J,A4J,L4J: parameters of the positronium wavefunction in the Ps
C bound channel JV
C GAMMA: parameter in the factor before the Neumann function
C
C Calling--
C   FBC_PSJU(..): bound-free matrix element with a Slater orbital as a
C   bound function of Ps
C
C Common Block--
C   H_PS_DATA, N_H_PS: details of the 18-state channel wavefunctions
C
C#####
FUNCTION FBC_VU(UK,JV,N4J,A4J,L4J,NU,LU,LU1,L,GAMMA)
IMPLICIT REAL*8(A-H,O-Z)
EXTERNAL FBC_PSJU
COMMON/E_18/EH(9),EPS(9)/H_PS_DATA/AHJ(9,4),CHJ(9,4),APSJ(9,4),

```

```

#CPSJ(9,4)/N_H_PS/NHJ(9,4),LHJ(9),NPSJ(9,4),LPSJ(9)

      SUM=0.

      DO J=1,4
      IF(CPSJ(JV,J) .NE. 0.)THEN
      SUM=SUM+CPSJ(JV,J)*FBC_PSJU(UK,NPSJ(JV,J),APSJ(JV,J),N4J,A4J
      ,LPSJ(JV),L4J,NU,LU,LU1,L,GAMMA)
      ENDIF

      ENDDO
      FBC_VU=SUM+FBC2
      RETURN
      END

*****
C   * < PS; J | H-E | PS; NU LU LU1,L> *
*****
C##### Descriptions #####
C
C Input--N3J,A3J,N4J,A4J,L3J,L4J: parameters in bound slater orbitals of the
C           Ps and mass center of Ps
C       NU,LU,LU1,L: quantum numbers of the free channel U of Ps with the Neumann
C           UK:          positronium momentum
C
C Calling--
C     FACT: factorial function
C     VV1: integration related to one spherical Neumann function
C     GN: integration related to one spherical Neumann function and interaction
C     F6J: six J symbol
C     B4: normalization factor of a Slater orbital
C     B3PS: coeffs of Ps physical wavefunction
C
C#####
FUNCTION FBC_PSJU(UK,N3J,A3J,N4J,A4J,L3J,L4J,NU,LU,LU1,L,GAMMA)
IMPLICIT REAL*8(A-H,O-Z)
EXTERNAL P6J,GN,B4,VV1,FACT,B3PS

      K1=MAX(ABS(L3J-LU),ABS(L4J-LU1))
      K2=MIN(ABS(L3J+LU),ABS(L4J+LU1))
      IF(L3J.EQ.LU .AND. L4J.EQ.LU1)THEN
      FBC1=-0.25D0*(A4J*UK*UK)*VV1(N4J+1,LU1,A4J,GAMMA,UK)
      #+0.25D0*(L4J*(L4J+1)-N4J*(N4J-1))*VV1(N4J-1,LU1,A4J,GAMMA,UK)
      #+0.5D0*A4J*N4J*VV1(N4J,LU1,A4J,GAMMA,UK)
      SS=0.
      DO JU=0,NU-LU-1
      SS=SS+B3PS(NU,LU,JU)*FACT(N3J+LU+JU+1)/
      #(A3J+0.5D0/NU)**(N3J+LU+JU+2)
      ENDDO
      FBC2=FBC1*SS
      ELSE
      FBC2=0.
      ENDIF

      SUM=0.
      IF(K1/2*2.NE.K1)THEN
      DO K=K1,K2,2

      SUM1=0.
      DO JU=0,NU-LU-1
      SUM1=SUM1+B3PS(NU,LU,JU)*2D0**((N3J+LU+JU+3)*
      #GN(N4J+1,A4J,UK,LU1,N3J+LU+JU-K,2*A3J+1D0/NU,K,GAMMA)
      ENDDO

      SUM=SUM+CT(L3J,K,LU)*CT(L4J,K,LU1)*P6J(
      #L3J,L4J,L,LU1,LU,K)*SUM1
      ENDDO
      ENDIF

      FBC_PSJU=-2D0**0.5D0*UK*(FBC2+(-1D0)**(LU+L4J+L)*SUM)
      #*B44(N3J,A3J)*B44(N4J,A4J)
      RETURN
      END

*****
C   * <PS;J,V(pseudo)| H-E| H; NP LP LP1,L;C> *
*****
C##### Descriptions #####
C

```

```

C Input-- NP,LP,LPI,L: quantum numbers of a H channel P with the Neumann free
C                           function of the positronium
C   PK: positron momentum in channel P
C   JV: channel number of Ps from 0 to 9, which specifies a bound
C         wavefunction of Ps
C   N4I,A4J,L4I: parameters of the positronium wavefunction in the Ps
C                   bound channel JV
C   beta: parameter in the factor before the Neumann function
C
C Calling--
C   FBC_PSJP(..): bound-free matrix element with a Slater orbital as a
C                   bound function of Ps
C
C Common Block--
C   H_PS_DATA, N_H_PS: details of the 18-state channel wavefunctions
C
C#####
C
FUNCTION FBC_VJP(PK,JV,N4J,A4J,L4J,NP,LP,LPI,L,beta)
IMPLICIT REAL*8(A-H,O-Z)
EXTERNAL FBC_PSJP
COMMON/E_18/EH(9),EPS(9)/H_PS_DATA/AHJ(9,4),CHJ(9,4),APSJ(9,4),
#CPSJ(9,4)/N_H_PS/NHJ(9,4),LHJ(9),NPSJ(9,4),LPSJ(9)
SUM=0.
DO J=1,4
  IF(CPSJ(JV,J) .NE. 0.)THEN
    SUM=SUM+CPSJ(JV,J)*FBC_PSJP(PK,NPSJ(JV,J),APSJ(JV,J),N4J,A4J
    #,LPSJ(JV),L4J,NP,LP,LPI,L,beta)
  ENDIF
ENDDO
FBC_VJP=SUM
RETURN
END
*****
* < Ps; J | H-E | H; NP LP LPI, L > *
*****
C#####
C Descriptions #####
C
C Input--N3J,A3J,N4J,A4J,L3J,L4J: parameters in bound slater orbitals of the
C                                     positron and positronium
C   NP,LP,LPI,L: quantum numbers of the free channel P of hydrogen with
C                 the Neumann function
C   PK:           positron momentum
C   beta: parameter in the factor before the Neumann function
C Calling--
C   VV1: integration related to one spherical Neumann function
C   B4: normalization factor of a Slater orbital
C   B3: coeffs of hydrogen physical wavefunction
C
C Common Block--
C   DHP(..): angular integration between Ps and H channels
C   DPSI_W_PSI: Gaussian nodes and weights of the spheroidal coordinate (psi)
C   DETA_W_ETA: Gaussian nodes and weights of the spheroidal coordinate (eta)
C
C#####
C
FUNCTION FBC_PSJP(PK,N3J,A3J,N4J,A4J,L3J,L4J,NP,LP,LPI,L,beta)
IMPLICIT REAL*8(A-H,O-Z)
EXTERNAL VV1,B4,B3
COMMON/D_MP/DHP(5,5,3,3,80,150)
#/PSI_ETA/DPSI(80),DETA(150)/W_W/W_PSI(80),W_ETA(150)
#/D_FACT/DFACT(150)

WW=0.5D0/NP**2-0.5D0*PK**2-A3J*A3J-0.25D0*A4J*A4J
A11=L3J*(L3J+1)-N3J*(N3J-1)
A12=L4J*(L4J+1)-N4J*(N4J-1)

L4J2=(L4J-INT(ABS(L-L3J)))/2
LP2=(LPI-INT(ABS(L-LP)))/2

SUM=0.
DO I=1,80
  PSI=1/DPSI(I)

  SUM1=0.
  DO J=1,150
    ETA=DETA(J)

```

```

X=DSQRT(PSI**2-6D0*ETA*PSI+ETA**2+8D0)
Y=0.5D0*(PSI-ETA)*A3J+0.5D0*(PSI+ETA)/NP+0.25D0*A4J*X
A1=A11*(2/(PSI-ETA))**2+0.25D0*A12*(4/X)**2
B1=(2*A3J*N3J-1)**2/(PSI-ETA)+A4J*N4J**2/X+1-2/(PSI+ETA)

SUM2=0.
DO JP=0,NP-LP-1

  SUM2=SUM2+B3(NP,LP,JP)*((PSI+ETA)/2)**(LP+JP)*(A1*
#VV1(1+N3J+N4J+LP+JP,LP1,Y,beta,PK)+B1*VV1(2+N3J+N4J+LP+JP
#,LP1,Y,beta,PK)+WW*VV1(3+N3J+N4J+LP+JP,LP1,Y,beta,PK))
ENDDO

  SUM1=SUM1+(PSI**2-ETA**2)*((PSI-ETA)/2)**(N3J-1)*(X/4)**2
#(N4J-1)*DHP(LP+1,LP2+1,L1J+1,L4J2+1,I,J)*SUM2*W_ETA(J)
ENDDO

  SUM=SUM+SUM1/DPSI(I)**2*W_PSI(I)
ENDDO

FBC_PSJP=-0.125d0*PK*B44(N3J,A3J)*B44(N4J,A4J)*SUM
RETURN
END

C **** -----
C * <H; J, Q(pseudo) | H-E | PS; NU LU LUI, L; C> *
C **** -----

C ##### Descriptions #####
C
C Input-- NU,LU,LUI,L: quantum numbers of a Ps channel U with the Bessel free
C function of the positron
C UK: positronium momentum in channel U
C JQ: channel number of H from 0 to 9, which specifies a bound
C wavefunction of H
C N2J,A2J,L2J: parameters of the positron wavefunction in the H bound
C channel JQ
C
C Calling--
C     FBC_HJU(...): bound-free matrix element with a Slater orbital as a bound
C function of H
C
C Common Block--
C     H_PS_DATA, N_H_PS: details of the 18-state channel wavefunctions
C #####
FUNCTION FBC_QJU(UK,JQ,N2J,A2J,L2J,NU,LU,LUI,L,GAMMA)
IMPLICIT REAL*8(A-H,O-Z)
EXTERNAL FBC_HJU
COMMON/E_18/EH(9),EPS(9)/H_PS_DATA/AHJ(9,4),CHJ(9,4),APSJ(9,4),
#CPSJ(9,4)/N_H_PS/NHJ(9,4),LHJ(9),NPSJ(9,4),LPSJ(9)

SUM=0.
DO J=1,4

  IF(CHJ(JQ,J) .NE. 0.)THEN
    SUM=SUM+CHJ(JQ,J)*FBC_HJU(UK,NHJ(JQ,J),AHJ(JQ,J),N2J,A2J,
#LHJ(JQ),L2J,NU,LU,LUI,L,GAMMA)
  ENDIF

ENDDO
FBC_QJU=SUM
RETURN
END

C **** -----
C * < H; J | H-E | PS; NU LU LUI, L; C> *
C **** -----

C ##### Descriptions #####
C
C Input--NIJ,A1J,N2J,A2J,L1J,L2J: parameters in bound slater orbitals of the
C electron and Ps
C NU,LU,LUI,L: quantum numbers of the free channel U of Ps with the Neumann
C UK: positronium momentum
C GAMMA: parameter in the factor before the Neuman function
C
C Calling--
C     VV1: integration related to one spherical Neumann function
C     B4: normalization factor of a Slater orbital

```

```

C      B3PS: coeffs of Ps physical wavefunction
C
C#####
C
FUNCTION FBC_HJU(UK,N1J,A1J,N2J,A2J,L1J,L2J,NU,LU,LUI,L,GAMMA)
IMPLICIT REAL*8(A-H,O-Z)
EXTERNAL VV1,B4,B3PS
COMMON/D_HP/DHP(5,5,3,3,80,150)/PSI_ETA/DPSI(80),
# DETA(150)/W_W/W_PSI(80),
# W_ETA(150)

WW=0.25D0/NU**2-0.25D0*UK**2-0.5D0*(A1J**2+A2J**2)
L2J2=(L2J-INT(ABS(L-L1J)))/2
LU2=(LUI-INT(ABS(L-LU)))/2

SUM=0.
DO I=1,80
PSI=1/DPSI(I)

SUM1=0.
DO J=1,150
ETA=DETA(J)

X=DSQRT(PSI**2+6D0*ETA*PSI+ETA**2+8D0)
Y=0.5d0*(PSI+ETA)*A1J+A2J+0.25D0*(PSI-ETA)/NU
GAM=0.25D0*GAMMA*X
UK1=0.25D0*UK*X

A1=0.5D0*(L1J*(L1J+1)-N1J*(N1J-1))*(2/(PSI+ETA))**2+0.5D0*
#(L2J*(L2J+1)-N2J*(N2J-1))
B1=(A1J*N1J-1)*2/(PSI+ETA)+A2J*N2J+1-2/(PSI-ETA)

SUM2=0.
DO JU=0,NU-LU-1
SUM2=SUM2+B3PS(NU,LU,JU)*((PSI-ETA)/2)**(LU+JU)*
#(A1*VV1(1+N1J+N2J+LU+JU,LUI,Y,GAM,UK1)+B1*VV1(2+N1J+N2J
#+LU+JU,LUI,Y,GAM,UK1)+WW*VV1(3+N1J+N2J+LU+JU,LUI,Y,GAM,UK1))
ENDDO

SUM1=SUM1+((PSI**2-ETA**2)*((PSI+ETA)/2)**(N1J-1)*
#DHP(L1J+1,L2J2+1,LU+1,LU2+1,I,J)*SUM2*W_ETA(J)
ENDDO

SUM=SUM+SUM1/DPSI(I)**2*W_PSI(I)
FBC_HJU=-0.125D0*2D0**0.5D0*UK*B44(N1J,A1J)*B44(N2J,A2J)*SUM

RETURN
END

*****
C      * NORMALIZATION FACTOR B44      *
C#####
C
FUNCTION B44(N,A)
IMPLICIT REAL*8(A-H,O-Z)
EXTERNAL FACT

B4=((2*A)**(2*N+1)/FACT(2*N))**0.5D0

RETURN
END

*****
C      *COEFF. OF RADIAL WAVEFUNCTION B3(N,L,M)  *
C#####
C
REAL*8 FUNCTION B3(N,L,M)
IMPLICIT REAL*8(A-H,O-Z)
EXTERNAL FACT
B3=SQRT(FACT(N-L-1)*FACT(N+L))/FACT(M)/FACT(N-L-1-M)/
& FACT(2*L+1-M)*(-1D0)**M*(2D0/N)**(M+L+1)/N
RETURN
END

*****
C      *PROG-COEFF. OF RADIAL Ps-WAVEFUNCTION B3PS(N,L,M)  *
C#####
C
FUNCTION B3PS(N,L,M)
IMPLICIT REAL*8(A-H,O-Z)
EXTERNAL FACT
B3PS=(-1)**M*DSQRT(0.5D0*FACT(N-L-1)*FACT(N+L))/FACT(M)/
& FACT(N-L-1-M)/FACT(2*L+1+M)*(1D0/N)**(M+L+1)/N

```

```

      RETURN
      END

C *****
C *   DELTA(ABC) OF 6J-FUNCTION  *
C *****
      REAL*8 FUNCTION DELTA(J1,J2,J3,L1,L2,L3)
      IMPLICIT REAL*8(A-H,O-Z)
      EXTERNAL FACT
      D1=FACT(J1+J2+J3)*FACT(J1-J2+J3)*FACT(J2-J1+J3)/
      &     FACT(J1+J2+J3+1)
      DELTA=DSQRT(D1)
      RETURN
      END

C *****
C *CALCULATE 6J-FUNCTION:          /J1  J2  J3\   *
C *J1,J2,J3,L1,L2,L3 HAVE AN ORDER  \L1  L2  L3/   *
C *****
      REAL*8 FUNCTION F6J(J1,J2,J3,L1,L2,L3)
      IMPLICIT REAL*8(A-H,O-Z)
      EXTERNAL FACT,DELTA
      M=MAX(J1+J2+J3,J1+L2+L3)
      M=MAX(M,L1+J2+L3)
      M=MAX(M,L1+L2+J3)
      N=MIN(J1+J2+L1+L2,J2+J3+L2+L3)
      N=MIN(N,J1+J3+L1+L3)
      IF (M .GE. 0 .OR. N .GE. 0)THEN
      F6J=DELTA(J1,J2,J3)*DELTA(J1,L2,L3)*
      &     DELTA(L1,J2,L3)*DELTA(L1,L2,J3)
      S=0.D0
      DO K=M,N
      S=S+(-1D0)**K*FACT(K+1)/FACT(K-J1-J2-J3)/FACT(K-J1-L2-L3)/
      &     FACT(K-L1-J2-L3)/FACT(K-L1-L2-J3)/FACT(J1+J2+L1+L2-K)/
      &     FACT(J2+J3+L2+L3-K)/FACT(J1+J3+L1+L3-K)
      ENDDO
      F6J=F6J*S
      ELSE
      WRITE(8,*) 'BIG-PROBLEM-K<0, IN-F6J'
      STOP
      ENDIF
      RETURN
      END

C *****
C * C(L,K,LP)=<L||C^(K)|||L'>  *
C *****
      REAL*8 FUNCTION CT(L,K,LP)
      IMPLICIT REAL*8(A-H,O-Z)
      EXTERNAL FACT
      IF (K .GE. ABS(L-LP) .AND. K .LE. L+LP) THEN
      J=0.5D0*(L-K+LP)
      C1=FACT(2*(J-L))*FACT(2*(J-K))*FACT(2*(J-LP))/FACT(2*j+1)
      C2=(-1D0)**(J+L)*DSQRT((2*L+1)*(2*LP+1)*C1)
      CT=C2*FACT(J)/FACT(J-L)/FACT(J-K)/FACT(J-LP)
      ENDIF
      RETURN
      END

C *****
C *           pi
C * PM(N,K,L,M)= |dx (cosx)**n (sinx)**k P_l^m(cosx)   *
C *           0
C *****
      FUNCTION PM(N,K,L,M)
      IMPLICIT REAL*8(A-H,O-Z)
      EXTERNAL FACT,PM1,GAMA
      SUM=0.
      DO J=0,(L-M)/2
      SUM=SUM+PM1(L,M,J)*((-1D0)**(N+L-2*j-M)+1D0)*0.5D0*
      &     GAMA(0.5D0*(N+L-2*j-M+1D0))*GAMA(0.5D0*(K+M+1D0))/
      &     GAMA(0.5D0*(N+L-2*j+K+2D0))
      ENDDO
      PM=SUM
      RETURN
      END

C *****
C * COEFFICIENT BEFORE (z/r)**(l-m-2k) in spherical harmonics *
C *****
      FUNCTION PM1(L,M,K)
      IMPLICIT REAL*8(A-H,O-Z)

```

```

      EXTERNAL FACT
      PML=(-1d0)**K*FACT(2*L-2*K)/FACT(K)/FACT(L-K)/FACT(L-2*K-M)
#/2D0***L
      RETURN
      END

C
C ***** * FACTOR BEFORE SUM IN spherical harmonics *
C *****

      FUNCTION APM(L,M)
      IMPLICIT REAL*8(A-H,O-Z)
      EXTERNAL FACT
      APM=(-1D0)**M*((2*L+1D0)*0.25D0/3.1415926535897932D0
#      *FACT(L-M)/FACT(L+M))**0.5D0
      RETURN
      END

C
C ***** * F3J(J1,J2,J3,M1,M2,M3)=| J1 J2 J3 \
C      *          |   *
C      *          \M1 M2 M3 /   *
C *****

      REAL*8 FUNCTION F3J(J1,J2,J3,M1,M2,M3)
      IMPLICIT REAL*8(A-H,O-Z)
      EXTERNAL FACT
      MM=M1+M2+M3
      N=MIN(J1+J2-J3,J1-M1)
      N=MIN(N,J2+M2)
      M=MAX(0,J2-J3-M1)
      M=MAX(M,J1-J3+M2)
      IF(MM .EQ. 0) THEN
      F3J1=DLOG(FACT(J1+J2-J3))+DLOG(FACT(J1-J2+J3))+*
        DLOG(FACT(-J1+J2+J3))+DLOG(FACT(J1-M1))+*
        DLOG(FACT(J1+M1))+DLOG(FACT(J2-M2))+DLOG(FACT(J2+M2))+*
        +DLOG(FACT(J3-M3))+DLOG(FACT(J3+M3))
      DO I=2,J1+J2+J3+1
      F3J1=F3J1-DLOG(1D0*I)
      ENDDO
      SUM=0.
      DO 601 K=M,N
        SUM=SUM+(-1)**K/FACT(K)/FACT(J1+J2-J3-K)/FACT(J1-M1-K)/
          FACT(J2-M2-K)/FACT(J3-J2+M1+K)/FACT(J3-J1-M2+K)
601    CONTINUE
      F3J=(-1)**(J1-J2-M3)*SUM*DEXP(0.5D0*F3J1)
      ELSE
      F3J=0.
      ENDIF
      RETURN
      END

C
C ***** * GJ(A,B,L,N,C,K)=|dx x**m exp(-ax) j_[L](bx) f(N,C,K,X) *
C      *          0
C *****

      FUNCTION GJ(M,A,B,L,N,C,K)
      IMPLICIT REAL*8(A-H,O-Z)
      EXTERNAL VV
      COMMON/D_FACT/DPACT(150)/D_BINC/dbinc(21,21)

      X=DFACT(N+2*K+2)/C***(N+2*K+2)

      SUM0=0.
      DO I=0,N+2*K
        SUM0=SUM0+VV(M+I-K-1,L,A+C,B)/DPACT(I+1)*C**I
      ENDDO

      SUM1=0.
      DO J=0,N-1
        SUM1=SUM1+VV(M+K+J,L,A+C,B)/DPACT(J+1)*C**J
      ENDDO

      GJ=X*(GJ1-SUM0)+DPACT(N+1)/C***(N+1)*SUM1

      RETURN
      END

C
C ***** * GN(M,A,B,L,N,C,K)=|dx x**M exp(-ax) n_[L](bx) f(N,C,K,X) *
C      *          0
C *****
```

```

C   *(1-exp(-alx))**(2L+1)
C ****
C FUNCTION GN(M,A,B,L,N,C,K,A1)
C IMPLICIT REAL*8(A-H,O-Z)
C EXTERNAL VV1
C COMMON/D_FACT/DFACT(150)/D_BINC/dbinc(21,21)

X=DFACT(N+2*K+2)/C**(N+2*K+2)

SUM0=0.
DO I=0,N+2*K
    SUM0=SUM0+VV1(M+I-K-1,L,A+C,A1,B)/DFACT(I+1)*C**I
ENDDO

SUM1=0.
DO J=0,N-1
    SUM1=SUM1+VV1(M+K+J,L,A+C,A1,B)/DFACT(J+1)*C**J
ENDDO

GN=X*(G11-SUM0)+DFACT(N+1)/C**(N+1)*sum1

RETURN
END

C ****
C * GEOMETRIC FUNCTION: M *
C * GEOF(A,B,C,X)= 1 + SGMA PI(M,A,B,C)*X^M *
C *          0 *
C ****

REAL*8 FUNCTION GEOF(A,B,C,X)
IMPLICIT REAL*8(A-H,O-Z)
IF (ABS(B-C).LT. 1D-14) THEN
    GEOF=(1D0-X)**(-A)
ELSE
    PIM=1D0
    SUM=0.33d0           ! avoid sum=0. at some argument
    M=1
399   SUM0=SUM
    M1=M-1
    PIM=PIM*(A+M1)*(B+M1)*X/((C+M1)*M)
    SUM=SUM+PIM
    M=M+1
    IF (ABS(1D0-SUM0/SUM)-1D-13) 400,400,399
400   GEOF=SUM+0.67d0      ! see above
ENDIF
RETURN
END

C ****
C SN(N1,L1,L2,L,A,PK)=<U_n111(r1) r2^12 exp(ZJ.r2)Y_L1112|1/r12|U_1s(r1)*
C   (1-exp(-beta.r2)^{2*L1+1}n_L(pk r2) Y_L0L(r1.r2)>
C n_L(b r)--- neuman function
C ****

REAL*8 FUNCTION SN(N1,L1,L2,L,ZJ,BETA,PK)
IMPLICIT REAL*8(A-H,O-Z)
EXTERNAL B3,CT,F6J,SN1
SN11=(-1D0)**(L2+L)*2D0*CT(L2,L1,L)*F6J(L1,L2,L,L,0,L1)
SUM=0.
DO NU=0,N1-L1-1
    SUM=SUM+B3(N1,L1,NU)*SN1(N1,L1,L2,L,NU,ZJ,BETA,PK)
ENDDO
SN=SN11*SUM
RETURN
END

C ****
C * SN1(N1,L1,L2,L,NU,ZJ,B,PK)--->RADIAL FREE-BOUND INTEGRAL *
C * ZJ,B---> PARAMETERS ; PK--->PK MOMENTUM
C ****

REAL*8 FUNCTION SN1(N1,L1,L2,L,NU,ZJ,B,PK)
IMPLICIT REAL*8(A-H,O-Z)
EXTERNAL VV1,FACT
X1=FACT(NU+2*L1+2)
X2=1D0+1D0/FLOAT(N1)
A0=ZJ+X2
SN11=X1/X2** (NU+2*L1+3)*VV1(L2-L1+1,L,ZJ,B,PK)

SN12=0.
DO I=0,NU+2*L1+1
    SN12=SN12+VV1(L2-L1+1+I,L,A0,B,PK)/FACT(I)/X2** (NU+2*L1+3-I)
ENDDO

```

```

SN13=0
DO J=0,NU
  SN13=SN13+VV1(L1+L2+2+J,L,A0,B,PK)/FACT(J)/X2** (NU+2-J)
ENDDO
SN1=SN11-X1*SN12+FACT(NU+1)*SN13
RETURN
END

C*****
C          OO          -a r1 _b r2      s^k      *
C SR(N,M,A,B,C,L,K)= | dr1 dr2 f(r1,r2,n,m,k) e   e   j_L(c r2) ----
C          0           t^(k+1)      *
C f(r1,r2,n,m,k)= r1^(n+k+1) r2^(m+k+1); s=r<; t=r>
C*****
REAL*8 FUNCTION SR(N,M,A,B,C,L,K)
IMPLICIT REAL*8(A-H,O-Z)
EXTERNAL VV,FACT
X=FACT(N+2*K+1)/A** (N+2*K+2)
SR11=X*VV(M,L,B,C)
SR12=0.
DO I=0,N+2*K
  SR12=SR12+VV(M+I,L,A+B,C)*A** I/FACT(I)
ENDDO
SR13=0D0
DO J=0,N-1
  SR13=SR13+VV(M+2*K+1+J,L,A+B,C)*A** J/FACT(J)
ENDDO
SR=SR11-SR12*X+SR13*FACT(N)/A** (N+1)
RETURN
END

C*****
C          OOO
C VV1(N,L,A,B,C)= | dx x^(n) exp(-ax) (1-exp(-bx))^(2L+1) n_(L)(cx)
C          0
C*****
FUNCTION VV1(N,L,A,B,C)
IMPLICIT REAL*8(A-H,O-Z)
EXTERNAL BESELN,SNV1
COMMON/GAUS/QX(354),QW(354)
if ( b/a .le. 1d-3)then
  vv1=0.
  return
elseif ( b/a .le. 2d-2)then
  VV1=0.
  DO I=1,354
    X=QX(I)
    VV1=VV1+X**N*EXP(-A*X)*BESSELN(2*L+1,L,B,C,X)*QW(I)
    IF(I .LE. 30)GO TO 3303
    IF (ABS(VV1) .LE. 1D-35)RETURN
    IF (ABS(1-VV1/VV1) .LE. 1D-12)return
3303  VV11=VV1
  ENDDO
else
  vv1=snvv1(N,L,A,B,C)
endif
RETURN
END

C*****
C          OOO
C VV1(N,L,A,B,C)= | dx x^(n) exp(-ax) (1-exp(-bx))^(2L+1) n_(L)(cx)
C          0
C*****
REAL*8 FUNCTION SNV1(N,L,A,B,C)
IMPLICIT REAL*8(A-H,O-Z)
EXTERNAL CVII1,FACT
SUM=0.
DO M=0,L/2
  SUM=SUM+(-1)**M*FACT(L+2*M)/FACT(2*M)/FACT(L-2*M)/
  (2D0*C)**(2*M)*CVII1(N-1-2*M,2*L+1,L,A,B,C)
ENDDO
IF (L) 1026,1026,1025
1025 DO K=0,(L-1)/2
  SUM=SUM+(-1D0)**K*FACT(L+2*K+1)/FACT(2*K+1)/FACT(L-2*K-1)/
  (2D0*C)**(2*K+1)*CVII1(N-2-2*K,2*L+1,L,A,B,C)
ENDDO
1026 SNV1=(-1D0)**(L+1)/C*SUM
RETURN
END

```

```

C ****
C *          000
C * CVIII1(N,N1,L,A,B,C)=|dx x^n(1-exp(-bx))^n1 exp(-ax)cos(cx+l.pi/2)*
C *          0
C ****
REAL*8 FUNCTION CVIII1(N,N1,L,A,B,C)
IMPLICIT REAL*8(A-H,O-Z)
EXTERNAL BINC,FACT
SUM=0.
IF(N .GE. 0) THEN
  DO J=0,N1
    X=DATAN(C/(A+J*B))
    Y=((A+J*B)**2+C*C)**(-N-1)
    SUM=SUM+(-1D0)**J*BINC(N1,J)*DSQRT(Y)*DCOS((N+1D0)*X+
      L*3.1415926535897932D0/2D0)
  ENDDO
  CVIII1=SUM*FACT(N)
ELSE
  N3=-N
  DO J=0,N1
    A1=(A+J*B)**2+C*C
    X=DATAN(C/(A+J*B))
    X1=0.5D0*DLOG(A1)
    XX=0.5D0*L*3.1415926535897932D0-(N3-1)*X
    SUM=SUM+(-1D0)**J*BINC(N1,J)*A1**((0.5D0*(N3-1))*
      *(DCOS(XX)*X1+DSIN(XX)*X))
  ENDDO
  CVIII1=(-1D0)**N3/FACT(N3-1)*SUM
ENDIF
RETURN
END

C ****
C * GAUSSIAN-QUADRATURE METHOD: POINTS-->QX(N); WEIGHT-->QW(N) *
C ****
SUBROUTINE GAUSS
IMPLICIT REAL*8(A-H,O-Z)
COMMON/GAUS/QX(354),QW(354)
OPEN(UNIT=31,FILE='QXQW_GAUS.DAT',STATUS='OLD')
DO I=1,354,3
  READ(31,11)QX(I),QX(I+1),QX(I+2)
  READ(31,11)QW(I),QW(I+1),QW(I+2)
ENDDO
CLOSE(31)
11 FORMAT(1X,3(D22.16,1X))
RETURN
END

C ****
C * BINC(N,I)=N!/(N-I)!/I!   *
C ****
REAL*8 FUNCTION BINC(N,I)
IMPLICIT REAL*8(A-H,O-Z)
IF( I .EQ. 0 .OR. I .EQ. N) THEN
  BINC=1D0
ELSE
  BINC=1D0
  DO J=0,I-1
    BINC=BINC*(N-J)/(J+1D0)
  ENDDO
ENDIF
RETURN
END

C ****
C * FACTORIAL OF A GIVEN INTEGER N   *
C ****
REAL*8 FUNCTION FACT(N)
IMPLICIT REAL*8(A-H,O-Z)
FACT=1D0
148 IF (N ) 148,153,149
  WRITE(8,'????$&&N=',N
  STOP
149 DO I=1,N
  FACT=FACT*FLOAT(I)
ENDDO
153 RETURN
END

C ****

```

```

C      * VV(N,L,A,B)= | dx x^N exp(-ax) j_L(bx) *
C      *          0
C ****
REAL*8 FUNCTION VV(N,L,A,B)
IMPLICIT REAL*8(A-H,O-Z)
EXTERNAL GEOP,FACT,GAMA
COMMON/D_FACT/DFACT(150)
AB=A*A+B*B
VV=DSQRT(3.1415926535897932D0)*DFACT(N+L+1)*B**L/2D0** (L+1)
$ /GAMA(L+1.5D0)*(1D0/AB)**(0.5D0*(N+L+1D0))
% *GEOP(0.5D0*(N+L+1D0),0.5D0*(1D0-N+L),L+1.5D0,B*B/AB)
RETURN
END
*****
C      * GAMA(X): X= +N; +N+.5; -N+0.5; *
C ****
REAL*8 FUNCTION GAMA(X)
IMPLICIT REAL*8(A-H,O-Z)
EXTERNAL FACT
PI=3.1415926535897932D0
X1=ABS(X)
N=INT(ABS(X))
IF (FLOAT(N) .LT. X1) THEN
  GAMA=DSQRT(PI)
  DO I=1,N
    GAMA=GAMA*(X1-I)
  ENDDO
  IF(X .LT. 0.)THEN
    GAMA=-PI/X1/DSIN(PI*X1)/GAMA
  ELSE
    ENDIF
  ELSEIF (X .GT. 0. .AND. FLOAT(N) .EQ. ABS(X)) THEN
    GAMA=FACT(N-1)
  ELSE
    WRITE(*,*) 'X>>>??'
  ENDIF
RETURN
END
*****
C      * PRODUCE PARAMETERS FOR H AND Ps STATES *
C ****
SUBROUTINE PS_H_DATA
IMPLICIT REAL*8(A-H,O-Z)
COMMON/E_18/EH(9),EPS(9)/H_PS_DATA/AMJ(9,4),CMJ(9,4),APSJ(9,4),
#CP SJ(9,4)/N_H_PS/NHJ(9,4),LHJ(9),NPSJ(9,4),LPSJ(9)

C##### eigenvalues of 9-hydrogen pseudostates
DATA(EH(I),I=1,9)/-0.5D0,-0.125D0,-0.125D0,-4.665304694881356D-6,
#5.4633840887524d-5,1.282846926346426d-5,0.755916874472686D0,
#0.525460522287252d0,0.472675820578354d0/

DO I=1,9
  EPS(I)=0.5D0*EH(I)
ENDDO

DATA(NHJ(1,J),J=1,4)/1.0,0,0,0/ !1s in s-orbitals
DATA(NHJ(2,J),J=1,4)/1.2,0,0,0/ !2s
DATA(NHJ(3,J),J=1,4)/2.0,0,0,0/ !2p

DATA(NHJ(4,J),J=1,4)/1.2,3,4/ !3s_
DATA(NHJ(5,J),J=1,4)/2.3,4,0/ !3p_
DATA(NHJ(6,J),J=1,4)/3.4,0,0/ !3d_

DATA(NHJ(7,J),J=1,4)/1.2,3,4/ !4s_
DATA(NHJ(8,J),J=1,4)/2.3,4,0/ !4p_
DATA(NHJ(9,J),J=1,4)/3.4,0,0/ !4d_

C##### THE FOLLOWING ARE PARAMETERS FOR THE H-12-STATES #####
C angular momentum quantum numbers
DATA(LHJ(J),J=1,9)/0,0,1,0,1,2,0,1,2/

C coeff. in the exponent parts
DATA(AMJ(1,J),J=1,4)/1d0,0.,0.,0./ !1s
DATA(AMJ(2,J),J=1,4)/0.5D0,0.5D0,0.,0./ !2s
DATA(AMJ(3,J),J=1,4)/0.5D0,0.0,0.,0./ !2p

DATA(AMJ(4,J),J=1,4)/0.6981D0,0.6981D0,0.6981D0,0.6981D0/ !3s_
DATA(AMJ(5,J),J=1,4)/0.753D0,0.753D0,0.753D0,0.753D0/ !3p_
DATA(AMJ(6,J),J=1,4)/0.9187D0,0.9187D0,0,0,/ !3d_

DATA(AMJ(7,J),J=1,4)/0.6981D0,0.6981D0,0.6981D0,0.6981D0/ !4s_

```

```

      DATA(AHJ(8,J),J=1,4)/0.753D0,0.753D0,0.753D0,0.753D0/      !4p_
      DATA(AHJ(9,J),J=1,4)/0.9187D0,0.9187D0,0,0/                  !4d_

C     coeffs. in Hls,2s,3s_,4s_
      DATA(CHJ(1,J),J=1,4)/1D0,0,0,0/                                !1s_
      DATA(CHJ(2,J),J=1,4)/1D0,-1.73205080756888D0,0.,0./          !2s_
      DATA(CHJ(3,J),J=1,4)/1d0,0.,0.,0./                           !2p_
      DATA(CHJ(4,J),J=1,4)/0.548204505284712d0,1.09033411051086d0,
#-5.34501185152612d0,4.09020873942977d0/                      !3s_
      DATA(CHJ(5,J),J=1,4)/-0.066399200837882d0,2.83931873582895d0,
#-2.88354263638701d0,0./                                         !3p_
      DATA(CHJ(6,J),J=1,4)/-0.440372063228619d0,1.39973551676968d0,
#0.,0./                                              !3d_
      DATA(CHJ(7,J),J=1,4)/4.04053052163474d0,-12.3533507661451d0,
#14.5266456777819d0,-6.195625233174c4d0/                      !4s_
      DATA(CHJ(8,J),J=1,4)/4.54980118724584d0,-8.36024797656426d0,
#4.37230438774340d0,0./                                         !4p_
      DATA(CHJ(9,J),J=1,4)/2.79393493945864d0,-2.45779179002078d0,
#0.,0./                                              !4d_

C ##### PARAMETERS FOR Ps PSEUDO-STATES   #####
      DO I=1,9
      LPSJ(I)=LHJ(I)
      DO J=1,4
      NPSJ(I,J)=NHJ(I,J)

      APSJ(I,J)=0.5D0*AHCJ(I,J)
      CPSJ(I,J)=CHJ(I,J)

      ENDDO
      ENDDO

      RETURN
      END

```

```

***** MAIN PROGRAM *****
C THIS PROGRAM IS TO CARRY OUT CALCULATIONS OF POSITRON-HYDROGEN SCATTERING
C BY USING THE HARRIS-NESBET ALGEBRAIC APPROACH. 1s-2s-2p-3p_ H +
C 1s-2s-2p Ps ARE ASSOCIATED WITH A GREAT NUMBER OF CORRELATION FUNCTIONS.
C

C INPUT -- L: THE TOTAL ANGULAR MOMENTUM QUANTUM NUMBER
C
C CALLINGS-- BB_7(L): TO GENERATE THE BOUND-BOUND MATRICES: A AND B
C
C EIGEN_NAG: TO DIAGONALIZE THE EIGENVALUE EQUATION: A X = E B X
C
C CC_7(L): TO CALCULATE THE SCATTERING PHASE SHIFTS AND CROSS
C SECTIONS.
C
C SUBROUTINES SHARED WITH 18_CC.f:
C
C =====
C 1. BOUND-BOUND SUBROUTINES RELATED:
C -----
C BB_HH,S_HH,BET,F6J,CT,YRSP,B44,BB_PSPS,BB_HPS,S_HPS,B3,B3PS,AA,EIGEN_NAG,
C
C 2. ALL FREE-FREE SUBROUTINES:
C -----
C R_MATRIX,T_MATRIX,AA_INVERSE,ludcmp,lubksb,ETA_PSI,MATRIX_HP,HP,HPMM,
C COMMON_DATA, FFSS_PQ,FFSS_UV,FFCS_PQ,FFCS_UV,FFCC_PQ,
C FF_N,FFCC_UV,FFSS_PU,FFCS_PU,FFCS_UP,FFCC_PU,BESSELN,WWJJ,Wjj,DWjj,
C FLEG2Q,BJ,WJN,WWJN,UR,WM,WR,H_PQ,PS_UV,PHI
C
C 3. FREE-BOUND SUBROUTINES RELATED:
C -----
C FBS_HJP,FBS_PSJU,FBS_PSJB,FBS_HJU,FBC_HJP,FBC_PSJU,FBC_PSLP,FBC_HJU,GN,
C GJ,GEOP,SN,SN1,SR,VVI,SNVVI,CVIII,GAUSS,BINC,FACT,VV,GAMA
C
C =====
C***** parameters of pseudo H3p *****
C
C IMPLICIT REAL*8 (A-H,O-Z)
C EXTERNAL BB_7,EIGEN_NAG, CC_7
C
C L=3
C
C CALL BB_7(L)
C
C CALL EIGEN_NAG
C
C CALL CC_7(L)
C
C END
C
C *****
C SUBROUTINE BB_7(L)
C *****
C
C IMPLICIT REAL*8 (A-H,O-Z)
C PARAMETER(NH=18,N_H=144,N_P=108,N=432)
C DIMENSION A(N,N),B(N,N),EVAL(N),EVEC(N,N),N24(NH),A2(NH),A4(NH)
C #,DL(N),E(N),N1J(N_H),A1J(N_H),N2J(N_H),A2J(N_H),L1(N_H),L2(N_H)
C #,N3J(N_P),A3J(N_P),N4J(N_P),A4J(N_P),L3(N_P),L4(N_P),bb1(5),bb2(7)
C #,N22(6),BB3(3),BB44(6),D2(NH)
C EXTERNAL COMMON_DATA,ETA_PSI,MATRIX_HP
C COMMON/N3PH/N3P(3)/A3PH/A3P(3)/B3PH/B3P(3)
C
C ##### parameters of pseudo H3p #####
C DATA (N3P(I),I=1,3)/1.1,2/
C DATA (A3P(I),I=1,3)/0.5D0,1D0,1D0/
C DATA (B3P(I),I=1,3)/0.339224553D0,-0.966001481D0,-0.48300074D0/
C ##### parameters of pseudo H3p #####
C
C DATA(N22(I),I=1,6)/1.2,1.2,1.2/
C DATA(BB1(I),I=1,4)/0.7d0,0.8d0,0.9d0,1.1d0/
C DATA(BB2(I),I=1,6)/0.3d0,0.4d0,0.5d0,0.6d0,0.8d0,1.1d0/
C DATA(BB3(I),I=1,3)/0.2d0,0.6d0,1d0/
C
C DATA(N24(I),I=1,NH)/1.2,3,1.2,3,1.2,3,1.2,3,1.2,3/
C DATA(BB44(I),I=1,6)/0.2d0,0.5d0,0.9d0,1.4d0,1.7d0,2.1d0/
C
C DATA(A2(I),I=1,NH)/0.05d0,0.05d0,0.05d0,0.2d0,0.2d0,0.2d0
C #,0.4d0,0.4d0,0.4d0,0.8d0,0.8d0,1.2d0,1.2d0,1.2d0
C #,1.8d0,1.8d0,1.8d0/
C
C OPEN(UNIT=8,FILE='BB_18_144_108F',STATUS='new')
C L=3

```

```

C##### parameters of H(I) correlation functions#####
M=0
DO L11=0,2
DO L21=INT(ABS(L-L11)),L+L11,2
DO I=1,4
DO J=1,6
M=M+1

if(L11.eq.1)then
N1J(M)=3
else
N1J(M)=L11+1
endif

N2J(M)=L21+N24(J)
L1(M)=L11
L2(M)=L21
A1J(M)=BB1(I)
A2J(M)=BB2(J)
ENDDO
ENDDO
ENDDO
ENDDO

C##### parameters of Ps(I) correlation functions #####
M=0
DO L31=0,2
DO L41=INT(ABS(L-L31)),L+L31,2
DO I=1,3
DO J=1,6
M=M+1
N3J(M)=L31+1
N4J(M)=L41+N24(J)
L3(M)=L31
L4(M)=L41
A3J(M)=BB3(I)
A4J(M)=BB44(J)
ENDDO
ENDDO
ENDDO
ENDDO

CALL COMMON_DATA
CALL ETA_PSI
CALL MATRIX_HP(L)

DO I=1,NH
A4(I)=A2(I)
ENDDO

DO I=1,NH
DO J=1,NH
NI=N24(I)+L
NJ=N24(J)+L
      !H1s-H1s
A(I,J)=BB_HH(1,1D0,NI,A2(I),1,1D0,NJ,A2(J),L,0,L,0,L)
B(I,J)=S_HH(1,1D0,NI,A2(I),1,1D0,NJ,A2(J),L,0,L,0,L)
      !H2s-H1s
IH2=NH+I
A(IH2,J)=BB_2SJ(NI,A2(I),1,1D0,NJ,A2(J),L,0,L)
B(IH2,J)=S_H2SJ(NI,A2(I),1,1D0,NJ,A2(J),L,0,L)
      !H2p-H1s
L20=INT(ABS(L-1))
N2P=0
DO L2I=L20,L+1,2
N2P=N2P+1
IH3=IH2+N2P*NH
NPI=N24(I)+L2I
A(IH3,J)=BB_HH(2,0.5D0,NPI,A2(I),1,1D0,NJ,A2(J),L,1,L2I,0,L)
B(IH3,J)=S_HH(2,0.5D0,NPI,A2(I),1,1D0,NJ,A2(J),L,1,L2I,0,L)
ENDDO

      !1sPs-H1s
IP1=IH3+NH
A(IP1,J)=BB_HPS(1,1D0,NJ,A2(J),1,0.5D0,NI,A4(I),L,0,L,0,L)
B(IP1,J)=S_HPS(1,1D0,NJ,A2(J),1,0.5D0,NI,A4(I),L,0,L,0,L)
      !2sPs-H1s

```

```

IP2=IP1+NH
A(IP2,J)=BB_2SPS_J12(NI,A4(I),L,1D0,NJ,A2(J),L,0,L)
B(IP2,J)=S_2SPS_J12(NI,A4(I),L,1D0,NJ,A2(J),L,0,L)
!2pPs-Hls
L40=INT(ABS(L-1))
N2P=0
DO L4I=L40,L+1,2
N2P=N2P+1
IP3=IP2+N2P*NH
NPI=N24(I)+L4I
A(IP3,J)=BB_HPS(1,1D0,NJ,A2(J),2,0.25D0,NPI,A4(I),L,0,L,1,L4I)
B(IP3,J)=S_HPS(1,1D0,NJ,A2(J),2,0.25D0,NPI,A4(I),L,0,L,1,L4I)
ENDDO

NI=N24(I)+L
NJ=N24(J)+L
JH2=NH+J
!2sH-2sH
A(IH2,JH2)=BB2S(NI,A2(I),NJ,A2(J),L)
B(IH2,JH2)=S_H2S(NI,A2(I),NJ,A2(J),L)
!2pH-2sH
L20=INT(ABS(L-1))
N2P=0
DO L2I=L20,L+1,2
N2P=N2P+1
IH3=IH2+N2P*NH
NPI=N24(I)+L2I
A(IH3,JH2)=BB_2SJ(NJ,A2(J),2,0.5D0,NPI,A2(I),L,1,L2I)
B(IH3,JH2)=S_H2SJ(NJ,A2(J),2,0.5D0,NPI,A2(I),L,1,L2I)
ENDDO
!1sPs-2sH

A(IP1,JH2)=BB_H2S_J34(NJ,A2(J),1,0.5D0,NI,A4(I),L,0,L)
B(IP1,JH2)=S_H2S_J34(NJ,A2(J),1,0.5D0,NI,A4(I),L,0,L)
!2sPs_2sH

A(IP2,JH2)=BB_2S2S(NJ,A2(J),NI,A4(I),L)
B(IP2,JH2)=S_2S2S(NJ,A2(J),NI,A4(I),L)
!2pPs-2sH
L40=INT(ABS(L-1))
N2P=0
DO L4I=L40,L+1,2
N2P=N2P+1
IP3=IP2+N2P*NH
NPI=N24(I)+L4I
A(IP3,JH2)=BB_H2S_J34(NJ,A2(J),2,0.25D0,NPI,A4(I),L,1,L4I)
B(IP3,JH2)=S_H2S_J34(NJ,A2(J),2,0.25D0,NPI,A4(I),L,1,L4I)
ENDDO

L20=INT(ABS(L-1)) !....-2pH
N2P=0
DO L2J=L20,L+1,2
N2P=N2P+1
NPJ=N24(J)+L2J
NI=N24(I)+L
NJ=N24(J)+L2J
JH3=JH2+N2P*NH
!2pH-2pH
L2I0=INT(ABS(L-1))
N2PI=0
DO L2I=L2I0,L+1,2
N2PI=N2PI+1
IH3=IH2+N2PI*NH
NPI=N24(I)+L2I
NPJ=N24(J)+L2J
A(IH3,JH3)=BB_HH(2,0.5D0,NPI,A2(I),2,0.5D0,NPJ,A2(J)
#,L,1,L2I,1,L2J)
B(IH3,JH3)=S_HH(2,0.5D0,NPI,A2(I),2,0.5D0,NPJ,A2(J)
#,L,1,L2I,1,L2J)
ENDDO
!1sPs-2pH
A(IP1,JH3)=BB_HPS(2,0.5D0,NPJ,A2(J),1,0.5D0,NI,A4(I),L,1,L2J,0,L)
B(IP1,JH3)=S_HPS(2,0.5D0,NPJ,A2(J),1,0.5D0,NI,A4(I),L,1,L2J,0,L)
!2sPs-2pH

A(IP2,JH3)=BB_2SPS_J12(NI,A4(I),2,0.5D0,NPJ,A2(J),L,1,L2J)
B(IP2,JH3)=S_2SPS_J12(NI,A4(I),2,0.5D0,NPJ,A2(J),L,1,L2J)
!2pPs-2pH
L4I0=INT(ABS(L-1))
N2PS=0

```

```

DO L4I=L4IO,L+1,2
N2PS=N2PS+1
NPI=N24(I)+L4I
IP3=IP2+N2PS*NH
A(IP3,JH3)=BB_HPS(2,0.5D0,NPJ,A2(J),2,0.25D0,NPI,A4(I),L,1,
#L2J,1,L4I)
B(IP3,JH3)=S_HPS(2,0.5D0,NPJ,A2(J),2,0.25D0,NPI,A4(I),L,1,
#L2J,1,L4I)
ENDDO

ENDDO
!.....-1sPs

JP1=JH3+NH
NI=N24(I)+L
NJ=N24(J)+L
!1sPs-1sPs
A(IP1,JP1)=BB_PSPS(1,0.5D0,NI,A4(I),1,0.5D0,NJ,A4(J),L,O,L,O,L)
B(IP1,JP1)=S_HH(1,0.5D0,NI,A4(I),1,0.5D0,NJ,A4(J),L,O,L,O,L)
!2sPs-1sPs

A(IP2,JP1)=BB_2SPSJ(NI,A4(I),1,0.5D0,NJ,A4(J),L,O,L)
B(IP2,JP1)=S_2SPSJ(NI,A4(I),1,0.5D0,NJ,A4(J),L,O,L)
!2pPs-1sPs

L4IO=INT(ABS(L-1))
N2P=0
DO L4I=L4IO,L+1,2
N2P=N2P+1
NPI=N24(I)+L4I
IP3=IP2+N2P*NH
A(IP3,JP1)=BB_PSPS(2,0.25D0,NPI,A4(I),1,0.5D0,NJ,A4(J),L,1,L4I,O,L)
B(IP3,JP1)=S_HH(2,0.25D0,NPI,A4(I),1,0.5D0,NJ,A4(J),L,1,L4I,O,L)
ENDDO
!.... -2s

Ps

JP2=JP1+NH
NI=N24(I)+L
NJ=N24(J)+L
!2sPs-2sPs
A(IP2,JP2)=BB2SPS(NI,A4(I),NJ,A4(J),L)
B(IP2,JP2)=S_2SPS(NI,A4(I),NJ,A4(J),L)
!2pPs-2sPs

L4IO=INT(ABS(L-1))
N2P=0
DO L4I=L4IO,L+1,2
N2P=N2P+1
NPI=N24(I)+L4I
IP3=IP2+N2P*NH
A(IP3,JP2)=BB_2SPSJ(NJ,A4(J),2,0.25D0,NPI,A4(I),L,1,L4I)
B(IP3,JP2)=S_2SPSJ(NJ,A4(J),2,0.25D0,NPI,A4(I),L,1,L4I)
ENDDO
!2pPs-2p_Ps

L4IO=INT(ABS(L-1))
NPJ=N24(J)+L4IO
N2PP=0
DO L4I=L4IO,L+1,2
N2PP=N2PP+1
IP3=IP2+N2PP*NH
JP3=JP2+NH
NPI=N24(I)+L4I
A(IP3,JP3)=BB_PSPS(2,0.25D0,NPI,A4(I),2,0.25D0,NPJ,A4(J),
#L,1,L4I,1,L4IO)
B(IP3,JP3)=S_HH(2,0.25D0,NPI,A4(I),2,0.25D0,NPJ,A4(J),
#L,1,L4I,1,L4IO)
ENDDO

!2pPs-2p+Ps

IF (L .GT. 0) THEN
NPJ=N24(J)+L+1
JP3=JP3+NH
NPI=N24(I)+L+1
A(IP3,JP3)=BB_PSPS(2,0.25D0,NPI,A4(I),2,0.25D0,NPJ,A4(J),
#L,1,L+1,1,L+1)
B(IP3,JP3)=S_HH(2,0.25D0,NPI,A4(I),2,0.25D0,NPJ,A4(J),
#L,1,L+1,1,L+1)
ENDIF

ENDDO
ENDDO

```

```

C#####the following is to calculate matrix elements #####
C##### related to correlation functions #####
1023  DO I=1,N_H
      I_H1=IP3+I
      DO J=1,NH
         J_H1=J
         !H(I)-H1s
         A(I_H1,J_H1)=BB_HH(N1J(I),A1J(I),N2J(I),A2J(I),1,1D0,N24(J)
#+L,A2(J),L,L1(I),0,L)
         B(I_H1,J_H1)=S_HH(N1J(I),A1J(I),N2J(I),A2J(I),1,1D0,N24(J)
#+L,A2(J),L,L1(I),L2(I),0,L)
         !H(I)-H2s
         J_H2=J_H1+NH
         A(I_H1,J_H2)=BB_2SJ(N24(J)+L,A2(J),N1J(I),A1J(I),N2J(I),A2J(I)
#,L,L1(I),L2(I))
         B(I_H1,J_H2)=S_H2SJ(N24(J)+L,A2(J),N1J(I),A1J(I),N2J(I),A2J(I)
#,L,L1(I),L2(I))
         !H(I)-H2p
         N2P=0
         DO L22=INT(ABS(L-1)),L+1,2
         N2P=N2P+1
         J_H3=J_H2+N2P*NH
         A(I_H1,J_H3)=BB_HH(N1J(I),A1J(I),N2J(I),A2J(I),2,0.5D0,
#N24(J)+L22,A2(J),L,L1(I),L2(I),1,L22)
         B(I_H1,J_H3)=S_HH(N1J(I),A1J(I),N2J(I),A2J(I),2,0.5D0,
#N24(J)+L22,A2(J),L,L1(I),L2(I),1,L22)
         ENDDO
         !H(I)-Ps(1s)
         J_P1=J_H3+NH
         A(I_H1,J_P1)=BB_HPS(N1J(I),A1J(I),N2J(I),A2J(I),1,0.5D0,
#N24(J)+L,A2(J),L,L1(I),L2(I),0,L)
         B(I_H1,J_P1)=S_HPS(N1J(I),A1J(I),N2J(I),A2J(I),1,0.5D0,
#N24(J)+L,A2(J),L,L1(I),L2(I),0,L)
         !H(I)-Ps(2s)
         J_P2=J_P1+NH
         A(I_H1,J_P2)=BB_2SPS_J12(N24(J)+L,A4(J),N1J(I),A1J(I),N2J(I)
#,A2J(I),L,L1(I),L2(I))
         B(I_H1,J_P2)=S_2SPS_J12(N24(J)+L,A4(J),N1J(I),A1J(I),N2J(I)
#,A2J(I),L,L1(I),L2(I))
         !H(I)-Ps(2p)
         N2P=0
         DO L42=INT(ABS(L-1)),L+1,2
         N2P=N2P+1
         J_P3=J_P2+N2P*NH
         A(I_H1,J_P3)=BB_HPS(N1J(I),A1J(I),N2J(I),A2J(I),2,0.25D0,
#N24(J)+L42,A4(J),L,L1(I),L2(I),1,L42)
         B(I_H1,J_P3)=S_HPS(N1J(I),A1J(I),N2J(I),A2J(I),2,0.25D0,
#N24(J)+L42,A4(J),L,L1(I),L2(I),1,L42)
         ENDDO
         ENDDO
         ENDDO
         DO I=1,N_P
         I_P1=I_H1+I
         DO J=1,NH
            !Ps(I)-H1s
            J_PH1=J
            A(I_P1,J_PH1)=BB_HPS(1,1D0,N24(J)+L,A4(J),N3J(I),A3J(I),
#N4J(I),A4J(I),L,0,L,L3(I),L4(I))
            B(I_P1,J_PH1)=S_HPS(1,1D0,N24(J)+L,A4(J),N3J(I),A3J(I),
#N4J(I),A4J(I),L,0,L,L3(I),L4(I))
            !Ps(I)-H2s
            J_PH2=J_PH1+NH
            A(I_P1,J_PH2)=BB_H2S_J34(N24(J)+L,A2(J),N3J(I),A3J(I),
#N4J(I),A4J(I),L,L3(I),L4(I))
            B(I_P1,J_PH2)=S_H2S_J34(N24(J)+L,A2(J),N3J(I),A3J(I),
#N4J(I),A4J(I),L,L3(I),L4(I))
            !Ps(I)-H2p
            N2P=0
            DO L22=INT(ABS(L-1)),L+1,2
            N2P=N2P+1
            J_PH3=J_PH2+N2P*NH
            A(I_P1,J_PH3)=BB_HPS(2,0.5D0,N24(J)+L22,A2(J),N3J(I),A3J(I),
#N4J(I),A4J(I),L,1,L22,L3(I),L4(I))
            B(I_P1,J_PH3)=S_HPS(2,0.5D0,N24(J)+L22,A2(J),N3J(I),A3J(I),
#N4J(I),A4J(I),L,1,L22,L3(I),L4(I))
            ENDDO
            !Ps(I)-Ps(1s)

```

```

J_PP1=J_PH3+NH
A(I_P1,J_PP1)=BB_PSPS(N3J(I),A3J(I),N4J(I),A4J(I),1,0.5D0,
#N24(J)+L,A4(J),L,L3(I),L4(I),0,L)
B(I_P1,J_PP1)=S_HH(N3J(I),A3J(I),N4J(I),A4J(I),1,0.5D0,
#N24(J)+L,A4(J),L,L3(I),L4(I),0,L)
!Ps(I)-Ps(2s)

J_PP2=J_PP1+NH
A(I_P1,J_PP2)=BB_2SPSJ(N24(J)+L,A4(J),N3J(I),A3J(I),N4J(I),
#A4J(I),L,L3(I),L4(I))
B(I_P1,J_PP2)=S_2SPSJ(N24(J)+L,A4(J),N3J(I),A3J(I),N4J(I),
#A4J(I),L,L3(I),L4(I))
!Ps(I)-Ps(2p)

N2P=0
DO L42=INT(ABS(L-1)),L+1,2
N2P=N2P+1
J_PP3=J_PP2+N2P*NH

A(I_P1,J_PP3)=BB_PSPS(N3J(I),A3J(I),N4J(I),A4J(I),2,0.25D0,
#N24(J)+L42,A4(J),L,L3(I),L4(I),1,L42)
B(I_P1,J_PP3)=S_HH(N3J(I),A3J(I),N4J(I),A4J(I),2,0.25D0,
#N24(J)+L42,A4(J),L,L3(I),L4(I),1,L42)
ENDDO

ENDDO
ENDDO

DO I=1,N_H
I_HH=I_P3+I
DO J=1,N_H
J_HH=J_P3+J
!H(I)-H(J)
A(I_HH,J_HH)=BB_HH(N1J(I),A1J(I),N2J(I),A2J(I),N1J(J),A1J(J)
#,N2J(J),A2J(J),L,L1(I),L2(I),L1(J),L2(J))
B(I_HH,J_HH)=S_HH(N1J(I),A1J(I),N2J(I),A2J(I),N1J(J),A1J(J)
#,N2J(J),A2J(J),L,L1(I),L2(I),L1(J),L2(J))
ENDDO
ENDDO

DO I=1,N_P
I_PH=I_HH+I
!Ps(I)-H(J)
DO J=1,N_H
J_PH=J_P3+J
A(I_PH,J_PH)=BB_HPS(N1J(J),A1J(J),N2J(J),A2J(J),N3J(I),A3J(I)
#,N4J(I),A4J(I),L,L1(J),L2(J),L3(I),L4(I))
B(I_PH,J_PH)=S_HPS(N1J(J),A1J(J),N2J(J),A2J(J),N3J(I),A3J(I)
#,N4J(I),A4J(I),L,L1(J),L2(J),L3(I),L4(I))
ENDDO
!Ps(I)-Ps(J)

DO J=1,N_P
J_PP=J_PH+J
A(I_PH,J_PP)=BB_PSPS(N3J(I),A3J(I),N4J(I),A4J(I),N3J(J),A3J(J)
#,N4J(J),A4J(J),L,L3(I),L4(I),L3(J),L4(J))
B(I_PH,J_PP)=S_HH(N3J(I),A3J(I),N4J(I),A4J(I),N3J(J),A3J(J)
#,N4J(J),A4J(J),L,L3(I),L4(I),L3(J),L4(J))
ENDDO

ENDDO

C#####pseudo H3p #####
1025 DO I=1,NH

I3P=-1
DO L2I=INT(ABS(L-1)),L+1,2
I3P=I3P+1
IH4=I_PH+I3P*NH+I

DO J=1,NH
N3PI=N24(I)+L2I
JH1=J
!H3p_-+H1s
A(IH4,JH1)=BB_Q3P(1,0,L,N24(J)+L,A2(J),N3PI,A2(I),L2I,L)
B(IH4,JH1)=0.
!H3p_-+H2s
JH2=JH1+NH
A(IH4,JH2)=BB_Q3P(2,0,L,N24(J)+L,A2(J),N3PI,A2(I),L2I,L)
B(IH4,JH2)=0.
!H3p_-+H2p

N2P=0
DO L2J=INT(ABS(L-1)),L+1,2
N2P=N2P+1
JH3=JH2+N2P*NH
A(IH4,JH3)=BB_Q3P(2,1,L2J,N24(J)+L2J,A2(J),N3PI,A2(I),L2I,L)

```

Aug 14 1996 09:47

## Fortran Program - 7\_mixing.f

198

```

      B(IH4,JH3)=0.
      ENDDO

      !H3p_-+Ps(1s)
      JP1=JH3+NH
      A(IH4,JP1)=BB_U3P(1,0,N24(J)+L,A4(J),L,N3PI,A2(I),L2I,L)
      B(IH4,JP1)=OVER_U3P(1,0,N24(J)+L,A4(J),L,N3PI,A2(I),L2I,L)
      !H3p_-+Ps(2s)
      JP2=JP1+NH
      A(IH4,JP2)=BB_U3P(2,0,N24(J)+L,A4(J),L,N3PI,A2(I),L2I,L)
      B(IH4,JP2)=OVER_U3P(2,0,N24(J)+L,A4(J),L,N3PI,A2(I),L2I,L)
      !H3p_-+Ps(2p)

      N2P=0
      DO L4J=INT(ABS(L-1)),L+1,2
      N2P=N2P+1
      JP3=JP2+N2P*NH
      A(IH4,JP3)=BB_U3P(2,1,N24(J)+L4J,A4(J),L4J,N3PI,A2(I),L2I,L)
      B(IH4,JP3)=OVER_U3P(2,1,N24(J)+L4J,A4(J),L4J,N3PI,A2(I),L2I,L)
      ENDDO

      ENDDO          !END J LOOP:H1s,2s,2p,Ps 1s,2s,2p

      !BEGIN J LOOP FOR H(J)          !H3p_-+H(J)
      DO J=1,N_H
      JHJ=JP3+J
      A(IH4,JHJ)=BB_H3PIJ(N3PI,A2(I),N1J(J),A1J(J),N2J(J),A2J(J),
      #L,L2I,L1(J),L2(J))
      B(IH4,JHJ)=S_H3PIJ(N3PI,A2(I),N1J(J),A1J(J),N2J(J),A2J(J),
      #L,L2I,L1(J),L2(J))
      ENDDO

      !H3p_-+Ps(J)
      DO J=1,N_P
      JPJ=JHJ+J
      A(IH4,JPJ)=BB_H3PPS(N3PI,A2(I),N3J(J),A3J(J),N4J(J),A4J(J),
      #L,L2I,L3(J),L4(J))
      B(IH4,JPJ)=S_H3PPS(N3PI,A2(I),N3J(J),A3J(J),N4J(J),A4J(J),
      #L,L2I,L3(J),L4(J))
      ENDDO

      !H3p_-+H3p_-
      DO J=1,NH
      J3P=-1
      DO L2J=INT(ABS(L-1)),L+1,2
      J3P=J3P+1
      JH4=JPJ+J3P*NH+J
      A(IH4,JH4)=BB_3P3P(N3PI,A2(I),L2I,N24(J)+L2J,A2(J),L2J,L)
      B(IH4,JH4)=OVER_3P3P(N3PI,A2(I),L2I,N24(J)+L2J,A2(J),L2J,L)
      ENDDO
      ENDDO          !for L2I loop
      ENDDO          !for I loop
      ENDDO          !H3p_-+H(J)

C#####
C
      DO I=1,N
      DO J=1,I
      WRITE(8,23)A(I,J),B(I,J)
      ENDDO
      ENDDO

23   FORMAT(1X,2(D27.20,1X))
30   FORMAT(1X,3(d23.17,1X))

      RETURN
      END

C#####
C
C  < NP LP;H; I | H | H_COR; J >
C  # NP,LP--> quantum numbers of H state P
C  # N2I,A2I,L2I--> continuum fuction centred
C  # N1J,A1J,N2J,A2J,L1J,L2J--> parameters of
C  # correlation function J
C#####
FUNCTION BB_HPJ(NP,N2I,A2I,N1J,A1J,N2J,A2J,L,LP,L2I,L1J,L2J)
IMPLICIT REAL*8(A-H,O-Z)
```

```

      EXTERNAL BB_HH,B3,B44

      SUM=0.
      DO JP=0,NP-LP-1
      SUM=SUM+B3(NP,LP,JP)*BB_HH(LP+JP+1,1D0/NP,N2I,A2I,N1J,A1J,
      #N2J,A2J,L,LP,L2I,L1J,L2J)/B44(LP+JP+1,1D0/NP)
      ENDDO
      BB_HPJ=SUM
      RETURN
      END

C
C      # < NP LP; H; I | H_COR; J >
C      # NP,LP--> quantum numbers of H state P
C      # N2I,A2I,L2I--> continuum fuction centred
C      # N1J,A1J,N2J,A2J,L1J,L2J--> parameters of
C      # correlation function J
C
C      FUNCTION S_HPJ(NP,N2I,A2I,N1J,A1J,N2J,A2J,L,LP,L2I,L1J,L2J)
      IMPLICIT REAL*8(A-H,O-Z)
      EXTERNAL S_HH,B3,B44

      SUM=0.
      DO JP=0,NP-LP-1
      SUM=SUM+B3(NP,LP,JP)*S_HH(LP+JP+1,1D0/NP,N2I,A2I,N1J,A1J,
      #N2J,A2J,L,LP,L2I,L1J,L2J)/B44(LP+JP+1,1D0/NP)
      ENDDO
      S_HPJ=SUM
      RETURN
      END

C
C      # < NP LP; H; I | NQ,LQ; H; J >
C      # NP,LP--> quantum numbers of H state P
C      # NQ,LQ-->quantum numbers of H state q
C      # N2I,A2I,L2I--> continuum fuction centred; I
C      # N2J,A2J,L2J--> continuum fuction centred; J
C
C      FUNCTION BB_HPJ(NP,N2I,A2I,NQ,N2J,A2J,L,LP,L2I,LQ,L2J)
      IMPLICIT REAL*8(A-H,O-Z)
      EXTERNAL BB_HH,B3,B44

      SUM=0.
      DO JP=0,NP-LP-1
      SUM1=0.

      DO JQ=0,NQ-LQ-1
      SUM1=SUM1+B3(NQ,LQ,JQ)*BB_HH(LP+JP+1,1D0/NP,N2I,A2I,LQ+JQ+1,
      #1D0/NQ,N2J,A2J,L,LP,L2I,LQ,L2J)/B44(LP+JP+1,1D0/NP)
      #/B44(LQ+JQ+1,1D0/NQ)
      ENDDO

      SUM=SUM+B3(NP,LP,JP)*SUM1
      ENDDO
      BB_HPJ=SUM
      RETURN
      END

C
C      # < NP LP; H; I | NQ,LQ; H; J >
C      # NP,LP--> quantum numbers of H state P
C      # NQ,LQ-->quantum numbers of H state q
C      # N2I,A2I,L2I--> continuum fuction centred; I
C      # N2J,A2J,L2J--> continuum fuction centred; J
C
C      FUNCTION S_HPJ(NP,N2I,A2I,NQ,N2J,A2J,L,LP,L2I,LQ,L2J)
      IMPLICIT REAL*8(A-H,O-Z)
      EXTERNAL S_HH,B3,B44

      SUM=0.
      DO JP=0,NP-LP-1
      SUM1=0.

      DO JQ=0,NQ-LQ-1
      SUM1=SUM1+B3(NQ,LQ,JQ)*S_HH(LP+JP+1,1D0/NP,N2I,A2I,LQ+JQ+1,
      #1D0/NQ,N2J,A2J,L,LP,L2I,LQ,L2J)/B44(LP+JP+1,1D0/NP)
      #/B44(LQ+JQ+1,1D0/NQ)
      ENDDO

      SUM=SUM+B3(NP,LP,JP)*SUM1

```

```

ENDDO
S_HPQ=SUM
RETURN
END

C ****
C * <H2s; I | H | H2s; J >
C ****
FUNCTION BB2S(N2I,A2I,N2J,A2J,L)
IMPLICIT REAL*8 (A-H,O-Z)
EXTERNAL YRSF,AA,FACT,B44

N2IJ=N2I+N2J
A2IJ=A2I+A2J
B4I=B44(N2I,A2I)
B4J=B44(N2J,A2J)

BB2S1=(-0.125D0-0.5d0*A2I**2+0.5d0*AA(N2I,L)*A2IJ**2/N2IJ/
#(N2IJ-1)+(A2I*N2I+1)*A2IJ/N2IJ)*B4I*FACT(N2IJ)/A2IJ***(N2IJ+1)*B4J
BB2S2=YRSF(1,N2IJ-1,1D0,A2IJ,0)-YRSF(2,N2IJ-1,1D0,A2IJ,0)
#+0.25D0*YRSF(3,N2IJ-1,1D0,A2IJ,0)

BB2S=BB2S1-B4I*BB2S2*B4J/2
RETURN
END

C ****
C * <H2s; I | H | theta; J >
C ****
FUNCTION BB_2SJ(N2I,A2I,N1J,A1J,N2J,A2J,L,L1J,L2J)
IMPLICIT REAL*8 (A-H,O-Z)
EXTERNAL AA,FACT,CT,F6J,YRSF

N2IJ=N2I+N2J
A2IJ=A2I+A2J
C12=FACT(N2IJ)/A2IJ***(N2IJ+1)*FACT(N1J+1)/(0.5D0+A1J)
#***(N1J+2)*(1-(N1J+2)/(1+2*A1J))
IF (L1J .EQ. 0 .AND. L2J .EQ. L)THEN
  BB=(-0.125D0-0.5D0*A2I**2+0.5D0*AA(N2I,L)*A2IJ**2/N2IJ
#/ (N2IJ-1)+(A2I*N2I+1)*A2IJ/N2IJ)*C12
ELSE
  BB=0.
ENDIF
  BB_2SJ=BB-CT(L,L1J,L2J)*F6J(0,L,L,L2J,L1J,L1J)
#*(YRSF(N1J-L1J,N2IJ-L1J-1,0.5D0+A1J,A2IJ,L1J)-0.5D0*
# YRSF(N1J-L1J+1,N2IJ-L1J-1,0.5D0+A1J,A2IJ,L1J))

BB_2SJ=1/2d0**0.5d0*B44(N2I,A2I)*BB_2SJ*B44(N1J,A1J)*B44(N2J,A2J)
RETURN
END

C ****
C * OVERLAP <H2s; I | H2s; J >
C ****
FUNCTION S_H2S(N2I,A2I,N2J,A2J,L)
IMPLICIT REAL*8 (A-H,O-Z)
EXTERNAL FACT,B44

S_H2S=B44(N2I,A2I)*FACT(N2I+N2J)/(A2I+A2J)***(N2I+N2J+1)*
#B44(N2J,A2J)

RETURN
END

C ****
C * OVERLAP: <H2s; I theta; J >
C ****
FUNCTION S_H2SJ(N2I,A2I,N1J,A1J,N2J,A2J,L,L1J,L2J)
IMPLICIT REAL*8 (A-H,O-Z)
EXTERNAL FACT,B44

IF (L1J .EQ. 0 .AND. L2J .EQ. L)THEN
N2IJ=N2I+N2J
A2IJ=A2I+A2J
S_H2SJ=B44(N2I,A2I)*FACT(N2IJ)/A2IJ***(N2IJ+1)*FACT(N1J+1)/
#(0.5D0+A1J)***(N1J+2)*(1-(N1J+2)/(1+2*A1J))*B44(N1J,A1J)*
#B44(N2J,A2J)/2d0**0.5d0
ELSE
S_H2SJ=0.

```

```

      ENDIF
      RETURN
      END

C #####  

C # <NU,LU;Ps;I | H | Ps_COR; J >  

C # NU,LU-- quantum numbers of Ps  

C # N4I,L4I,A4I--continuum function of Ps mass center  

C # N3J,A3J,N4J,A4J,L3J,L4J--parameters of the  

C # correlation functions  

C # L--- total angular momentum  

C #####  

FUNCTION BB_PS_34J(NU,N4I,A4I,N3J,A3J,N4J,A4J,L,LU,L4I,L3J,L4J)
IMPLICIT REAL*8(A-H,O-Z)
EXTERNAL BB_PSPS

SUM=0.
DO JU=0,NU-LU-1
SUM=SUM+B3PS(NU,LU,JU)*BB_PSPS(LU+JU+1,0.5D0/NU,N4I,A4I,
#N3J,A3J,N4J,A4J,L,LU,L4I,L3J,L4J)/B44(LU+JU+1,0.5D0/NU)
ENDDO

BB_PS_34J=SUM
RETURN
END

C #####  

C # <NU,LU;Ps;I | H | Ps_COR; J >  

C # NU,LU-- quantum numbers of Ps  

C # N4I,L4I,A4I--continuum function of Ps mass center  

C # N3J,A3J,N4J,A4J,L3J,L4J--parameters of the  

C # correlation functions  

C # L--- total angular momentum  

C #####  

FUNCTION S_PS_34J(NU,N4I,A4I,N3J,A3J,N4J,A4J,L,LU,L4I,L3J,L4J)
IMPLICIT REAL*8(A-H,O-Z)
EXTERNAL S_HH,B3PS,B44

SUM=0.
DO JU=0,NU-LU-1
SUM=SUM+B3PS(NU,LU,JU)*S_HH(LU+JU+1,0.5D0/NU,N4I,A4I,
#N3J,A3J,N4J,A4J,L,LU,L4I,L3J,L4J)/B44(LU+JU+1,0.5D0/NU)
ENDDO

S_PS_34J=SUM
RETURN
END

C #####  

C # <NU,LU;Ps;I | H | NV,LV-Ps; J >  

C # NU,LU;NV,LV-- quantum numbers of Ps  

C # N4I,L4I,A4I--continuum function of Ps mass center;I#
C # N4J,L4J,A4J--continuum function of Ps mass center;J#
C # L--- total angular momentum  

C #####  

FUNCTION BB_UV(NU,N4I,A4I,NV,N4J,A4J,L,LU,L4I,LV,L4J)
IMPLICIT REAL*8(A-H,O-Z)
EXTERNAL BB_PSPS,B44,B3PS

SUM=0.
DO JU=0,NU-LU-1

SUM1=0.
DO JV=0,NV-LV-1
SUM1=SUM1+B3PS(NV,LV,JV)*BB_PSPS(LU+JU+1,0.5D0/NU,N4I,A4I
#,LV+JV+1,0.5D0/NV,N4J,A4J,L,LU,L4I,LV,L4J)/B44(LU+JU+1,
#0.5D0/NU)/B44(LV+JV+1,0.5D0/NV)
ENDDO

SUM=SUM+B3PS(NU,LU,JU)*SUM1
ENDDO

BB_UV=SUM
RETURN
END

C #####  

C # <NU,LU;Ps;I | NV,LV-Ps; J >  

C # NU,LU;NV,LV-- quantum numbers of Ps  

C # N4I,L4I,A4I--continuum function of Ps mass center;I#

```

```

C      # N4J,L4J,A4J--continuum function of Ps mass center;J#
C      # L--- total angular momentum
C ###### ##### ##### ##### ##### ##### ##### #####
FUNCTION S_UV(NU,N4I,A4I,NV,N4J,A4J,L,LU,L4I,LV,L4J)
IMPLICIT REAL*8(A-H,O-Z)
EXTERNAL S_HH,B44,B3PS

SUM=0.
DO JU=0,NU-LU-1

SUML=0.
DO JV=0,NV-LV-1
SUM1=SUM1+B3PS(NV,LV,JV)*S_HH(LU+JU+1,0.5D0/NU,N4I,A4I
#,LV+JV+1,0.5D0/NV,N4J,A4J,L,LU,L4I,LV,L4J)/B44(LU+JU+1,
#0.5D0/NU)/B44(LV+JV+1,0.5D0/NV)
ENDDO

SUM=SUM+B3PS(NU,LU,JU)*SUM1
ENDDO

S_UV=SUM
RETURN
END

C ****
C * <Ps(2S);I | H | Ps(2s);J>
C ****
FUNCTION BB2SPS(N4I,A4I,N4J,A4J,L)
IMPLICIT REAL*8(A-H,O-Z)
EXTERNAL YRSF,AA,FACT

N4IJ=N4I+N4J
A4IJ=A4I+A4J
B4IJ=B44(N4I,A4I)*B44(N4J,A4J)

BB2SPS=0.5D0*(-0.125D0+0.5D0*AA(N4I,L)*A4IJ**2/N4IJ/(N4IJ-1)
#+A4I*N4I*A4IJ/N4IJ-0.5D0*A4I**2)*B4IJ*FACT(N4IJ)/A4IJ**2(N4IJ+1)

RETURN
END

C ****
C * <2sPs; I | 2sPs; J >
C ****
FUNCTION S_2SPS(N4I,A4I,N4J,A4J,L)
IMPLICIT REAL*8(A-H,O-Z)
EXTERNAL AA,FACT

N4IJ=N4I+N4J
A4IJ=A4I+A4J
B4IJ=B44(N4I,A4I)*B44(N4J,A4J)

S_2SPS=B4IJ*FACT(N4IJ)/A4IJ**2(N4IJ+1)

RETURN
END

C ****
C * < 2SPs; I | H | theta; J >
C ****
FUNCTION BB_2SPSJ(N4I,A4I,N3J,A3J,N4J,A4J,L,L3J,L4J)
IMPLICIT REAL*8(A-H,O-Z)
EXTERNAL AA,FACT,CT,P6J,YRSF,B44

N4IJ=N4I+N4J
A4IJ=A4I+A4J
B4I=0.25D0*B44(N4I,A4I)
B4J=B44(N3J,A3J)*B44(N4J,A4J)
C13=B4I*FACT(N4IJ)/A4IJ**2(N4IJ+1)*FACT(N3J+1)/(0.25D0+A3J)**2
#(N3J+2)*(1-(N3J+2)/(1+4*A3J))*B4J
IF (L3J .EQ. 0 .AND. L4J .EQ. L) THEN
  BB_2SPSJ=(-0.0625-0.25D0*AA(N4I,L)*A4IJ**2/N4IJ/(N4IJ-1) +
#0.5D0*A4I*N4I*A4IJ/N4IJ)*C13
ELSEIF(L3J .EQ. 1) THEN
  BB_2SPSJ=B4I*CT(L,1,L4J)*P6J(0,L,L,L4J,1,1)*2**2*(N3J+3)*
#(YRSF(N3J-1,N4IJ-2,0.5D0+2*A3J,A4IJ,1)-0.5D0*YRSF(N3J,N4IJ-2,
#0.5D0+2*A3J,A4IJ,1))*B4J
ELSEIF(L3J .EQ. 2) THEN
  BB_2SPSJ=0.
ENDIF

```

```

      BB_2SPSJ=BB_PS_34J(2,N4I,A4I,N3J,A3J,N4J,A4J,L,0,L,L3J,L4J)
      RETURN
      END

C ****
C * OVERLAP: <2SPs;I | theta; J> *
C ****
      FUNCTION S_2SPSJ(N4I,A4I,N3J,A3J,N4J,A4J,L,L3J,L4J)
      IMPLICIT REAL*8(A-H,O-Z)
      EXTERNAL FACT,B44

      IF (L3J .EQ. 0 .AND. L4J .EQ. L)THEN
      N4IJ=N4I+N4J
      A4IJ=A4I+A4J
      B4I=0.25d0*B44(N4I,A4I)
      B4J=B44(N3J,A3J)*B44(N4J,A4J)
      S_2SPSJ=B4I*FACT(N4IJ)/A4IJ**(N4IJ+1)*FACT(N3J+1)/
      #(0.25D0+A3J)**(N3J+2)*(1-(N3J+2)/(1+4*A3J))*B4J
      ELSE
      S_2SPSJ=0.
      ENDIF

      RETURN
      END

C ****
C * <H2s; I | H | theta;J (3,4) > *
C ****
      FUNCTION BB_H2S_J34(N2I,A2I,N3J,A3J,N4J,A4J,L,L3J,L4J)
      IMPLICIT REAL*8(A-H,O-Z)
      EXTERNAL FACT,B44,B3,B3ps
      COMMON/D_MP/DHP(5,5,3,3,80,130)/PSI_ETA/DPSI(80),
      # DETA(130)/W_W/W_PSI(80),
      # W_ETA(130)

      L4J0=INT(ABS(L-L3J))

      SUM1=0.
      DO I=1,80
      PSI=1/DPSI(I)

      SUM2=0.
      DO J=1,130
      ETA=DETA(J)

      X00=(PSI**2+6*PSI*ETA+ETA**2+8)**0.5D0
      X11=(PSI**2-ETA**2)*(0.5D0*(PSI-ETA))**((N3J-1)*(0.25D0*X00))
      S**((N4J-1)*DHP(1,1,L3J+1,(L4J-L4J0)/2+1,I,J))

      Y=0.25D0*(PSI+ETA)+0.5D0*(PSI-ETA)*A3J+0.25D0*A4J*X00+A2I

      SUM3=0.
      DO K=0,1
      M=2+N2I+N3J+N4J+K
      SUM3=SUM3+(-1D0)**K/(K+1D0)*(0.5D0*(PSI+ETA))**K*(-0.125D0-0.5D0
      $*A2I**2+(0.5D0*AA(N2I,L)*Y/(M-1)+A2I*N2I+1-2/(PSI-ETA))*Y/M)*
      #FACT(M)/Y**((M+1)
      ENDDO

      SUM2=SUM2+SUM3*X11*W_ETA(J)
      ENDDO

      SUM1=SUM1+SUM2*W_PSI(I)*PSI**2
      ENDDO

      BB_H2S_J34=B44(N2I,A2I)*B44(N3J,A3J)*B44(N4J,A4J)/2**3.5D0*SUM1
      RETURN
      END

C ****
C * < 2sH; I | H | 2sPs; J > *
C ****
      FUNCTION BB_2S2S(N2I,A2I,N4J,A4J,L)
      IMPLICIT REAL*8(A-H,O-Z)
      EXTERNAL FACT
      DIMENSION BA(3)
      COMMON/D_MP/DHP(5,5,3,3,80,130)/PSI_ETA/DPSI(80),
      # DETA(130)/W_W/W_PSI(80),W_ETA(130)

      SUM1=0.
      DO I=1,80

```

```

PSI=1/DPSI(I)

SUM2=0.
DO J=1,130
ETA=DETA(J)

X00=(PSI**2+6*PSI*ETA+ETA**2+8)**0.5D0
X11=(PSI**2-ETA**2)*(X00/4)**(N4J-1)*DHP(1,1,1,1,I,J)

Y=0.25D0*(PSI+ETA)+0.125D0*(PSI-ETA)+0.25D0*A4J*X00+A2I

BA(1)=1D0
BA(2)=-(0.25D0*(PSI+ETA)+0.125D0*(PSI-ETA))
BA(3)=(PSI**2-ETA**2)/32
SUM3=0.
DO M=0,2
M1=3+N2I+N4J+M
SUM3=SUM3+BA(M+1)*(-0.125D0-0.5D0*A2I**2+(A2I*N2I+1-2/(PSI-ETA))
#*Y/M1+0.5D0*AA(N2I,L)*Y*Y/M1/(M1-1))*FACT(M1)/Y**(M1+1)
ENDDO

SUM2=SUM2+SUM3*X11*W_ETA(J)
ENDDO

SUM1=SUM1+SUM2*W_PSI(I)*PSI**2
ENDDO

BB_2S2S=B44(N2I,A2I)*B44(N4J,A4J)/2D0**5.5D0*SUM1
RETURN
END

*****
C * < 2sH; I | 2sPs; J > *
*****
FUNCTION S_2S2S(N2I,A2I,N4J,A4J,L)
IMPLICIT REAL*8(A-H,O-Z)
EXTERNAL FACT
DIMENSION BA(3)
COMMON/D_HP/DHP(5,5,3,3,80,130)/PSI_ETA/DPSI(80),
# DETA(130)/W_W/W_PSI(80),W_ETA(130)

SUM1=0.
DO I=1,80
PSI=1/DPSI(I)

SUM2=0.
DO J=1,130
ETA=DETA(J)

X00=(PSI**2+6*PSI*ETA+ETA**2+8)**0.5D0
X11=(PSI**2-ETA**2)*(X00/4)**(N4J-1)*DHP(1,1,1,1,I,J)
Y=0.25D0*(PSI+ETA)+0.125D0*(PSI-ETA)+0.25D0*A4J*X00+A2I

BA(1)=1D0
BA(2)=-(0.25D0*(PSI+ETA)+0.125D0*(PSI-ETA))
BA(3)=(PSI**2-ETA**2)/32
SUM3=0.
DO M=0,2
M1=3+N2I+N4J+M
SUM3=SUM3+BA(M+1)*FACT(M1)/Y**(M1+1)
ENDDO

SUM2=SUM2+SUM3*X11*W_ETA(J)
ENDDO

SUM1=SUM1+SUM2*W_PSI(I)*PSI**2
ENDDO

S_2S2S=B44(N2I,A2I)*B44(N4J,A4J)/2D0**5.5D0*SUM1
RETURN
END

C ****
C * <H2s ; I | theta; J(3,4)> *
*****
FUNCTION S_H2S_J34(N2I,A2I,N3J,A3J,N4J,A4J,L,L3J,L4J)
IMPLICIT REAL*8(A-H,O-Z)
EXTERNAL FACT,B44
COMMON/D_HP/DHP(5,5,3,3,80,130)/PSI_ETA/DPSI(80),
# DETA(130)/W_W/W_PSI(80),W_ETA(130)

L4JO=INT(ABS(L-L3J))

```

```

SUM1=0.
DO I=1,80
PSI=1/DPSI(I)

SUM2=0.
DO J=1,130
ETA=DETA(J)

X00=(PSI**2+6*PSI*ETA+ETA**2+8)**0.5D0
X11=(PSI**2-ETA**2)*(0.5D0*(PSI-ETA))**((N3J-1)*(0.25D0*X00)
S**((N4J-1)*DHP(1,1,L3J+1,(L4J-L4J0)/2+1,I,J))

Y=0.25D0*(PSI+ETA)+0.5D0*(PSI-ETA)*A3J+0.25D0*A4J*X00+A2I

SUM3=0.
DO K=0,1
M=2+N2I+N3J+N4J+K
SUM3=SUM3+(-1D0)**K/(K+1D0)*(0.5D0*(PSI+ETA))**K*FACT(M)/Y**((M+1)
ENDDO

SUM2=SUM2+SUM3*X11*W_ETA(J)
ENDDO

SUM1=SUM1+SUM2*W_PSI(I)*PSI**2
ENDDO

S_H2S_J34=B44(N2I,A2I)*B44(N3J,A3J)*B44(N4J,A4J)/2**3.5D0*SUM1
RETURN
END

C ****
C * <2sPs; I | H | theta; J > *
C ****
FUNCTION BB_2SPS_J12(N4I,A4I,N1J,A1J,N2J,A2J,L,L1J,L2J)
IMPLICIT REAL*8(A-H,O-Z)
EXTERNAL FACT,B44
COMMON/D_HP/DHP(5,5,3,3,80,130)/PSI_ETA/DPSI(80),
DETA(130)/W_W/W_PSI(80),
# W_ETA(130)

L2J0=INT(ABS(L-L1J))

SUM1=0.
DO I=1,80
PSI=1/DPSI(I)

SUM2=0.
DO J=1,130
ETA=DETA(J)

X00=(PSI**2+6*PSI*ETA+ETA**2+8)**0.5D0
X11=(PSI**2-ETA**2)*(0.5D0*(PSI+ETA))**((N1J-1)*(0.25D0*X00)
S**((N4I-1)*DHP(L1J+1,(L2J-L2J0)/2+1,I,1,I,J))

Y=0.125D0*(PSI-ETA)+0.5D0*(PSI+ETA)*A1J+0.25D0*A4I*X00+A2J

a0=-0.5d0*a1j*a1j-0.5d0*a2j*a2j
a1=(a1j*n1j-1)**2/(psi+eta)+(a2j*n2j+1)-2/(psi-eta)
a2=0.5d0*AA(n1j,11j)*(2/(psi+eta))**2+0.5d0*AA(n2j,12j)

SUM3=0.
DO K=0,1
M=2+N4I+N1J+N2J+K
SUM3=SUM3+(-1D0)**K/(K+1)**2*((PSI-ETA)/2)**K*(A0+(A1+A2*Y/
#(M-1))*Y/M)*FACT(M)/Y**((M+1)
ENDDO

SUM2=SUM2+X11*SUM3*W_ETA(J)
ENDDO

SUM1=SUM1+SUM2*W_PSI(I)*PSI**2
ENDDO

BB_2SPS_J12=B44(N4I,A4I)*B44(N1J,A1J)*B44(N2J,A2J)/32D0*SUM1
RETURN
END

C ****
C * <2SPs; I | htheta; J > *
C ****
FUNCTION S_2SPS_J12(N4I,A4I,N1J,A1J,N2J,A2J,L,L1J,L2J)

```

```

IMPLICIT REAL*8 (A-H,O-Z)
EXTERNAL FACT,B44
COMMON/D_HF/DHP(5,5,3,3,80,130)/PSI_ETA/DPSI(80),
# DETA(130)/W_W/W_PSI(80).W_ETA(130)

L2J0=INT(ABS(L-L1J))

SUM1=0.
DO I=1,80
PSI=1/DPSI(I)

SUM2=0.
DO J=1,130
ETA=DETA(J)

X00=(PSI**2+6*PSI*ETA+ETA**2+8)**0.5D0
X11=(PSI**2-ETA**2)*(0.5D0*(PSI+ETA))**2*(N1J-1)*(0.25D0*X00)
S***(N4I-1)*DHP(L1J+1,(L2J-L2J0)/2+1,1,I,J)

Y=0.125D0*(PSI-ETA)+0.5D0*(PSI+ETA)*A1J+0.25D0*A4I*X00+A2J

SUM3=0.
DO K=0,1
M=2+N4I-N1J+N2J+K
SUM3=SUM3+(-1D0)**K/(K+1)**2*((PSI-ETA)/2)**K*FACT(M)/Y***(M+1)
ENDDO

SUM2=SUM2+X11*SUM3*W_ETA(J)
ENDDO

SUM1=SUM1+SUM2*W_PSI(I)*PSI**2
ENDDO

S_2SPS_J12=B44(N4I,A4I)*B44(N1J,A1J)*B44(N2J,A2J)/32D0*SUM1
RETURN
END

C ######
C # BOUND-BOUND INTEGRALS INCLUDING H3p_
C #####
FUNCTION BB_Q3P(N1,L1,L2,N2I,A2I,N2J,A2J,L21,L)
IMPLICIT REAL*8 (A-H,O-Z)
EXTERNAL BB_HH,B44
COMMON/N3PH/N3P(3)/A3PH/A3P(3)/B3PH/B3P(3)

SS1=0.
DO K=1,3
SS2=0.
DO NU=0,N1-L1-1
SS2=SS2+B3(N1,L1,NU)*BB_HH(L1+NU+1,1D0/N1,
#N2I,A2I,N3P(K)+1,A3P(K),N2J,A2J,L,L1,L2,1,L21)
#/B44(N3P(K)+1,A3P(K))/B44(L1+NU+1,1D0/N1)
ENDDO

SS1=SS1+B3P(K)*SS2
ENDDO

BB_Q3P=SS1
RETURN
END

C *****
C * <H3p_ | H | H3p_> *
C *****
FUNCTION BB_3P3P(N2I,A2I,L2,N2J,A2J,L21,L)
IMPLICIT REAL*8 (A-H,O-Z)
EXTERNAL B44,BB_HH
COMMON/N3PH/N3P(3)/A3PH/A3P(3)/B3PH/B3P(3)
SSI=0.
DO J=1,3
SS2=0.
DO K=1,3
SS2=SS2+B3P(K)*BB_HH(N3P(J)+1,A3P(J),N2I,A2I,N3P(K)+1,
#A3P(K),N2J,A2J,L,1,L2,1,L21)/B44(N3P(J)+1,A3P(J))/
#B44(N3P(K)+1,A3P(K))
ENDDO
SSI=SSI+B3P(J)*SS2
ENDDO
BB_3P3P=SSI
RETURN
END

```

```

C   ****
C   * <H3P_ | H3P_ >
C   ****
C
FUNCTION OVER_3P3P(N2I,A2I,L2,N2J,A2J,L21,L)
IMPLICIT REAL*8(A-H,O-Z)
EXTERNAL FACT
IF ( L2 .EQ. L21)THEN
OVER_3P3P=B44(N2I,A2I)*B44(N2J,A2J)*FACT(N2I+N2J)
#/(A2I+A2J)**(N2I+N2J+1)
ELSE
OVER_3P3P=0.
ENDIF
RETURN
END

C   ****
C   * <NU LU L1I L | H | H3P_ >
C   ****
C
FUNCTION BB_U3P(NU,LU,N4I,A4I,L4I,N2J,A2J,LP1,L)
IMPLICIT REAL*8(A-H,O-Z)
EXTERNAL B44,BB_HPS,B3PS
COMMON/D_HP/DHP(5,5,3,3,80,130)/PSI_ETA/DPSI(80),
# DETA(130)/W_W/W_PSI(80),W_ETA(130)/N3PH/N3P(3)
# /A3PH/A3P(3)/B3PH/B3P(3)/D_FACT/DFACT(130)

SS1=0.
DO K=1,3
SS2=0.
DO JU=0,NU-LU-1
SS2=SS2+B3PS(NU,LU,JU)*BB_HPS(N3P(K)+1,
#A3P(K),N2J,A2J,LU+JU+1,0.5D0/NU,N4I,A4I,L,1,LP1,LU,L4I)
#/B44(N3P(K)+1,A3P(K))/B44(LU+JU+1,0.5D0/NU)
ENDDO

SS1=SS1+B3P(K)*SS2
ENDDO
BB_U3P=SS1

RETURN
END

C   ****
C   * <NU LU L1I L | H3P_ >
C   ****
C
FUNCTION OVER_U3P(NU,LU,N4I,A4I,L4I,N2J,A2J,LP1,L)
IMPLICIT REAL*8(A-H,O-Z)
EXTERNAL B44,S_HPS,B3PS
COMMON/D_HP/DHP(3,3,2,2,80,130)/PSI_ETA/DPSI(80),
# DETA(130)/W_W/W_PSI(80),W_ETA(130)/N3PH/N3P(3)
# /A3PH/A3P(3)/B3PH/B3P(3)/D_FACT/DFACT(130)

SS1=0.
DO K=1,3
SS2=0.
DO JU=0,NU-LU-1
SS2=SS2+B3PS(NU,LU,JU)*S_HPS(N3P(K)+1,
#A3P(K),N2J,A2J,LU+JU+1,0.5D0/NU,N4I,A4I,L,1,LP1,LU,L4I)
#/B44(N3P(K)+1,A3P(K))/B44(LU+JU+1,0.5D0/NU)
ENDDO

SS1=SS1+B3P(K)*SS2
ENDDO
OVER_U3P=SS1

RETURN
END

C   ****
C   * < H3P_ ; I | H | theta J; H >
C   ****
C
FUNCTION BB_H3PIJ(N2I,A2I,N1J,A1J,N2J,A2J,L,L2I,L1J,L2J)
IMPLICIT REAL*8(A-H,O-Z)
EXTERNAL BB_HH,B44
COMMON/N3PH/N3P(3)/A3PH/A3P(3)/B3PH/B3P(3)

SUM=0.
DO K=1,3
SUM=SUM+B3P(K)*BB_HH(N3P(K)+1,A3P(K),N2I,A2I,N1J,A1J,N2J,A2J,
#L,1,L2I,L1J,L2J)/B44(N3P(K)+1,A3P(K))
ENDDO
BB_H3PIJ=SUM

```

```

      RETURN
      END

C ****
C * < H3p_ ; I | theta J; H > *
C ****
      FUNCTION S_H3PIJ(N2I,A2I,N1J,A1J,N2J,A2J,L,L2I,L1J,L2J)
      IMPLICIT REAL*8(A-H,O-Z)
      EXTERNAL BB_HH,B44
      COMMON/N3PH/N3P(3)/A3PH/A3P(3)/B3PH/B3P(3)

      SUM=0.
      DO K=1,3
      SUM=SUM+B3P(K)*S_HH(N3P(K)+1,A3P(K),N2I,A2I,N1J,A1J,N2J,A2J,
      #L,1,L2I,L1J,L2J)/B44(N3P(K)+1,A3P(K))
      ENDDO
      S_H3PIJ=SUM
      RETURN
      END

C ****
C * <H3p_ ; I | H | theta (3,4); Ps>   *
C ****
      FUNCTION BB_H3PPS(N2I,A2I,N3J,A3J,N4J,A4J,L,L2I,L3J,L4J)
      IMPLICIT REAL*8(A-H,O-Z)
      EXTERNAL BB_HPS,B44
      COMMON/N3PH/N3P(3)/A3PH/A3P(3)/B3PH/B3P(3)

      SUM=0.
      DO K=1,3
      SUM=SUM+B3P(K)*BB_HPS(N3P(K)+1,A3P(K),N2I,A2I,N3J,A3J,N4J,
      #A4J,L,1,L2I,L3J,L4J)/B44(N3P(K)+1,A3P(K))
      ENDDO

      BB_H3PPS=SUM
      RETURN
      END

C ****
C * <H3p_ ; I | H | theta (3,4); Ps>   *
C ****
      FUNCTION S_H3PPS(N2I,A2I,N3J,A3J,N4J,A4J,L,L2I,L3J,L4J)
      IMPLICIT REAL*8(A-H,O-Z)
      EXTERNAL S_HPS,B44
      COMMON/N3PH/N3P(3)/A3PH/A3P(3)/B3PH/B3P(3)

      SUM=0.
      DO K=1,3
      SUM=SUM+B3P(K)*S_HPS(N3P(K)+1,A3P(K),N2I,A2I,N3J,A3J,N4J,
      #A4J,L,1,L2I,L3J,L4J)/B44(N3P(K)+1,A3P(K))
      ENDDO

      S_H3PPS=SUM
      RETURN
      END

C ****
C * SUBROUTINE CC_7(L)
C ****

      IMPLICIT REAL*8(A-H,O-Z)
      EXTERNAL Q1_MATRIX,Q2_MATRIX,COMMON_DATA,ETA_PSI,MATRIX_HP
      COMMON/N3PH/N3P(3)/A3PH/A3P(3)/B3PH/B3P(3)/B_G/BETA,GAMMA

      DATA (N3P(I),I=1,3)/1.1,2/
      DATA (A3P(I),I=1,3)/0.5D0,1D0,1D0/
      DATA (B3P(I),I=1,3)/0.339224553D0,-0.966001481D0,-0.48300074D0/

      OPEN(UNIT=5,FILE='EIGEN_RES_21_120_90P',STATUS='OLD')
      OPEN(UNIT=8,FILE='Q_RES_21_120_90P.res1',STATUS='new')

      CALL GAUSS
      CALL COMMON_DATA
      CALL ETA_PSI
      CALL MATRIX_HP(L)
      beta=0.8d0
      gamma=0.8d0

```

```

      write(8,*)'P-WAVE,H(1s,2s,2p,3p_)+Ps(1s,2s,2p),21 function/ch'
      write(8,*)'factor 2*L+1 has been multiplied,120_H+90_Ps'
      write(8,*)'Beta=',beta,'Gamma=',gamma

      CALL Q1_MATRIX(L)
      CALL Q2_MATRIX(L)

      RETURN
      END
*****
C      * OPEN CHANNEL: H1s      *
*****
C      SUBROUTINE Q1_MATRIX(L)
C      IMPLICIT REAL*8(A-H,O-Z)
C      PARAMETER(N=1)
C      external R_MATRIX,T_MATRIX,FFM,BFMATRIX
C      DIMENSION X00(N,N),X01(N,N),X10(N,N),X11(N,N),Y(N,N),INDX(N)
C      # ,R1(N,N),R2(N,N),T11(N,N),T12(N,N),T21(N,N),T22(N,N),PPK(13)
C      # ,PKK(N)

C      DATA(PPK(I),I=1,13)/0.1D0,0.2D0,0.3D0,0.4D0,0.5D0,0.6D0,
C      # 0.62d0,0.64d0,0.66d0,0.68d0,0.69d0,0.7D0,0.705D0/

      WRITE(8,123)'PK','PHASE_K','PHASE-IK','Q1-K','Q2-IK'
      WRITE(8,*)
      DO KK=1,6

      PKK(1)=PPK(KK)

      NO=N
      CALL FFM(NO,PKK(1),L,X00,X10,X01,X11)      !FREE-FREE

      CALL BFMATRIX(NO,PKK(1),L,X00,X10,X01,X11)  !(FREE-FREE)+(FREE-BOUND)
      !---->M_matrices

      DO I=1,NO
      DO J=1,NO
      PKIJ=DSQRT(PKK(I)*PKK(J))
      X00(I,J)=X00(I,J)/PKIJ
      X01(I,J)=X01(I,J)/PKIJ
      X10(I,J)=X10(I,J)/PKIJ
      X11(I,J)=X11(I,J)/PKIJ
      ENDDO
      ENDDO

      CALL R_MATRIX(X00,X01,X10,X11,Y,INDX,R1,R2,N)

      CALL T_MATRIX(R1,T11,T12,INDX,N)
      CALL T_MATRIX(R2,T21,T22,INDX,N)

      DO I=1,N
      DO J=1,N
      T11(I,J)=T11(I,J)**2+T12(I,J)**2           !T11(I,J)=|Tk(I,J)|^2
      T22(I,J)=T21(I,J)**2+T22(I,J)**2           !T22(I,J)=|Ti(I,J)|^2
      ENDDO
      ENDDO

      PI=1D0/PPK(1)**2*(2*L+1)
      Q1=T11(1,1)*PI
      Q2=T22(1,1)*PI
      WRITE(8,124)PPK(1),atan(R1(1,1)),ATAN(R2(1,1)),Q1,Q2
      write(2,124)PPK(1),atan(R1(1,1)),ATAN(R2(1,1)),Q1,Q2
      close(2)
      ENDDO

123  FORMAT(A5,2x,A13,3(5x,A13))
124  FORMAT(f7.5,4(2x,E15.10))

      RETURN
      end
*****
C      * OPEN CHANNELS: H1s,Ps(1s),or H2s,H2p  *
*****
C      SUBROUTINE Q2_MATRIX(L)
C      IMPLICIT REAL*8(A-H,O-Z)
C      PARAMETER(N=2)
C      external R_MATRIX,T_MATRIX,FFM,BFMATRIX
C      DIMENSION X00(N,N),X01(N,N),X10(N,N),X11(N,N),Y(N,N),INDX(N)
C      # ,R1(N,N),R2(N,N),T11(N,N),T12(N,N),T21(N,N),T22(N,N),PPK(25)
C      # ,PKK(N)

```

```

      DATA(PPK(I),I=1,17)/0.71D0,0.72D0,0.725D0,0.73D0,0.74D0,0.75D0,
#0.76D0,0.77D0,0.78D0,0.79D0,0.80D0,0.81D0,0.82D0,0.83D0,0.84D0,
#0.85D0,0.86D0/
      !Open channel:Ps(1s);N=2

      NO=N
      WRITE(8,124)'PK','Q11(1,1)', 'Q22(1,1)', 'Q11(1,2)', 'Q22(1,2)'
      WRITE(8,124)'QK','Q22(2,2)', 'Q11(2,2)', 'Q11(2,1)', 'Q22(2,1)'
      WRITE(8,'-----')

      DO KK=1,17

      PPK(1)=PPK(KK)
      IF(NO .EQ. 2)THEN
      PPK(2)=(2*PPK(1)**2-1)**0.5D0
      ENDIF

      CALL FFM(NO,PPK(1),L,X00,X10,X01,X11)    !FREE-FREE
      CALL BMATRIX(NO,PPK(1),L,X00,X10,X01,X11) ! (FREE-FREE)+(FREE-BOUND)
      !----> M_matrices

      DO I=1,N
      DO J=1,N
      PKIJ=DSQRT(PPK(I)*PPK(J))
      X00(I,J)=X00(I,J)/PKIJ
      X01(I,J)=X01(I,J)/PKIJ
      X10(I,J)=X10(I,J)/PKIJ
      X11(I,J)=X11(I,J)/PKIJ

      ENDDO
      ENDDO

      CALL R_MATRIX(X00,X01,X10,X11,Y,INDX,R1,R2,N)

      CALL T_MATRIX(R1,T11,T12,INDX,N)
      CALL T_MATRIX(R2,T21,T22,INDX,N)

      DO I=1,N
      DO J=1,N
      T11(I,J)=T11(I,J)**2+T12(I,J)**2           !T11(I,J)=|Tk(I,J)|^2
      T22(I,J)=T21(I,J)**2+T22(I,J)**2           !T22(I,J)=|Ti(I,J)|^2
      ENDDO
      ENDDO

      DO I=1,N
      PI=1D0/PPK(I)**2*(2*L+1)                   !Transition cross sections
      DO J=1,N
      T11(I,J)=PI*T11(I,J)
      T22(I,J)=PI*T22(I,J)
      ENDDO
      IF(NO .GT. 4 )THEN
      T11(I,4)=T11(I,4)+T11(I,5)
      T22(I,4)=T22(I,4)+T22(I,5)
      ENDIF
      ENDDO

      IF(NO .EQ. 2)THEN
      C H entrance channel kp   ls->ls_k ls->ls_i ls->Ps_k ls->Ps_i
      WRITE(8,126)PPK(1),T11(1,1),T22(1,1),T11(1,2),T22(1,2)
      write(2,126)PPK(1),T11(1,1),T22(1,1),T11(1,2),T22(1,2)

      C Ps entrance channel kq   Ps->Ps_k Ps->Ps_i Ps->ls_K Ps->ls_i
      WRITE(8,126)PPK(2),T11(2,2),T22(2,2),T11(2,1),T22(2,1)
      WRITE(8,'')
      write(2,126)PPK(1),T11(1,1),T22(1,1),T11(1,2),T22(1,2)
      close(2)

      ELSEIF(NO .GT. 2 .AND. NO .LT. 6)THEN
      C H entrance channel kp,  ls->ls   ls->Ps  ls->2s   ls->2p_, 2p+
      WRITE(8,126)PPK(1),T11(1,1),T11(1,2),T11(1,3),T11(1,4)
      WRITE(8,126)PPK(1),T22(1,1),T22(1,2),T22(1,3),T22(1,4)

      C Ps entrance channel kq   Ps->ls   Ps->Ps   Ps->2s   Ps->2p_, 2p+
      WRITE(8,126)PPK(2),T11(2,1),T11(2,2),T11(2,3),T11(2,4)
      WRITE(8,126)PPK(2),T22(2,1),T22(2,2),T22(2,3),T22(2,4)

      ENDIF

      ENDDO
      124 FORMAT(A5,4(5X,A13))
      126 FORMAT(F10.8,1X,4(1X,E14.9))

```

```

      RETURN
      END

C *****
C * CALCULATE FREE-FREE MATRICE:FFSS,FFCS,FFSC,FFCC *
C * NO --> NO. OF OPEN CHANNEL *
C *****
      SUBROUTINE FFM(NO,PK,L,FFSS,FFCS,FFSC,FFCC)
      IMPLICIT REAL*8(A-H,O-Z)
      EXTERNAL FFSS_PQ,FFCS_PQ,FFCC_PQ,FFSS_PU,FFCS_PU,FFCS_UP,
#FFCC_PU
      DIMENSION FFSS(NO,NO),FFCS(NO,NO),FFSC(NO,NO),FFCC(NO,NO)
      COMMON/B_G/BETA,GAMMA

      FFSS(1,1)=FFSS_PQ(PK,PK,L,1,0,L,1,0,L)
      FFCS(1,1)=FFCS_PQ(PK,PK,L,1,0,L,1,0,L,beta)
      FFSC(1,1)=FFCS(1,1)+0.5D0*PK
      FFCC(1,1)=FFCC_PQ(PK,PK,L,1,0,L,1,0,L,BETA,BETA)
      write(*,*)'finish free-free 1'

      IF (NO .GT. 1) THEN                                !Ps channel open
      PK2=DSQRT(2*PK*PK-1)
      FFSS(1,2)=FFSS_PU(PK,PK2,L,1,0,L,1,0,L)
      FFSS(2,1)=FFSS(1,2)
      FFSS(2,2)=0.

      FFCS(1,2)=FFCS_PU(PK,PK2,L,1,0,L,1,0,L,BETA)
      FFCS(2,1)=FFCS_UP(PK2,PK,L,1,0,L,1,0,L,GAMMA)
      FFCS(2,2)=0.

      FFSC(1,2)=FFCS(2,1)
      FFSC(2,1)=FFCS(1,2)
      FFSC(2,2)=0.5D0*PK2

      FFCC(1,2)=FFCC_PU(PK,PK2,L,1,0,L,1,0,L,BETA,GAMMA)
      FFCC(2,1)=FFCC(1,2)
      FFCC(2,2)=FFCC_UV(PK2,PK2,L,1,0,L,1,0,L,BETA,GAMMA)
      ENDIF

      RETURN
      END

C *****
C * CALCULATE PBS(P,J) AND FBC(P,J) MATRICE;NO->NO. OF OPEN CHANNEL*
C *****
      SUBROUTINE BFMATRIX(NO,PK,L,PB00,PB10,PB01,PB11)
      IMPLICIT REAL*8(A-H,O-Z)
      PARAMETER(NH=18,NPS=18,N_H=144,N_P=108,NHN=432)
      EXTERNAL FBC_UQ,FBS_UP,FBS_PU,FBC_PU,FBS_PQ,FBS_VU,FBC_PQ,FBC_VU
      DIMENSION ZII(NPS),ZJJ(NH),FBS(5,NHN),FBC(5,NHN),PB00(NO,NO),
#PB01(NO,NO),PB10(NO,NO),PB11(NO,NO),BFMS(10,NHN),BFMC(10,NHN),
#EVAL(NHN),EVEC(NHN,NHN),N24(NH)

      DIMENSION N1J(N_H),A1J(N_H),N2J(N_H),A2J(N_H),L1(N_H),L2(N_H),
#N3J(N_P),A3J(N_P),N4J(N_P),A4J(N_P),L3(N_P),L4(N_P),BB1(5),bb2(6)
#,N22(6),BB3(3),BB44(6)
      COMMON/B_G/BETA,GAMMA

      DATA(N22(I),I=1,6)/1,2,1,2,1,2/
      DATA(BB1(I),I=1,4)/0.7D0,0.8D0,0.9D0,1.1D0/
      DATA(BB2(I),I=1,6)/0.3D0,0.4D0,0.5D0,0.6D0,0.8D0,1.1D0/
      DATA(BB3(I),I=1,3)/0.2D0,0.6D0,1D0/
      DATA(BB44(I),I=1,6)/0.2D0,0.5D0,0.9D0,1.4D0,1.7D0,2.1D0/
      DATA(N24(I),I=1,NH)/1,2,3,1,2,3,1,2,3,1,2,3,1,2,3,1,2,3,
#1,2,3/

      DATA(A2(I),I=1,NH)/0.05D0,0.05D0,0.05D0,0.2D0,0.2D0,0.2D0
#,0.4D0,0.4D0,0.4D0,0.8D0,0.8D0,1.2D0,1.2D0,1.2D0
#,1.8D0,1.8D0,1.8D0/

      N_COR=1
C ##### parameters of H(I) correlation functions#####
      M=0
      DO L11=0,2
      DO L21=INT(ABS(L-L11)),L+L11,2
      DO I=1,4
      DO J=1,6
      M=M+1

      if(L11.eq.1)then

```

Aug 14 1996 09:47

## Fortran Program - 7\_mixing.f

212

```

N1J(M)=3           !n1j=3 for S,P,D ,for H N1j(m)=2+N22(I)
else
N1J(M)=L11+1
endif

N2J(M)=L21+N24(J)
L1(M)=L11
L2(M)=L21
AL1(M)=BB1(I)
A2J(M)=BB2(J)
ENDDO
ENDDO
ENDDO
ENDDO

C##### parameters of Ps(I) correlation functions #####
M=0
DO L31=0,2
DO L41=INT(ABS(L-L31)),L+L31,2
DO I=1,3
DO J=1,6
M=M+1
N3J(M)=L31+1
N4J(M)=L41+N24(J)
L3(M)=L31
L4(M)=L41
A3J(M)=BB3(I)
A4J(M)=BB4(J)
ENDDO
ENDDO
ENDDO
ENDDO

C#####
DO I=1,NH
ZJJ(I)=ZII(I)
ENDDO

DO J=1,NH
ZJ=ZJJ(J)
NJ=N24(J)+L
PBS(1,J)=PBS_PQ(PK,NJ,ZJ,L,1,0,L,1,0,L)      !H1s(b)-H1s(f)
FBC(1,J)=FBC_PQ(PK,NJ,ZJ,L,1,0,L,1,0,L,BETA)

JH2=J+NH
PBS(1,JH2)=PBS_PQ(PK,NJ,ZJ,L,2,0,L,1,0,L)      !H2s(b)-H1s(f)
FBC(1,JH2)=FBC_PQ(PK,NJ,ZJ,L,2,0,L,1,0,L,BETA)

N2P=0
DO LP1=INT(ABS(L-1)),L+1,2
N2P=N2P+1
NPJ=N24(J)+LP1
JH3=JH2+N2P*NH
PBS(1,JH3)=PBS_PQ(PK,NPJ,ZJ,L,2,1,LP1,1,0,L)
FBC(1,JH3)=FBC_PQ(PK,NPJ,ZJ,L,2,1,LP1,1,0,L,BETA)
ENDDO

JP1=JH3+NH
PBS(1,JP1)=PBS_UP(PK,NJ,ZJ,L,1,0,L,1,0,L)      !Ps(1s)(b)-H1s(f)
FBC(1,JP1)=FBC_UQ(PK,NJ,ZJ,L,1,0,L,1,0,L,BETA)

JP2=JP1+NH
PBS(1,JP2)=PBS_UP(PK,NJ,ZJ,L,2,0,L,1,0,L)      !2sPs(b)-H1s(f)
FBC(1,JP2)=FBC_UQ(PK,NJ,ZJ,L,2,0,L,1,0,L,BETA)

N2PP=0
L2U0=INT(ABS(L-1))
DO LU1=L2U0,L+1,2
N2PP=N2PP+1
NPPJ=N24(J)+LU1
JP3=JP2+N2PP*NH
PBS(1,JP3)=PBS_UP(PK,NPPJ,ZJ,L,2,1,LU1,1,0,L)
FBC(1,JP3)=FBC_UQ(PK,NPPJ,ZJ,L,2,1,LU1,1,0,L,BETA)
ENDDO

ENDDO

DO K=1,N_H
NH_C=JP3+K
      !H_COR-H1s

```

```

FBS(1,NH_C)=FBS_HJP(PK,N1J(K),A1J(K),N2J(K),A2J(K),L1(K)
#,L2(K),1,0,L,L)
FBC(1,NH_C)=FBC_HJP(PK,N1J(K),A1J(K),N2J(K),A2J(K),L1(K)
#,L2(K),1,0,L,L,BETA)
ENDDO

DO K=1,N_P                                !Ps_COR-H1s
NPS_C=NH_C+K
FBS(1,NPS_C)=FBS_PSJP(PK,N3J(K),A3J(K),N4J(K),A4J(K),L3(K)
#,L4(K),1,0,L,L)
FBC(1,NPS_C)=FBC_PSJP(PK,N3J(K),A3J(K),N4J(K),A4J(K),L3(K)
#,L4(K),1,0,L,L,BETA)
ENDDO

DO J=1,NH                                !H3p_+H1s
ZJ=ZII(J)
J3P=-1
DO L2J=INT(ABS(L-1)),L+1,2
J3P=J3P+1
JH4=NPS_C+J3P*NH+J
N3PJ=N24(J)+L2J
FBS(1,JH4)=FBS_H3PQ(PK,N3PJ,ZJ,L2J,1,0,L,L)
FBC(1,JH4)=FBC_H3PQ(PK,N3PJ,ZJ,L2J,1,0,L,L,BETA)
ENDDO

ENDDO

IF(NO .GT. 1)THEN                         !Ps(1s) open
PK2=DSQRT(2*PK*PK-1)
DO J=1,NH
NJ=N24(J)+L
ZJ=ZJJ(J)
FBS(2,J)=FBS_PU(PK2,NJ,ZJ,L,1,0,L,1,0,L)      !H1s-Ps(f)
FBC(2,J)=FBC_PU(PK2,NJ,ZJ,L,1,0,L,1,0,L,GAMMA)

JH2=NH+J
FBS(2,JH2)=FBS_PU(PK2,NJ,ZJ,L,2,0,L,1,0,L)      !H2s(b)-Ps(f)
FBC(2,JH2)=FBC_PU(PK2,NJ,ZJ,L,2,0,L,1,0,L,GAMMA)

N2P=0                                         !H2p(b)-Ps(f)
DO LP1=INT(ABS(L-1)),L+1,2
N2P=N2P+1
NPJ=N24(J)+LP1
JH3=JH2+N2P*NH
FBS(2,JH3)=FBS_PU(PK2,NPJ,ZJ,L,2,1,LP1,1,0,L)
FBC(2,JH3)=FBC_PU(PK2,NPJ,ZJ,L,2,1,LP1,1,0,L,GAMMA)
ENDDO

JP1=JH3+NH
FBS(2,JP1)=FBS_VU(PK2,NJ,ZJ,L,1,0,L,1,0,L)      !Ps(1s)-Ps(f)
FBC(2,JP1)=FBC_VU(PK2,NJ,ZJ,L,1,0,L,1,0,L,GAMMA)

JP2=JP1+NH
FBS(2,JP2)=FBS_VU(PK2,NJ,ZJ,L,2,0,L,1,0,L)      !2sPs(b)-1sPs(f)
FBC(2,JP2)=FBC_VU(PK2,NJ,ZJ,L,2,0,L,1,0,L,gamma)

N2PP=0                                         !2pPs(b)-1sPs(f)
DO LU1=INT(ABS(L-1)),L+1,2
N2PP=N2PP+1
NPPJ=N24(J)+LU1
JP3=JP2+N2PP*NH
FBS(2,JP3)=FBS_VU(PK2,NPPJ,ZJ,L,2,1,LU1,1,0,L)
FBC(2,JP3)=FBC_VU(PK2,NPPJ,ZJ,L,2,1,LU1,1,0,L,GAMMA)
ENDDO

ENDDO

DO K=1,N_H                                !H_COR-1sPs
NH_C=JP3+K
FBS(2,NH_C)=FBS_HJU(PK,N1J(K),A1J(K),N2J(K),A2J(K),L1(K)
#,L2(K),1,0,L,L)
FBC(2,NH_C)=FBC_HJU(PK,N1J(K),A1J(K),N2J(K),A2J(K),L1(K)
#,L2(K),1,0,L,L,GAMMA)
ENDDO

DO K=1,N_P                                !PS_COR-1sPs
NPS_C=NH_C+K
FBS(2,NPS_C)=FBS_PSJU(PK,N3J(K),A3J(K),N4J(K),A4J(K),L3(K)
#,L4(K),1,0,L,L)

```

```

FBC(2,NPS_C)=FBC_PSJU(PK2,N3J(K),A3J(K),N4J(K),A4J(K),L3(K)
#,L4(K),1,0,L,L,GAMMA)
ENDDO

DO J=1,NH

ZJ=ZII(J)
J3P=-1
DO L2J=INT(ABS(L-1)),L+1,2
J3P=J3P+1
JH4=NPS_C+J3P*NH+J
N3PJ=N24(J)+L2J
FBS(2,JH4)=PBS_H3PPS(PK2,N3PJ,ZJ,L2J,1,0,L,L)
FBC(2,JH4)=FBC_H3PPS(PK2,N3PJ,ZJ,L2J,1,0,L,L,GAMMA)
ENDDO
ENDDO

ENDIF

C##### READ IN THE EIGENVALUES AND EIGENFUNCTIONS #####
IF(NO_READ .NE. 1)THEN
DO I=0,NHN
DO J=1,NHN,3
  IF (I .EQ. 0)THEN
    READ(5,30) EVAL(J), EVAL(J+1), EVAL(J+2)
  ELSE
    READ(5,30) EVEC(I,J), EVEC(I,J+1), EVEC(I,J+2)
  ENDIF
ENDDO
ENDDO
NO_READ=1
close(5)
ENDIF

C##### CALCULATE FB00,FB01,FB10,FB11 #####
E=-0.5D0+0.5D0*PK**2
DO I=1,NO
  DO J=1,NHN
    BFMS(I,J)=0.
    BFMC(I,J)=0.
    DO K=1,NHN
      BFMS(I,J)=BFMS(I,J)+FBS(I,K)*EVEC(K,J)
      BFMC(I,J)=BFMC(I,J)+FBC(I,K)*EVEC(K,J)
    ENDDO
  ENDDO
ENDDO

DO I=1,NO
DO J=1,NO
s00=0.
s01=0.
s10=0.
s11=0.

DO K=1,NHN
  S00=S00+BFMS(I,K)/(E-EVAL(K))*BFMS(J,K)
  S01=S01+BFMS(I,K)/(E-EVAL(K))*BFMC(J,K)
  S10=S10+BFMC(I,K)/(E-EVAL(K))*BFMS(J,K)
  S11=S11+BFMC(I,K)/(E-EVAL(K))*BFMC(J,K)
ENDDO
FB00(I,J)=FB00(I,J)+S00
FB01(I,J)=FB01(I,J)+S01
FB10(I,J)=FB10(I,J)+S10
FB11(I,J)=FB11(I,J)+S11

ENDDO
ENDDO

30 FORMAT(1X,3(d23.17,1X))

RETURN
END

C ****
* FBS_UP(..)=<Ps CHANNEL-U;bound|H-E| H CHANNEL P;free *
C ****
FUNCTION FBS_UP(PK,N4J,ZJ,L,NU,LU,LUL,NP,LP,LP1)
IMPLICIT REAL*8(A-H,O-Z)
EXTERNAL VV,B4,B3,B3PS
COMMON/D_HP/DHP(5,5,3,3,80,150)
# /PSI_ETA/DPSI(80),DETA(150)/W_W/W_PSI(80),W_ETA(150)

```

```

* /D_FACT/DFACT(150)

LP2=(LP1-INT(ABS(L-LP)))/2
LU2=(LU1-INT(ABS(L-LU)))/2
SUM=0.
DO I=1,80
PSI=1/DPSI(I)

SUM1=0.
DO J=1,150
ETA=DETA(J)

X=DSQRT(PSI**2+6D0*ETA*PSI+ETA**2+8D0)
Y=0.25D0*((2D0/NP+1D0/NU)*PSI+(2D0/NP-1D0/NU)*ETA+ZJ*X)

SUM2=0.
DO JU=0,NU-LU-1

SUM3=0.
DO JP=0,NP-LP-1
SUM3=SUM3+B3(NP,LP,JP)*(0.5D0*(PSI+ETA))**((LP+JP)-
#DHP(LP+1,LP2+1,LU+1,LU2+1,I,J)*VV(3+N4J+LU+JU+LP+JP,LP1,Y,PK)
ENDDO

SUM2=SUM2+B3PS(NU,LU,JU)*(0.5D0*(PSI-ETA))**((LU+JU)*SUM3
ENDDO

SUM1=SUM1+SUM2*(PSI**2-ETA**2)*(0.25D0*X)**(N4J-1)*(1-2/(PSI-ETA))
#*W_ETA(J)
ENDDO

SUM=SUM+SUM1/DPSI(I)**2*W_PSI(I)
ENDDO
FBS_UP=0.125D0*PK*B44(N4J,ZJ)*SUM
RETURN
END

*****
C *FBC_UQ(PK,L) = <CHANNEL-U:Ps(bound) | H- E | CHANNEL-Q:H(free)>*
C ****
FUNCTION FBC_UQ(QK,N4J,ZJ,L,NU,LU,LUL,NQ,LQ,LQ1,BETA)
IMPLICIT REAL*8(A-H,O-Z)
EXTERNAL VV1,B4,B3,B3PS
COMMON/D_HP/DHP(5,5,3,3,80,150)
#/PSI_ETA/DPSI(80),DETA(150)/W_W/W_PSI(80),W_ETA(150)
#/D_FACT/DFACT(150)

WW=0.5D0*(1D0/NQ**2-0.5D0/NU**2-0.5D0*ZJ*ZJ-QK*QK)
AA1=LUL*(LUL+1)-N4J*(N4J-1)
LQ2=(LQ1-INT(ABS(L-LQ)))/2
LU2=(LU1-INT(ABS(L-LU)))/2
SUM=0.
DO I=1,80
PSI=1/DPSI(I)

SUM1=0.
DO J=1,150
ETA=DETA(J)

X=DSQRT(PSI**2+6D0*ETA*PSI+ETA**2+8D0)
Y=0.5D0*((1D0/NQ+0.5D0/NU)*PSI+(1D0/NQ-0.5D0/NU)*ETA+ZJ*X/2)

SUM2=0.
DO JU=0,NU-LU-1
AJU=B3PS(NU,LU,JU)*(0.5D0*(PSI-ETA))**((LU+JU)*
SUM3=0.
DO JQ=0,NQ-LQ-1
AJQ=B3(NQ,LQ,JQ)*(0.5D0*(PSI+ETA))**((LQ+JQ)*DHP(LQ+1,
#LQ2+1,LU+1,LU2+1,I,J)
AJQ1=WW*VV1(4+LU+JU+N4J+LQ+JQ,LQ1,Y,BETA,QK)+(2*ZJ*N4J/X
#+1-2/(PSI+ETA))*VV1(3+LU+JU+N4J+LQ+JQ,LQ1,Y,BETA,QK)+4*AA1/X**2*
#VV1(2+LU+JU+N4J+LQ+JQ,LQ1,Y,BETA,QK)
SUM3=SUM1+AJQ*AJQ1
ENDDO

SUM2=SUM2+AJU*SUM3
ENDDO

SUM1=SUM1+SUM2*(PSI**2-ETA**2)*(0.25D0*X)**(N4J-1)*W_ETA(J)
ENDDO

```

```

SUM=SUM+SUM1/DPSI(I)**2*W_PSI(I)
ENDDO

FBC_UQ=-0.125D0*QK*B44(N4J,ZJ)*SUM
RETURN
END

C ****
C * FBS_PU(..)= <H CHANNEL-P;bound|H-E|Ps CHANNEL-U;free> *
C ****
FUNCTION FBS_PU(UK,N2J,ZJ,L,NP,LP,LPI,NU,LU,LU1)
IMPLICIT REAL*8(A-H,O-Z)
EXTERNAL VV,B4
COMMON/D_HP/DHP(5,5,3,3,80,150)/PSI_ETA/DPSI(80),
DETA(150)/W_W/W_PSI(80),W_ETA(150)
LP2=(LPI-INT(ABS(L-LP)))/2
LU2=(LU1-INT(ABS(L-LU)))/2

SUM=0.
DO I=1,80
PSI=1/DPSI(I)

SUM1=0.
DO J=1,150
ETA=DETA(J)

UK1=0.25D0*UK*DSQRT(PSI**2+6D0*ETA*PSI+ETA**2+8D0)
Y=0.25D0*((2D0/NP+1D0/NU)*PSI+(2D0/NP-1D0/NU)*ETA+4*ZJ)
SUM2=0.
DO JP=0,NP-LP-1

SUM3=0.
DO JU=0,NU-LU-1
SUM3=SUM3+B3PS(NU,LU,JU)*(0.5D0*(PSI-ETA))**((LU+JU)*
*VV(3+JP+LP+N2J+JU+LU,LU1,Y,UK1)
ENDDO

SUM2=SUM2+B3(NP,LP,JP)*(0.5D0*(PSI+ETA))**((LP+JP))*SUM3
ENDDO

SUM1=SUM1+((PSI**2-ETA**2-(PSI-ETA))*SUM2*W_ETA(J)*
*DHP(LP+1,LP2+1,LU+1,LU2+1,I,J)
ENDDO

SUM=SUM+SUM1/DPSI(I)**2*W_PSI(I)
ENDDO

FBS_PU=0.125D0*2d0**0.5d0*UK*B44(N2J,ZJ)*SUM
RETURN

END
C ****
C * FBC_PU(..)= <H CHANNEL-P;bound|H-E|Ps CHANNEL-U;free> *
C ****
FUNCTION FBC_PU(UK,N2J,ZI,L,NP,LP,LPI,NU,LU,LU1,GAMMA)
IMPLICIT REAL*8(A-H,O-Z)
EXTERNAL VV1,B4
COMMON/D_HP/DHP(5,5,3,3,80,150)/PSI_ETA/DPSI(80),
DETA(150)/W_W/W_PSI(80),W_ETA(150)
WW=0.25D0*(1D0/NU**2-2D0/NP**2-2*ZI*ZI-UK*UK)

LP2=(LPI-INT(ABS(L-LP)))/2
LU2=(LU1-INT(ABS(L-LU)))/2

SUM=0.
DO I=1,80
PSI=1/DPSI(I)

SUM1=0.
DO J=1,150
ETA=DETA(J)

X=DSQRT(PSI**2+6D0*ETA*PSI+ETA**2+8D0)
Y=0.25d0*((2D0/NP+1D0/NU)*PSI+(2D0/NP-1D0/NU)*ETA+4*ZI)
UK1=0.25D0*UK*X
GAM=0.25D0*GAMMA*X

SUM2=0.
DO JP=0,NP-LP-1

SUM3=0.
DO JU=0,NU-LU-1

```

```

NN=4+JP+LP+N2J+JU+LU
CC=NN*VV1(NN,LU1,Y,GAM,UK1)+(ZI*N2J+1-2/(PSI-ETA))* 
#VV1(NN-1,LU1,Y,GAM,UK1)+0.5D0*(LP1*(LP1+1)-N2J*(N2J-1))* 
#VV1(NN-2,LU1,Y,GAM,UK1)
SUM3=SUM3+B3PS(NU,LU,JU)*(0.5D0*(PSI-ETA))**((LU+JU)*CC
ENDDO

SUM2=SUM2+B3(NP,LP,JP)*(0.5D0*(PSI+ETA))**((LP+JP)*SUM3
ENDDO
SUM1=SUM1+(PSI**2-ETA**2)*SUM2*W_ETA(J)*
#DHP(LP+1,LP2+1,LU+1,LU2+1,I,J)
ENDDO

SUM=SUM+SUM1/DPSI(I)**2*W_PSI(I)
ENDDO

FBC_PU=-0.125D0*2d0**0.5d0*UK*B44(N2J,ZI)*SUM
RETURN
END
*****
C *FBS_PQ(..)=<H channel-p;bound[H-E|H channel-q;free(S)> *
*****
FUNCTION FBS_PQ(QK,N2J,ZJ,L,NP,LP,LP1,NQ,LQ,LQ1)
IMPLICIT REAL*8(A-H,O-Z)
EXTERNAL VV,F6J,B4,GJ

IF(NP .EQ. NQ .AND. LP .EQ. LQ .AND. LP1 .EQ. LQ1)THEN
FBS=VV(N2J,LQ1,ZJ,QK)
ELSE
FBS=0.
ENDIF

APQ=1D0/NP+1D0/NQ
K1=MAX(ABS(LP-LQ),ABS(LP1-LQ1))
K2=MIN(LP+LQ,LP1+LQ1)

SUM0=0.
DO JP=0,NP-LP-1
SUM1=0.
DO JQ=0,NQ-LQ-1

SUM2=0.
DO K=K1,K2,2
SUM2=SUM2+CT(LP,K,LQ)*CT(LP1,K,LQ1)*F6J(LP,LP1,L
#,LQ1,LQ,K)*GJ(N2J+1,ZJ,QK,LQ1,LP+JP+LQ+JQ+1-K,APQ,K)
ENDDO
SUM1=SUM1+B3(NQ,LQ,JQ)*SUM2
ENDDO

SUM0=SUM0+B3(NP,LP,JP)*SUM1
ENDDO
FBS_PQ=QK*B44(N2J,ZJ)*(FBS-(-1D0)**(LQ+LP1+L)*SUM0)
RETURN
END

*****
C *FBS_VU(..)=<Ps channel-V;bound[H-E|Ps channel-U;free(S)> *
*****
FUNCTION FBS_VU(UK,N4J,ZJ,L,NV,LV,LV1,NU,LU,LU1)
IMPLICIT REAL*8(A-H,O-Z)
EXTERNAL F6J,GJ,B4

AUV=1D0/NU+1D0/NV
K1=MAX(ABS(LV-LU),ABS(LV1-LU1))
K2=MIN(LV+LU,LV1+LU1)

IF(K1/2*2 .EQ. K1)THEN
FBS_VU=0.
RETURN
ENDIF
SUM0=0.
DO JU=0,NU-LU-1

SUM1=0.
DO JV=0,NV-LV-1

SUM2=0.
DO K=K1,K2,2
SUM2=SUM2+CT(LV,K,LU)*CT(LV1,K,LU1)*F6J(LU,LU1,L
#,LV1,LV,K)*GJ(N4J+1,ZJ,UK,LU1,LU+JU+LV+JV+1-K,AUV,K)
ENDDO

```

```

SUM1=SUM1+D0** (LU+JU+LV+JV+4) *B3PS(NV,LV,JV) *SUM2
ENDDO

SUM0=SUM0+B3PS(NU,LU,JU) *SUM1
ENDDO

PBS_VU=2d0**0.5d0*(-1D0)**(LV+LU1+L)*UK*B44(N4J,ZJ)*SUM0
RETURN
END

C ****
C *FBC_PQ(..)=<H channel-p;bound|H-E|H channel-q;free(C) > *
C ****
FUNCTION FBC_PQ(QK,N2J,ZJ,L,NP,LP,LP1,NQ,LQ,LQ1,BETA)
IMPLICIT REAL*8(A-H,O-Z)
EXTERNAL F6J,GN,B4,VV1,B3

IF(NP.EQ.NQ .AND. LP.EQ.LQ .AND. LP1.EQ.LQ1)THEN
  WW=-0.5D0*(ZJ*ZJ+QK*QK)
  FBC=WW*VV1(N2J+1,LQ1,ZJ,BETA,QK)+(ZJ*N2J+1)*VV1(N2J,LQ1,
#ZJ,BETA,QK)+0.5D0*(LP1*(LP1+1)-N2J*(N2J-1))*VV1(N2J-1,LQ1,
#ZJ,BETA,QK)
ELSE
  FBC=0.
ENDIF

APQ=1D0/NP+1D0/NQ
K1=MAX(ABS(LP-LQ),ABS(LP1-LQ1))
K2=MIN(LP+LQ,LP1+LQ1)
SUM0=0.
DO JP=0,NP-LP-1
  SUM1=0.
  DO JQ=0,NQ-LQ-1
    SUM2=0.
    DO K=K1,K2,2
      SUM2=SUM2+CT(LP,K,LQ)*CT(LP1,K,LQ1)*F6J(LP,LP1,L
#,LQ1,K)*GN(N2J+1,ZJ,QK,LQ1,LP+JP+LQ+JQ+1-K,APQ,K,BETA)
    ENDDO
    SUM1=SUM1+B3(NQ,LQ,JQ)*SUM2
  ENDDO
  SUM0=SUM0+B3(NP,LP,JP)*SUM1
ENDDO

FBC_PQ=-QK*B44(N2J,ZJ)*(FBC-(-1D0)**(LQ+LP1+L)*SUM0)
return
end

C ****
C *FBC_VU(..)=<Ps channel-V;bound|H-E|Ps channel-U;free(C) > *
C ****
FUNCTION FBC_VU(UK,N4J,ZJ,L,NV,LV,LV1,NU,LU,LU1,GAMMA)
IMPLICIT REAL*8(A-H,O-Z)
EXTERNAL F6J,GN,B4,VV1

IF(NV.EQ.NU .AND. LV.EQ.LU .AND. LV1.EQ.LU1)THEN
  WW=-0.25D0*(ZJ*ZJ+UK*UK)
  FBC=WW*VV1(N4J+1,LU1,ZJ,GAMMA,UK)+0.5D0*ZJ*N4J*VV1(N4J
#,LU1,ZJ,GAMMA,UK)+0.25D0*(LV1*(LV1+1)-N4J*(N4J-1))*VV1(N4J-1,
#LU1,ZJ,GAMMA,UK)

ELSE
  FBC=0.
ENDIF

AUV=1D0/NU+1D0/NV
K1=MAX(ABS(LV-LU),ABS(LV1-LU1))
K2=MIN(LV+LU,LV1+LU1)

SUM0=0.

IF(K1/2**2 .EQ. K1)GO TO 3031

```

```

      DO JU=0,NU-LU-1
      SUM1=0.
      DO JV=0,NV-LV-1
      SUM2=0.
      DO K=K1,K2,2
      SUM2=SUM2+CT(LV,K,LU)*CT(LV1,K,LU1)*F6J(LU,LU1,L
      ,LV1,LV,K)*GN(N4J+1,ZJ,UK,LU1,LU+JU+LV+JV+1-K,AUV,K,GAMMA)
      ENDDO
      SUM1=SUM1+2D0** (LU+JU+LV+JV+4) *B3PS(NV,LV,JV)*SUM2
      ENDDO
      SUM0=SUM0+B3PS(NU,LU,JU)*SUM1
      ENDDO
      3031 FBC_VU=-2D0**0.5D0*UK*B44(N4J,ZJ)*(FBC+(-1D0)**(LV+LU1+L)*SUM0)
      RETURN
      END

C #####  

C # < H3P_ ; I | H-E | np lp ; S > #
C #####  

C FUNCTION PBS_H3PQ(PK,N2I,A2I,L2I,NQ,LQ,LQ1,L)
C IMPLICIT REAL*8(A-H,O-Z)
C EXTERNAL FBS_HJP
C COMMON/N3PH/N3P(3)/A3PH/A3P(3)/B3PH/B3P(3)

      SUM=0.
      DO K=1,3
      SUM=SUM+B3P(K)*PBS_HJP(PK,N3P(K)+1,A3P(K),N2I,A2I,1,L2I,
      #NQ,LQ,LQ1,L)/B44(N3P(K)+1,A3P(K))
      ENDDO

      PBS_H3PQ=SUM
      RETURN
      END

C #####  

C # < H3P_ ; I | H-E | np lp ; C > #
C #####  

C FUNCTION FBC_H3PQ(PK,N2I,A2I,L2I,NQ,LQ,LQ1,L,BETA)
C IMPLICIT REAL*8(A-H,O-Z)
C EXTERNAL FBC_HJP
C COMMON/N3PH/N3P(3)/A3PH/A3P(3)/B3PH/B3P(3)

      SUM=0.
      DO K=1,3
      SUM=SUM+B3P(K)*FBC_HJP(PK,N3P(K)+1,A3P(K),N2I,A2I,1,L2I,
      #NQ,LQ,LQ1,L,BETA)/B44(N3P(K)+1,A3P(K))
      ENDDO

      FBC_H3PQ=SUM
      RETURN
      END

C #####  

C # H3P_ ; I | H-E| NU LU LU1; S>#
C #####  

C FUNCTION PBS_H3PPS(UK,N2I,A2I,L2I,NU,LU,LU1,L)
C IMPLICIT REAL*8(A-H,O-Z)
C EXTERNAL PBS_HJU
C COMMON/N3PH/N3P(3)/A3PH/A3P(3)/B3PH/B3P(3)

      SUM=0.
      DO K=1,3
      SUM=SUM+B3P(K)*PBS_HJU(UK,N3P(K)+1,A3P(K),N2I,A2I,1,L2I,
      #NU,LU,LU1,L)/B44(N3P(K)+1,A3P(K))
      ENDDO

      PBS_H3PPS=SUM
      RETURN
      END

C #####  

C # H3P_ ; I | H-E| NU LU LU1; C>#
C #####  

C FUNCTION FBC_H3PPS(UK,N2I,A2I,L2I,NU,LU,LU1,L,GAMMA)
C IMPLICIT REAL*8(A-H,O-Z)
C EXTERNAL FBC_HJU
C COMMON/N3PH/N3P(3)/A3PH/A3P(3)/B3PH/B3P(3)

```

Aug 14 1996 09:47

## Fortran Program - 7\_mixing.f

220

```
SUM=0.  
DO K=1,3  
SUM=SUM+B3P(K)*FBC_HJU(UK,N3P(K)+1,A3P(K),N2I,A2I,I,L2I,  
*NU,LU,LU1,L,GAMMA)/B44(N3P(K)+1,A3P(K))  
ENDDO  
  
FBC_H3PPS=SUM  
RETURN  
END
```





